Space-Based Power Conversion and Power Relay Systems

Preliminary Analysis of Alternate Systems

Interim Report

NAS 8-31628

Boeing Aerospace Company

INTERIM REPORT

SPACE-BASED POWER CONVERSION

AND

POWER RELAY SYSTEMS

PRELIMINARY ANALYSIS OF ALTERNATE SYSTEMS

Submitted to:

The National Aeronautics and Space Administration
George C. Marshall Space Flight Center

Study Contract NAS 8-31628

(This document covers contract activities from July 8, 1975 to May 26, 1976.)

The Boeing Aerospace Company

CONTENTS

1.0 INTRODUCTION, BACKGROUND AND SUMMARY

1.1 INTRODUCTION

1.1.1 The Study Effort

This document summarizes the results of nine months of technical study of non-photovoltaic options for the generation of electricity for terrestrial use by satellite power stations (SPS). A concept for the augmentation of ground-based solar power plants by orbital sunlight reflectors was also studied.

During the period of this study, the George C. Marshall Space Flight Center (MSFC) was also administering a parallel study of a photovoltaic SPS and studies of space transportation system which may be associated with the placement and servicing of the SPS. These studies contributed to the data base for this study.

This study investigated three SPS types having a solar energy source and two which used nuclear reactors. Data derived for each included:

- o configuration definition, including mass statement
- o information for use in environmental impact assessment
- o energy balance (ratio of energy produced to that required to achieve operation)
- o development and other cost estimates

Cost estimates were dependent upon the total program (development, placement and operation of a number of satellites) which was postulated. This postulation was based upon an analysis of national power capacity trends and guidelines received from MSFC.

1.1.2 Contributors

In addition to personnel of the Boeing Aerospace Company, Research and Engineering Division, the following contributed to this study:

1. AiResearch Manufacturing Company of Arizona (A division of the Garrett Corporation), Turbomachines.
2. Dr. J. Richard Williams (Georgia Inst. of Tech), Consultant, Nucleonics and Thermionics

1.2 BACKGROUND

1.2.1 The Satellite Power Station Concept

Fig. 1-1 may be used to understand the basic principle of the Satellite Power Station (SPS). A power generating system produces electric power which is converted into a narrow (total divergence angle of approximately 1/100 degree) microwave beam by the microwave transmitter. These systems are located in equatorial geosynchronous orbit and thus remain in line-of-sight of their associated microwave power receiving stations on the ground. At these stations the microwave power is converted into a form of electricity suitable for insertion into the local power network.

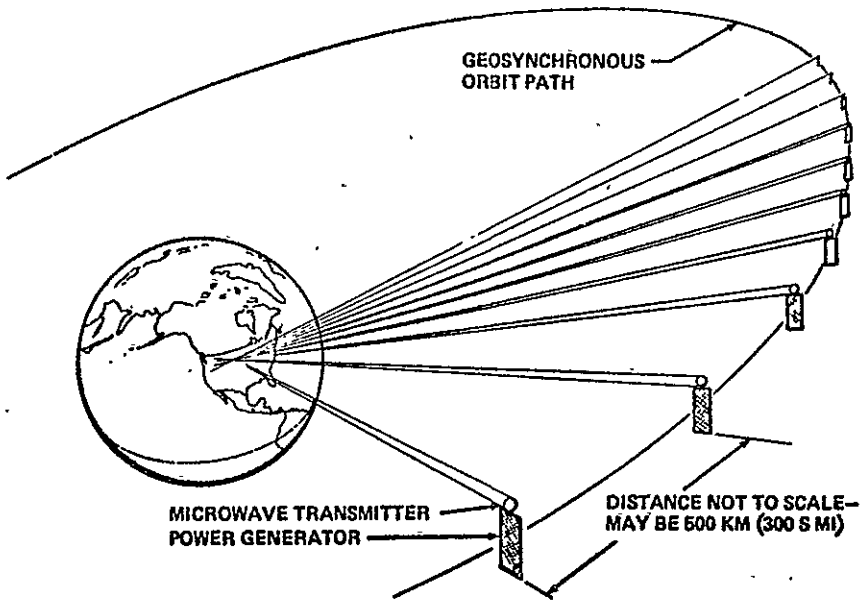

Figure 1-1 Satellite Power Stations

In this study the power generating systems were either non-photovoltaic solar types, or used nuclear reactors as the energy source.

The receiving stations for the SPS consist of a large number ($\approx 10^9$) of small receiving antennas integrated in an oval array. Rectification of the received energy to direct current is accomplished by circuit elements which are integral to the antennas. Fig.1-2 shows such an array.

Figure 1-2 Receiving Antenna

Since the antenna blocks most of the microwave energy but is nearly transparent to sunlight, it is possible that agriculture could be accomplished beneath it. Surrounding the antenna is a buffer zone to contain those microwave "side-lobes" which are more energetic than the continuous exposure standard (assumed to be more than 10 times more stringent than the current standard). These antennas could be placed relatively near demand points (Note the city in the background of Figure 1-2.)

Fig. 1-3 shows one of the concepts studied; a solar Brayton SPS. Four power generator modules feed the circular microwave transmitter. Each power module consists of a reflector which concentrates solar energy into a cavity absorber at the focal point. The resultant high temperatures are used to energize turbomachines which turn electrical generators. This option and the others studied are described in greater detail in Table 3-0.

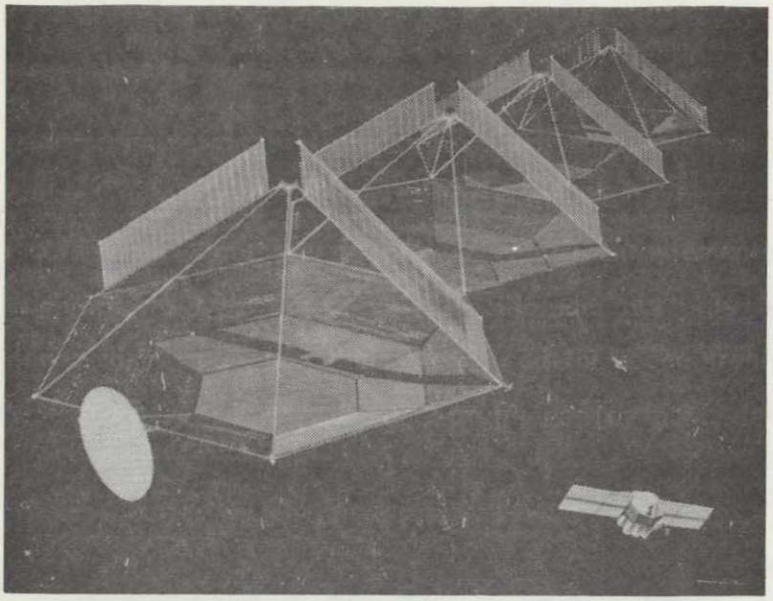

Figure 1-3 Solar Turbomachine Power Satellite Option

In this study the technical and economic practicality of these systems was investigated. While these systems produce large quantities of power (e.g., 10,000,000 kilowatts per satellite), the forecasted demands of the United States alone are sufficient to require a significant number of satellites. In the program baselined in this study, 62 satellites are made operational by the year 2011.

1.2.2 Auxiliary Systems

The criterion for optimization of these systems was minimum cost per kilowatt hour of energy produced (while maintaining set standards on factors such as environmental impact). To achieve low cost per kWhr, all significant elements of the program must also be appropriately low in cost. This includes not only the power generation and transmission systems, but also the systems used for space transportation and space assembly. These auxiliary systems were of necessity considered in this study although their investigation was not a primary goal.

2.0 PROGRAMMATICS

2.1 DERIVATION OF SATELLITE ENERGY SYSTEM PROGRAM DEFINITION

The methodology used to select the system size guidelines is as follows:

Background

Utilization of space-based power generation could conceivably occur as a legislated action, prompted by the resultant increase of national energy independency, reduced pollution, infinite source, etc. However, about three-fourths of our electric powe currently is produced by private utilities, suggesting that economics may be a majo factor influencing space-based power incorporation. Thus, market elasticity must be considered, i.e. sales will be influenced by the price of the product.

Many factors have contributed to the increases in installed capacity (kW) and consumption (kWh).

1. Population growth - from 1956 to 1973 the rate was 1.3% per year. The rate is predicted to decline to 0.8% in the 1973 to 1990 period. Resultant populations millions (1):

1964	192
1974	212
1984	231
1994	249

2. Rising standard of living - disposable income per person has been increasing; the trend is expected to continue (1):

Year	1974 $/year per person disposable income
1964	3248
1974	4592
1984	5677
1994	7071

3. Relative reduction in electricity cost - as pointed out by Hannon (2), the cost of electricity energy has reduced relative to labor costs (electricity does not strike for higher wages). It thus seems appropriate that about 40% of our national electricity use is for process heat and industrial power while only 9% goes for lighting (3). In the following plot (Figure 1) from (2) the ratio of manufacturing workers hourly wage to industrial kWh cost of electricity is represented as 1.0 in 1951 on the ratio index scale.

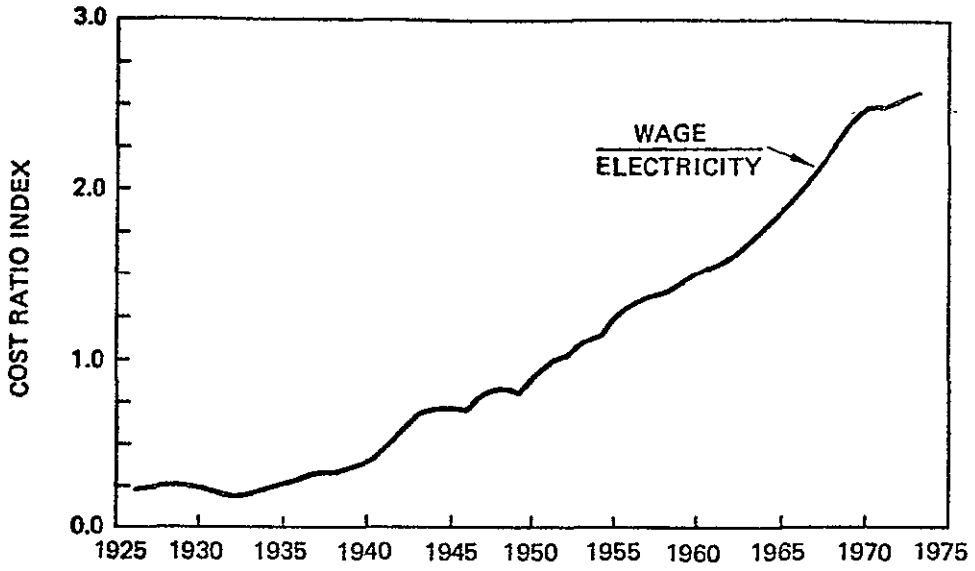

FIG. 2-1 ELECTRICITY/LABOR COST RATIO

Forecasts

Fig. 2-2 shows trends in national installed generating capacity. Note the difference between the 1973 and 1974 forecasts. It is significant that the 1973 article in (5) was titled "Utilities Plan Expansion to Meet Record Demands" and that the 1974 title in (1) was "Slower Growth In Sales and Peaks Sparks Sharp Cut in Expansion Plans and Cost."

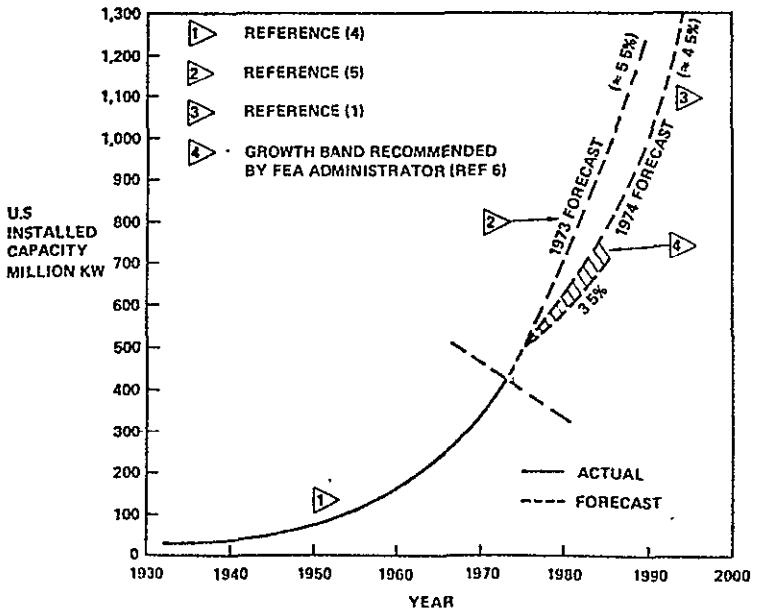

FIG. 2-2 GROWTH IN U.S. INSTALLED CAPACITY

An explanation for the change in forecast is given in (1): at the end of 1973 an increase of 33,100 MW in the summer peak requirement was forecast. An increase of 43,607 MW in capacity was planned for 1974 to meet this peak, retire some obsolescent units and raise the national reserve margin to 21%. However, energy conservation (partly from recession-caused production decreases) cut the load growth, to only 15,530 MW, resulting in a generating margin of 26.2%. Consequently, some of this margin can be applied to subsequent growth needs, depressing the growth curve. Fig. 2-3 shows variation of this margin with time. 18% is generally considered by utilities to be desirable; the margin was 16.6% in 1969 when reductions and curtailments occurred.

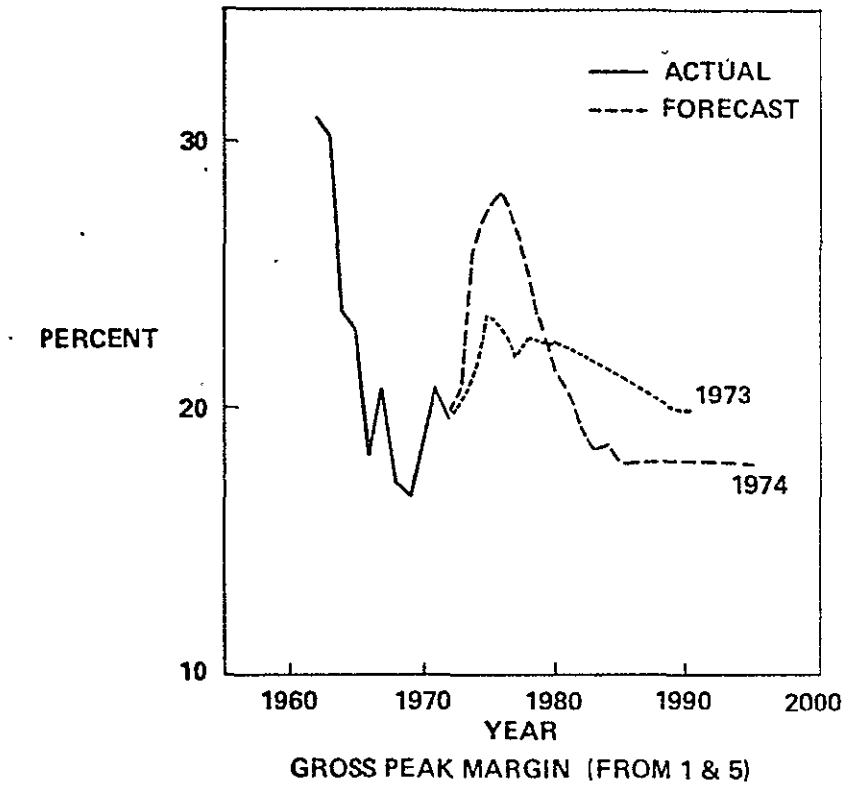

FIG.2-3 U.S. CAPACITY MARGIN

Some authors have forecast and/or recommended very low or even zero energy growth rate. Hannon (2) recommends a more labor intensive economy, i.e. one in which, in essence, human muscles perform rather than electric motors, thereby making more (lower paying) jobs. One factor is the growing labor pool resulting from population growth; if the birth rate instantly dropped to zero, the labor pool would still increase in size for two decades.

A more middle-of-the-road view is that energy growth is essential to economic health. Federal Energy Administrator Zarb has recommended a 3.5% to 4.5% installed capacity growth rate for 1975 to 1985 (6). This range was plotted in Figure 2-2.

It is possible for national energy consumption to remain constant while the amount of electricity generated increases. In 1968 the U.S. Energy Consumption was as shown in Table 2-1 (from 3).

TABLE 2-1 1968 U.S. ENERGY CONSUMPTION PATTERNS BY END USE

	Natural gas utilization by %	Oil utilization by %	Coal utilization by %	Electricity by %	% of total U.S. energy consumption	Potential electrical by %
Transportation					24.9	
Aircraft Vehicles	3.1	} 49.4				
Trains		2.1				
Ships		2.2		0.4		1.1
Chemical feedstock	2.3	10.2	1.1		5.5	
Process heat	40.7	9.7	37.3	2.5	26.2	26.2
Industrial power				37.2	7.9	7.9
Lighting				9.3	2.0	2.0
Miscellaneous					13.6	13.6
Household	7.0	0 8		16.9		
Commercial	3.3			23.1		
Industrial				7.1		
Space heating					19 9	19.9
Home	16.5	11.2		3.5		
Commercial	6.2	9.0	4.3			
Industrial	3.1	0.7	3.0			
Electricity gen	17.8	4.7	54.3	—	—	
Totals, %	100.0	100 0	100.0	100.0	100.0	
% of total U.S. consumption	26.5	42.1	10.1	21.2	—	70.7

In 1968, 21.2% of the energy expended went to produce electricity. The last column shows a potential of 70.7% utilization without significant changes in energy use technology; for example, electricity could be used for all process heat.

Current Predictions

Fig.2-4 shows historical (4) and forecasted (1 and 5) annual additions to U.S. installed capacity. Note that these are net additions after retirement of obsolete capacity. Actual sales are 1% to 2% greater. Again note the dramatic changes resulting from the capacity margin produced by reduced electricity consumption. The projected 1973 addition rate for the year 1990 was 64 GW (64000 MW); the 1974 projection is for 53 GW per year for 1990.

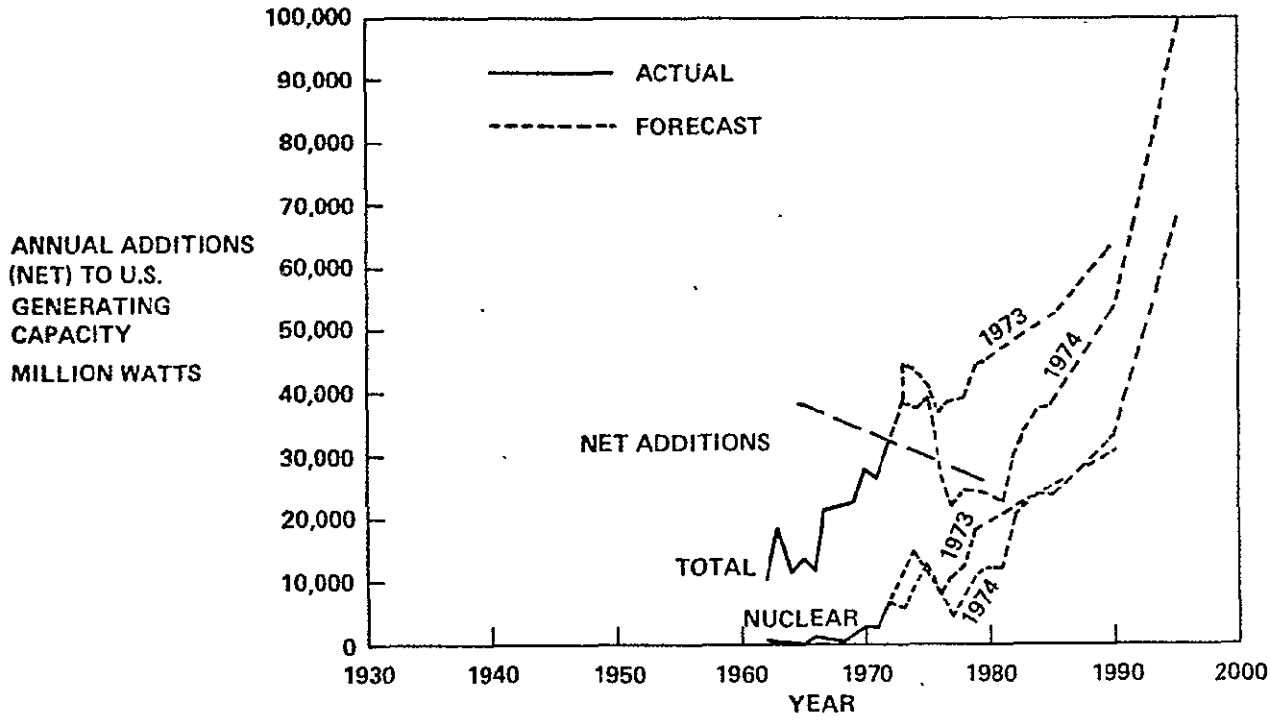

FIG.2-4 ANNUAL ADDITIONS TO INSTALLED CAPACITY

Figure 4 also shows the trend and forecast for the addition rate of nuclear-generated electricity. In 1973, nuclear provided 4.8% of our capacity. This was 16 years from the initial power reactor and nine years after the first "commercially competitive" reactor of 1964. In the 16 years from 1964 until 1980 nuclear energy is forecasted to grow to capture 13.6% of the electric power market. In another 15 years it will represent 30% of our capacity (but provide over 50% of the kWh) (1). It thus appears reasonable to assume early market capture rates of 15% for powersats (assuming equivalent economics). In England, nuclear capacity was added at approximately five times the percentage rate of the United States. Should superior

economics be achieved, i.e. very low costs for space based power, the capture rate could be even higher. Other factors could also accelerate space power incorporation, such as nuclear power moratoriums or legislation which levies the full "social" costs of fossil fuel usage on the electric power customer. The current social cost for the use of coal may be 13 to 15 mills/kWh (7). In consideration of this, it appears appropriate to also consider a high market capture rate of 30%. From these possibilities Table 2-2 is constructed.

TABLE 2-2 SPACE-BASED POWER ADDITION RATE

	Initial operation in 1990				Initial operation in 2000			
Capacity growth	U.S. capacity (gw)	Annual additions (gw/yr)	15% capture (gw/yr)	30% capture (gw/yr)	U.S. capacity (gw)	Annual additions (gw/yr)	15% capture (gw/yr)	30% capture (gw/yr)
"Low" (3.5% growth)	827	29	4.5	9	1,167	41	6	12
"Intermediate" (4.5% growth)	956	43	6	12	1,485	67	10.5	21
"High" (5.5% growth)	1,102	61	9	18	1,883	104	15	30

Based on a 1975 installed U.S. capacity of 494 gw

2.2 HIGH LEVEL PROGRAM REQUIREMENTS (SPACE-BASED POWER)

R1. Provide electric power for commercial utilization within the United States.

R2. Power output of the associated individual ground installations is baselined at 10 GW (10^{10} watts) each, 60 Hz.

R3. The power source (either solar or nuclear) for these ground stations shall be located in geostationary orbit, with power transfer by a microwave link.

R4. The associated programs shall be based on materials and technology concepts available for:

	Technology Availability (Demonstrated on sub-scale units)	First Unit Initial Operational Capability (IOC)
Program A	1985	1990
Program B	1995	2000

R5 The system concepts for these programs, including facilities, launch equipment, etc., shall provide for annual system additions over a range of rates:

	Low Rate (GW/year)	High Rate (GW/YEAR)
Program A	4.5	18
Program B	6.0	30

R6. Nominal life of the space power units and the ground receiving stations shall be 30 years, assuming appropriate maintenance.

R7. System safety is to be such that:

a) No failure mode shall cause non-program personnel to be exposed to microwave radiation flux greater than the current U.S. exposure standard of 10 mW/cm^2.

b) Public exposure to nuclear radiation from either system operation or failure (including reactor meltdown/vaporization/release) shall not exceed the current U.S. public exposure standard.

R8. The system optimization criterion shall be minimum cost per kilowatt hour; both recurring and non-recurring costs shall be recovered from operational revenues.

R9. Man will be utilized in space as required appropriate to the above minimum cost goal.

R10. Nuclear reactors shall be of the breeder type.

R11. In-space power conversion will be by thermionic diodes or closed Brayton cycle thermal engines, or a combination thereof.

ADDITIONAL PROGRAM REQUIREMENTS (PROVISIONAL REQUIREMENTS ESTABLISHED FOR THE CONVENIENCE OF THIS STUDY)

PR1. Microwave power transmission concepts, efficiencies, etc., shall be based on the Grumman/Raytheon studies (5,6).

PR2. Launch site will be the John F. Kennedy Space Center.

PR3. As a guideline, nuclear reactors will use the nation's UF_6 stockpile as a fuel source.

PR4. Radiator system meteoroid resistance capability shall be such as to provide a degradation of 30% or less of the total area when exposed to the environment as defined in (4), without repair or replacement of damaged panels, over a period of 30 years. This does not preclude such repair or replacement.

PR5. Program economics analyses shall be based on a 30-year investment horizon and an eight percent discount rate.

REFERENCES

1. Electrical World, September 15, 1974.

2. Hannon, B., "Energy Conservation and the Consumer," Science, 11 July, 1975 (Vol. 189, No. 4197)

3. Hauser, L. G., "Future Trends in Energy Supply," 1974 Textile Industry Conference.

4. Moody's Public Utility Manual, 1974.

5. Electrical World, September 15, 1973.

6. "World News Beat," Electrical World, July 1, 1975.

7. Morgan, M. G., Barkovich, B. R. and Meier, A. K., "The Social Costs of Producing Electric Power from Coal: A First Order Calculation," IEEE Proceedings, Vol. 61, No. 10, October 1973.

3.0 SYSTEMS STUDIED

Five power conversions systems were studied. All will be located in geostationary orbit. Three utilize solar energy; two use nuclear reactors. Two power conversion methods are baselined. The closed Brayton cycle system involves rotating machinery; the thermionic system is passive except for coolant pumps. The cascaded system employs thermionic diodes and the Brayton cycle in series, i.e., the diodes are cooled by the Brayton cycle, with each extracting a portion of the solar energy available.

A power relay system was also studied. This consists of a mirror in geostationary orbit which reflects sunlight to an area on the earth, potentially allowing night operation of ground solar power plants.

Table 3-0 lists the systems that were studied.

Table 3-0 Systems Studied

o Space-based power conversion systems:

Energy Source	Energy Converter
Solar	Thermionic . Direct radiation cooled . Liquid cooled
Solar	Closed Brayton cycle
Solar	Cascaded thermionic/closed Brayton cycle
Nuclear	Thermionic
Nuclear	Closed Brayton cycle

o Space-based power relay system:

Orbital solar mirror

3.1 SOLAR THERMIONIC, DIRECT RADIATION COOLED

In a thermionic diode, electrons are produced at the emitter (cathode) due to its elevated temperature, and travel to the lower temperature collector (anode). The

circuit is completed through the load. Several processes within the emitter-collector gap tend to reduce the efficiency of power generation from the applied thermal energy. For example, the electrons in the gap tend to repel those being produced at the emitter.

The diodes are mounted in the wall of the solar cavity absorber; the emitters are heated by the concentrated solar energy. By allowing the collectors to dissipate waste heat to space, the temperature differential required for operation is produced. Fins are added to the collectors to improve cooling.

Individual diodes have outputs of approximately 0.8 volts, and it is not practical (due to insulation breakdown) to use series strings to produce the 20,000 volts required by the transmitter. Therefore, rotary converters/transformers are used to step up the voltage. An AC to DC converter is used to provide the DC necessary to energize the transmitter.

The solar thermionic direct radiation cooled system is shown in Figure 3-1.

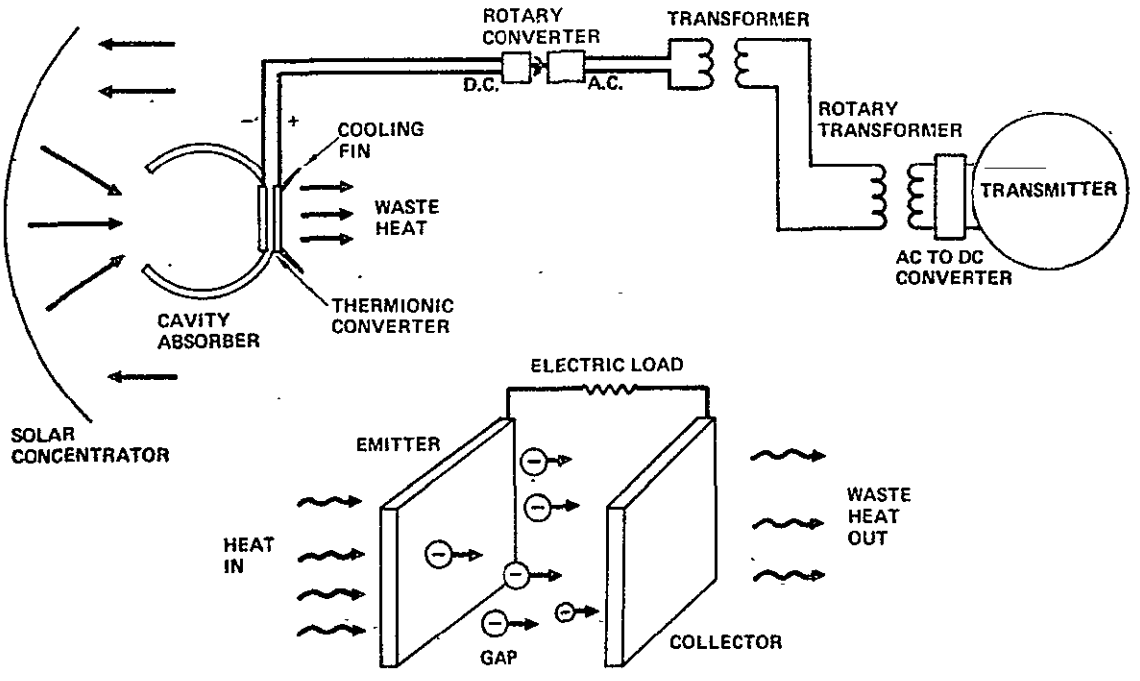

Figure 3-1 Solar Thermionic Direct Radiation Cooled System

3.2 SOLAR THERMIONIC, ACTIVELY COOLED

In this configuration a liquid metal cooling loop is used to remove waste heat from the diode collectors. In effect, the coolant loop couples the diodes to a greater radiating area than is practical for fins directly attached to the diodes, thereby producing a lower collector temperature, a greater temperature differential across the diode and greater electrical output. Thus the diodes are more efficient, so that fewer diodes are required; however, active cooling uses power drawn from the diodes and requires a liquid metal loop with thermal radiator.

Rotary converters/transformers are used to step-up the diode output voltage. An AC to DC converter is used to provide the DC necessary to energize the transmitter.

The solar thermionic, actively-cooled system is shown in Figure 3-2 .

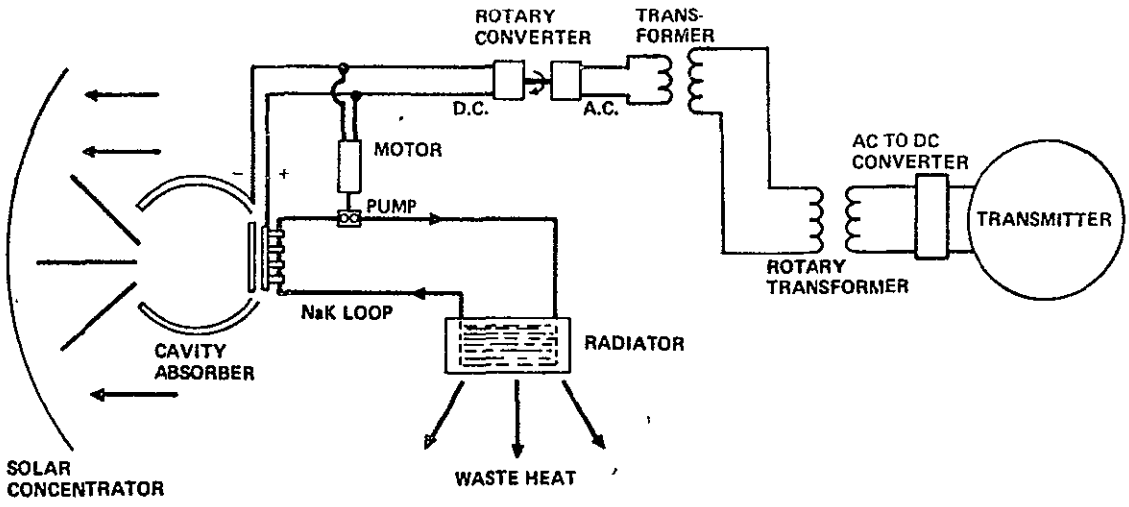

Figure 3-2 Solar Thermionic, Actively-Cooled System

3.3 SOLAR BRAYTON CYCLE

The Brayton cycle turbomachine provides a rotating shaft output which drives the generators. Thermal energy is added to the helium working fluid in heat exchanger tubing located within the cavity absorber. The hot gas is expanded through the turbine, providing power to turn both the compressor and generator. The recuperator exchanges energy across the loop to increase the system efficiency. Waste heat is rejected through a gas-to-liquid heat exchanger to a liquid metal cooling loop; the liquid metal pumps use power drawn from the generators.

The 60,000 volt AC output of the generators is stepped-up to 382,000 volts in transformers; this high voltage facilitates on-board distribution. Step-down occurs in the rotary transformers. An AC to DC converter is used to provide the DC required to energize the transmitter.

The solar Brayton cycle system is shown in Figure 3-3.

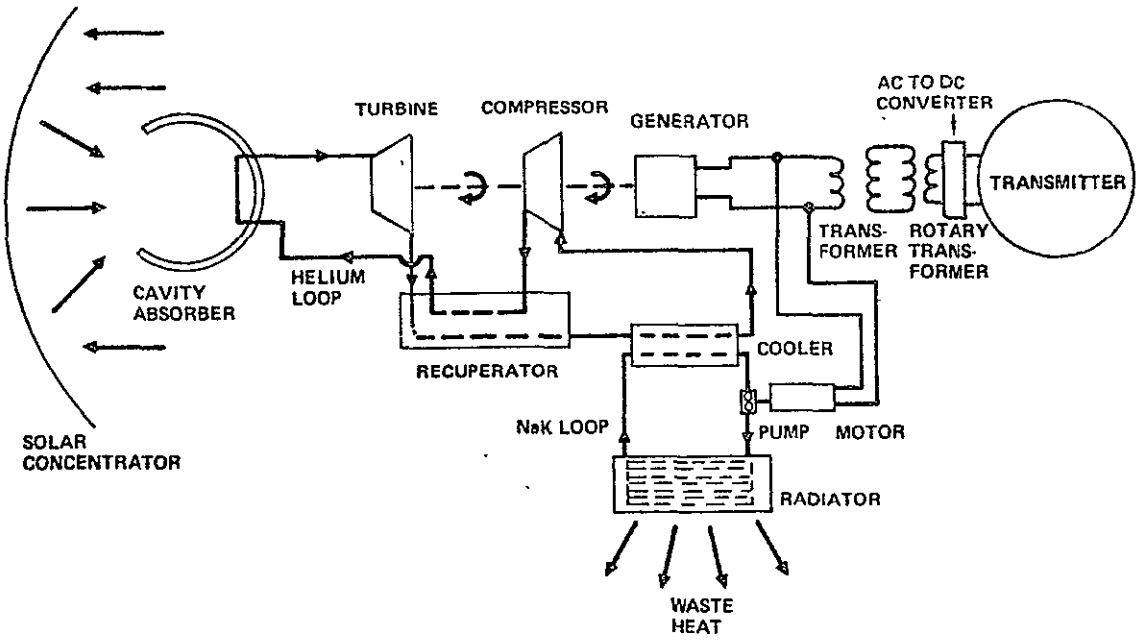

Figure 3-3 Solar Brayton Cycle System

3.4 SOLAR THERMIONIC/BRAYTON CYCLE

This "cascaded" system offers potentially high efficiency. All waste heat from the thermionic diodes is available to the Brayton cycle; the diodes are cooled by the helium flow in the Brayton loop. The Brayton loop is cooled by a liquid metal radiator.

The DC output of the diodes is stepped-up to 50,000 volts AC in the rotary converters/transformers; the turbomachine generators produce 50,000 volts AC which is combined with the output of the rotary converters/ transformers. An AC to DC converter is used to provide the DC required to energize the transmitter.

The cascaded solar thermionic/Brayton cycle system is shown in Figure 3-4.

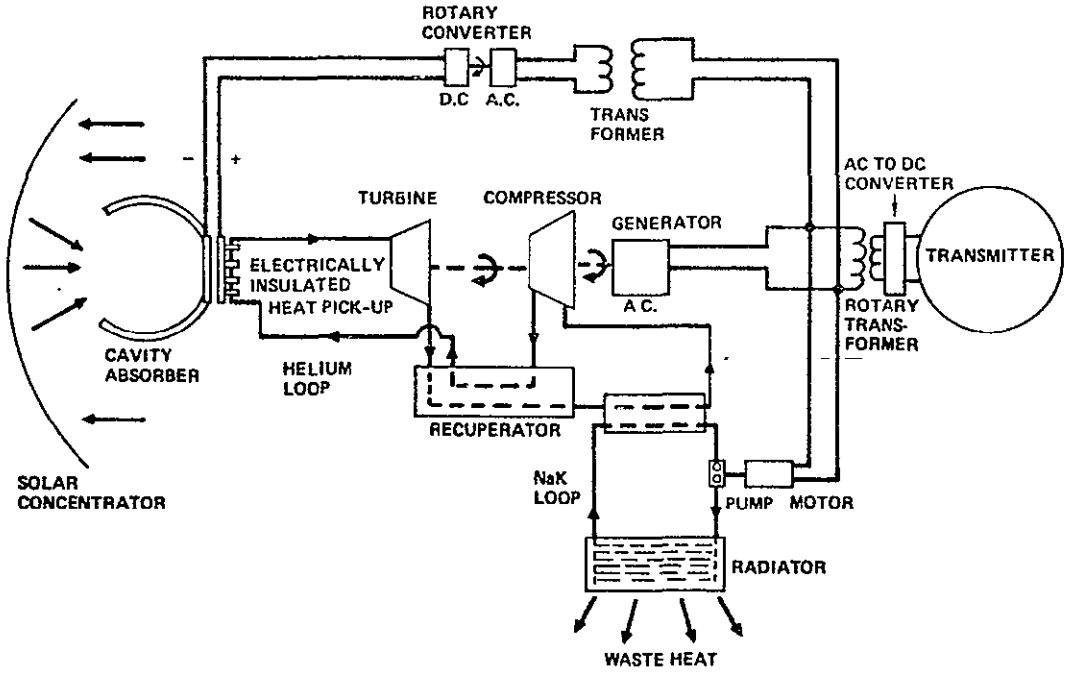

Figure 3-4 Cascaded Solar Thermionic/Brayton Cycle System

3.5 NUCLEAR THERMIONIC

The energy source in this system is nuclear; a molten salt breeder reactor (MSBR) is used. The salt mixture contains both fissile fuel, the energy source, and fertile fuel, which breeds to become fuel for subsequent use. The salt mixture is circulated out of the reactor core through a heat exchanger which transfers energy to a sodium loop. The sodium loop is used since there is insufficient salt flow for the diode emitter area.

A small secondary salt flow is continuously passed through a fuel process system. This system removes the protactinium and wastes which would "poison" the reactor by excessive neutron capture. The fuel process system introduces fertile fuel and removes bred fuel. The MSBR is an unique breeder concept in that a single liquid fuel mixture contains both fissile and fertile fuels, and that processing of solid fuel elements is not required.

The diode collectors are cooled by a liquid metal radiator loop. The low voltage DC output of the collectors is stepped-up and converted to AC by rotary converters/ transformers. An AC to DC converter is used to provide the DC necessary to energize the transmitter.

The nuclear thermionic system is shown in Figure 3-5.

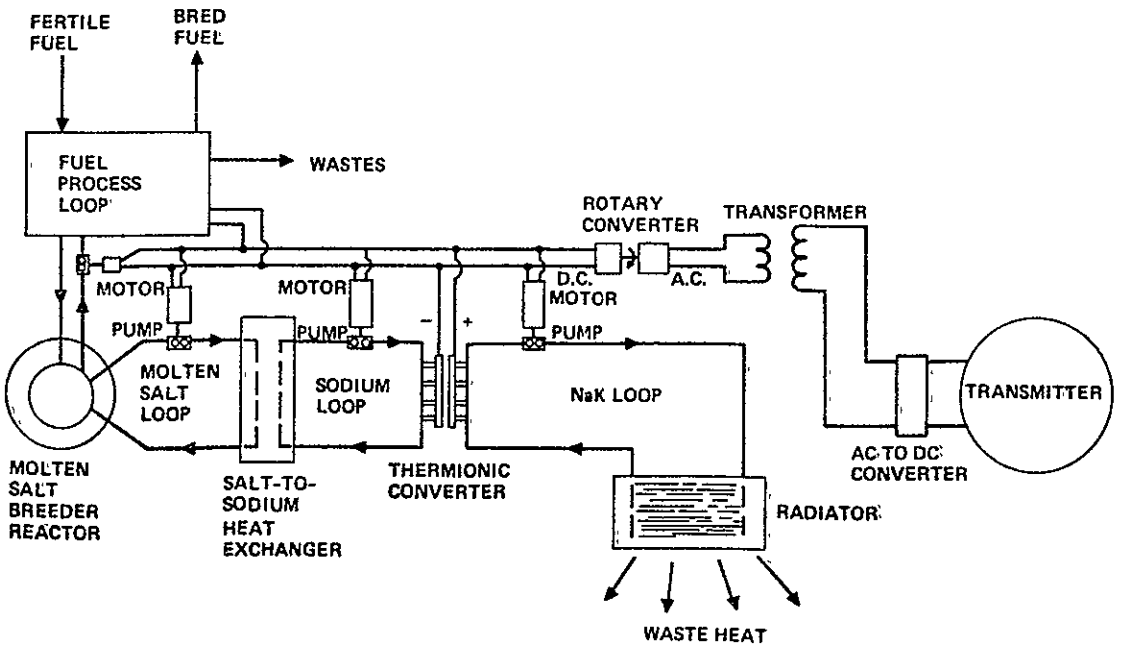

Figure 3-5 Nuclear Thermionic System

3.6 NUCLEAR BRAYTON CYCLE

The energy source in this system is nuclear; a molten salt breeder reactor (MSBR) is used. The salt mixture contains both fissile fuel, the energy source, and fertile fuel, which breeds to beome fuel for subsequent use. The salt mixture is circulated out of the reactor core through a heat exchanger which transfers energy to the helium loop of the Brayton turbomachines.

A small secondary salt flow is continuously passed through a fuel process system. This system removes the protactinium and wastes which would "poison" the reactor by excessive neutron capture. The fuel process system introduces fertile fuel and removes bred fuel. The MSBR is an unique breeder concept in that a single fuel mixture contains both fissile and fertile fuels, and that processing of solid fuel elements is not required.

The Brayton cycle turbomachine provides a rotating shaft output which drives the generators. Hot helium is expanded through the gas turbine, providing power to drive both the compressors and generators. The recuperator exchanges energy across the loop to increase efficiency. Waste heat is rejected through a gas-to-liquid heat exchanger to a liquid metal cooling loop; the liquid metal pumps use power drawn from the generators.

The 60,000 volt AC output of the generators is stepped-up to 382,000 volts in transformers; this high voltage facilitates on-board distribution. Step-down occurs in the rotary transformers. An AC to DC converter is used to provide the DC required to energize the transmitter.

The nuclear Brayton cycle system is shown in Figure 3-6.

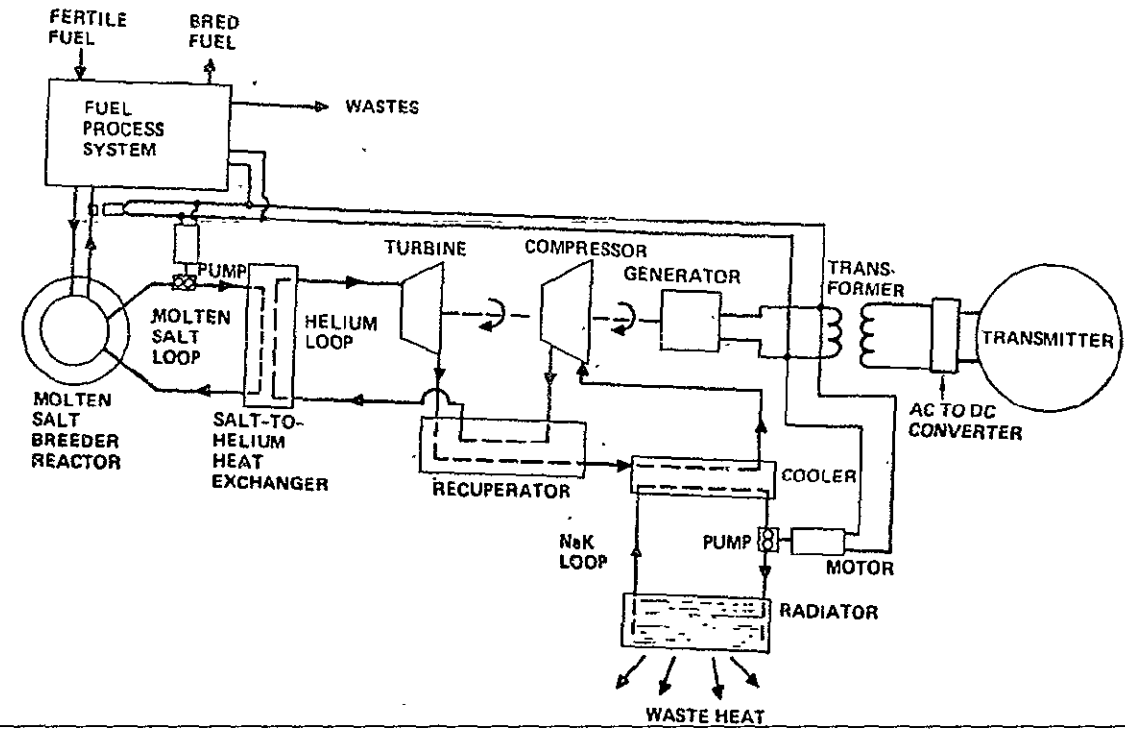

Figure 3-6. Nuclear Brayton Cycle System

4.0 SUBSYSTEMS

4.1 MATERIALS

Many of the material requirements of the SPS will be satisfied by the use of aluminum, magnesium and titanium alloys. However, some subsystems contain components which operate at elevated temperatures. Selection of alloys for these SPS applications is based on the temperature range involved, as shown in Figure 4-1. The tungsten/rhenium and tantalum alloys are less well defined than the columbium and cobalt alloys.

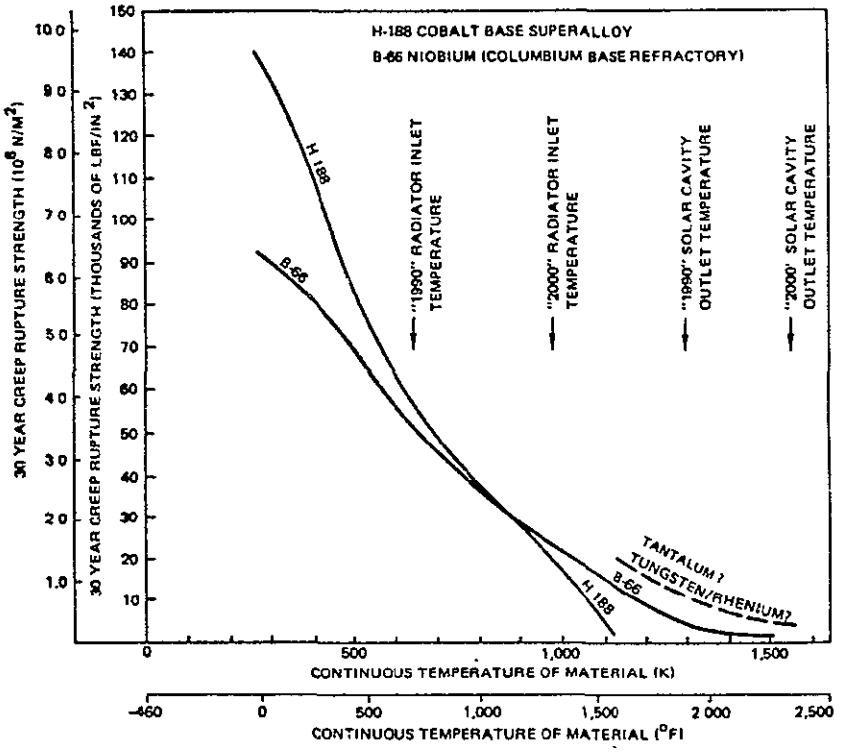

Figure 4-1 Material Selection

The materials identified will be used for heat exchanger tubing (e.g., within solar cavity absorbers) and for manifolds, etc, in the radiator systems.

Note that the material strength shown in Figure 4-1 is the predicted 30-year creep rupture strength. Many SPS subsystems require long term confinement of pressurized

gases or liquid at high temperatures, thus a fundamental problem is the long-term creep rupture at high temperatures.

Table 4-1 shows additional considerations in material selection, and alloys considered as options.

Table 4-1 Material Considerations

DESIGN REQUIREMENT	IMPORTANT MATERIAL CHARACTERISTICS
SERVICE TEMPERATURE AND PRESSURE	• STRESS-RUPTURE STRENGTH
SERVICE LIFE	• METALLURGICAL STABILITY • SUBLIMATION EFFECTS ON STRESS-RUPTURE STRENGTH
SYSTEM SIZE	FABRICABILITY
ECONOMICS	• DENSITY • CHEMICAL COMPOSITION (COST & CRITICAL/STRATEGIC METAL CONTENT)

ALLOY SYSTEMS

STAINLESS STEEL
- AISI 316
- AISI 347

NICKEL BASE SUPERALLOYS
- INCONEL
- HASTELLOY X
- INCONEL X
- INCONEL 617

COBALT BASE SUPERALLOYS
- HS-25
- HA-188

REFRACTORY ALLOYS
- COLUMBIUM BASE – B-66

IRON BASE (HI TEMP)
- 19-9 DL
- A-286

A trend of improvement of alloys for service above 1000K (1340°F) is shown in Figure 4-2. Iron, cobalt, columbium and nickel base systems were compared. A number of alloys having good strength properties were not considered due to their poc fabrication capabilities. While strength rupture capabilities of the nickel and cobalt base alloys have shown only a modest advance in the past 25 years, significant improvements in thermal fatigue, oxidation resistance, and stability characteristics have been achieved.

CONCLUSIONS:

1. Little or no improvement trend in the cobalt base alloys.
2. Nickel base alloys have been improving at the rate of approximately 3.4K (6.2°F) per year.
3. Introduction of a new alloy type, e.g., columbium-based B-66, can cause the most dramatic increase.

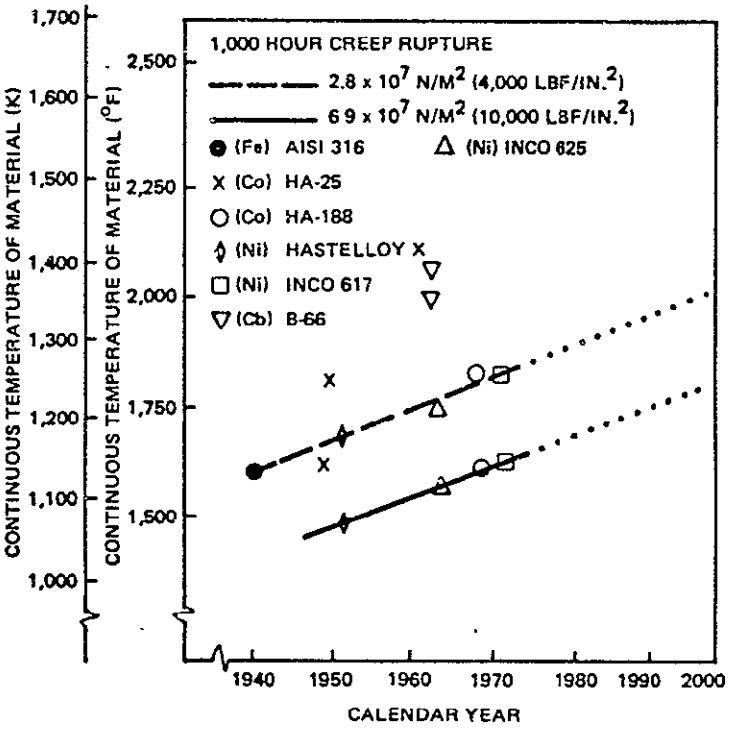

Figure 4-2 MATERIAL TECHNOLOGY TREND

4.2 SOLAR CONCENTRATOR

The solar power generating systems require large solar concentrators with low mass per unit area. Concentration ratios of one thousand or more are required. Highest optical efficiency would be obtained with a rigid paraboloid; yet the structure required to provide accurate form despite thermal and gravity loads, aging and assembly inaccuracies is estimated to have a mass of at least 2.0 kg/m^2 (0.41 lbm/ft^2). The baselined concentrator consists of a large number of individually steerable plastic film mirrors mounted on a relatively light framework. Active mirror control maintains focusing despite the disturbing forces mentioned above. Total concentrator mass for this type of system is estimated to be 0.29 kg/m^2 (0.059 lbm/ft^2). A 20 percent contingency is included in this estimate.

The faceted concentrator is shown in Figure 4-3.

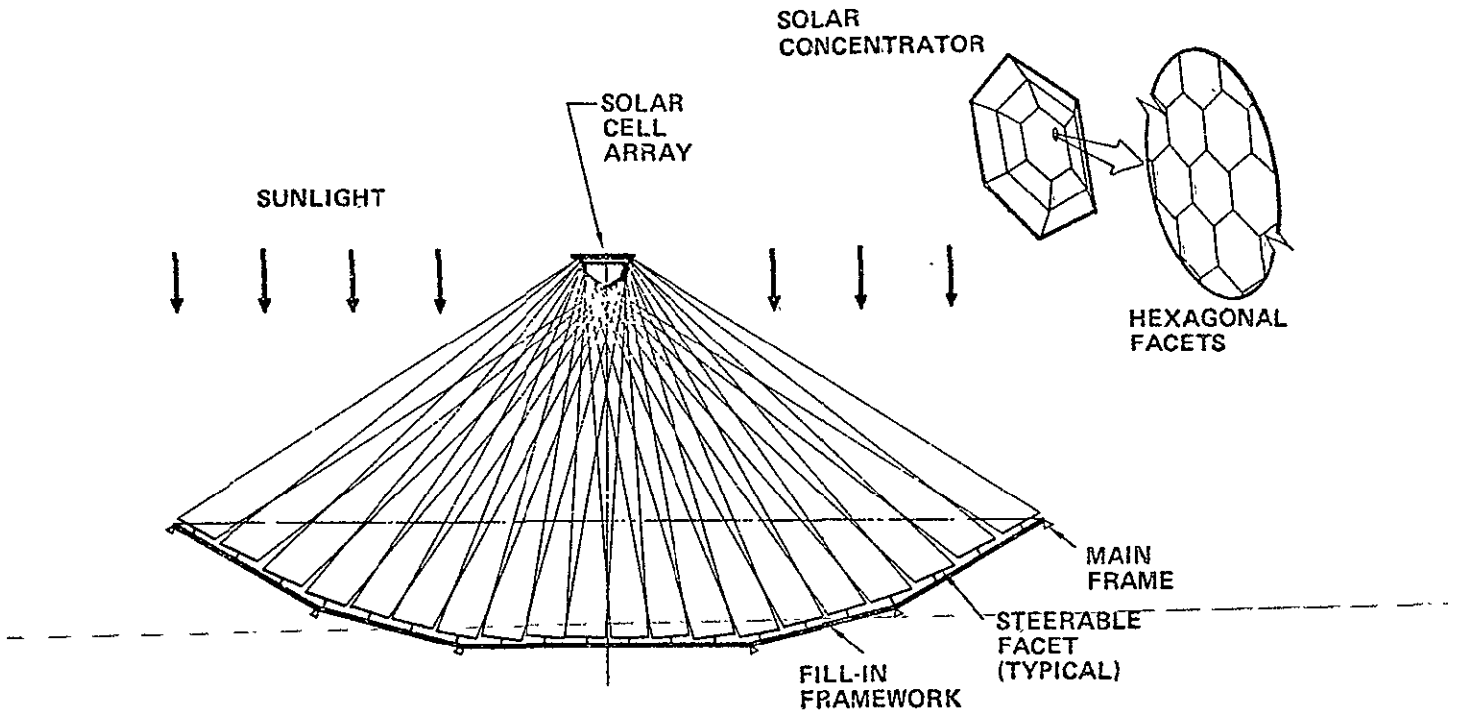

Figure 4-3 Faceted Concentrator
(Individual Steerable Facets Direct Solar
Impages into Cavity Absorber)

Figure 4-4 shows a typical reflective facet. Metallized plastic film (baseline is aluminized Kapton) is tensioned to form a plane surface. The support system consists of three edge members with bridles tensioned by springs. The inherent action of this system causes the three edge members to be co-planar. Each reflector facet is fitted with a two axis servo drive which causes the sunlight reflected by the facet to enter the aperture of the cavity absorber.

The number of facets used influences the achievable solar concentration. The most efficient concentrator would of course be a paraboloid, consisting, in effect, of an infinite number of very small reflectors. With reflectors of a finite size the image of each reflector also increases in size. Since the sun has an apparent width of 0.53°, the light reflected by the facets must spread at least at this angle. A total angle of one degree was used in this analysis. Perfect reflectivity was assumed.

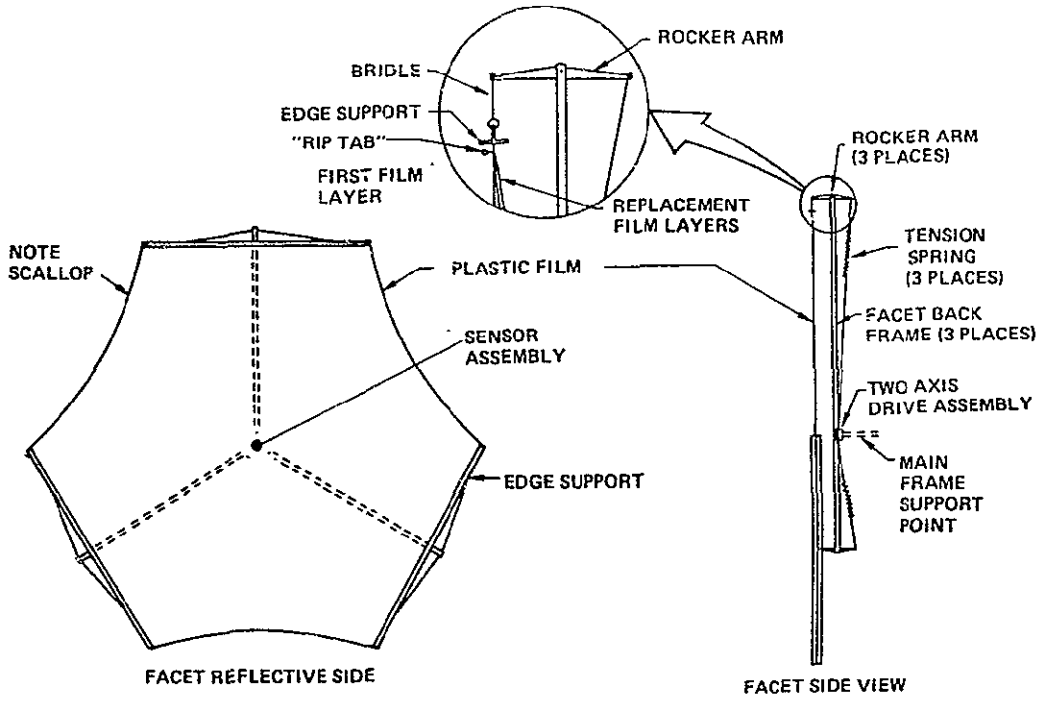

Figure 4-4 Typical Reflective Facet

Figure 4-5 shows the actual concentration of solar energy achieved for various numbers of facets and geometric concentration ratios. It was developed by dividing a paraboloid into five zones and then taking the performance of facets in the center of each zone.

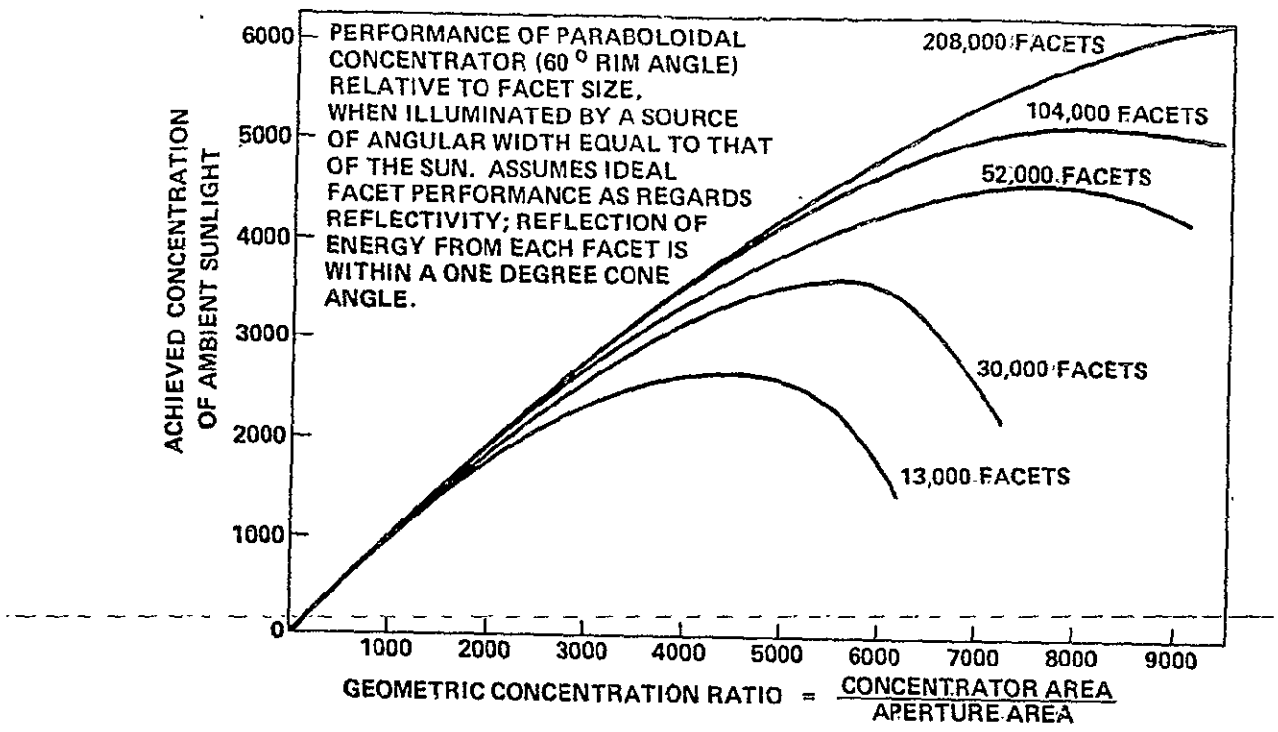

Figure 4-5 Number of Facets Used Influences Achievable Solar Concentration

Solar Reflector Susceptibility to Degradation in the Geosynchronous Environment

Damage to the solar concentrators by meteoroid particles has been assessed. The optical characteristics of the concentrators will be impaired by the scouring effect of small particles and by penetration of larger particles. All particles striking the concentrators will damage an area far greater than the cross section of the particle. The damage will consist of penetration, cratering and spallation. For the purpose of this assessment the particle specific gravity was assumed to be 0.05, and the diameter of the area damaged to be twenty times the particle diameter. This latter figure may appear conservative but spall zones of this ratio of damage to particle diameter were encountered on the Apollo windows (2). Although there is a difference in materials, it is possible that the material chosen for the concentrators may become embrittled with age and suffer a similar type of damage to the Apollo windows.

To estimate the damage rate the omnidirectional meteoroid flux model given in (3) was used. The model provides the cumulative flux corresponding to meteoroid mass, which was reduced to yield a total damaged area per unit area and time, using the criteria given previously. The estimated damage is 2.05×10^{-6} meter^2 per meter^2-day (2.05×10^{-6} foot^2 per foot^2-day).

This is a maximum figure since it assumes no two hits in the same place. Since this represents only 2.25% area damage in 30 years, meteoroids appear to pose no threat to the optical qualities of the solar concentrator.

However, the specular reflectance of metallized films may be significantly degraded by the proton flux. A possible explanation for this damage may be as follows: low energy protons are stopped within the metal layer and form hydrogen after gathering an electron. Hydrogen accumulation causes small "bubbles" to form in the metal, so that the surface is no longer planar. Some tests at relatively high exposure rates (to shorten the test period) were run by Boeing in connection with project ABLE (orbital reflectors for ground illumination). At a flux corresponding to 900 times the geosynchronous proton flux, reflectivity decreased to only 0.59 from an original value of 0.92 in a period of 3.25 days, which may correspond to only eight years of orbital exposure (4). There was some indication of a dose rate effect, so that the actual correspondence period may be much longer. However, it is evident that radiation damage may be quite severe for conventional metallized films.

In the SPS, large electric currents have to be carried considerable distances. In order to minimize mass, members carrying these currents must also be primary structure and carry physical loads. Typical of these members are the truss beams connecting the solar concentrators to the solar absorbers. Ideal cross sections were derived to provide a minimum sum of beam mass and generator penalty.

A family of curves were derived for beams configured as shown in Figure 4-6. The spacing between tubes, the tube diameters and thicknesses was varied, and mass per beam length plotted against beam length for a given load. The dotted line is an estimate of the locus of minimum mass. However, since the tubes of the beam are designed to carry current and heat loss (I^2R) has to be dissipated, there is a minimum cross section of the beam capable of carrying both the current and the applied load. This is indicated in Figure 4-6 for a typical SPS truss.

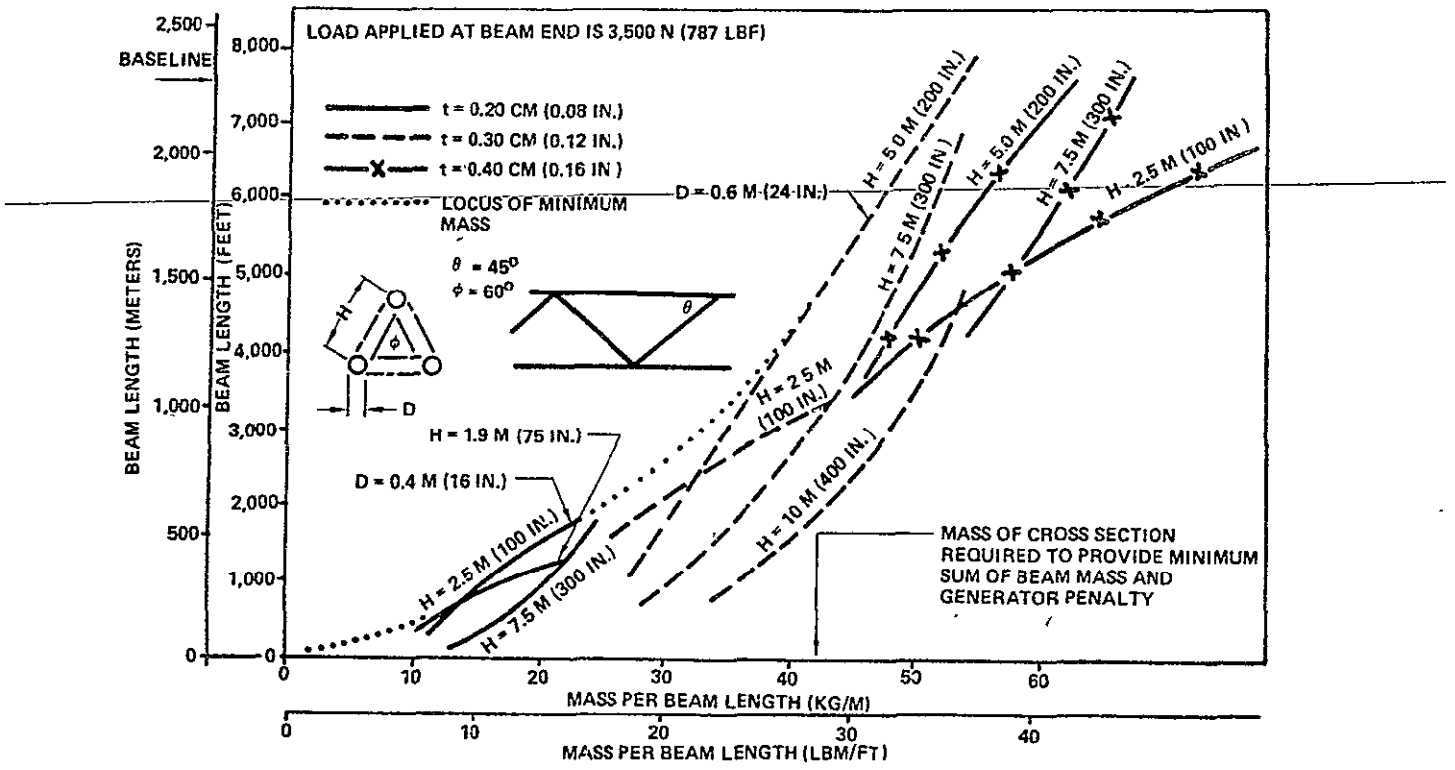

Figure 4-6 Derivation of Ideal Beam Dimensions

Typical primary structure (trusses) of the SPS consists of three tubes equispaced as shown in Figure 4-7 . The tubes are supported by diagonals which are hinged together. Since the tubes carry the primary satellite power the diagonals are insulated as shown. Prior to assembly in low earth orbit the diagonals are folded together tightly. On assembly the diagonals are unfolded and tubes 25.4M (83.3 ft.) long are inserted into the clamps at the ends of the diagonals. The sections of tube are welded together and to the clamps where they butt, and the snatch clamps are secured to the tubes.

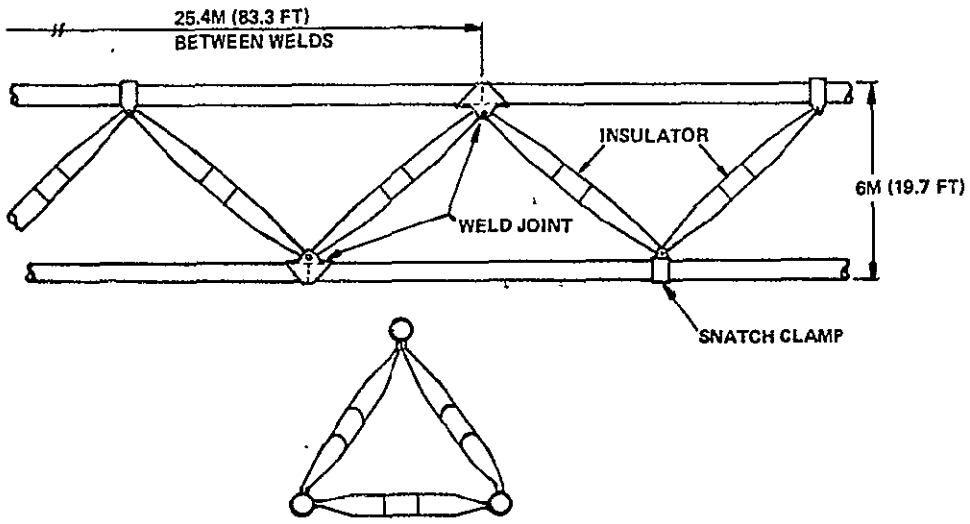

Figure 4-7 Typical Power Satellite Primary Structure (Conducting)

4.3 CAVITY SOLAR ABSORBER

Solar heat flux from the solar concentrator is reflected into the cavity absorber. The cavity is a spherical structure with an aperture for receiving solar radiation as shown by Figure 4-8.

Solar energy flux into a cavity absorber is for the most part absorbed into the walls. This is because multiple reflections must in general take place before reflection back ou of the aperture can occur. Once absorbed, the energy is available for removal by the energy converter (Brayton cycle or thermionics). The hot walls radiate thermal energy

back and forth between them; some of this energy escapes through the aperture. Insulation and a low emissivity exterior coating are used to limit energy loss through the walls.

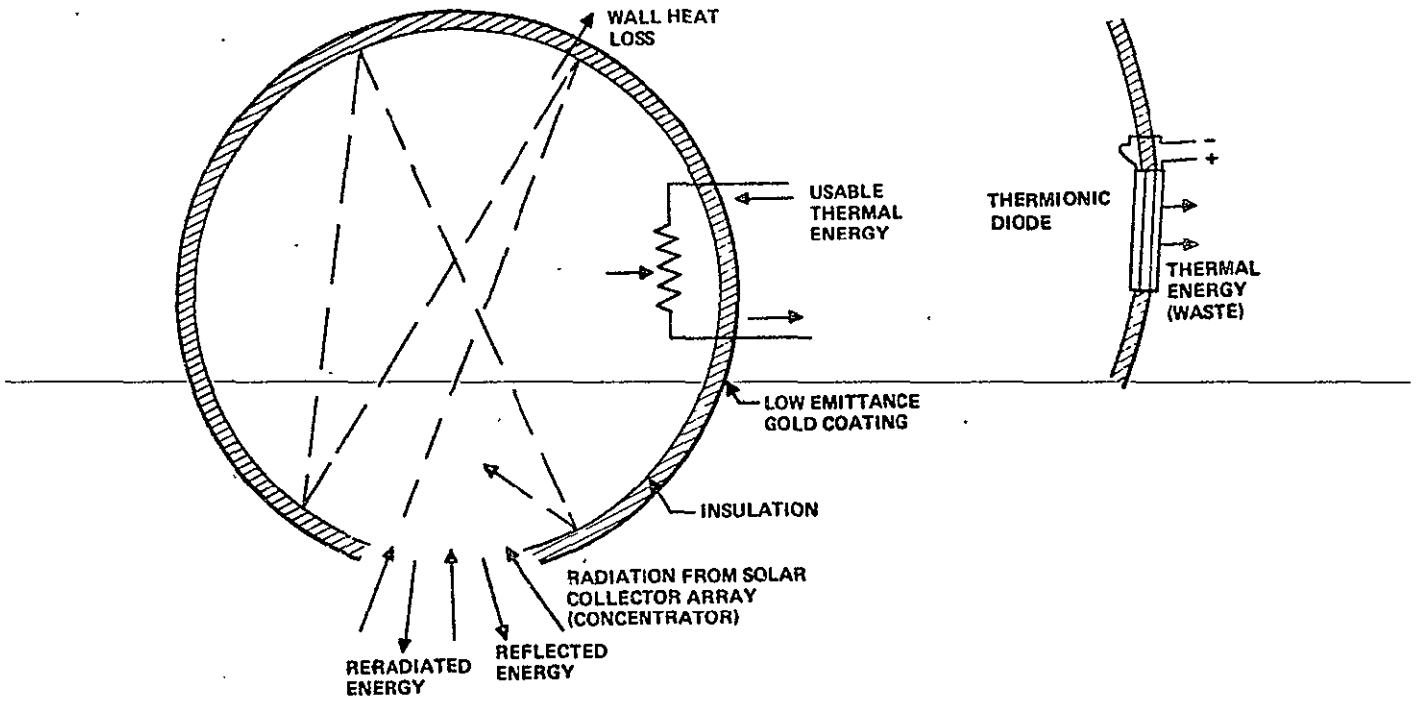

Figure 4-8 Cavity Solar Absorber

Heat loss through the aperture is comprised of reflected heat energy and reradiated energy Figure 4-9 shows the effect of the wall area-to-aperture ratio on reflection out of the aperture. It is based on the analysis of Stephens and Haire. (Reference 1)

Reference 1 - Stephens, C. W., and Haire, A. M., "Internal Design Consideration for Cavity-Type Solar Absorbers," ARS Journal, July 1961, pp. 896-901.

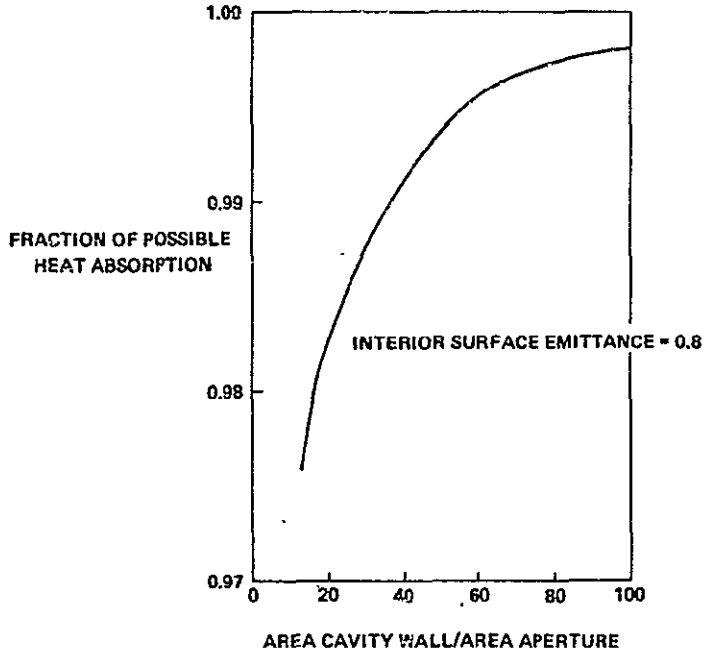

Figure 4-9 Cavity Solar Heat Absorption

Thermal energy loss by radiation is influenced by the emissivity of the surface and the fourth power of its absolute temperature. Thermal engine efficiency requires high cavity temperatures, therefore reradiation must be controlled if cavity efficiency is to be high. The chart shows the effect of wall area-to-aperture ratio; it is based on the analysis of Stephens and Haire (Reference 1). The fraction of heat absorbed lost by reradiation is the ratio of loss from the cavity to the loss which would occur from an equivalent flat plate area. The loss by reradiation as a function of cavity inner wall area to aperture area ratio is shown by Figure 4-10.

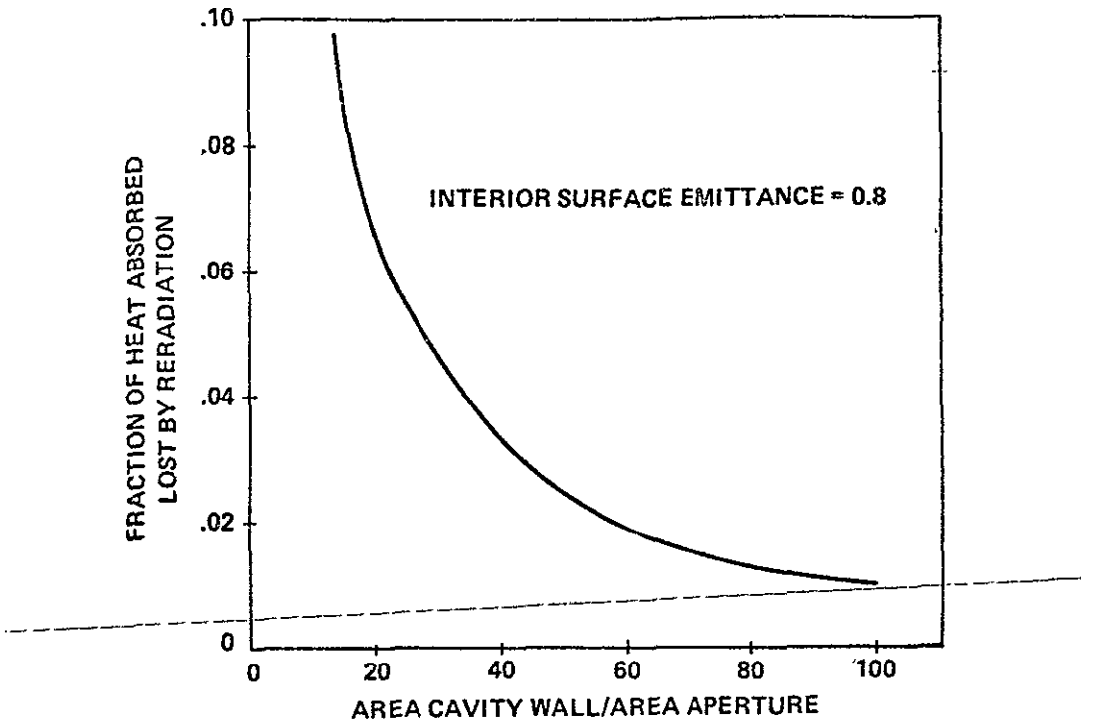

Figure 4-10 Cavity Heat Loss by Reradiation

All energy passing through the walls must eventually be reradiated from the cavity exterior. Therefore, a low emissivity coating (gold is baselined) is used. To provide a low exterior temperature, thermal insulation is provided. Alumina-silica fiber, 128 kg/m^3 (8 lb/ft^3) density, is baselined. Multi-layer high temperature insulation may provide higher performance; however, good data was not available. Figure 4-11 shows how the insulation mass per unit wall area influences reradiation.

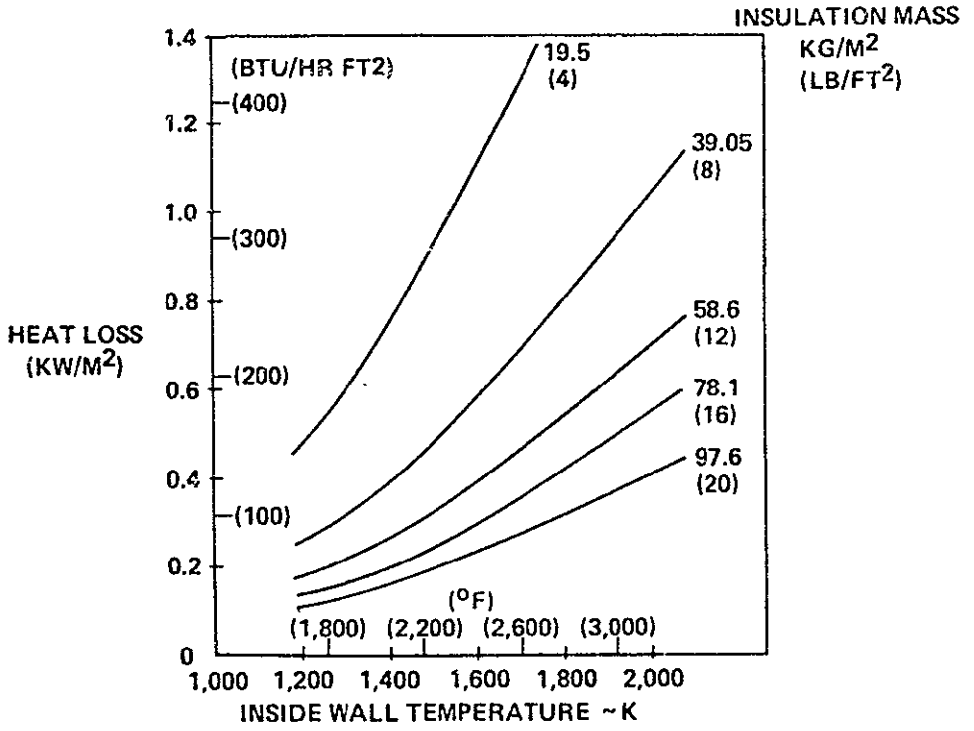

Figure 4-11 Cavity Condution Heat Loss

Cavity Heat Exchanger

The cavity heat exchanger is comprised of banks of circular tubes spaced near the interior walls of the cavity solar energy collector. Solar energy impinges on the interior wall of the spherical cavity heating it to a high temperature. The wall radiates to the tube banks through which a Helium-Xenon gas mixture is circulated. The cavity heat exchanger parameters shown in Figure 4-12 are input as tables for computer modeling of the various systems utilizing the Brayton cycle.

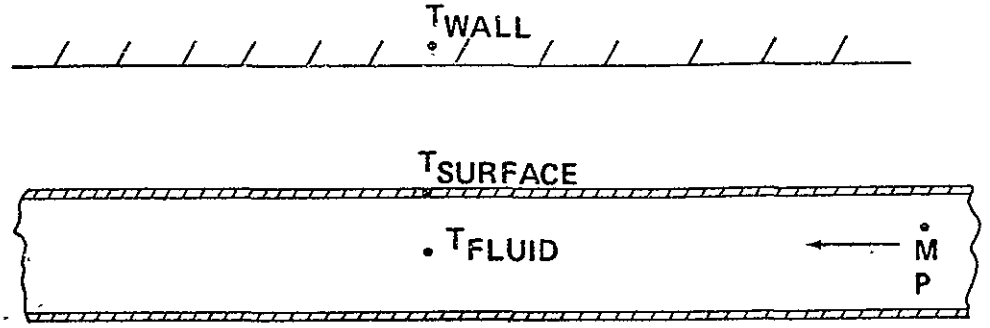

Independent variables	Dependent variables
Cavity wall temperature	Pressure drop per unit length
Fluid temperature	Tube weight per unit length
Fluid flow rate	Tube-wall-temperature
Fluid pressure	Heat input per unit length
Tube wall allowable stress	
Fluid properties	

Assumed tube diameter 12.5 mm (I.D.) (0.492 inch)

Figure 4-12 Cavity Heat Exchanger

The heat input to the Brayton cycle Helium-Xenon gas mixture (molecular weight = 8) is determined by the effective cavity wall temperature, radiation exchange factor, and convective film coefficient to the flowing gas. A radiation exchange factor of 0.9 was assumed which can be updated when a more detailed design configuration has been established. The internal heat transfer coefficient was calculated, allowing for the variation of fluid properties with pressure and temperature, assuming full developed turbulent flow in circular tubes.

The curves shown in Figure 4-13 are for a cavity wall temperature of 1800K (2780°F). Similar data were calculated for wall temperatures ranging from 1200K (1700°F) to 2100K (3320°F).

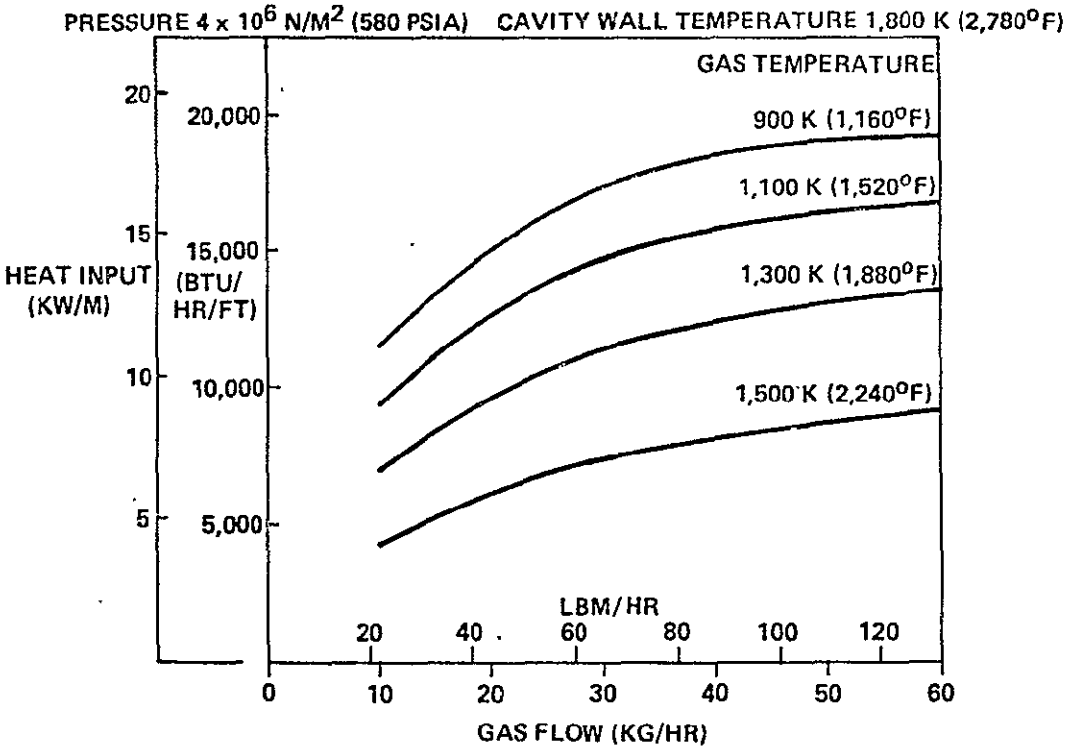

Figure 4-13 Cavity Heat Exchanger Heat Input

Figure 4-14 shows pressure drop per unit length as a function of a Helium-Xenon gas flow rate and mean gas temperature. The analysis was based on fully developed turbulent flow in circular, smooth wall tubes allowing for variation in friction factor with Reynolds number.

The curves shown are for a gas pressure of 4,000,000 N/M^2 (580 PSIA). Similar data were calculated for pressures ranging from 3,000,000 N/M^2 (290 PSIA) to 8,000,000 N/M^2 (1160 PSIA).

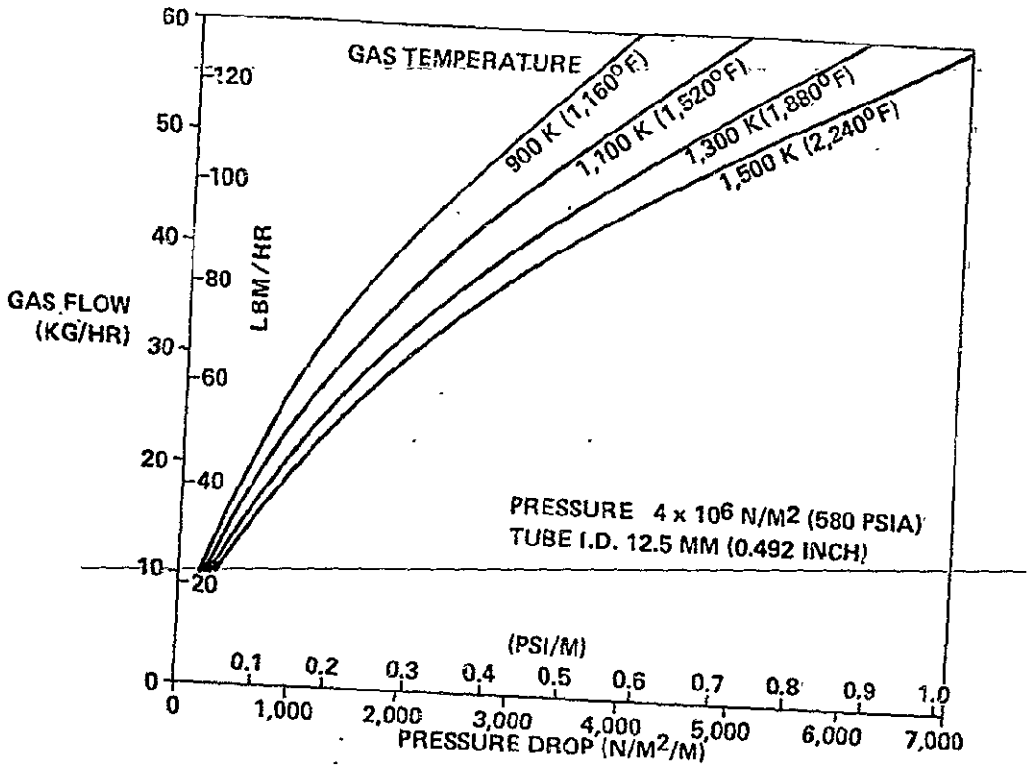

Figure 4-14 Cavity Heat Exchanger Pressure Drop

To determine the tube mass per unit length, it is necessary to calculate the tube wall temperature which influences the tube material allowable stress and required wall thickness. The wall temperature is calculated from a thermal balance of energy received by thermal radiation to the outer tube surface and energy removed by convective heat transfer to the Helium-Xenon gas mixture flowing through the tubes.

Figure 4-15 shows tube wall temperatures for a cavity wall temperature of 1800K (2870°F). Similar data were calculated for wall temperatures ranging from 1200K (1700°F) to 2100K (3320°F).

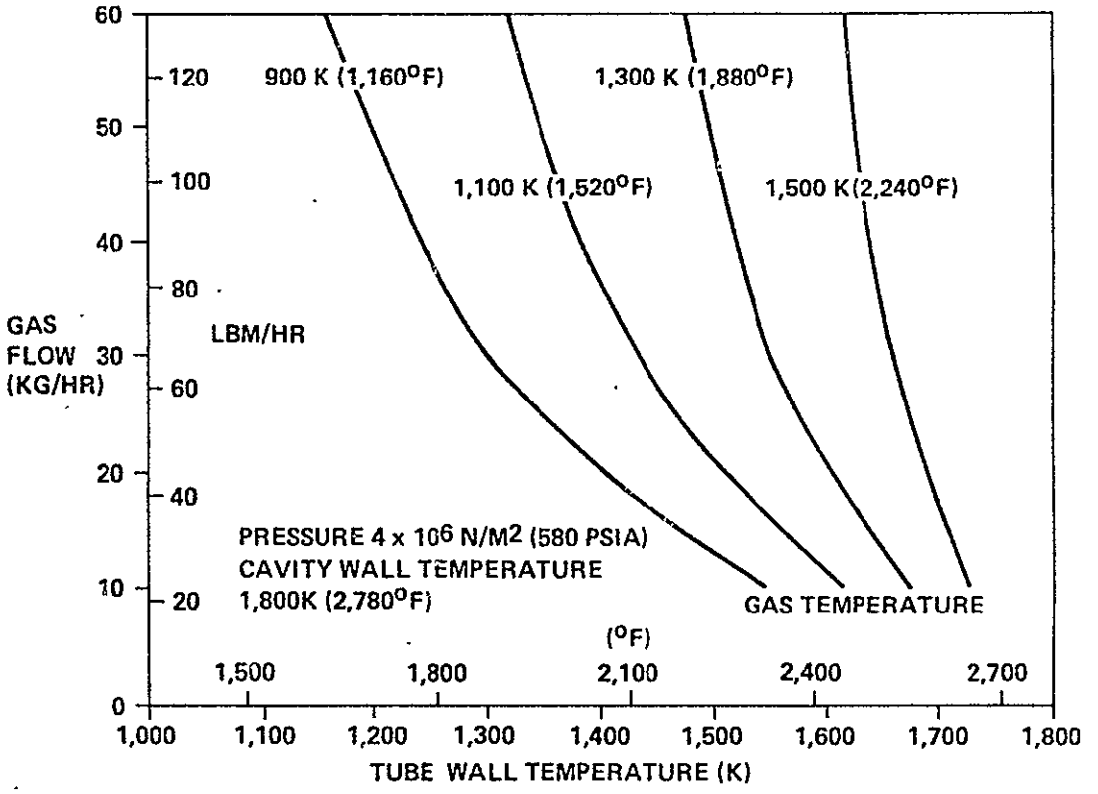

Figure 4-15 Cavity Heat Exchanger Tube Wall Temperature

The tube mass per unit length shown by Figure 4-16 is a function of the tube material properties, internal fluid pressure and tube wall temperature. An internal tube diameter of 12.5 MM (0.492 inch) was assumed to calculate wall thickness and resulting tube mass.

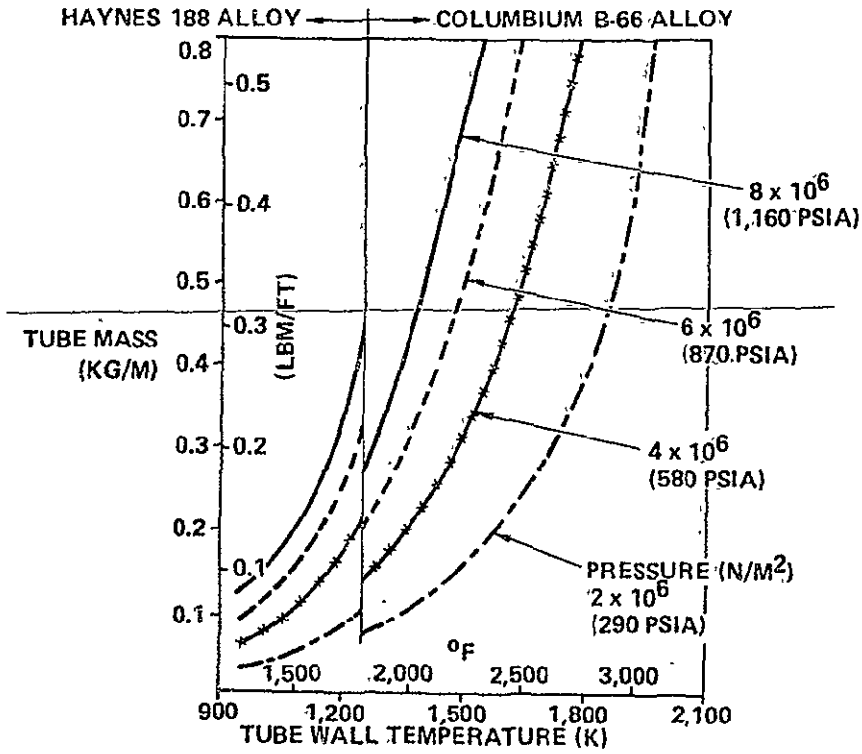

Figure 4-16 Cavity Heat Exchanger Tube Mass

4.4 BRAYTON CYCLE TURBINE PARAMETRIC DESIGN STUDY

A parametric design study of the Brayton cycle turbine has been performed. The study approach consisted of initially defining a baseline system about the Boeing selected turbine inlet temperature (T_3 = 1300K) and cycle temperature ratio (T_0/T_3 = 0.35). This baseline system included a recuperature and gas-to-NaK cooler contained within a pressure containment tank and the turbine and compressor package. Total estimated specific weight of these components was 1.717 kg/KW_e. Influence coefficients were generated that described the component specific weight variations versus major cycle design parameters. These influence coefficients were provided to Boeing for their trade-off studies, the results of which were reviewed by AiResearch and a second generation baseline system (turbocompressor and recuperator/cooler package) defined. The second generation specific weight is 1.669 kg/KW_e or 1.465 kg/KW_e including potential changes in the radiator. Figure 4-17 shows the study approach.

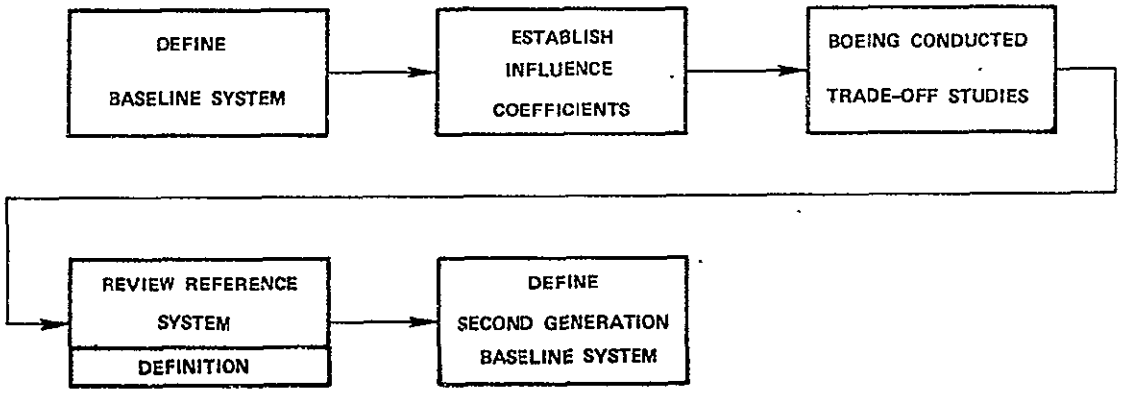

Figure 4-17 Study Approach

A comparison of the trade-off study results and the first generation baseline system definition, Figure 4-19 , shows that several major parameters were changed. These parameters and their influence on the specific weight are shown in Figure 4-18 . Table 4-2 defines the nomenclature used in the study and Tables 4-3 through 4-19 give the influence coefficients in discrete form.

		(W/Wr)			Figure
		TC	REC	Cooler	Reference
Turbine inlet temperature (T_3), °K	1300 → 1430	1.82	0.915	0.915	4.21
Pressure loss parameter (β)	0.94 → 0.95	0.99	0.968	0.980	4.22
Compressor discharge pressure (P_1), kN/M^2	3450 → 4500	0.785	0.810	0.955	4.23
Cooler gas side effectiveness (E_c)	0.90 → 0.92	---	---	1.36	4.24
Cooler thermal capacity ratio (ϕ)	0.80 → 0.85	---	---	1.98	4.24
Product of (W/Wr) column		1.414	0.717	2.306	
Specific Weight Changes, kg/kW_e					
Recuperator core	$0.974 \times (W/W_r)_{REC} = 0.974 \times 0.717 =$				0.699
Cooler core	$0.216 \times (W/W_r)_{CLR} = 0.216 \times 2.306 =$				0.498
Total heat exchanger core	1.190				1.197
Tank = 0.2 x Total heat exchanger core =	0.238				0.239
Turbo compressor	$0.289 \times (W/W_r)_{TC} = 0.289 \times 1.414 =$				0.409
Total Specific Weight	1.717				1.845

Figure 4-18 Influence of Parameter Changes on Specific Weights

4.4.1 First Baseline System

The first baseline system included the selection of a Xenon-Helium gas mixture working fluid with a molecular weight of 8 instead of Helium. This selection was based on the heat exchanger specific weight being equal with the turbocompressor variations as shown. The Xenon-Helium turbocompressor incorporates a lighter and shorter rotor which is more amenable to use of hydrostatic gas bearings. Longer turbine blading will result in increased efficiency potential. Figure 4-19 shows the layout of the first baseline system.

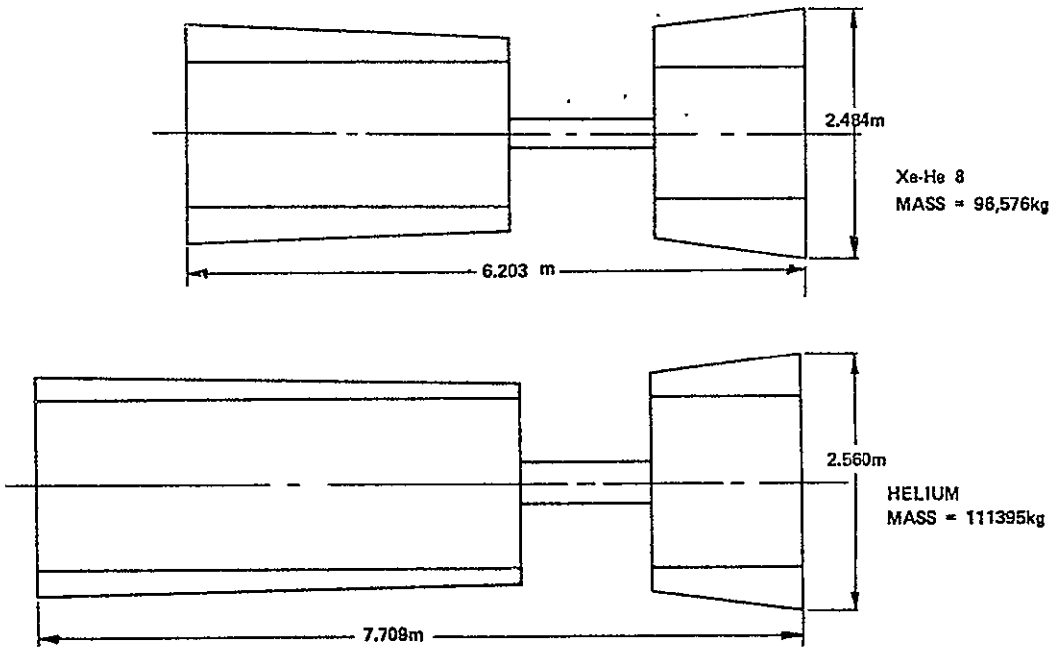

Figure 4-19 First Baseline System

DESIGN EQUATIONS

$$T_1 = \left(\frac{P_{rc}^{0.4} - 1}{\eta_c} + 1 \right)$$

$$T_2 = T_1 + E_R (T_4 - T_1)$$

$$T_4 = T_3 \left\{ 1 - \eta_T \left[1 - \left(\frac{F}{P_{rc}} \right)^{0.4} \right] \right\}$$

$$T_5 = T_4 - E_R (T_4 - T_1)$$

$$T_{L1} = T_5 - \frac{T_5 - T_o}{E_c}$$

$$T_{L2} = E_L (T_5 - T_{L1}) + T_{L1}$$

$$\text{Engine Efficiency} = \eta_{misc.} - \frac{\frac{P_{rc}^{0.4} - 1}{\eta_c} + \frac{(T_4 - T_1)(1 - E_R)}{T_o}}{\eta_T \left[\frac{1 - \left(\frac{1 + F}{P_{rc}} \right)^{0.4}}{\frac{T_o}{T_3}} + \frac{(T_4 - T_1)(1 - E_R)}{T_o} \right]}$$

TS DIAGRAM

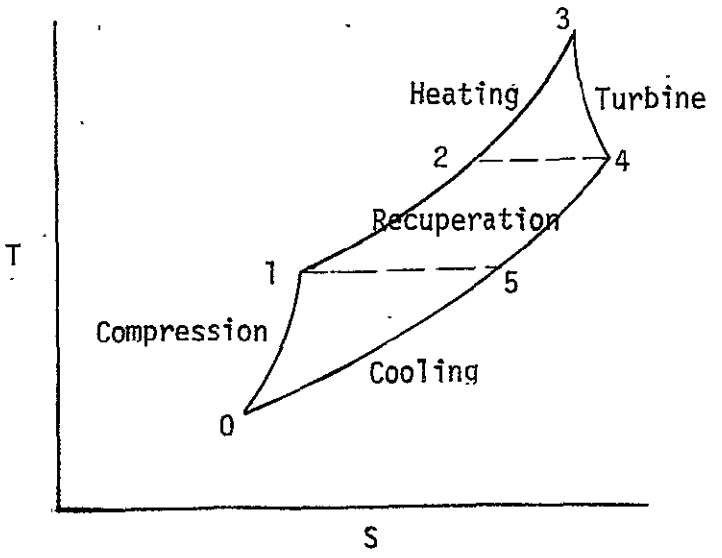

TABLE 4-2

T_o	Compressor inlet temperature
T_1	Compressor discharge temperature
T_2	Heat source inlet gas temperature
T_3	Turbine inlet temperature
T_4	Turbine discharge temperature
T_5	Cooler inlet temperature
T_{L_1}	Cooler liquid inlet temperature
T_{L_2}	Cooler liquid discharge temperature
P_1	Compressor discharge pressure
Pr_c	Compressor pressure ratio
Pr_t	Turbine pressure ratio
β	Pressure loss parameter = Pr_t/Pr_c
$\Delta P/P_t$	Closed loop total fractional pressure drop $\cong (1-\beta)$
E_R	Recuperator effectiveness = $\frac{T_2 - T_1}{T_4 - T_1} = \frac{T_4 - T_5}{T_4 - T_1}$
E_C	Cooler gas side effectiveness = $\frac{T_5 - T_o}{T_5 - T_{L_1}}$
E_1	Cooler liquid side effectiveness = $\frac{T_{L_2} - T_{L_1}}{T_5 - T_{L_1}}$
ϕ_C	Capacity ratio = E_1/E_C
$\Delta P/P_{REC}$	Total recuperator pressure drop for both sides
$\Delta P/P_{CLR}$	Cooler pressure drop = 0.32 x $\Delta P/P_{REC}$
η_{misc}	Miscellaneous efficiency losses, including bearing losses (approx. 1%)
η_c	Compressor efficiency
η_t	Turbine efficiency
F	Total pressure drop around gas loop

TABLE 4-3

T_3	1300°K	1525°K	1750 K
W/W_{ref}	1.000	0.866	0.763

TABLE 4-4

T_o/T_3	0.31	0.33	0.35	0.37	0.39
$(W/W_r)_{REC}$	0.769	0.873	1.000	1.157	1.358
$(W/W_r)_{CLR}$	0.085	0.894	1.000	1.127	1.281

TABLE 4-5

E_R	0.96	0.94	0.92	0.90
$(W/W_r)_{REC}$	1.508	1.000	0.746	0.594
$(W/W_r)_{CLR}$	1.039	1.000	0.972	0.950

TABLE 4-6

β	0.94	0.92	0.90
$(W/W_r)_{REC}$	1.000	1.072	1.160
$(W/W_r)_{CLR}$	1.000	1.056	1.122

TABLE 4-7

η_t	0.93	0.91	0.89
$(W/W_r)_{REC}$	1.000	1.085	1.170
$(W/W_r)_{CLR}$	1.000	1.068	1.135

TABLE 4-8

η_c	0.875	0.855	0.835
$(W/W_r)_{REC}$	1.000	1.061	1.121
$(W/W_r)_{CLR}$	1.000	1.049	1.098

TABLE 4-9

$\Delta P/P_{REC}$	0.042	0.036	0.030	0.024
$(W/W_r)_{REC}$	0.872	0.921	1.000	1.100
$(W/W_r)_{CLR}$	0.965	0.980	1.000	1.027

NOTE: $(\Delta P/P)_{CLR} = 0.32 \times \Delta P/P$

TABLE 4-10

P_1	2750 kN/m^2	3450 kN/m^2	4150kN/m^2
$(W/W_r)_{REC}$	1.217	1.000	0.862
$(W/W_r)_{CLR}$	1.041	1.000	0.968

TABLE 4-11

E_C	0.90	0.85	0.80
$(W/W_r)_{CLR}$	1.000	0.532	0.365

TABLE 4-12

ϕ_C	0.85	0.80	0.75
$(W/W_r)_{CLR}$	1.984	1.000	0.767

TABLE 4-13

T_3	1300°K	1350	1400	1450	1525
$(W/W)_{T-C}$	1.000	1.129	1.489	2.083	3.553

TABLE 4-14

T_o/T_3	0.31	0.33	0.35	0.37	0.39
$(W/W_r)_{T-C}$	0.791	0.888	1.000	1.134	1.297

TABLE 4-15

E_R	0.96	0.94	0.92	0.90
$(W/W_r)_{T-C}$	1.045	1.000	0.967	0.941

TABLE 4-16

β	0.94	0.92	0.90
$(W/W_r)_{T-C}$	1.000	1.052	1.115

TABLE 4-17

η_t	0.93	0.91	0.89
$(W/W_r)_{T-C}$	1.000	1.069	1.138

TABLE 4-18

η_c	0.875	0.855	0.835
$(W/W_r)_{T-C}$	1.000	1.051	1.103

TABLE 4-19

P_1	2750 kN/m^2	3450	4150
$(W/W_r)_{T-C}$	1.250	1.000	0.834

4.4.2 Compressor Pressure Ratio

The compressor pressure ratio is selected as the value that results in the maximum cycle efficiency. This value is a function of the recuperator effectiveness, (E_R), cycle temperature ratio (T_0/T_3) and the cycle pressure loss parameter (β). The cycle pressure loss parameter is defined as the ratio of the turbine pressure ratio divided by the compressor pressure ratio and is approximately equal to one minus the sum of the total fractional pressure losses around the closed cycle ($\beta = 1 - \Delta P/P_t$). See Figure 4-20 .

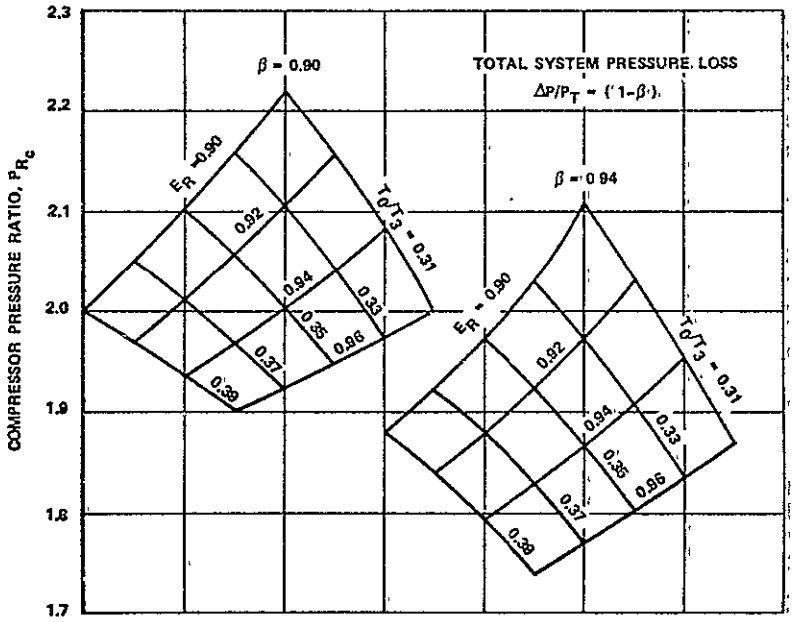

Figure 4-20 Compressor Pressure Ratio

4.4.3 Specific Weight Influence Coefficients

Turbine Inlet Temperature (T_3)

The specific weight of the recuperator and cooler cores decrease with increased T_3 due to the reduction in cycle mass flow. Turbocompressor specific weight increases because of the additional material required to contain the high pressure at the increased temperature. See Figure 4-21.

Cycle Temperature Ratio (T_0/T_3)

The specific weight variations are due to the change of the cycle mass flow rate and the resulting change in flow area. See Figure 4-21.

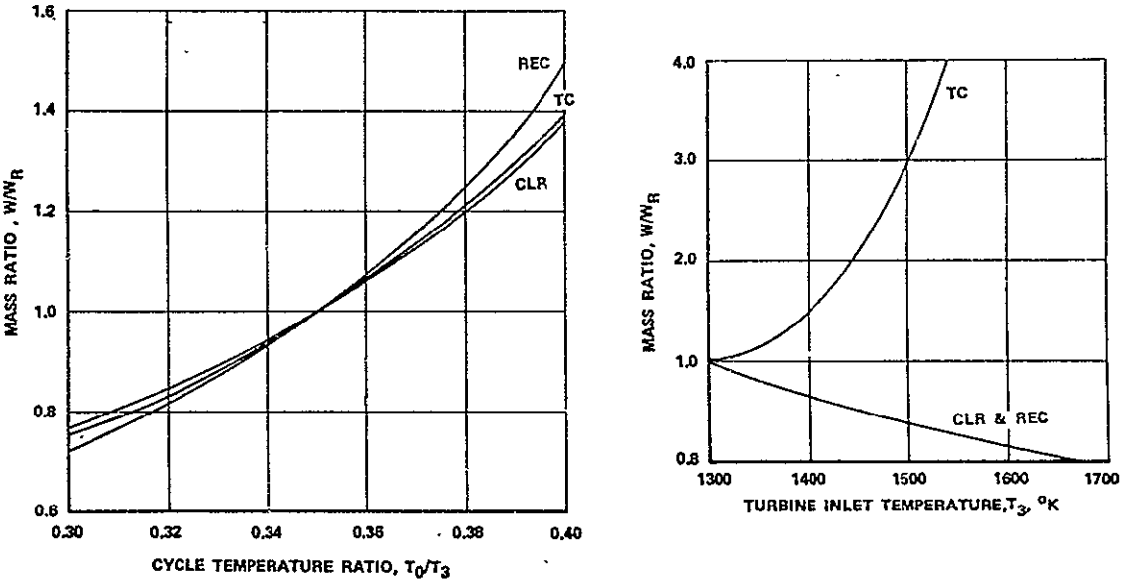

Figure 4-21 Specific Weight Influence Coefficients (T_3 and T_0/T_3)

Recuperator Effectiveness (E_R)

Changes in the recuperator effectiveness effect the cooler and turbocompressor due to the change in mass flow. The recuperator specific weight is changed due primarily to the change in the recuperator thermal conductance. See Figure 4-22.

Pressure Loss Parameter (β)

Reductions in β results in a lower cycle efficiency with a corresponding increase in the cycle mass flow rate. See Figure 4-22.

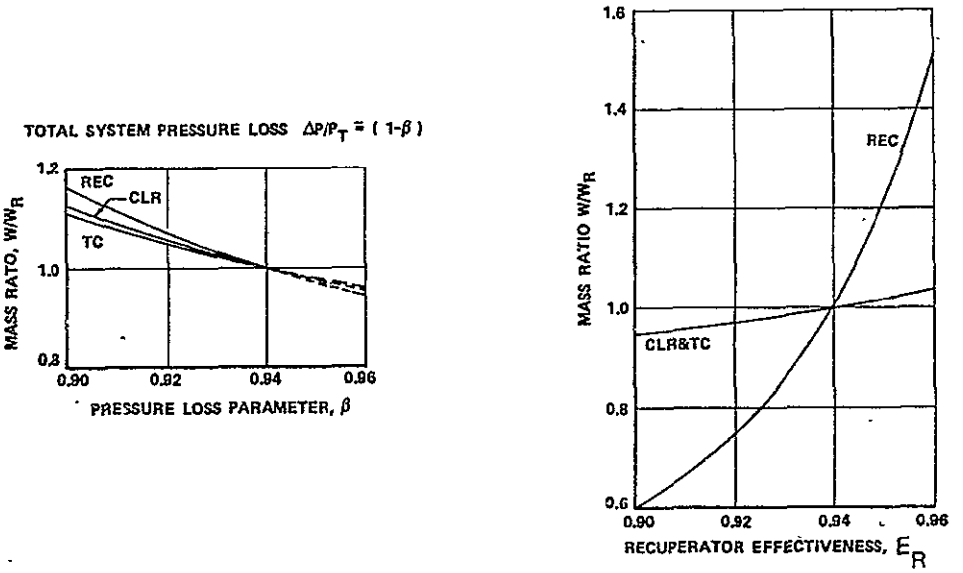

Figure 4-22 Specific Weight Influence Coefficients (β and E_R)

Compressor Discharge Pressure (P_1)

Variations in the compressor discharge pressure primarily effect the flow areas required for the recuperator and cooler. Changes in the amount of material required to contain the working fluid, particularly within the hot end of the turbocompressor, are also evident. See Figure 4-23.

Recuperator Pressure Drop ($\Delta P/P_r$)

Changes in the recuperator fraction pressure drop effect the cooler specific weight because the low pressure flow areas must be matched. Thus the cooler fractional pressure drop is a fixed ratio of the recuperator fractional pressure drop. See Figure 4-23.

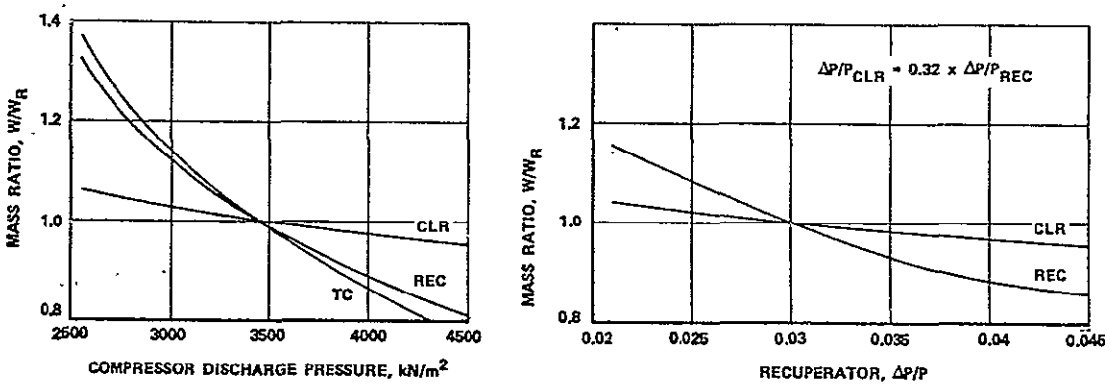

Figure 4-23 Specific Weight Influence Coefficients (P_1 and $\Delta P/P_r$)

Compressor and Turbine Efficiency (n_c and n_t)

Reduction in the compressor and turbine efficiency cause mass flow rate changes with corresponding increases in the required flow area. See Figure 4-24.

Cooler Effectiveness (E_c) and Thermal Capacity (ϕ)

These influence coefficients were generated for a three pass finned tube gas-to-NaK cooler with a fixed cooler gas discharge temperature or compressor inlet temperature (T_o). The cooler gas side effectiveness defines the minimum radiator NaK temperature delivered to the cooler. The thermal capacity ratio defines the NaK temperature rise across the cooler. The large cooler specific weight variations are due to the use of a three pass cooler configuration. Use of more passes would increase the cooler

weight at the baseline point but reduce the specific weight change for variations in ϕ and E_c. See Figure 4-24.

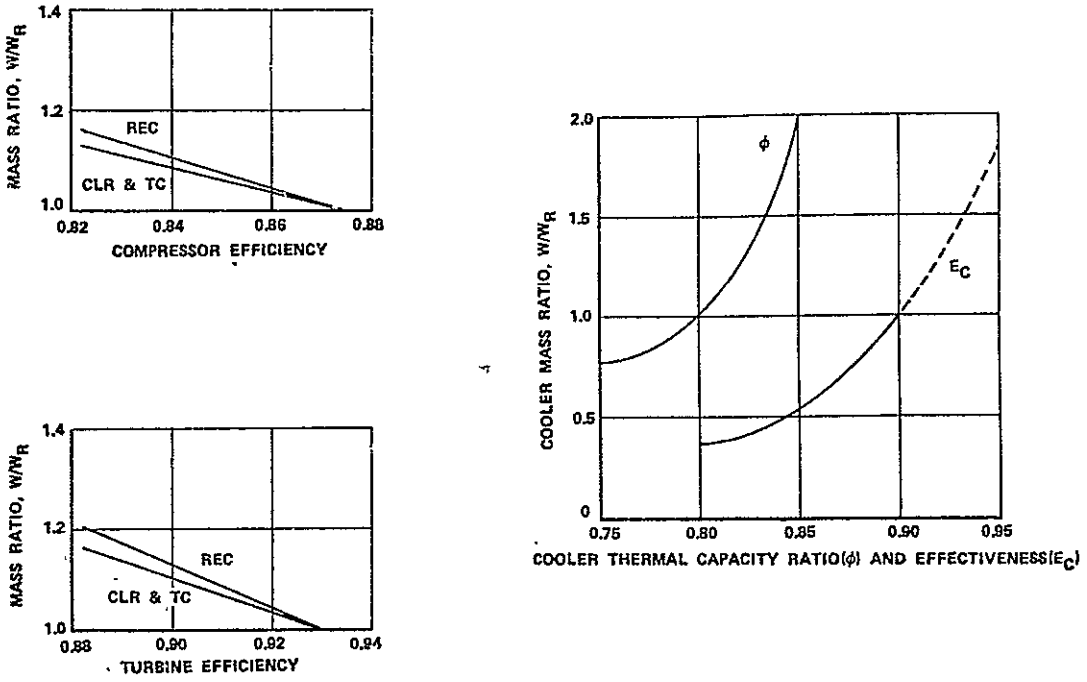

Figure 4-24 Specific Weight Influence Coefficients (n_c, n_t, ϕ and E_c)

4.4.4 Baseline Systems Design

The major parameters that define the baseline systems and the resulting component specific weights are shown in Table 4-20. Increasing the turbine inlet temperature resulted in the most significant changes between the first generation baseline and the trade-off study results. A review of these results indicated that the number of cooler passes should be increased from three to seven and the cooler thermal capacity ratio (ϕ) be increased to 0.95. These changes resulted in the second baseline system as defined in the third column. Note that the increased ϕ will result in an increase in the average radiator temperature with a potential radiator specific weight reduction of 0.204 kg/kW_e.

The specific weight variation of the turbocompressor is the result of sensitivity to the high turbine inlet temperatures.

Table 4-20 Baseline Systems Design

	FIRST GEN BASELINE SYSTEM	TRADE-OFF STUDY RESULTS	SECOND GEN BASELINE SYSTEM
TURBINE INLET TEMPERATURE (T_3), °K	1300	1430	1430
CYCLE TEMPERATURE RATIO (T_0/T_3)	0 35	0.35	0.35
RECUPERATOR EFFECTIVENESS (E_R)	0 94	0.94	0.94
PRESSURE LOSS PARAMETER (β)	0.94	0 95	0 95
COMP DISCHARGE PRESSURE (P_1), kN/m^2	3450	4500	4500
COMPRESSOR EFFICIENCY	0 875	0 875	0 875
TURBINE EFFICIENCY	0.930	0.930	0 930
RECUPERATOR PRESSURE DROP ($\Delta P/P_{rec}$)	0 03	0 03	0 03
COOLER GAS SIDE EFFECTIVENESS (E_C)	0 90	0.92	0 92
COOLER THERMAL CAPACITY RATIO ($\emptyset$)	0 80	0.85	0 95*
RECUPERATOR CORE SPECIFIC WEIGHT, kg/kW$_e$	0.974	0 699	0.681
COOLER CORE SPECIFIC WEIGHT, kg/kW$_e$	0 216	0.498	0.277
TANK SPECIFIC WEIGHT, kg/kW$_e$	0.238	0.239	0.191
TURBOCOMPRESSOR SPECIFIC WEIGHT, kg/kW$_e$	0.289	0 409	0.520
TOTAL SPECIFIC WEIGHT, g/W$_e$	1.717	1.845	1.669

*ESTIMATED TO REDUCE RADIATOR SPECIFIC WEIGHT BY 0.204 kg/kW$_e$.
NET SPECIFIC WEIGHT = 1.669 - 0.204 = 1.465 kg/kW$_e$

Second Generation Turbocompressor Layout

The second generation turbocompressor includes a sixteen stage axial compressor and a six stage axial turbine. The rotor is supported by hydrostatic gas journal bearings outboard of the aerodynamic wheels and a hydrostatic gas thrust bearing between the turbine and compressor. An axial thrust balancing piston will probably be required to limit the thrust loads and thus minimize the thrust bearing size.

The turbine end scrolls are shown to include internal insulation which is required to reduce the unit mass. No insulation benefit is included in the total turbocompressor mass figure however. The second generation turbocompressor layout is shown in Figure 4-25.

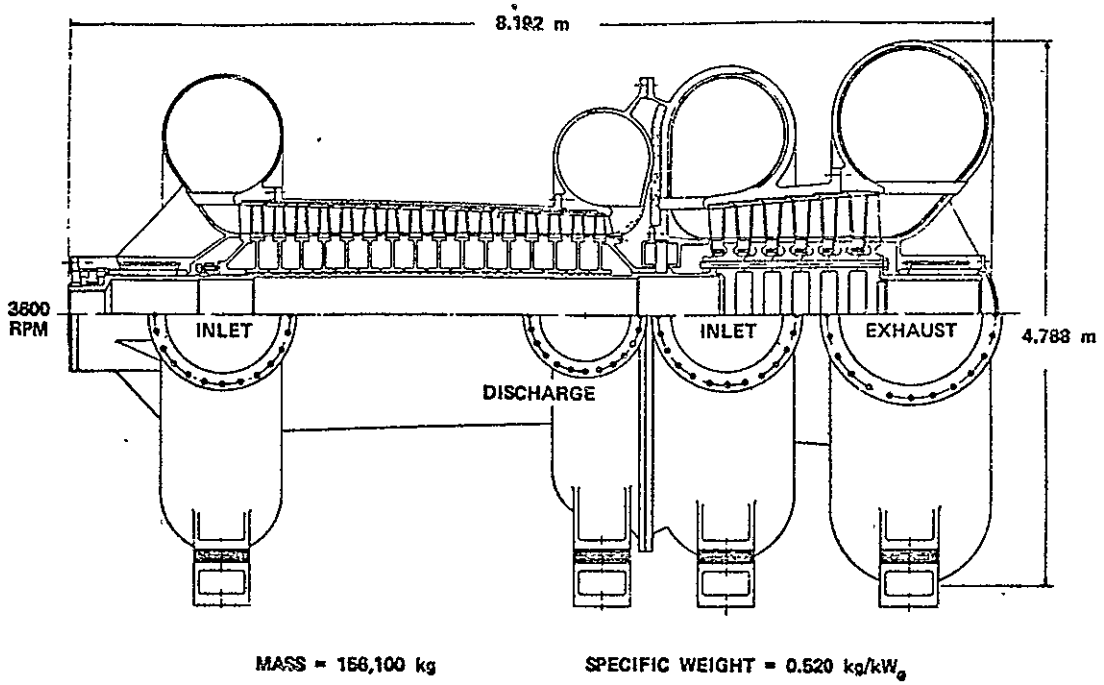

Figure 4-25 Second Generation Turbocompressor Layout

High Temperature Material Considerations

ASTAR 811C 1% Creep Data---The high temperature material creep strength data used during the baseline system definitions is shown in Figure 4-26. This material would be used for the turbine static structure and inlet piping.

Effect of Internal Insulation---Internal pipe and turbine scroll insulation design concepts have been investigated which allow separation of the high thermal and pressure loads imposed. Figure 4-26 shows the change in piping specific weight as a function of the metal temperature reduction achieved by applying internal insulation to the pipe.

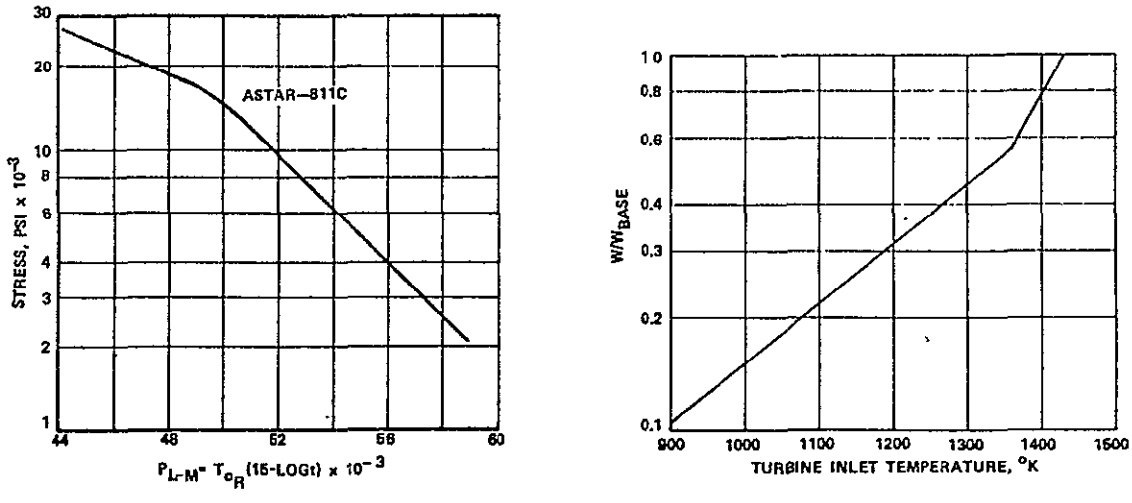

Figure 4-26 High Temperature Material Considerations

System Specific Weight Variations

The combined specific weight of the turbocompressor and recuperator/cooler package is shown in Figure 4-27 as a function of the module output power. Note that these results are for a system designed for 30 years life. Low power modules designed for one to two years operation as a pilot plant would have a significantly lower specific weight.

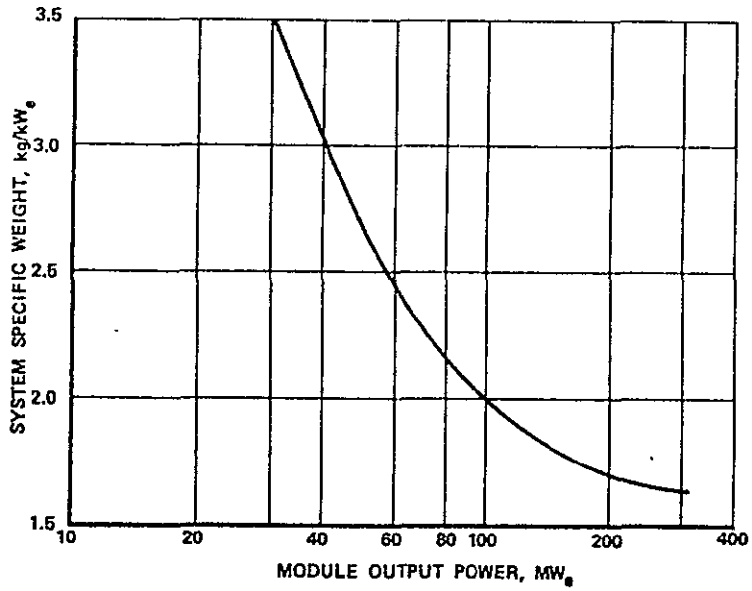

Figure 4-27 System Specific Weight Variations

4.5 THERMIONICS

The current NASA/ERDA program for thermionic converter is represented by efforts to improve electrodes (Contract AT (11-1)-3056 to Thermo Electron Corporation) and to reduce plasma losses (Contract to Rasor Associates, Inc.). These efforts have the promise of continuing the trend in efficiency improvement which has occurred since approximately 1960 (1) as shown in Table 4-20.

TABLE 4-20 THERMIONIC CONVERTER EFFICIENCY IMPROVEMENT

YEAR	"BARRIER INDEX"* (ELECTRON VOLTS)	EFFICIENCY AT EMITTER TEMP. OF 1800K (2780°F) AND COLLECTOR TEMPERATURE OF 900K (1160°F)
1960	3.0	0.03
1970	2.4	0.10
1975	2.1	0.15
1985 (Projection)	1.6	0.24
1995 (Projection)	1.2	0.36

*Barrier index is the difference between the ideal and actual electrode to electrode voltage.

For a barrier index of 1.6 electron volts, and allowing for emitter to collector radiative losses at an emissivity of 0.5, efficiency may be related to electrode temperature as shown in Figure 4-28.

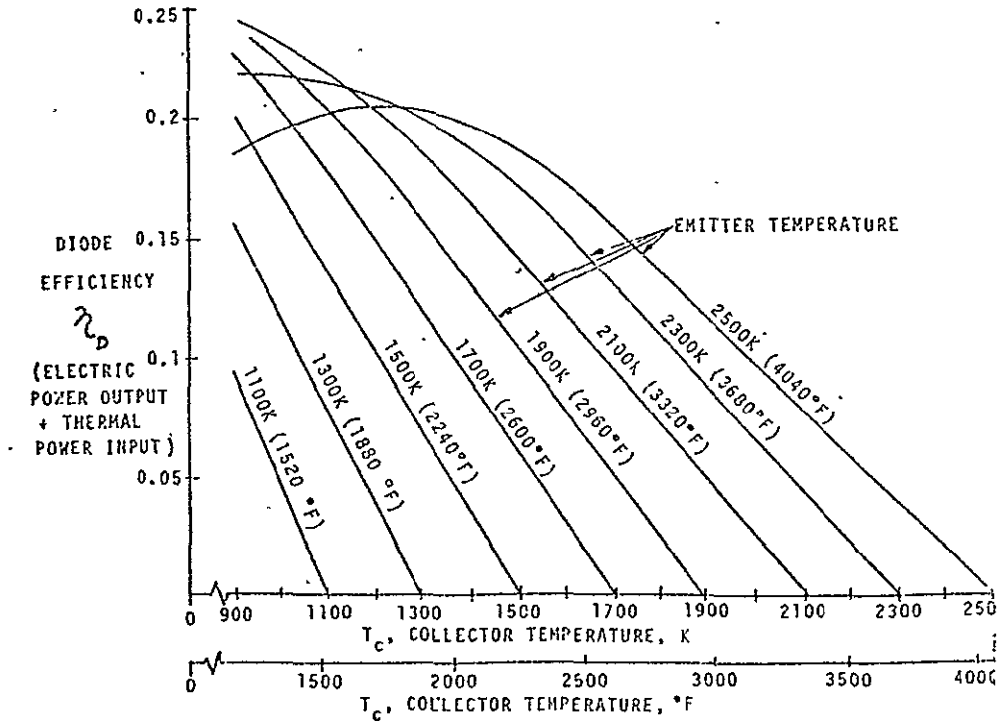

FIGURE 4-28 THERMIONIC CONVERTER EFFICIENCY

Figure 4-29 shows the baseline thermionic converter. The electrodes are tungsten, with a tungsten oxide deposit on the collector. The gap is filled with cesium vapor from the cesium reservoir. The electrodes are webbed for stiffness.

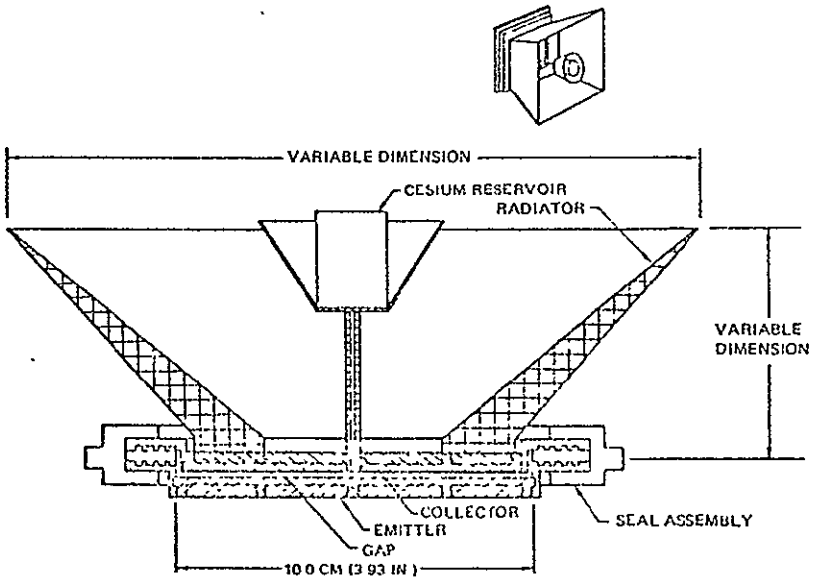

FIGURE 4-29 BASELINE THERMIONIC CONVERTER (DIRECT RADIATION COOLED VARIANT)

It is necessary to cool the collector to achieve thermionic operation. In either the nuclear or solar concepts cooling tubes would be bonded to the collector to conduct away the heat. Another option is passive cooling by the provision of collect fins as was shown in Figure 4-29.

A trade study was conducted to determine the optimum thickness for the electrodes, i.e. that thickness which causes the sum of the electrode mass and the mass penalty to counter the resistive (I^2R) loss in the diode to be a minimum. The optimum thickness was seen to range from 0.2 cm (0.079 in.) to 0.4 cm (0.157 in.) for the temperature range from 1000K (1340^{0}F) to 3000K (4940^{0}F).

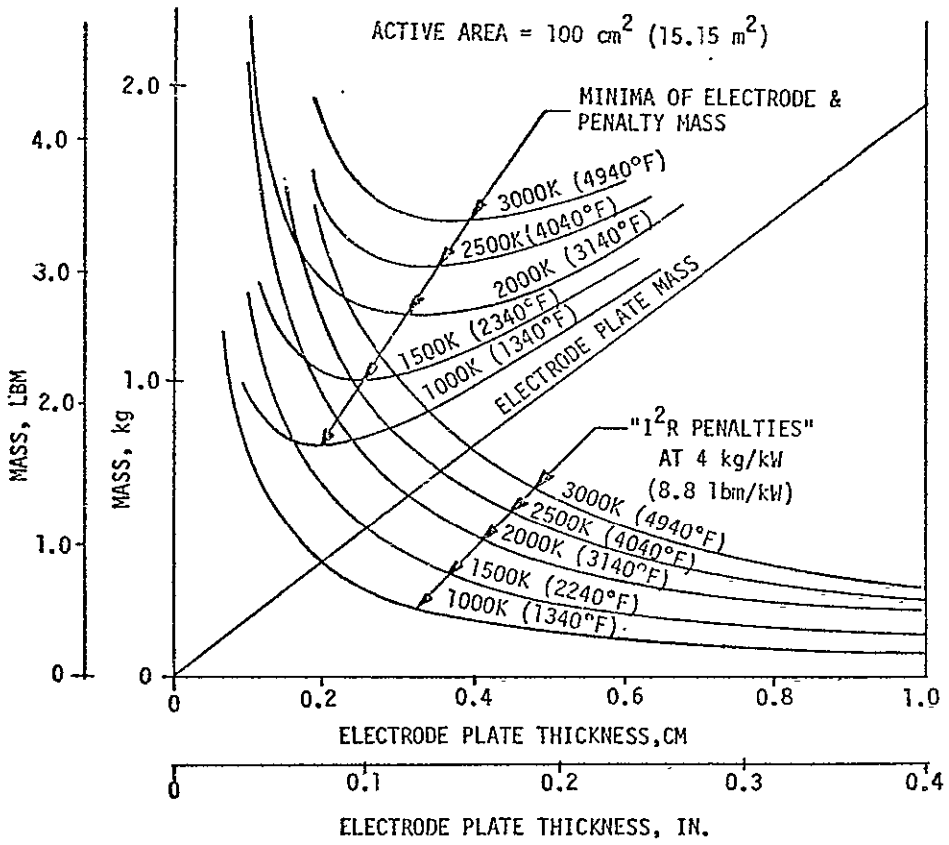

FIGURE 4-30 DERIVATION OF OPTIMUM ELECTRODE THICKNESS

Table 4-21 is a mass statement for the baseline diode.

TABLE 4-21 BASELINE DIODE MASS BREAKDOWN

ITEM	MASS	
	kg	LBM
ELECTRODES	1.00	2.20
SEAL ASSEMBLY	0.30	0.66
CESIUM RESERVOIR	0.03	0.07
CONTINGENCY (20%)	0.27	0.54
TOTAL	1.60	3.52

For an emitter temperature of 1900K (2960°F) and a collector temperature of 1000K (1340°F), the diode efficiency is 0.23, with a current output of 800 amperes at 0.80 volts (0.64 kw).

The thermionic diodes are mounted in the wall of the solar cavity absorber; their collectors and cooling fins are directly exposed on the outside of the cavity. The amount of heat to be rejected is a function of the diode efficiency, as shown in Figure 4-31.

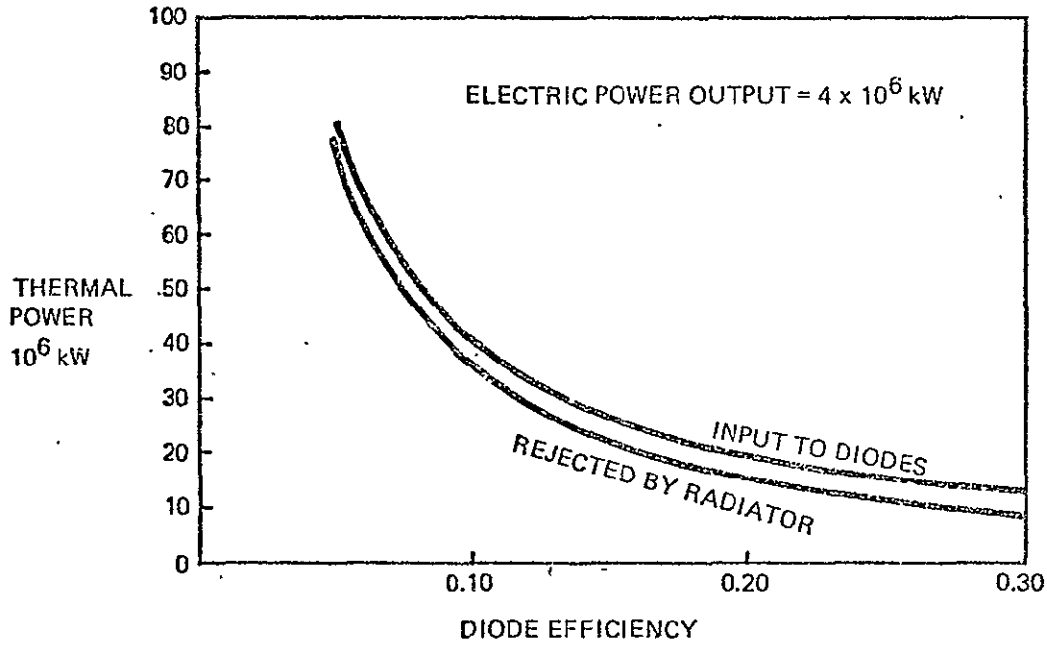

FIGURE 4-31 HEAT REJECTION FROM 4 GW_e THERMIONIC MODULE

The area required for the cavity exterior (which is nearly totally radiating area) is a function of the collector/fin temperature and the energy to be rejected, which is itself a function of diode efficiency. These factors are related in Figure 4-32. The minimum area for the cavity is 1.45×10^5 m^2 (1.56×10^6 ft^2) for a system wherein the diodes touch each other (i.e. radiating area equals collector area).

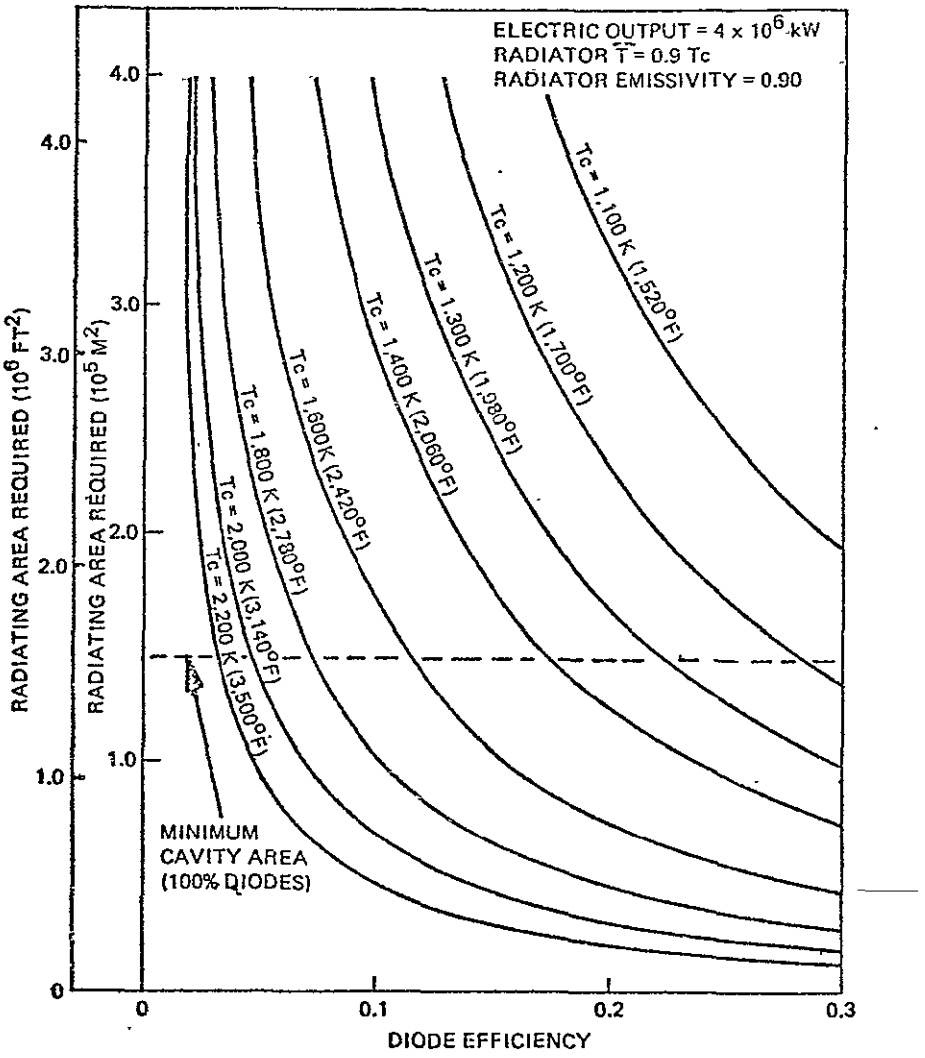

FIGURE 4-32 HEAT REJECTION AREA AS A FUNCTION OF DIODE EFFICIENCY (T_C = COLLECTOR TEMPERATURE)

The power generation module mass is composed of the cavity absorber with its diodes and rotary converters, the support framing and the hexagonal solar concentrator with its steerable plastic film reflectors. System mass optimization requires that the sum of these masses be a minimum. Rotary converters are used to step up the diode output to the voltage level required by the transmitter amplitrons. The limiting voltage for diodes in series is in the range of 50 to 100 volts as established by the breakdown characteristics of the electrical insulation at the temperature involved. Current insulation capability at 2000K (3140^{0}F) is approximately 25 volts (2). Baseline mass estimates used in the optimization are given in Table 4-22.

TABLE 4-22 BASELINE SPECIFIC MASSES

ITEM	SPECIFIC MASS
DIODES	2.50 kg/kW_e (5.51 lbm/kW)
FINS + UNDERLYING INSULATION	26 kg/m^2 (57 lbm/m^2)
ROTARY CONVERTORS	0.4 kg/kW_e (0.88 lbm/kW_e)
SOLAR CONCENTRATORS + FRAME & SUPPORT ARMS	0.3 kg/kW_T (0.66 lbm/kW_T)

Figure 4-33 shows the results of the system optimization process. For each emitter temperature/collector temperature combination the diode efficiency was derived to determine the heat rejection requirements and hence the cavity size and mass. Solar concentrator size and mass was taken as required to fulfill the 4 GW electrical output requirement.

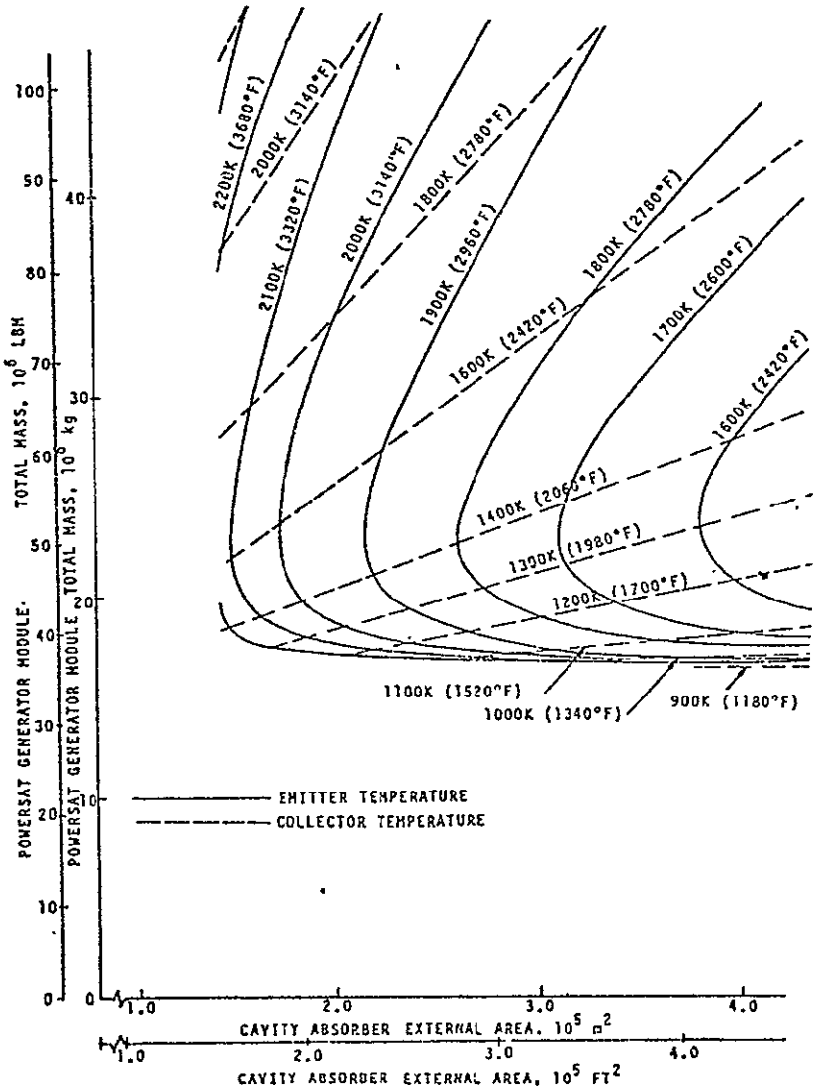

FIGURE 4-33 POWERSAT MODULE MASS OPTIMIZATION

Preliminary Concept Definition

The above modeling and optimization process indicates that near-minimum mass was achieved with an emitter temperature of 1900K (2960^{0}F) and a collector temperature of 1000K (1340^{0}F). The resultant configuration has a cavity surface area of 3.7 x 10^{5} m^{2} (39.8 x 10^{6} ft^{2}); the diameter of the sphere is 343m (1126 ft). It is composed of individual diode panels as shown in Figure 4-34.

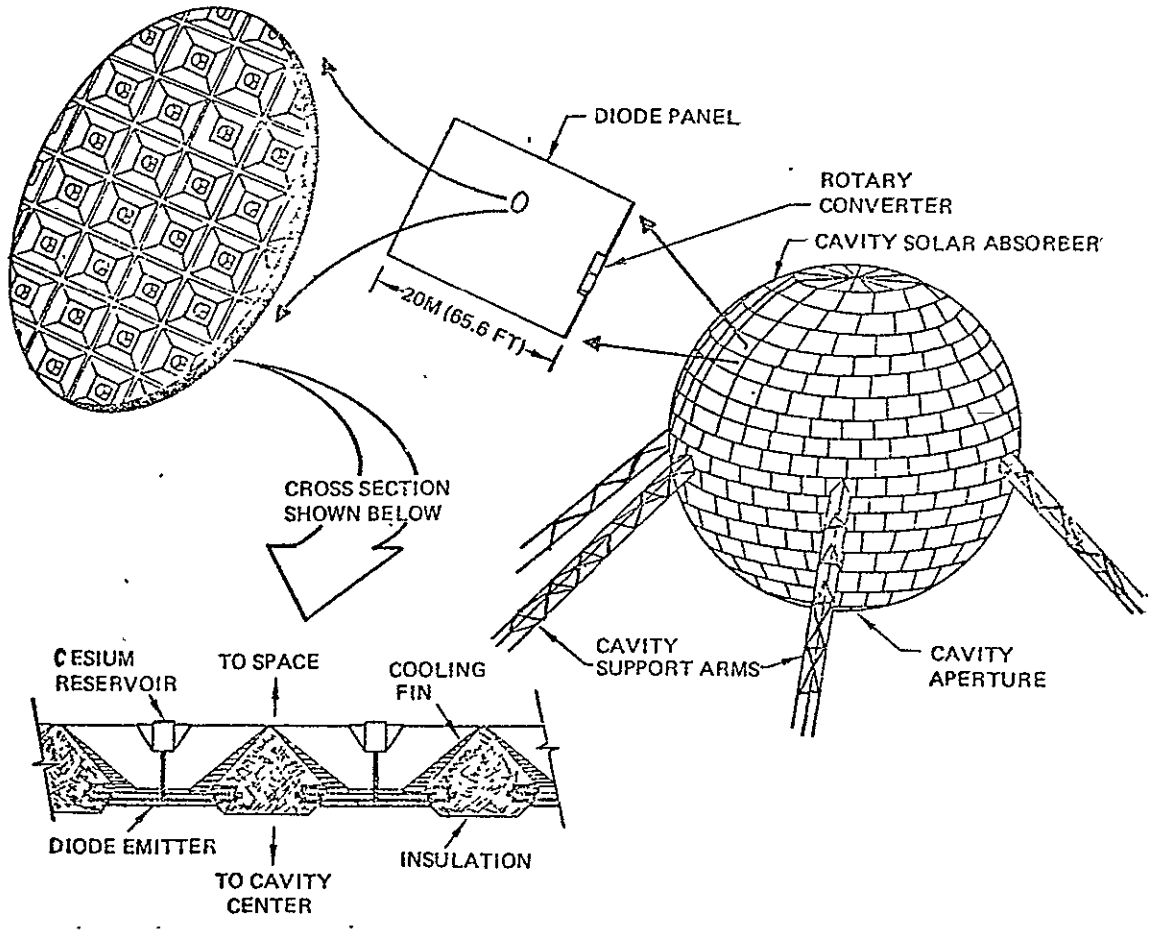

FIGURE 4-34 DIRECTLY COOLED CAVITY SOLAR ABSORBER

Total mass for a 40 GW generation module is 17.0 x 10^6 kg (37.5 x 10^6 lbm). A 10 GW ground output powersat composed of four of these modules and associated transmitter would have a mass of 79.03 x 10^6 kg (174.23 x 10^6 lbm).

The four associated solar concentrators are each 4490m (17,718 ft) across the flats of the hex.

REFERENCES

(1) Hatsopoulos, G.N., and Huffman, F. N., "The Growth of Thermionic Energy Conversion",Tenth Intersociety Energy Conversion Conference, August 1975.

(2) Private Communication with John W. Stearns, Jr. JPL.

4.6 BREEDER REACTOR PROGRAM CONCEPT

Reactor modules would be assembled and fueled in low orbit. Sixteen modules are baselined for a 10 GWe ground output nuclear SPS. Only two to four modules need be energized to provide the electric power necessary for the thrusters needed for a 100 day transfer to geosynchronous orbit (assuming 50% thruster efficiency). Thus when "self powering" away from low orbit, and still relatively near the atmosphere, only a relatively small quantity of fission products will be produced in the Molten Salt Breeder Reactor (MSBR) salt mixture. Some "bomb grade" material may be present in those power modules used for ascent.

In operation, a MSBR breeds U(233) from thorium. In a ractor module designed primarily for power production the fuel doubling time would be approximately six years. By placing design emphasis on breeding, this time could be reduced. Bred fuels are available for later SPS's. The basic fertile fuel which is carried up is thorium. All SPS's produce radioactive wastes. These could be accumulated at the SPS's, or accelerated to a remote location by a rocket disposal system. Geosynchronous orbital velocity and altitude provides an advantageous starting conditior for such a system.

The breeder reactor program concept is shown in Figure 4-35.

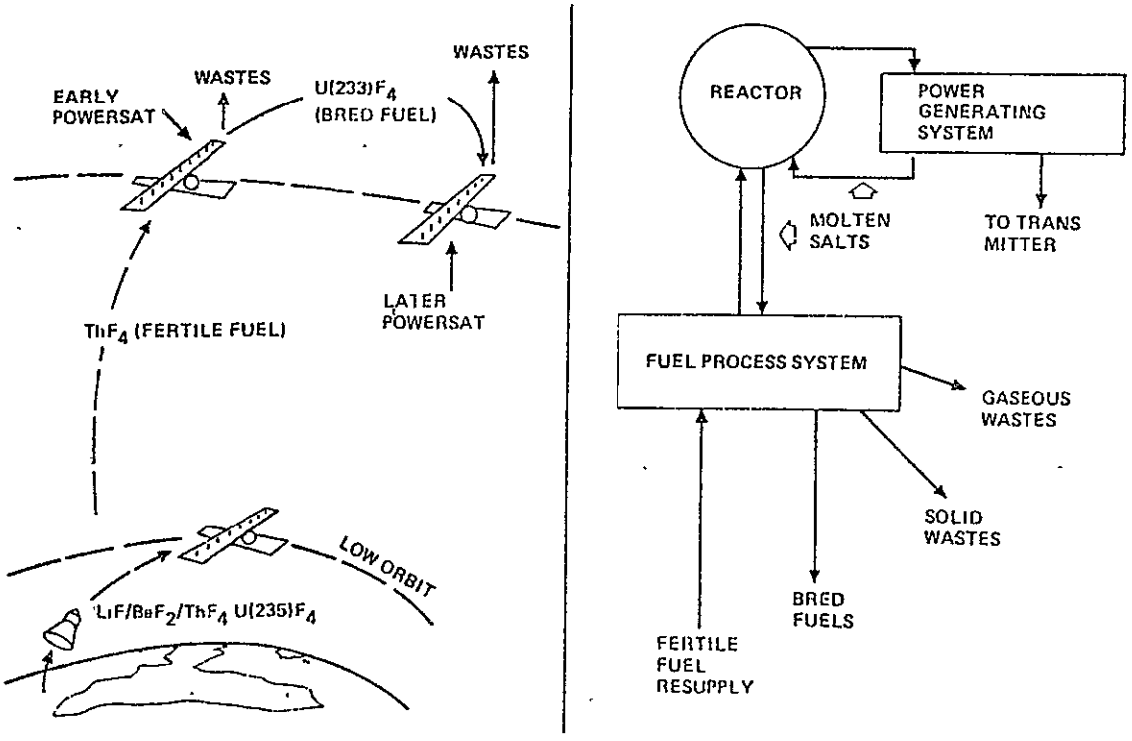

FIG 4-35 BREEDER REACTOR PROGRAM CONCEPT

4.6.1 Nuclear SPS

Two nuclear SPS designs were investigated, one using nuclear thermionic modules and the other, nuclear Brayton cycle modules.

Reactor Selection

For 1985 technology, 1990 operation, the most promising reactor type is the molten salt breeder reactor (MSBR) using a single circulating fuel loop containing both fissile and fertile materials. It was originally intended to use a beryllium moderator, but neutron induced swelling would limit life to only approximately five years (graphite would last approximately two years). To circumvent the problems of on-orbit moderator change-out, a self critical spherical cavity reactor with a molten salt moderator (LiF + BeF) is now baselined. Control would be by reflector drums and salt mixture control. Operation of the molten salt breeder reactor is as follows: The molten salt (^7LiF - BeF_2 - ThF_4 - UF_4) is circulated out-of-core by a pump system. The primary flow is either to a liquid-to-gas exchanger for the Brayton cycle system or to the diode assembly in the thermionic systems. A small side stream of salt is passed through a chemical processing system to remove protactinium and the salt-soluble fission products. Uranium is removed as UF_6 by fluorination. Liquid bismuth and lithium is used to extract protactinium. The remaining fission products are trapped in the bismuth contactor. The protactinium is held until it decays to U-233. This uranium and that removed by fluorination are reduced to UF_4 and either returned to the loop or transported to other systems. System wastes, including radioactive gases are held for disposal.

The molten salt breeder reactor flow is shown in Figure 4-36

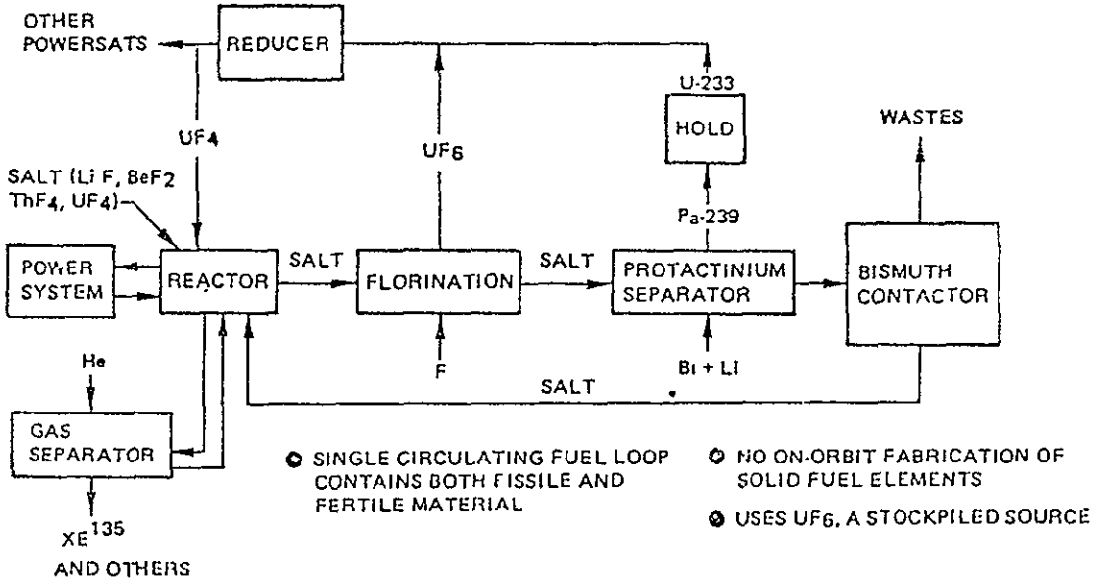

FIG 4-36 MOLTEN SALT BREEDER REACTOR FLOW SHEET

The highest practical tubing temperature for the 1985 technology molten salt breeder reactor was judged to be 1030K (1350^{o}F) for 30 years continuous utilization (with Hastalloy N). This relatively low temperature severely limits the temperature drop which can be achieved across the Brayton engine (and consequently the engine efficiency). Achieving a large temperature drop requires a low radiator temperature, with the resultant mass penalties shown in Fig. 4-37. In addition, large low temperature radiators require significant power for fluid pumping, which in turn increases the power to be dissipated by the radiator. Table 4-25 gives significant descriptive parameters for a 10GW ground output Nuclear Brayton power satellite.

TABLE 4-25. NUCLEAR BRAYTON POWER SATELLITE PARAMETERS

CYCLE TEMPERATURES:		
Radiator Inlet	401K	262^{o}F
Radiator Outlet	282K	48^{o}F
Minimum Gas Temperature	299K	78^{o}F
Reactor Inlet Temperature	766K	919^{o}F
Maximum Gas Temperature	1030K	1395^{o}F
ENGINE PRESSURE RATIO	2.2	
OVERALL BRAYTON EFFICIENCY	45.3%	
RADIATOR PUMP POWER	4.24×10^{6} kW	
ELECTRIC POWER TO TRANSMITTER	15.0×10^{6} kW	

The relatively large mass of the nuclear system is directly due to the low system maximum temperature. This low temperature limitation results from the effects of the molten salt mix on the out-of-core tubing system. The molten salt breeder reactor was selected as the best approach to on-orbit fuel processing. Future study of nuclear power satellites should include systems capable of higher maximum temperature, even though more complex fuel processing may be required. A single orbital fuel processing complex could perhaps serve many nuclear power satellites.

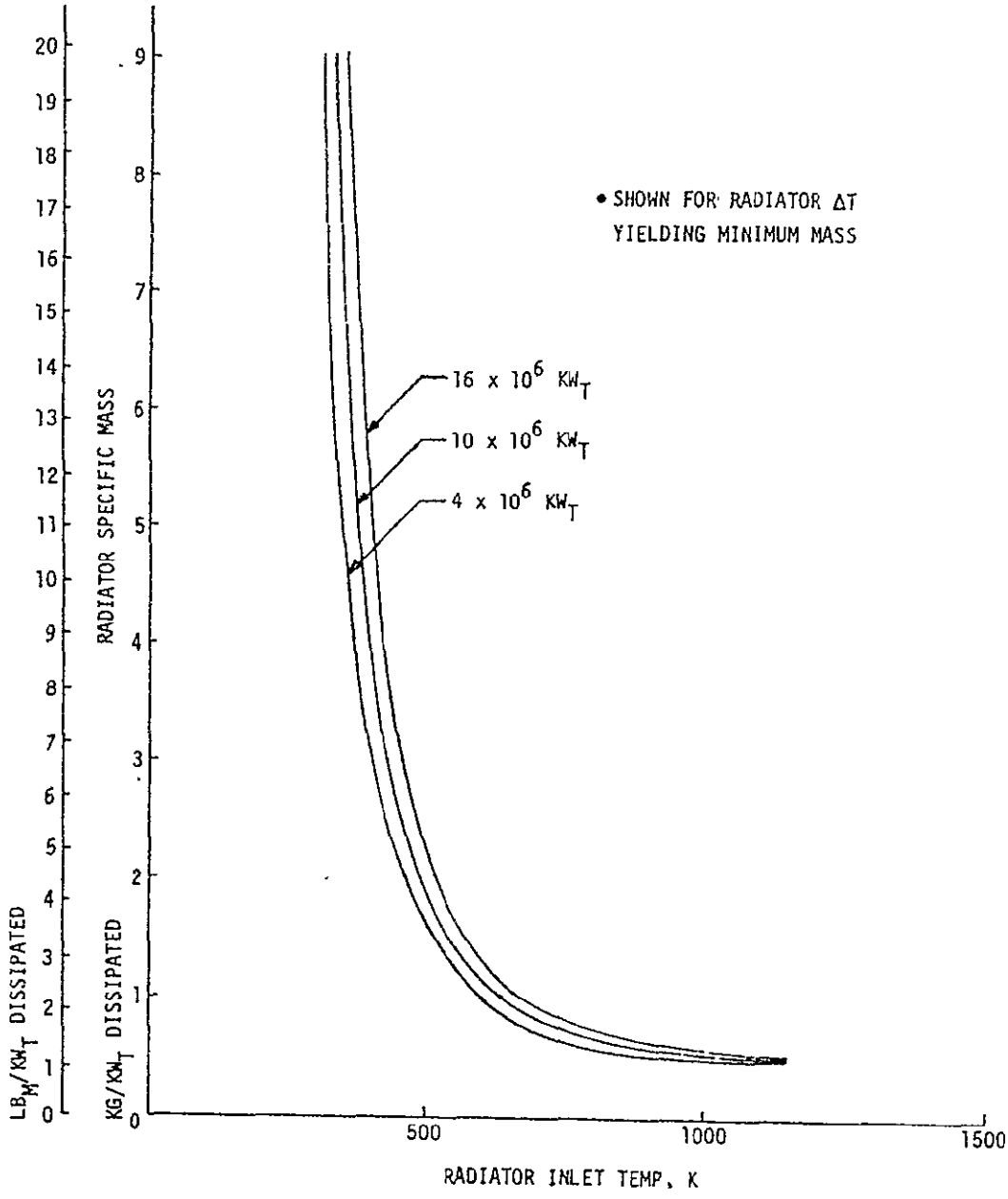

FIG 4-37. EFFECT OF INLET TEMPERATURE ON RADIATOR TOTAL MASS (OPTIMUM Δ T)

For the nuclear thermionic system, both in-core and out-of-core (with heat pipes) options appear viable. The following performances are predicted for systems employing 800K (980^{o}F) collectors (anodes):

	Emitter Temperature	Efficiency
Program A (1985 technology)	1450 K (2150^{o}F)	20%
Program B (1995 technology)	1600 K (2420^{o}F)	35%

Additional information is contained in (1) and (2).

4.6.2 MSBR Fuel Reprocessing

Operation of a molten-salt reactor as a high-performance breeder is made possible by the continuous processing of the fuel salt in a facility that is located at the reactor site. The most important operations consist in removing fission products (principally the rare earths) and isolating ^{233}Pa from the region of high neutron flux during its decay to ^{233}U in order to hold neutron absorption in these materials to an acceptably low level.

The rates at which the fuel salt must be processed for ^{233}Pa removal and rare-earth removal are mutually dependent. It will be convenient to define the term "processing cycle time" as the time required for processing a volume of fuel salt equal to that contained in the reactor system. The "removal time" for a given material is then an effective cycle time that is equal to the processing cycle time divided by the fraction of the material that is removed in a pass through the processing system. As shown in Fig. 4-38, for a particular single-fluid MSBR having a breeding ratio of 1.07, the required rare-earth removal time can range from 50 days for a protactinium removal time of 3 days to about 11 days for a protactinium removal time of 20 days. The optimum choice of protactinium and rare-earth removal times is largely dependent on the characteristics of the processes employed. For example, the present rare-earth removal process requires that protactinium be removed from the salt prior to the removal of rare earths. Hence, with this process, the rare-earth removal time will always be as long as or longer than the protactinium removal time. As will be discussed later, a protactinium removal time of 10 days and a rare-earth removal time of about 27 days are used with the reference processing system.

Processes involving the selective chemical reduction of materials from the fuel salt into liquid bismuth appear to be the most promising processing methods currently available (3). The isolation of protactinium is straightforward since its extraction behavior is significantly different from that of uranium, thorium, and lithium. However, until recently, the removal of rare earths was difficult since the rare earths and thorium extract in almost the same manner from molten fluoride mixture (4,5)

Bismuth is a low-melting (271°C) metal that is essentially immiscible with molten halide mixtures consisting of fluorides, chlorides, and bromides. The vapor pressure of bismuth in the temperature range of interest (500 to 700°C) is negligible,

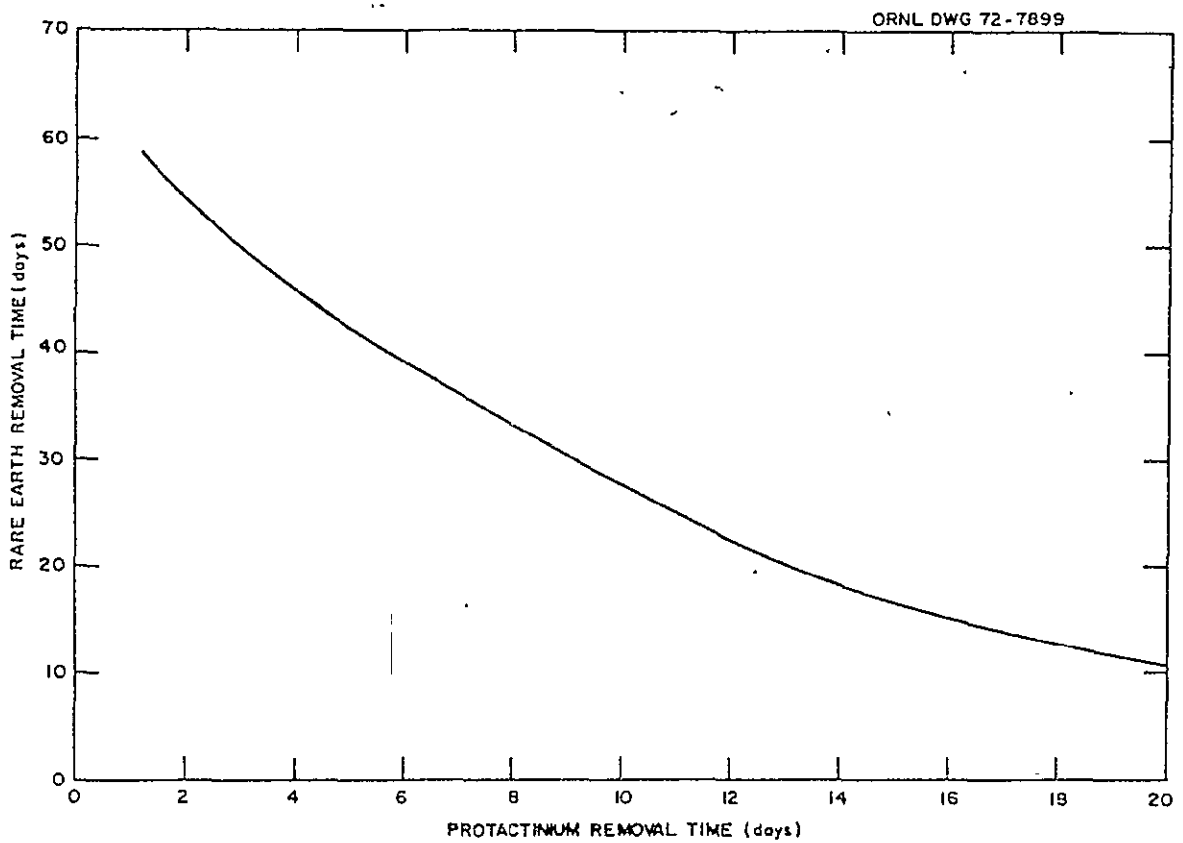

Figure 4-38. Rare earth and protactinium removal time combinations that result in a breeding ratio of 1.07.

and the solubilities of lithium, thorium, uranium, protactinium, and most of the fission products are adequate for processing applications.

Under the conditions of interest, reductive extraction reactions between materials in salt and metal phases can be represented by the following reaction:

$$MX_n \text{ (salt)} + n\text{Li(Bi)} \rightleftharpoons \text{M(Bi)} + n\text{LiX (salt)} ,$$

in which the metal halide MX_n in the salt reacts with lithium from the bismuth phase to produce M in the bismuth phase and the respective lithium halide in the salt phase. The valence of M in the salt is $+n$, and X represents fluorine, chlorine, and bromine. It has been found (6) that at a constant temperature the distribution coefficient D for metal M depends on the lithium concentration in the metal phase (mole fraction), X_{Li}, as follows:

$$\log D = n \log X_{Li} + \log K_m^* .$$

The quantity K_m^* is dependent only on temperature, and the distribution coefficient is defined by the relation:

$$D = \frac{\text{mole fraction of M in metal phase}}{\text{mole fraction of } MX_n \text{ in salt phase}} .$$

The ease with which one component can be separated from another is indicated by the ratio of the respective distribution coefficients, that is, the separation factor. As the separation factor approaches unity, separation of the components becomes increasingly difficult. On the other hand, the greater the deviation from unity, the easier the separation.

Distribution data obtained (6) for a number of materials between fuel salt (72-16-12 mole % $LiF-BeF_2-ThF_4$) and bismuth at 640°C are summarized in Figure 4-39. The lines for the various elements have slopes that correspond to the indicated oxidation states. Under the expected process conditions, the Pa-Th separation factor is about 1200, which indicates that protactinium as well as uranium and zirconium can be easily extracted from a salt stream containing ThF_4.

Distribution data for LiCl at 640°C are shown in Figure 4-40 (7-9). The data fall roughly into three groups. The divalent rare-earth and alkaline-earth elements distribute most readily to the LiCl, with thorium-rare-earth separation factors of about 10^8. The trivalent rare earths form the second group, and the thorium-rare-earth separation factors are about 10^4. Tetravalent materials, such as thorium and protactinium, distribute only slightly to the LiCl. Studies on the temperature dependence of the distribution data show essentially no effect for the divalent elements, a minor effect for the trivalent elements, and a somewhat greater effect for

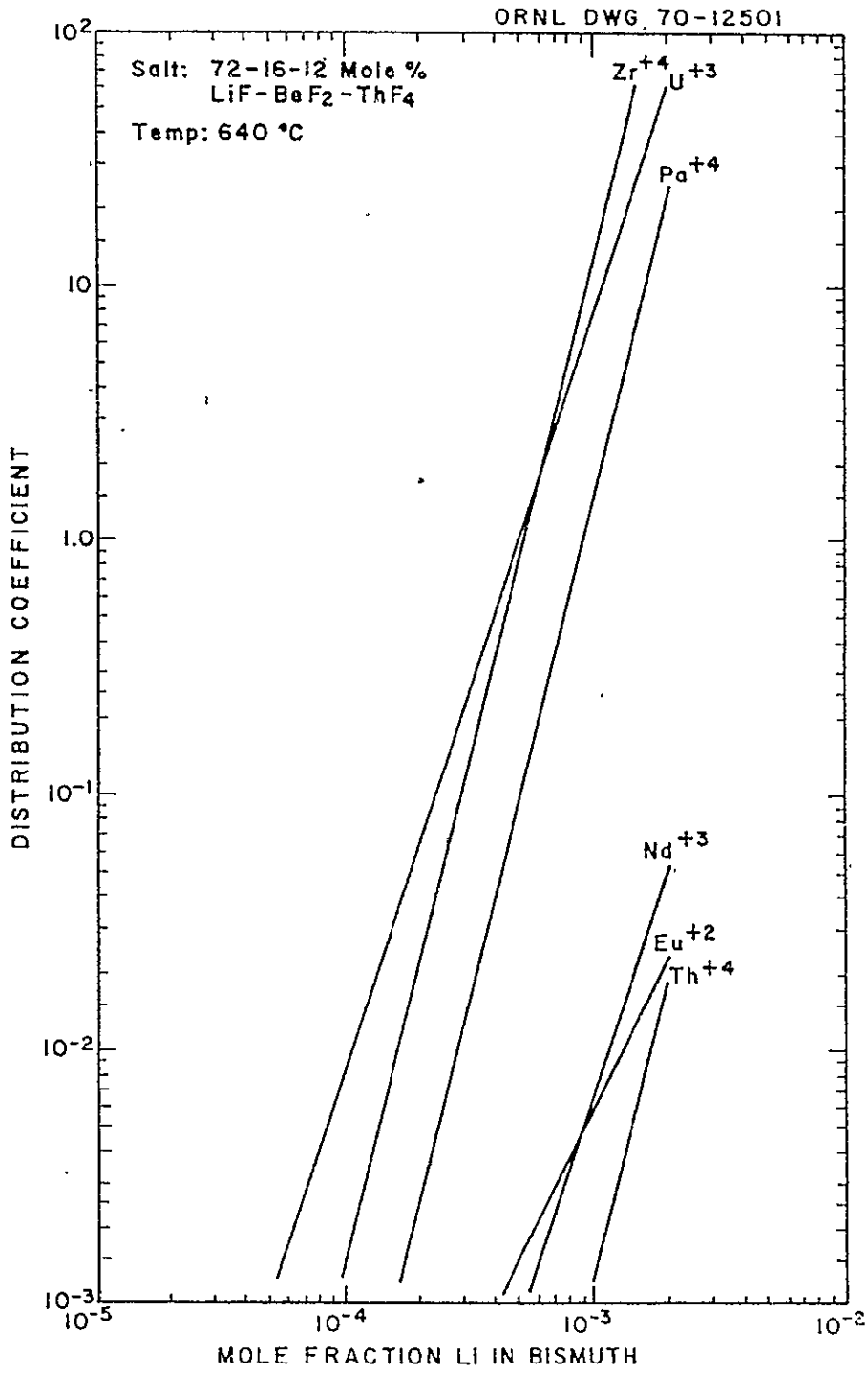

Figure 4-39. Distribution Data Between Fuel Salt and Bismuth.

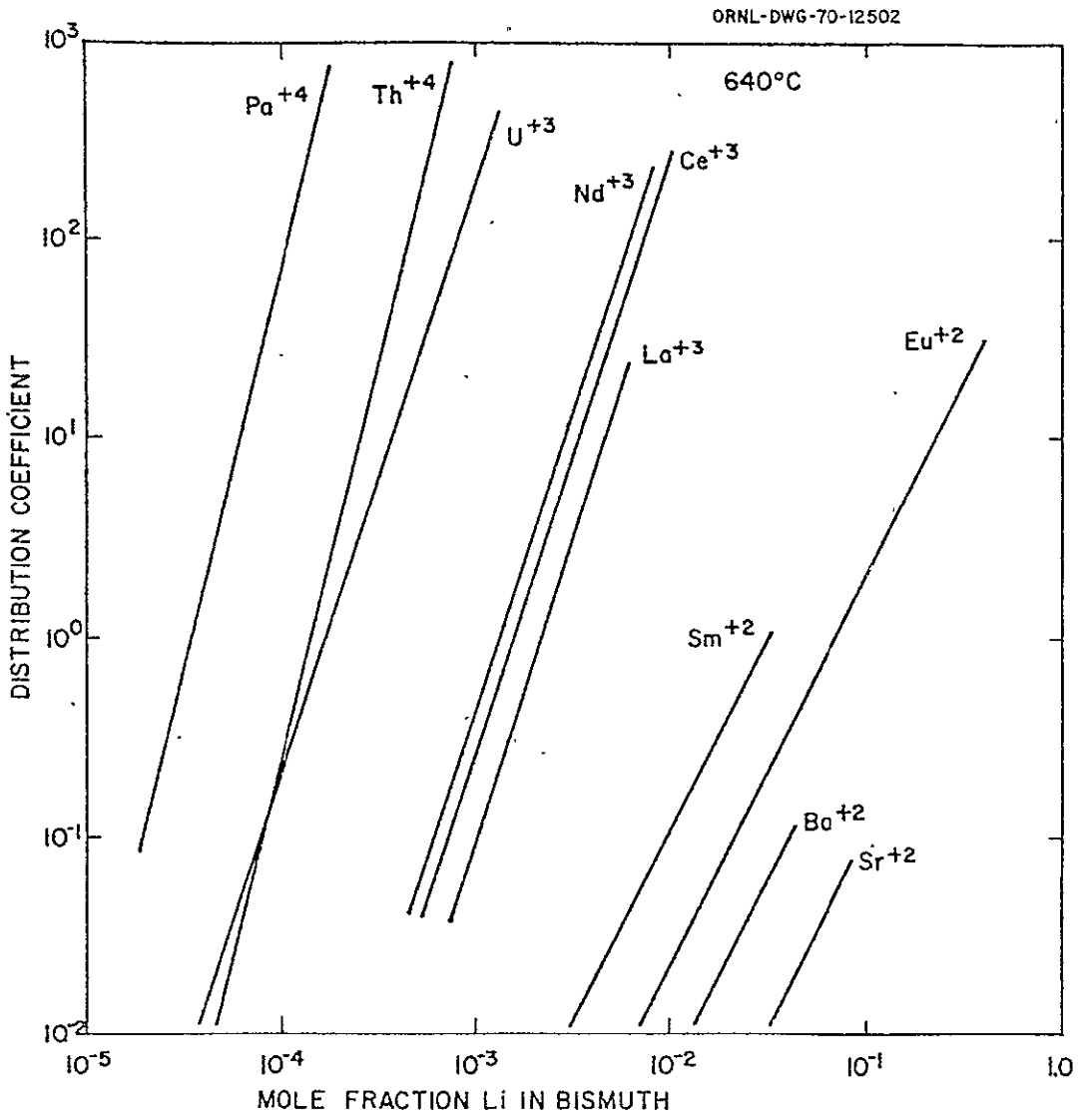

Fig. 4-40 Distribution Data Between Lithium Chloride and Bismuth.

the tetravalent elements. The distribution coefficient for thorium is decreased sharply by the addition of fluoride to the LiCl, although the distribution coefficients for the rare earths are affected by only a minor amount. Thus, contamination of the LiCl with several mole percent fluoride will not affect the removal of the rare earths but will cause a sharp increase in the thorium discard rate. Data with LiBr (9) are similar to those with LiCl, and the distribution behavior with LiCl-LiBr mixtures would likely not differ appreciably from the data with the pure materials.

The potential held by LiCl for selective extraction of the rare earths from MSBR fuel salt is best illustrated by considering the equilibrium concentrations of rare earths, thorium, and lithium in fuel salt, bismuth containing reductant, and LiCl as shown in Table 4-26. The concentrations of the rare earths and alkaline earths in the fluoride salt correspond to a 25-day removal time for these materials in the reference MSBR. The thorium concentration in the bismuth is 90% of the thorium solubility at 640°C. As can be seen, the rare-earth and alkaline-earth elements are present in the LiCl at low concentrations and are associated with a negligible amount of thorium.

The reference protactinium removal system (10) shown in Figure 4-41 is based on fluorination for uranium removal and reduction extraction for protactinium isolation. Fuel salt containing 0.33 mole % UF_4 and approximately 0.0035 mole % PaF_4 is withdrawn from the reactor. About 99% of the uranium is removed from the salt by fluorination. The salt stream is fed countercurrent to a bismuth stream containing lithium and thorium, where the remaining uranium and the protactinium transfer to the metal stream. These materials are transferred from the bismuth to a captive secondary salt by hydrofluorinating the bismuth stream leaving the extraction column in the presence of the secondary salt. The secondary salt which flows through the hydrofluorinator also circulates through a fluorinator, where about 90% of the uranium is removed, and through a tank that contains most of the protactinium. Lithium is added to the bismuth leaving the hydrofluorinator, and the resulting stream is returned to the top of the extraction column.

Table 4-26. Equilibrium Concentrations in Fuel Carrier Salt, Bismuth, and Lithium Chloride at 640°C

Element	Mole Fraction		
	In Fuel Carrier Salt[a]	In bismuth	In Lithium Chloride
Li	0.72	0.00201	
Be	0.16	0 approx	
Th	0.12	0.0025	3.31×10^{-6}
Zr	33.8×10^{-6}	0.00802	0.236×10^{-6}
Ba	2.83×10^{-6}	0.253×10^{-6}	0.00123
Ce	19.3×10^{-6}	1.38×10^{-6}	0.636×10^{-6}
Nd	12.1×10^{-6}	0.680×10^{-6}	0.219×10^{-6}
Pm	1.26×10^{-6}	0.0439×10^{-6}	0.0429×10^{-6}
Sm	1.34×10^{-6}	0.0622×10^{-6}	0.000019
Eu	1.55×10^{-6}	0.0359×10^{-6}	4.39×10^{-6}

[a]Concentrations of the fission products in the fuel carrier salt are based on an assumed processing cycle time of 10 days and a removal efficiency of 40%, which results in a 25-day removal time.

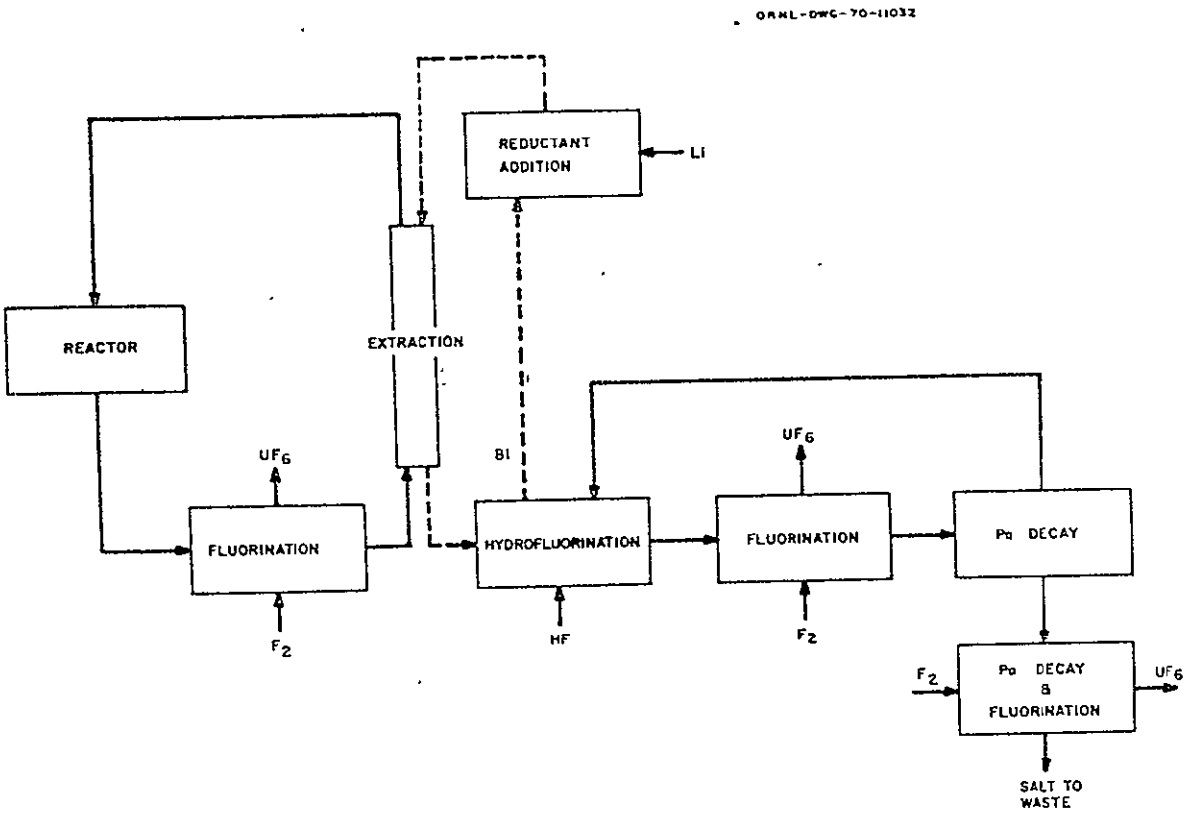

Fig. 4-41. Flowsheet for Isolation of Protactinium From a Single-Fluid MSBR by Fluorination-Reductive Extraction.

The salt leaving the extraction column is essentially free of uranium and protactinium but contains the rare earths at essentially the reactor concentration. This stream is fed to the rare-earth removal system.

Rare-Earth Removal Process

A simplified flowsheet for the rare-earth removal system (11) is shown in Figure 4-42. Fuel salt, which is free of uranium and protactinium but contains the rare earths, is countercurrently contacted with bismuth containing reductant in order to extract a significant fraction of the rare earths into the bismuth. The bismuth stream, which contains the rare earths and thorium, is then countercurrently contacted with lithium chloride. Because of highly favorable distribution coefficients, significant fractions of the rare earths transfer to the LiCl along with a negligible amount of thorium. The final steps of the process consist in extracting the rare earths from the LiCl by contact with bismuth having lithium concentrations of 5 and 50 atom %.

This process has a number of very desirable characteristics. Of primary importance is the fact that there is no net consumption of reductant in the two upper contactors. The process is not sensitive to minor variations in operating conditions. Essentially no materials other than the rare-earth and alkaline-earth elements are removed from or added to the fuel salt; the major change consists in replacing the extracted rare earths with an equivalent amount of lithium as LiF. The amount of LiF added to the fuel salt in this manner during 30 years of operation would be less than 10% of the LiF inventory in the reactor.

Conceptual Processing Flowsheet

The reference processing flowsheet (10) is shown in Figure 4-43. Fuel salt is withdrawn from the reactor on a 10-day cycle; for a 2300 MW reactor, this represents a flow rate of 0.88 gpm. The fluorinator, where 99% of the uranium is removed, has an active diameter of 8 inches and a height of 15 feet. The protactinium extraction column is 3 inches in diameter and is packed with 3/8 inch Raschig rings. The column is equivalent to five equilibrium stages and has a height of 15 feet. The bismuth flow rate through the column is 0.13 gpm, and the inlet thorium concentration in the stream is 90% of the thorium solubility at the operating temperature of 640°C. The protactinium decay tank has a volume of 160 ft^3. The uranium inventory in the tank is less than 0.2% of that in the reactor. Fluorides of lithium, thorium, zirconium, and nickel accumulate in the tank at a total rate of about 0.1 ft^3/day. These materials are removed by periodic withdrawal of salt to a final protactinium decay and fluorination operation.

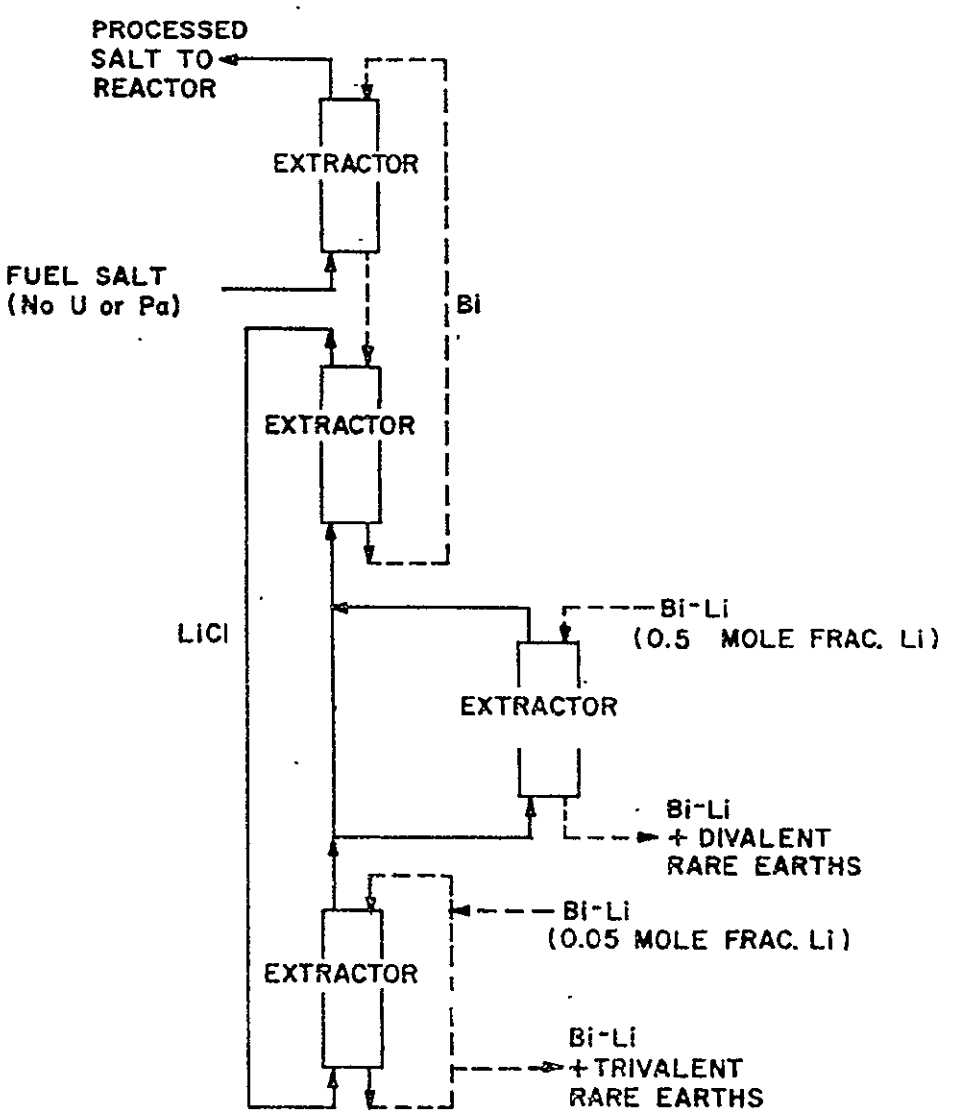

Fig. 4-42. Metal Transfer Process for Removal of Rare Earths From Single-Fluid MSBR Fuel Salt.

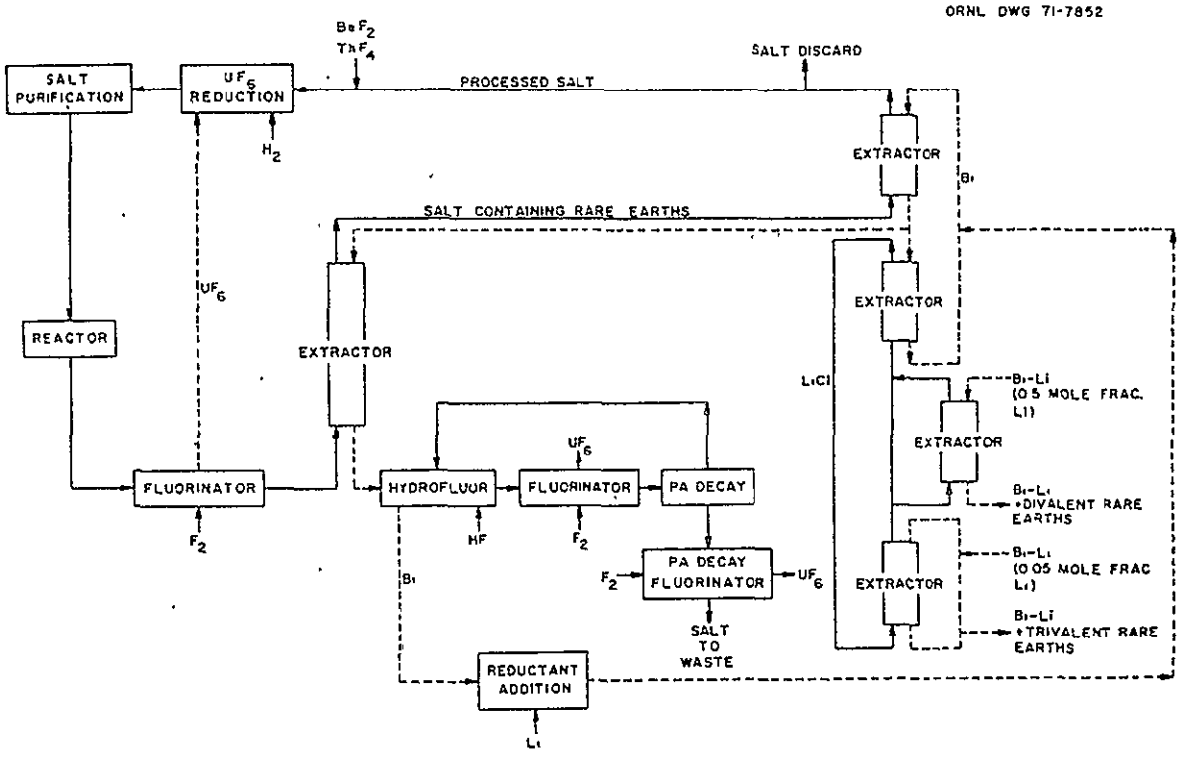

Fig. 4-43 Conceptual Flowsheet for Processing a Single-Fluid MSBR by Fluorination-Reductive Extraction and the Metal Transfer Process

The bismuth flow rate through the two upper contactors in the rare-earth removal system is 12.5 gpm, and the LiCl flow rate is 33 gpm. These extraction columns are 7 to 13 inch in diameter and are packed with 1/2-inch Raschig rings. Each is equivalent to three equilibrium stages.

The trivalent and divalent rare earths are removed in separate contactors in order to minimize the amount of lithium required. Only 2% of the LiCl, or 0.66 gpm is fed to the two-stage divalent rare-earth removal contactor, where it is contacted with 0.58-gal/day bismuth stream containing 50 atom % lithium. The trivalent stripper, where the LiCl is contacted with bismuth containing 5 atom % lithium, is equivalent to one equilibrium stage.

The bismuth stream containing the reductant necessary for the isolation of protactinium is actually fed to the recirculating bismuth stream in the rare-earth removal system. An equivalent amount of bismuth is withdrawn from the stream and is fed to the protactinium isolation column. This allows for more nearly complete extraction of the protactinium and provides a means for removing materials which might otherwise accumulate in the recirculating stream.

The remaining steps in the flowsheet consist in combining the processed salt with uranium and purifying the resulting fuel salt. The uranium addition is accomplished by absorbing the UF_6-F_2 stream from the fluorinators into fuel salt containing UF_4, which results in the formation of soluble, nonvolatile UF_5. The UF_5 is then reduced to UF_4 by contact with hydrogen. The HF resulting from reduction of UF_5 is electrolyzed in order to recycle the contained fluorine and hydrogen. Recycle of these materials is used in order to avoid waste disposal charges on the material that would be produced if the HF were absorbed in an aqueous solution of KOH. The salt will be contacted with nickel wool in the purification step in order to ensure that the final bismuth concentration is acceptably low.

The protactinium removal time obtained with the flowsheet is 10 days, and the rare-earth removal times range from 17 to 51 days, with the rare earths of most importance being removed on 27- to 30-day cycles. The flowsheet is relatively insensitive to minor variations in operating conditions such as changes in temperature, flow rates, reductant concentrations, etc. (10,11). The thorium/rare-earth separation factor decreases sharply as the concentration of fluoride in the LiCl is increased; contamination of the LiCl would result from entrainment of fuel salt by the bismuth stream leaving the upper contactor. The effect is largely an increase in the rate at which thorium is removed with the rar earths.

The thorium removal rate increases from about 0.4 mole/day with no fluoride in the LiCl to about 280 moles/day when the LiCl contains the equivalent of 5 mole % LiF. The effect of fluoride in the LiCl on the removal of rare earths is negligible. In fact, the rare-earth removal efficiency increases slightly as the fluoride concentration in the LiCl increases. In addition, contact of LiCl containing fluoride with BCl_3 has been found to result in formation of volatile BF_3 (12), and thus fluoride can be removed from LiCl easily by this means.

The reliable removal of decay heat from the processing plant is an important consideration because of the relatively short decay time before the salt enters the processing plant. A total of about 6 MW of heat would be produced in the processing plant for a 2300 MWt MSBR. Since molten bismuth, fuel salt, and LiCl are not subject to radiolytic degradation, there is not the usual concern encountered with processing of short-decayed fuel.

Waste Streams Produced by Processing Plant

All high-level waste streams produced by the protactinium and rare-earth removal systems can be combined (10) for uranium recovery prior to disposal, as shown in Fig 4-44. In this operation, waste salt from the protactinium decay tank would be combined with the discard stream of fuel carrier salt. The lithium-bismuth stream from the trivalent-rare-earth stripper would be hydrofluorinated in the presence of the resulting salt, and the combined stream would be held for protactinium decay. The protactinium concentration in the combined stream would be only 500 ppm initially, and the specific heat generation rate would be acceptably low. The salt in the waste holdup tank would be fluorinated before discard to recover uranium in order that the loss of fissile material can be made acceptably low. The composition of the discarded salt would be 74.7-13.5-9.5-0.8 mole % $LiF-ThF_4-BeF_2-ZrF_4$, 1.2 mole % trivalent-rare-earth fluorides, and 0.3 mole % divalent-rare-earth fluorides. The salt temperature would have to be maintained at about 600°C so that the trivalent-rare-earth fluorides would not precipitate. This processing scheme would require that salt be discarded at the rate of 60 ft^3 every 220 days.

Thorium is discarded from the system at the rate of about 50 moles/day. Flowsheet modifications have been developed, however, that will not require discard of thorium and which will result in almost complete utilization of thorium.

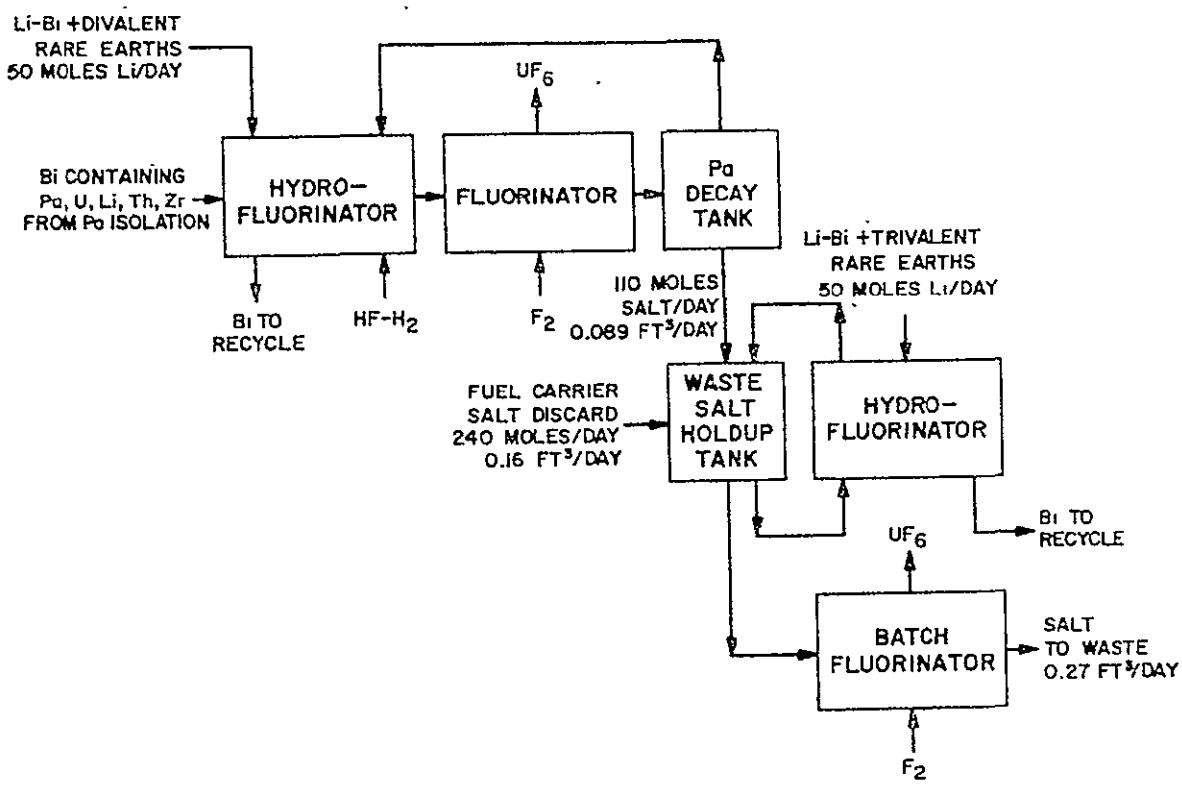

Fig. 4-44 Method for Combining Waste Streams From Protactinium Isolation and Rare Earth Removal Processes. Flow rates are shown for an assumed uranium removal efficiency in the primary fluorinator of 99%.

An additional high-level solid waste stream, which contains most of the iodine and bromine removed from the reactor, is produced by the H_2-HF purification and recycle system (shown in Fig. 4-45). The H_2-HF streams leaving the fuel reconstitution step, the hydrogen-reduction columns, purge columns, and hydrofluorinators are combined, compressed to about 2 atm pressure, and chilled to -40°C in order to condense HF from the stream for production of hydrogen and fluorine for recycle by electrolysis. Large fractions of the HI, HBr, SeF_6, and TeF_6 are expected to be dissolved in the hydrogen fluoride condensate. These compounds are more volatile than hydrogen fluoride and can be separated by low-temperature distillation at 2 atm pressure.

The gas stream leaving the top of the distillation column, which will contain HF, HBr, and HI, is combined with the gas stream leaving the HF condenser, which will contain a small quantity of HF, and the resulting stream is scrubbed with an aqueous KOH solution for removal of the halides. The gas stream is dried in regenerative silica gel sorbers and is recycled. About 5% of the hydrogen is fed through beds of activated alumina and charcoal for removal of SeF_6, TeF_6, and noble gases, which are not removed by the KOH.

The halides are accumulated in the KOH scrubber solution for a period of 34 days, after which the solution is held for a 45-day decay period. The solution is then evaporated in 24-inch-diameter, 10-foot-long waste containers. Two waste containers are filled annually.

A number of corrosion environments will be present in the processing plant, and materials that will withstand attack are required. The conditions of greatest severity consist of the following:

1. The presence of molten salt and gaseous mixtures of F_2 and UF_6 at 500 to 550°C.
2. The presence of molten salts and bismuth containing lithium and thorium at 550 to 650°C, and
3. The presence of HF-H_2 mixtures and mixtures of molten fluorides at 550 to 650°C.

Molten-salt fluorinators could be constructed of nickel or nickel-base alloys. Corrosion in these systems will be limited by frozen salt, so that the protective NiF_2 layer will not be removed from the metal surface by dissolution in the molten salt.

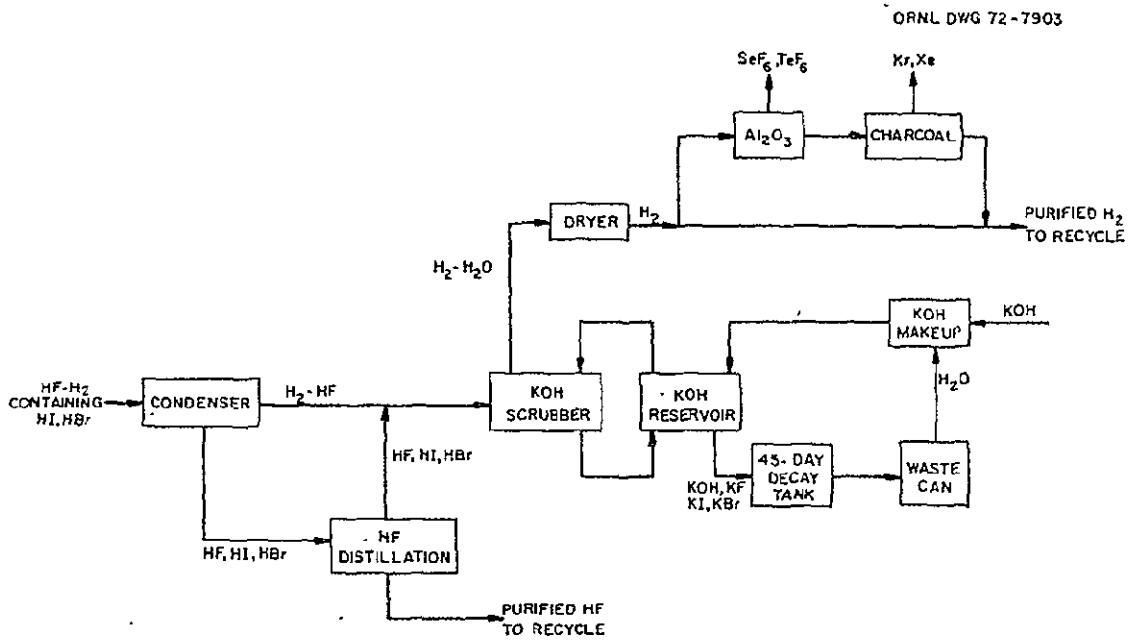

Fig. 4-45 Hydrogen - HF Purification and Recycle System.

The selection of molybdenum as a procession plant material was based on corrosion investigations at ORNL and elsewhere which showed it to resist dissolution and chemical attach in molten bismuth. The studies at ORNL were conducted in small thermal convective loops which provided a temperature gradient of 100 to 200°C in the bismuth circuit. Tests were conducted on low-carbon molybdenum and the allow TZM in pure bismuth and bismuth containing up to 0.01 wt % (0.3 atom %) Li. Mass transfer was negligible in the temperature range 500 to 700°C for periods as long as 3000 hour. Tests carried out in static bismuth also have shown no effect of stress on the corrosivity of molybdenum.

Studies have been carried out for the development of braze materials for joining molybdenum that are resistant to corrosion by bismuth and molten salts (14). An iron-base alloy (Fe-15%, Mo-5% Ge-4% C-1% B) has been found to have good wetting and flow properties, a moderately low brazing temperature (<1200°C), and adequate resistance to bismuth at 650°C.

The results of work to date on molybdenum fabrication techniques have been quite encouraging, and it is believed that the material can be used in building processing plants if proper attention is given to its fabrication characteristics.

Other refractory metals that are resistant to attack in molten bismuth include pure tungsten and certain tantalum alloys. Tungsten, because of its relatively high ductile-brittle transition temperature, may not be amenable to the fabrication and joining operations required for a full-sized processing plant. However, it is being used as a surface coating at several points in the molybdenum extraction facility. The coatings are deposited by chemical vapor deposition (8) and serve as additional seals on the joints made with tube expanders or by welding.

Corrosion tests in molten Bi and Bi-Li solutions have been conducted on pure tantalum and the tantalum alloy T-111 (8% W, 2% HF, bal Ta). In quartz thermal convection loops at 700°C, the mass transfer rate of pure tantalum in these liquid metals was greater than that of molybdenum, although the rate was still less than 3 mils/year. Mass transfer rates of the alloy T-111 were comparable to those for molybdenum, but the mechanical properties of the former alloy were strongly affected by interaction with interstitial impurities, primarily oxygen, in the quartz-pure-bismuth loop experiments. A test carried out at 700°C with the Bi-2.5 wt % Li mixture in a loop constructed of T-111 tubing did not measurably affect the mechanical properties of the T-111, and the mass transfer rate again was insignificant.

Several complex assemblies have been fabricated at ORNL using the T-111 alloy, the largest of which was a forced convection loop which circulated liquid lithium for 3000 hr at 1370°C. In contrast to molybdenum, the alloy is quite ductile in the as-welded condition; thus it appears promising for complex geometries that would operate principally in Bi or Bi-Li solutions and only occasionally in fuel salt.

Graphite, which has excellent compatibility with the fuel salt, also shows promise for the containment of bismuth. Of course, in a chemical processing application, the absence of a neutron flux allows greater flexibility in the selection of graphite grade and fabrication history than for a reactor core.

Compatibility tests to date have shown no evidence of chemical interaction between graphite and bismuth containing up to 3 wt % (48 atom %) Li. However, the largest open pores of most commercially available polycrystalline graphties are penetrated to some extent by liquid bismuth. Static capsule tests (15) of three commercial graphites (ATJ, AXF-5QBG, and Graphitite A) were conducted for 500 hours at 700°C using both high-purity bismuth and Bi-3 wt % (48 atom %) Li. Although penetration by pure bismuth was negligible, the addition of lithium to bismuth appeared to increase the depth of permeation and, presumably, the wetting characteristics of the bismuth.

There are several approaches that have potential for sealing a porous graphite against penetration by the bismuth and bismuth-lithium alloys. Two well-established ones are (1) multiple liquid hydrocarbon impregnations that are carbonized and/or graphitized and (2) pyrocarbon coatings. Another possible approach is the use of carbide-forming sealants. Each of these sealing approaches is being evaluated in bismuth loop experiments. We are also studying the wetting characteristics of graphite as a function of surface pretreatments such as dedusting, alcohol wash and oven dry, and vacuum degassing at 700 to 1000°C.

Nickel or a nickel-base alloy would be used for the oxide precipitation portions of a plate based on an oxide precipitation-metal transfer for fluorinators for removal of uranium from molten fluoride mixtures, and for portions of the plant that contain gaseous mixtures of F_2, UF_6, and HF. Many years of experience have been accumulated in the fabrication and joining of this class of alloys, stemming from the construction of reactors and associated hardware as well as fluoride salt purification equipment.

Although one would limit the corrosion rate in continuous fluorinators by the maintenance of a frozen-salt film next to the container wall, the chemical corrosion of nickel and nickel-base alloys has been evaluated at ORNL under the severe environmental conditions endemic to fluorination processes. Much of this information has evolved from fuel-recovery operations conducted with metallic reactor fuel elements using molten fluoride mixtures in which UF_4 was converted to volatile UF_6 by fluorine sparging.

During these studies, a number of materials were exposed to gaseous fluorine and molten salt. Most of the data were obtained during operation of two plant-scale fluorinators constructed of "L" nicket at temperatures ranging from 540 to 730°C. A number of corrosion specimens (20 different materails) were located in the fluorinators. The specimen showing the least attack, Hymu 80, had a maximum bulk loss rate of 11 mils/month based on total time in molten salt.

Overall Evaluation of Processing Capability

The probability is quite high that the technology required for processing the fuel salt from an MSBR will be developed. There are presently no major obstacles to the isolation of protactinium by the fluorination is progression well and is expected to culminate in the successful development of continuous fluorinators.

Although the metal transfer process for removal of rare earths requires the use of molten bismuth containing reductant, several candidate materials of construction for this portion of the plant appear to be acceptable. Careful design of salt-metal contactors will prevent entrainment of bismuth in the fuel salt and that the concentration of bismuth can be reduced to the required low levels. On-line instruments have been developed for use in processing experiments, and efforts to develop the additional instrumentation required for a processing plant should be successful.

4.6.3 Nuclear Thermionic SPS

Sixteen modules, each one GWe, are baselined for a 10 GWe ground output SPS. The transmitter and power generating systems are rigidly connected; the entire system is attitude controlled to mechanically point the transmitter to the rectenna (additional electronic pointing is of course required).

Each generating module is located in the center of the square radiator area associated with that module. Distributing the modules in this fashion increases the distance over which electrical distribution occurs. The resultant mass penalty is less than the radiator manifold mass penalty which would occur if the modules were clustered together. The radiators sections are arranged 90^{o} apart to minimize their mutual view factor (thermal interaction).

Modules requiring maintenance are undocked and separated as described in the preceding text section. The concept is shown in Figure 4-46.

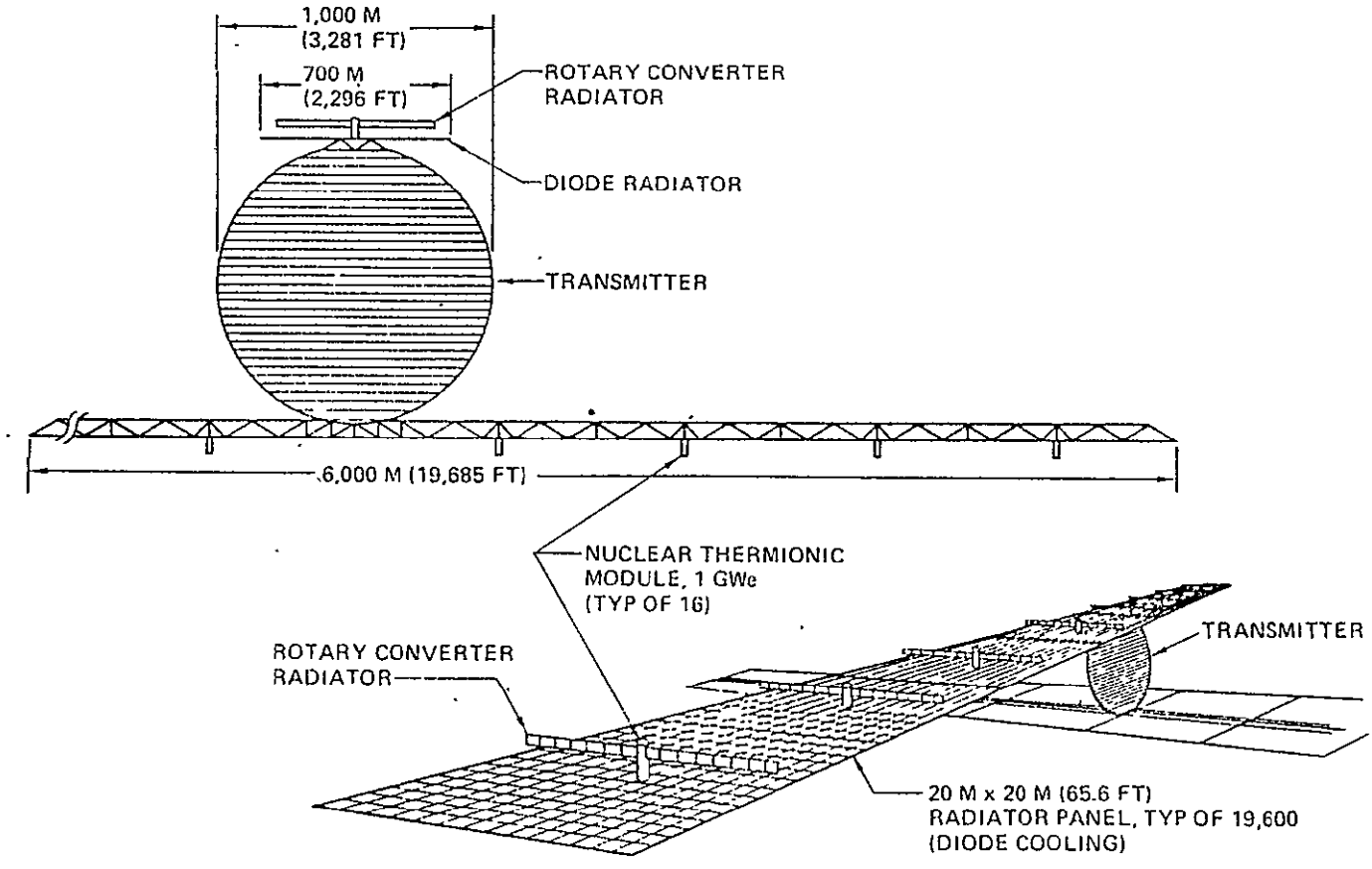

FIGURE 4-46 NUCLEAR THERMIONIC SPS

Subsequent analysis has shown that the nuclear thermionic SPS is not feasible with 1985 technology. Materials considerations limit the emitter temperature to 1,030K ($1,394^{o}$F) using a molten salt breeder reactor heat source. With a 1,030K emitter temperature and 400K (260^{o}F) radiator temperature, the thermionic diode efficiency

is only 23%. Thus, 77% of the total energy must be dissipated as waste heat and the required radiator needs more pumping power than the electric power produced by the diodes. An increase in radiator temperature to reduce pumping power produces a substantial decrease in diode efficiency; thereby increasing the required waste heat to be dissipated. As a result, the electric power produced is still less than the required pumping power.

4.6.4 Nuclear Brayton Cycle SPS

The nuclear Brayton cycle SPS contains sixteen 1 GW busbar output molten salt breeder reactor modules. The main structure of the satellite consists of a spine with sixteen ribs to which are attached the reactor modules and their primary radiators. Each reactor module has secondary radiators for cooling the generators and nuclear fuel processing systems. The ground output of the nuclear Brayton cycle power satellite is 10 GW. The concept is shown in Figure 4-47.

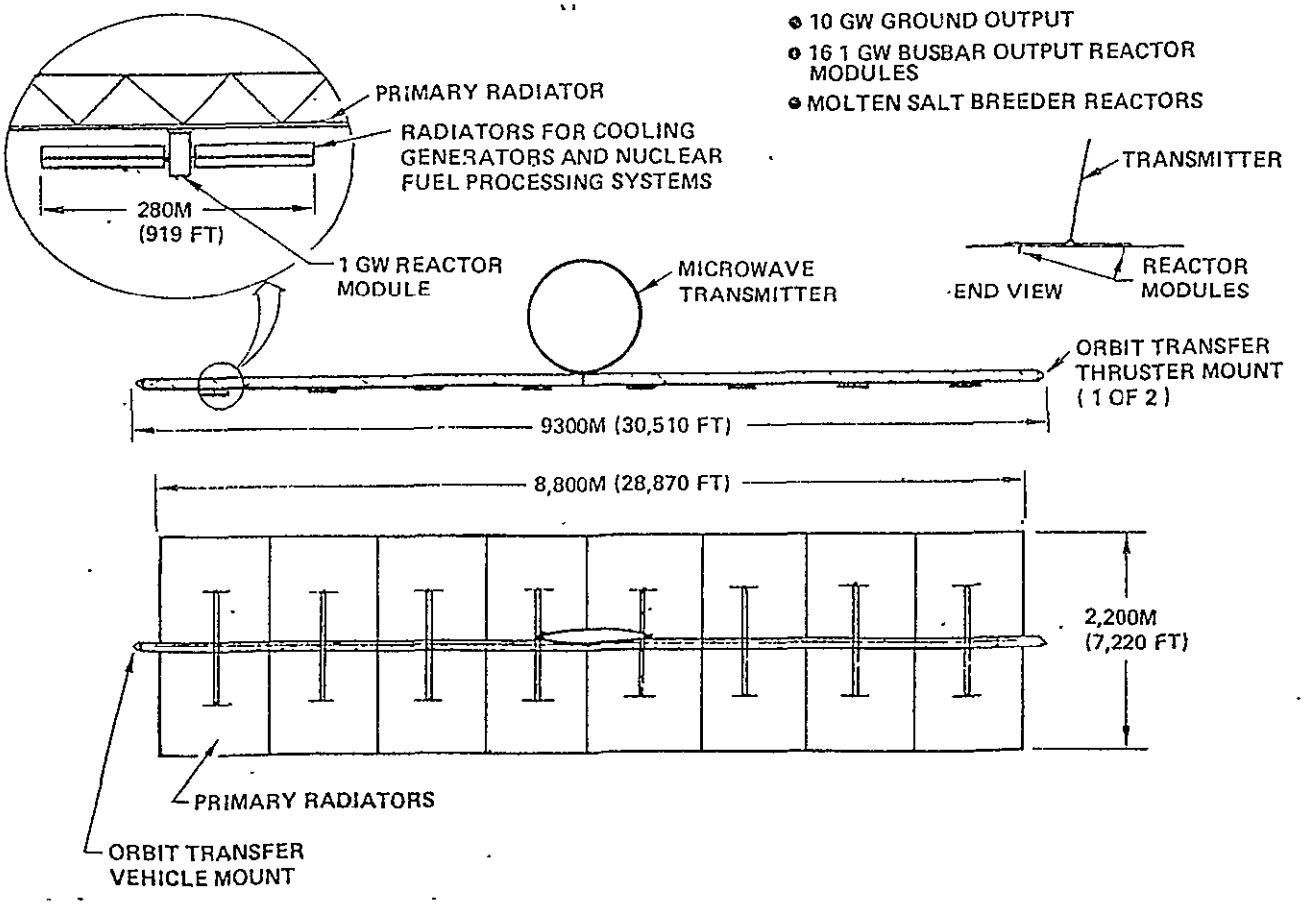

FIGURE 4-47. NUCLEAR BRAYTON CYCLE SPS

4.6.5.1 GWe Nuclear Brayton Cycle Module

In the baseline concept, Figure 4-48, sixteen of these modules are used to provide 10 GWe ground output. The molten salt breeder reactor (MSBR) is spherical. The shield to reduce the radiation level at the transmitter is located only along lines-of-sight to the transmitter. Molten salt flows to six salt-to-helium heat exchangers. Hot helium then flows to turbines of the Brayton rotating unit (three, with one generator each). Six recuperator modules surround the turbomachines. The helium-to-liquid metal (NaK) heat exchangers (coolers) are located in the recuperator housings. NaK accumulators (volume make-up) and pumps are located between the recuperators and the fuel process carousel. High and low temperature NaK and electrical power pass through the interface to the powersat main frame (on left).

A small flow of molten salt is continuously circulated through the fuel process module, which accomplishes the following:

- o Removes protactinium (which decays to uranium)
- o Removes other wastes
- o Removes bred fuel
- o Accepts fertile fuel
- o Adjusts salt mixture

The fuel process module is located on a continuously rotating carousel; the resultant inertial forces simulate gravity and permit operation of the countercurrent separation columns. Module servicing (e.g., waste removal) is accomplished through the docking port on the right.

The battery stack on the right is part of the system which allows the reactor module to separate and operate as an independent spacecraft. Propulsion and attitude control systems are located at the left, delta velocity capability is nominally 100m (328 ft/sec) which allows a malfunctioning reactor system to be undocked and separated a safe distance from the powersat which continues to operate at a reduced power level.

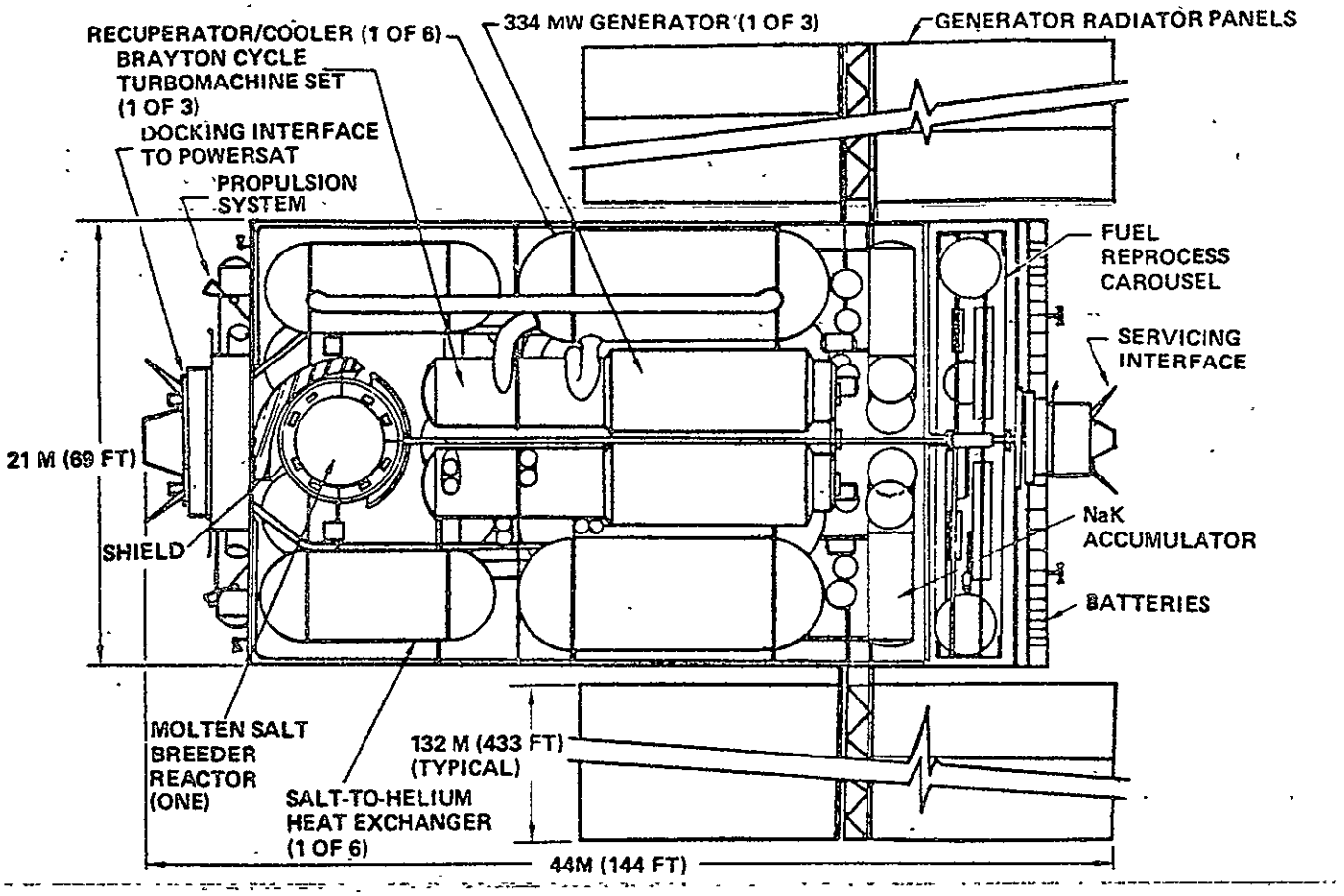

FIGURE 4-48 IGWe NUCLEAR BRAYTON CYCLE MODULE

References

(1) Lundholm, J. G., "NASA Thermionic Converter Research and Technology Program" 10th IECEC Proceedings, August 1975.

(2) Newby, G. A., "The ERDA Thermionic Program", 10th IECEC Proceedings, August 1975.

(3) M. E. Whatley, L. E. McNeese, W. L. Carter, L. M. Ferris and E. L. Nicholson, Nucl. Appl. Tech. 8, (1970)

(4) MSR Program Semiannu. Progr. Rep. Feb. 28, 1969, ORNL-4396.

(5) L. E. McNeese,Engineering Development Studies for Molten-Salt Breeder Reactor Processing No. 5, ORNL-TM-3140 (October 1971)

(6) L. M. Ferris, J. C. Mailen, J. J. Lawrence, F. J. Smith, and E. D. Nogueria, J. Inorg. Nucl. Chem. 32, 2019-35 (1970)

(7) L. E. McNeese, Engineering Development Studies for Molten-Salt Breeder Reactor Processing No. 2, ORNL-TM-3137 (February 1971).

(8) MSR Program Semiannu. Progr. Rep. Feb. 28, 1970, ORNL-4548.

(9) L. M. Ferris, F. J. Smith, J. C. Mailen, and M. J. Bell, J. Inorg. Nucl. Chem. 34, 313-20 (1972)

(10) L. E. McMeese, Engineering Development Studies for Molten-Salt Breeder Reactor Processing No. 8, ORNL-TM-3258 (May 1972).
(11) L. E. McNeese, Engineering Development Studies for Molten-Salt Breeder Reactor Processing No. 6, ORNL-TM-3141 (December 1971).
(12) MSR Program Semiannu. Progr. Rep. Aug. 31, 1970, ORNL-4622.
(13) C. E. Bamberger and C. F. Baes, Jr., J. Nucl. Mater. 35, 177 (1970).

4.7 RADIATORS

4.7.1 Analysis and Modeling

A computer analysis was conducted of radiator configurations designed to withstand the predicted meteoroid environment. Three basic radiator configurations were studied. Fig. 4-50 shows a section view and the thermal analysis nodal networks for each configuration.

Configuration A relies on increased armor thickness around each tube for meteoroid protection; whereas Configurations B and C utilize fin structure as a bumper to fragment the meteoroids.

45 parameter runs were conducted for each configuration to evaluate the optimum combination of tube pitch, tube diameter, and fin thickness.

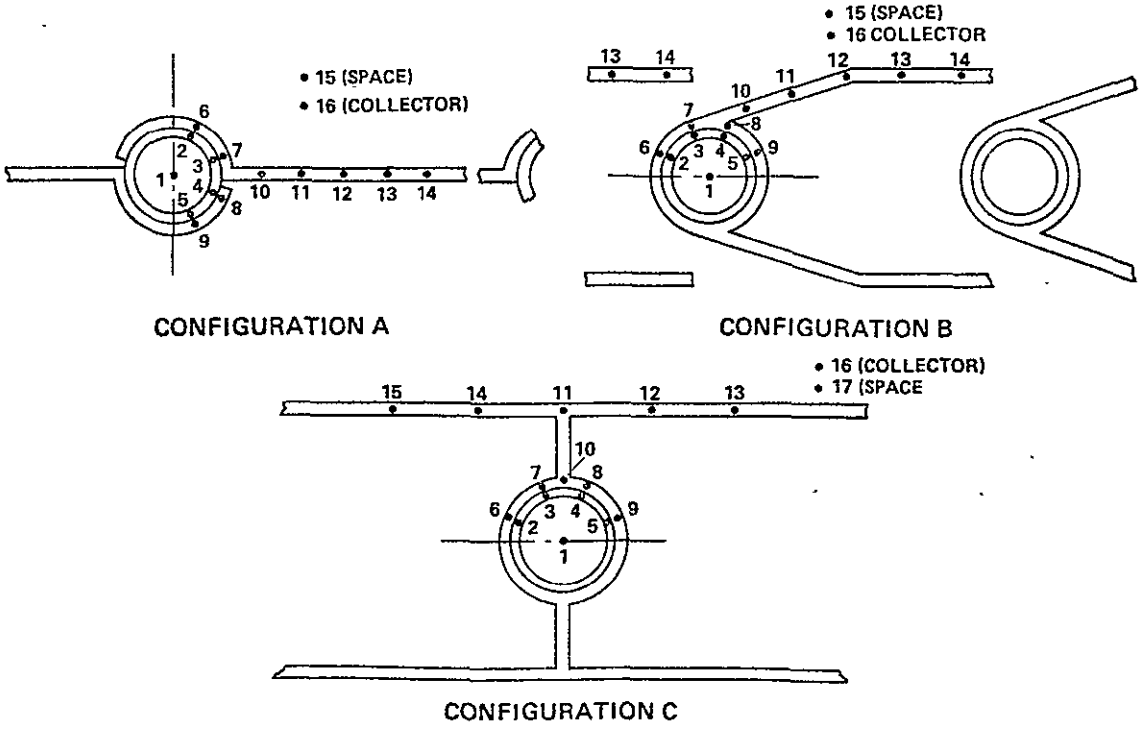

FIGURE 4-50 RADIATOR CONFIGURATIONS

A segment of radiator structure (Fig. 4-51) was divided into a nodal network and a steady-state energy balance was calculated at each node by a digital computer program. The Beta Computer Program solves steady-state and transient thermal problems when radiative, convective, and conductive thermal paths are defined.

The heat rejection of a unit area of radiator surface was calculated as a function of radiator fluid temperature and the results were then integrated along a tube length to determine the drop in fluid temperature (Figure 4-52). A summation of the results for a single tube enabled the calculation of total radiator performance.

A comparison was made of radiator performance when tube pitch, tube diameter, and fin thickness were systematically varied to achieve an optimum configuration

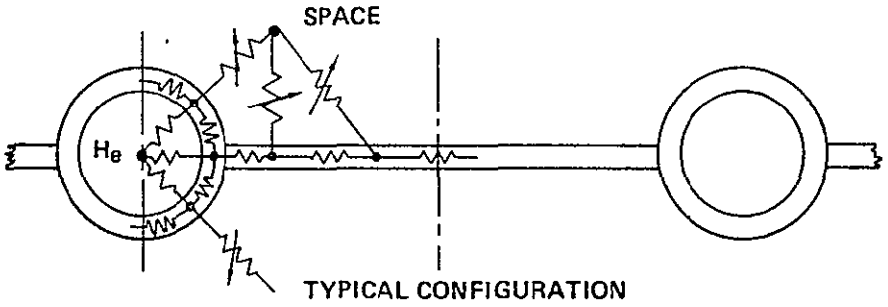

PARAMETER VARIABLES

- HELIUM FILM COEFFICIENT
- THERMAL CONDUCTIVITY
- FIN THICKNESS
- TUBE DIAMETER
- TUBE SPACING
- EMISSIVITY
- TUBE LENGTH

FIGURE 4-51 BETA PROGRAM SOLVES THERMAL NETWORK MODELING OF RADIATOR STRUCTURE

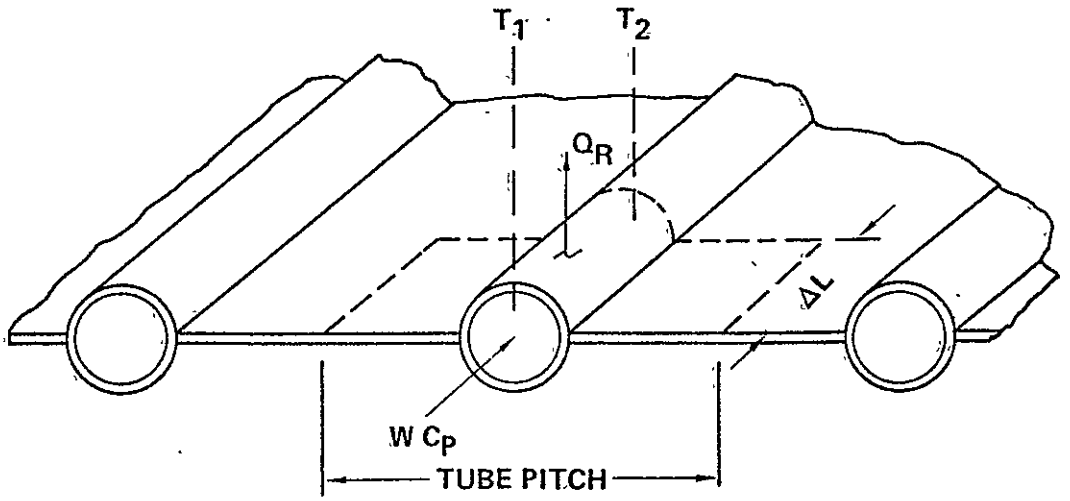

$W C_P (T_1 - T_2) = Q_R \cdot \Delta L$

Q_R = HEAT REJECTION/UNIT LENGTH

FIGURE 4-52 RADIATOR THERMAL MODEL

Two radiator concepts(Fig. 4-53) were baselined as a result of an optimization exercise which selected the ratio of radiator temperature to Brayton cycle turbine inlet temperature. For minimum system weight this ratio is approximately 0.35. For Program A (1990) the maximum turbine inlet temperatures with superalloys (e.g. columbium) is 1300 K (1880°F); for Program B (2000) a turbine inlet temperature of 1750 K (2690°F) is baselined for refractory metals or ceramics. (The feasibility of silicon carbide heat absorber tubing for Program A, at 1470 K (2186°F) is still under investigation.) The above turbine inlet temperatures were used in a preliminary cycle design to select the radiator concepts.

	1990 superalloy	2000
T_{in} K/°F	657/723	986/1315
T_{out} K/°F	459/366	702/804
$\bar{T}_{gas}$ K/°F	535/503	813/1003
$\bar{T}_{rad}$ K/°F	481/406	732/858
Q/A kW/m^2/btu/ft^2 sec	2.73/0.240	14.6/1.29
P_{in} N/m^2/lb/in.^{2}	3.4×10^6/500	3.4×10^6/500
ΔP	0.015	0.015
Total radiating area m^2/ft^2	10.9×10^6/1.17×10^8	2.5×10^6/2.67×10^7
Projected area of each of eight panels m^2/ft^2	6.8×10^5/7.32×10^6	1.56×10^5/1.68×10^6

FIGURE 4-53 BASELINE RADIATORS

Many of the early studies were based on the use of helium as a radiator fluid because a trade study comparing helium with NaK showed helium provided a lighter system. Hence, the results shown in Figures 4-54 to 4-57 are based on helium as the working fluid. However, it later developed that substantial advantages in the Brayton cycle turbomachinery loop resulted if heat were transferred from the Brayton gas loop to a radiator NaK loop. NaK radiator fluid was used as baseline for later studies (Figures 4-59 through 4-64).

Optimum configurations of three types of radiator are shown in Figure 4-54. All take advantage of the anisotropic meteoroid flux and preferential panel orientation. Configuration A uses solid armor around the tubes and radiates heat from both sides of the fin. Configurations B and C use meteoroid bumpers, the outer sheet breaks up the meteoroids so that dispersion occurs before the tube is reached. Each candidate was designed to provide protection against particles of at least .001 gm (.0000022 lbm). Tubes were suzed by the 30-year creep rupture strength with a minimum factor of safety of 2.0. For equivalent thermal and meteoroid protection, Configuration C yields the lightest radiator.

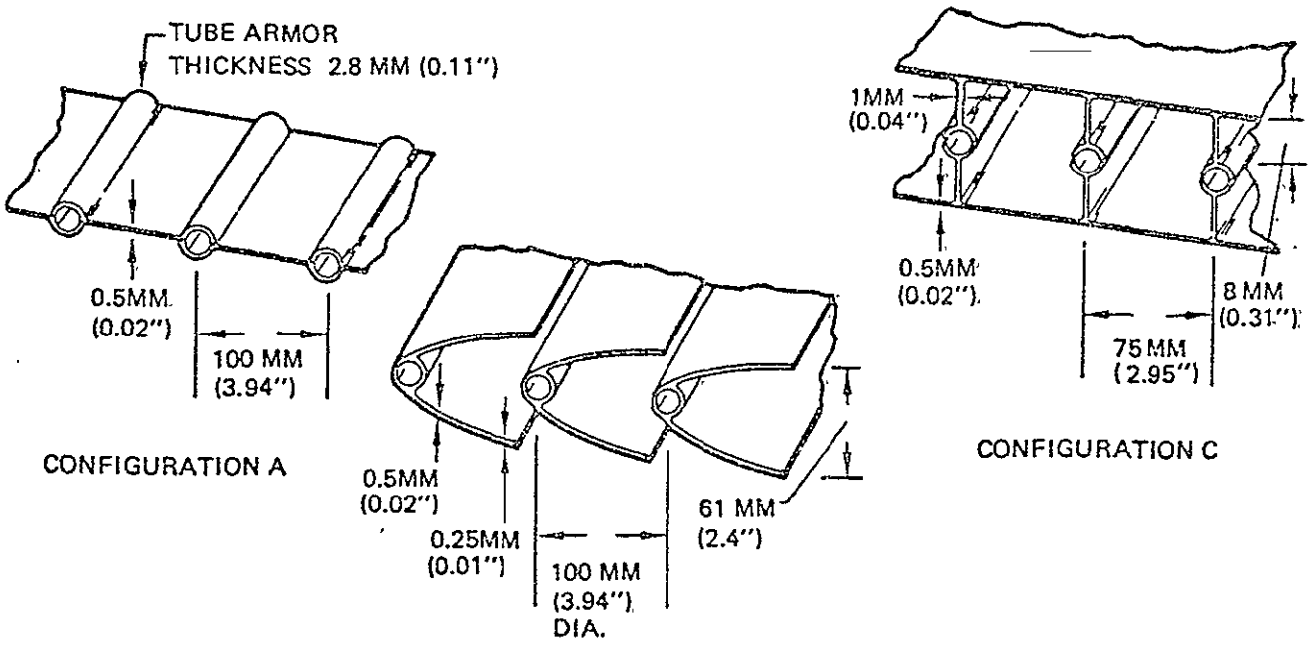

NOTE: TUBE DIAMETER IS 12.7 MM (0.5"), WALL THICKNESS 0.13MM (0.005")

FIGURE 4-54 OPTIMUM RADIATOR PANEL DIMENSIONS - LOW TEMPERATURE HELIUM RADIATOR

Fig. 4-55 shows radiator heat rejection on an area basis. It is relatively insensitive to tube diameter.

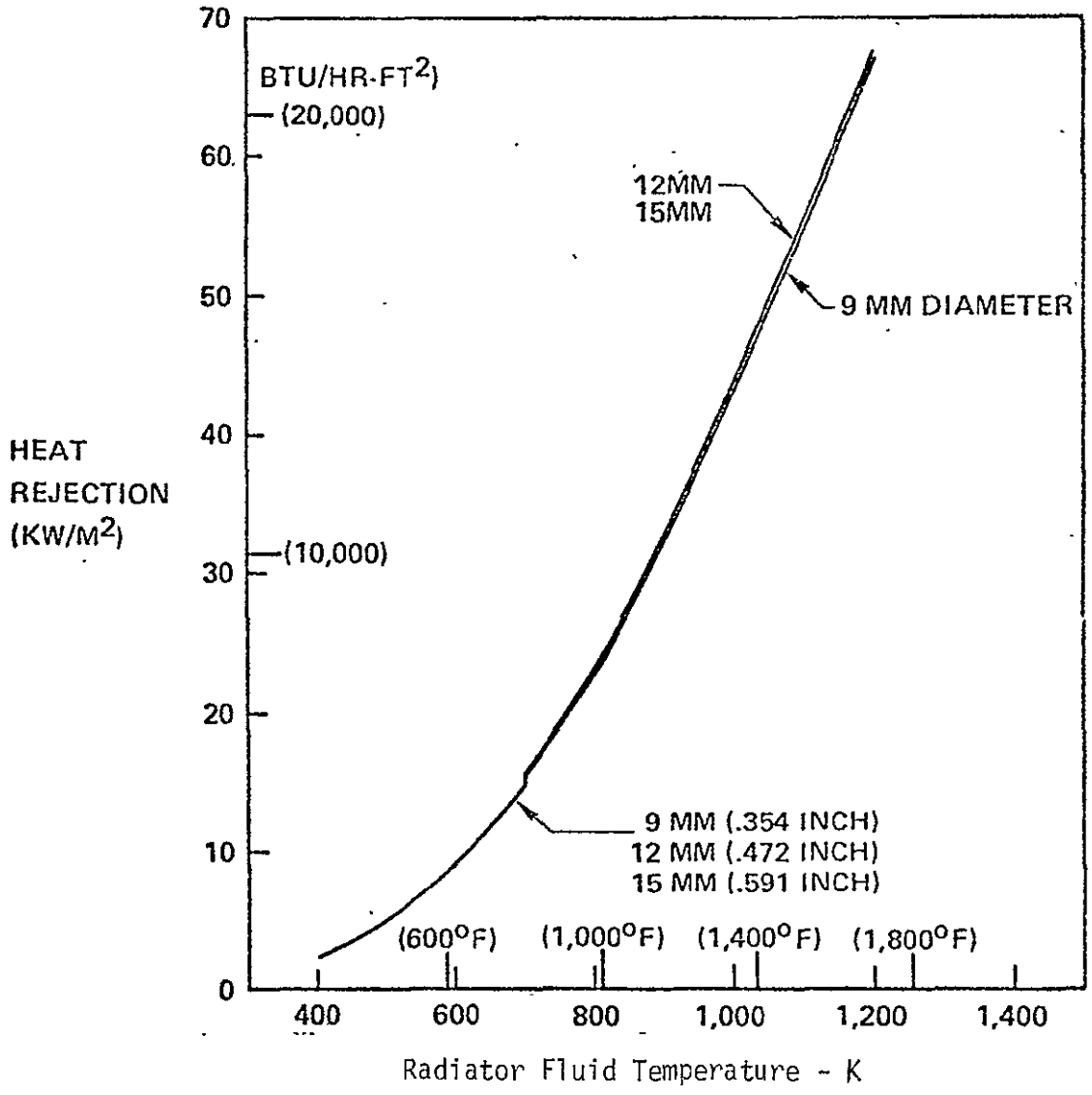

FIGURE 4-55 RADIATOR HEAT REJECTION HELIUM FLUID

Fig. 4-56 shows the specific heat rejection (kW/kg or BTU/hr lbm) of radiator tube/fin panels with various tube diameters.

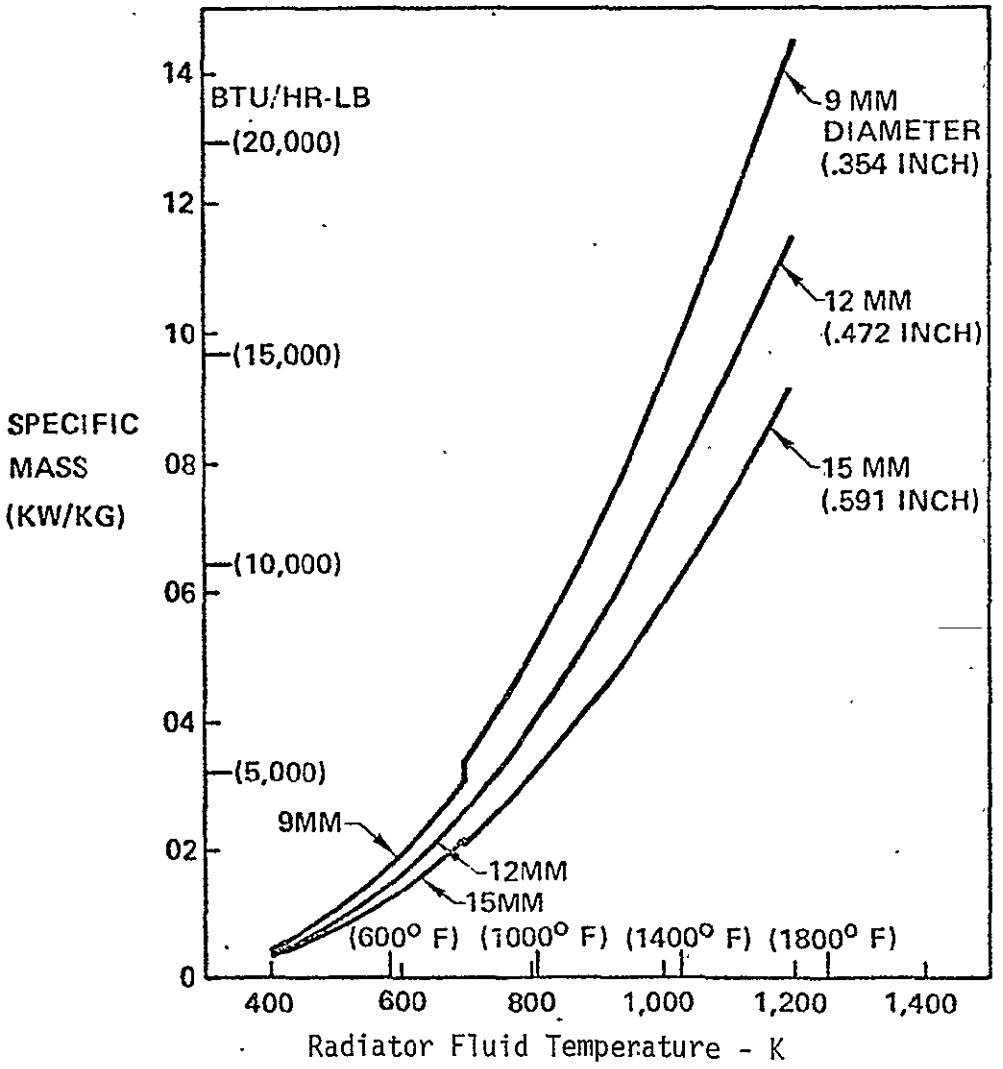

FIGURE 4-56 RADIATOR PANEL MASS HELIUM FLUID

Table 4-30 shows optimum dimensional and performance data for the three configurations analyzed. Configuration 3 provided the best performance with year 1990 materials and fluid temperatures.

Configuration 4 shows material and dimensional modifications providing optimum performance with year 2000 radiator requirements.

TABLE 4-30 OPTIMUM CONFIGURATIONS, HELIUM RADIATOR FLUID

Configuration	Average fluid temp K (°F)	Fin material	Tube material	Tube diameter mm(inches)	Fin thickness mm(inches)	Tube pitch mm(inches)	Heat rejection kw/m2 (Btu/hr-ft^2)	Heat rejection kw/kg (Btu/hr-lb)
 1	535 (503)	Aluminum 6061	Haynes 188	12.5 (.50)	.5 (.02)	100 (4.0)	5.55 (1759)	1.12 (1742)
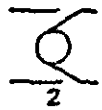 2	535 (503)	Aluminum 6061	Haynes 188	12.5 (.50)	.5 (.02)	75 (3.0)	4.33 (1373)	1.04 (1610)
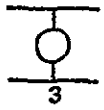 3	535 (503)	Aluminum 6061	Haynes 188	12.5 (.50)	.5 (.02)	75 (3.0)	5.95 (1889)	1.26 (1952)
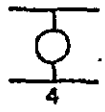 4	850 (1070)	Beryllium	Columbium B66	12.5 (.50)	.5 (.02)	50 (2.0)	25.6 (8127)	5.82 (9012)

Fig. 4-57 shows that a much greater portion of the total radiator mass is allocated to the panels with the low temperature (year 1990) radiator system. This results from the substantially greater radiating area required with the low temperature system since heat rejection is proportional to the fourth power of the absolute surface temperature.

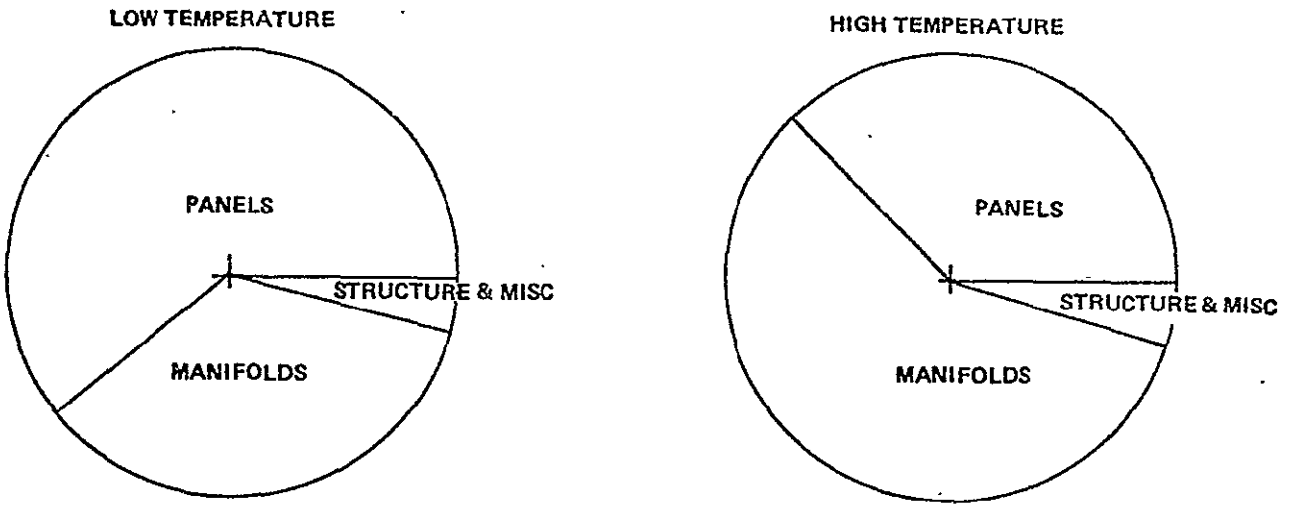

FIGURE 4-57 RADIATOR MASS DISTRIBUTION HELIUM

Tab. 4-31 shows the relative mass of radiators designed for the year 1990 and year 2000 powersats.

Substantial reduction in radiator surface area and panel mass results with year 2000 (high temperature) components due to the higher operating temperature.

A lesser mass reduction occurs in the manifolds of the high temperature configuration, because, although the headers are shorter, greater wall thickness is necessary due to lower allowable stresses.

TABLE 4-31 MASSES OF HIGH AND LOW TEMPERATURE HELIUM RADIATORS

Item	Low temperature		High temperature	
	10^6 kg	10^6 lbm	10^6 kg	10^6 lbm
Panels	24.7	54.4	7.0	15.4
Manifolds	13.3	29.3	10.6	23.4
Structures, miscellaneous	1.7	3.7	0.9	2.0
Total	39.7	87.4	18.5	40.8

A trade study was conducted to compare a gaseous helium radiator concept with a liquid NaK radiator. The use of liquid NaK will require an additional gas-liquid heat exchanger and a circulating pump.

Fig. 4-58 shows flow diagrams for the two systems. Pressure drop in the helium loop will be reduced with the NaK system with a resultant improvement in engine efficiency and the denser fluid allows smaller headers.

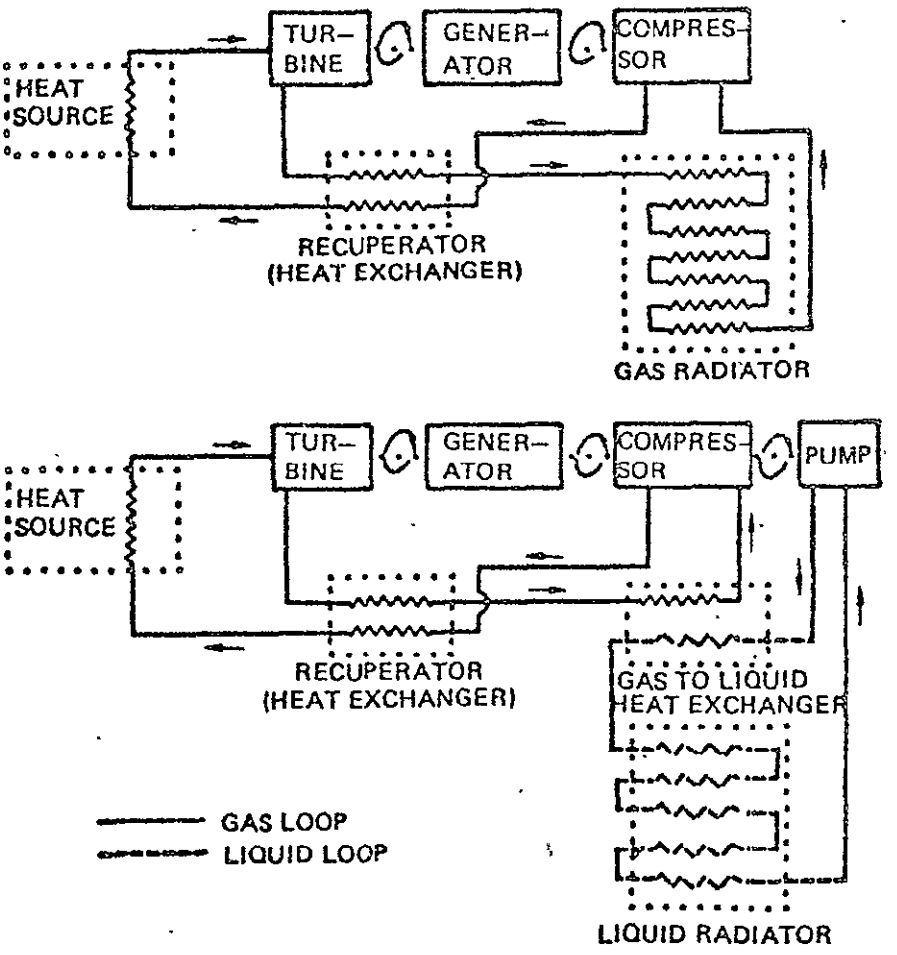

FIGURE 4-58 USE OF LIQUID RADIATOR WITH BRAYTON CYCLE REQUIRES ADDITIONAL HEAT EXCHANGER

All liquid radiator working fluid candidates for the inlet temperature range of interest of 657K to 986K (723°F to 1315°F) are alkali metals. Selection was based on compatibility with the tubing material, stability over the temperature range and the fusion point. A near-eutectic of sodium and potassium (NaK) was selected; the boiling point is 1057K (1443°F), the fusion point is 262K (+12°F). Compatibility with columbium for exposure times up to three years has been demonstrated. Liquids provide high transfer rates and, due to their density, small header dimensions relative to helium. However, a separate gas-to-liquid heat exchanger is required for the Brayton cycle variants, and pump power and weight must be considered. Use of a separate gas-to-liquid heat exchanger can significantly reduce the pressure drop in the gas cycle. Table 4-shows masses for helium and NaK radiators (high temperature variant) which reject heat appropriate to the generation of 16 GW by a helium Brayton cycle.

Each of these systems was optimized for minimum total weight. One factor contributing to the higher mass of the NaK system is the temperature drop across the gas-to-liquid heat exchanger of 30K (54°F) which reduces the radiator effectiveness. The "Brayton cycle efficiency factor" is the mass of solar concentrator and absorber system necessary to counter the efficiency loss resulting from the higher pressure drops in the gas system.

TABLE 4-32 MASSES OF GAS AND LIQUID RADIATORS

Item	Helium		NaK	
	10^6 kg	10^6 lbm	10^6 kg	10^6 lbm
Panels	7.0	15.4	5.5	12.1
Manifolds	10.6	23.4	4.0	8.8
Structure, miscellaneous	0.9	2.0	0.8	1.8
Working fluid	—	—	7.6	16.8
Gas-to-liquid heat exchanger	—	—	8.5	18.7
Pumps + pump power penalty	—	—	3.0	6.6
Brayton cycle efficiency factor	2.5	5.5	—	—
Totals	21.0	46.3	29.4	64.8

The optimum radiator panel configuration for the baseline Brayton cycle is shown in Fig 4-59. Liquid NaK is circulated through thin wall Haynes 188 alloy tubing.

Aluminum radiating fins are bonded to the tubing and provide a bumper for protection against meteoroids. Segmented construction is used to minimize thermal stresses.

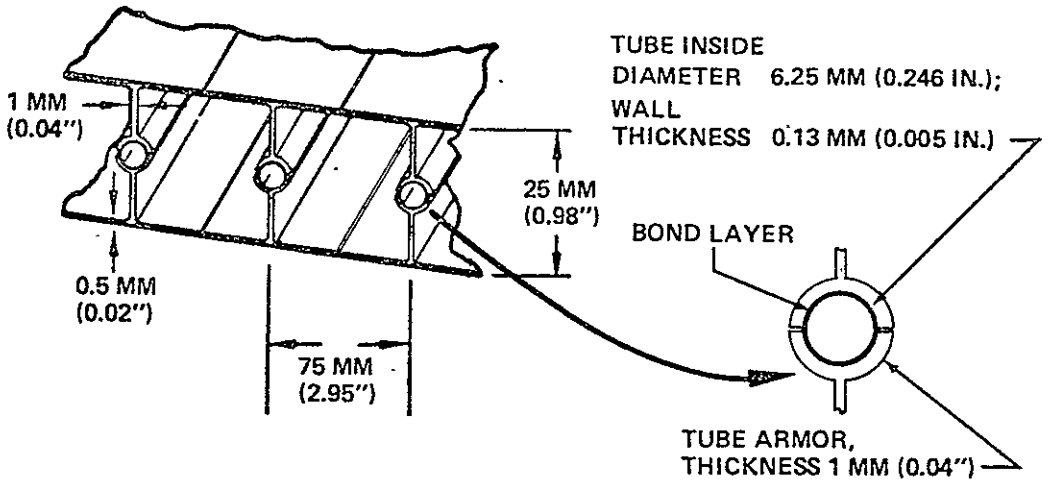

FIGURE 4-59 OPTIMUM RADIATOR PANEL DIMENSIONS LOW TEMPERATURE NaK RADIATOR

Fig. 4-60 is a portion of the interactions diagram of a liquid metal cooled generation system. It represents a math model which is computerized to determine minimum radiator system mass. It is a portion of a larger math model of the complete powersat module.

Each block labeled "t" or "T" represents a parametric relationship. Longer blocks represent equations. The Greek letter rho indicates the ratio of the two inputs; the Greek letter pi indicates product. + and - indicate addition and subtraction. Blocks with the lower right hand corners shaded are independent input variables. Note that the radiator mass is the sum of the mass of all feeders, headers and radiator panels (and the NaK therein) and the associated motors and pumps. Other significant factors include the total power to be radiated and the inlet and outlet temperatures. An independent variable of prime importance is "D HEAD", the diameter of the header manifolds. As this diameter is reduced, the stress in the headers tends to reduce, the area of metal reduces, and the volume of NaK (a significant mass factor) also reduces. However, the pressure drop in the manifolds increases, so that the sum of the pressure drops around the Loop ("P_3") increases, tending to increase the inlet pressure, which increases the stress in the manifolds. Higher inlet pressures require more pump power, so that the pumps and associated motors become heavier. More pump power also means more busbar power, so that more solar concentrator, cavity, etc., are required.

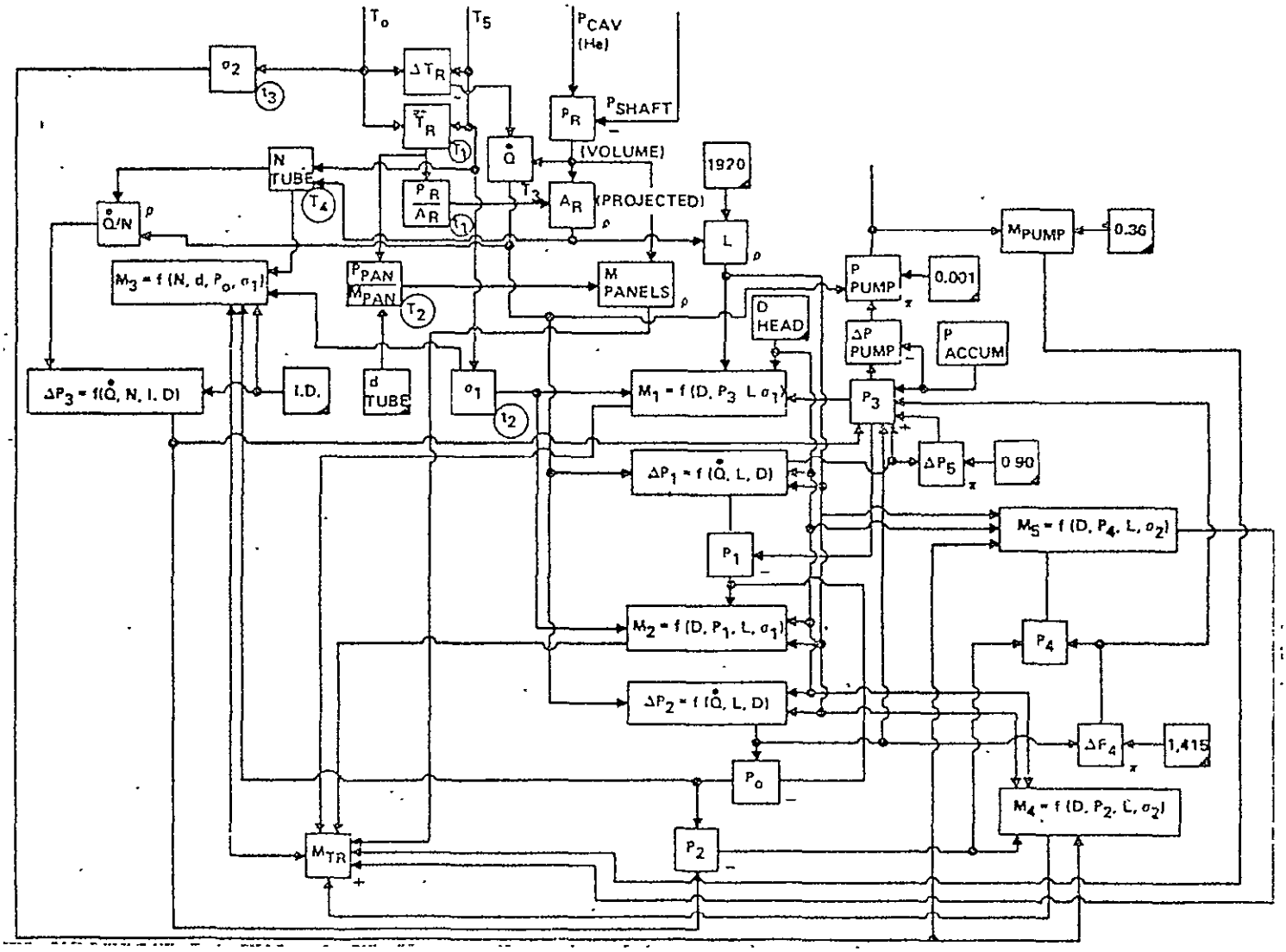

FIGURE 4-60 RADIATOR SYSTEM MODELING

Fig, 4-61 shows one of the parametric relationships used in the radiator modeling exercise; it was itself derived from computer analysis. It shows the effective temperature; i.e., temperature of an isothermal area equal in size to the radiator which rejects the same amount of energy. T_5 is the radiator inlet temperature; T_o is the outlet temperature.

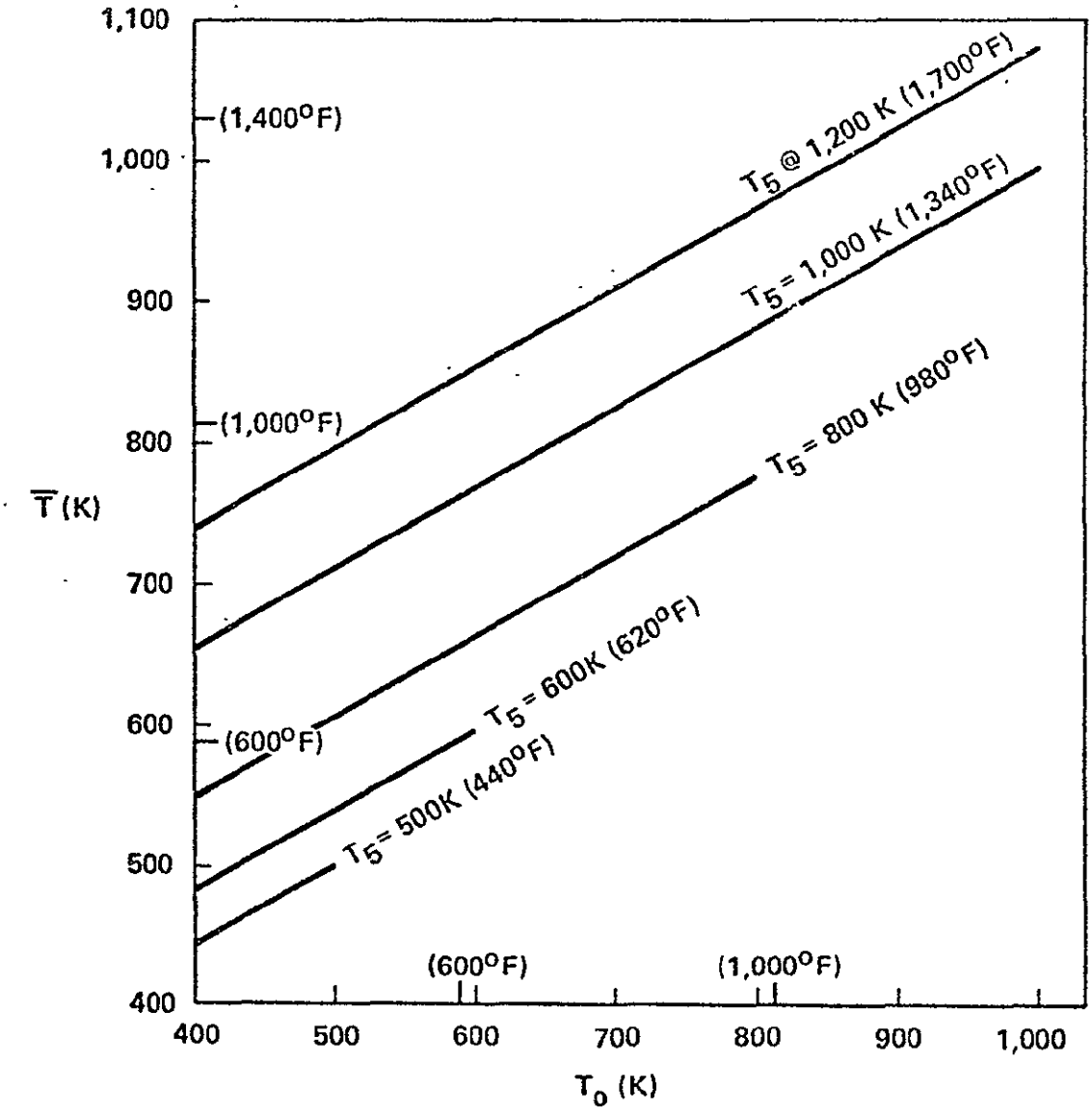

FIGURE 4-61 RADIATOR $\overline{T}$

Fig. 4-62 shows total radiator system mass for the range of primary variables judged to be potentially applicable to power satellite usage. For each inlet temperature there is a temperature drop across the radiator (ΔT) which yields minimum mass. Note the drop in mass as inlet temperature is increased up to 1150K (1611°F); beyond this point the trend is less dramatic. This is because the model includes material strength allowables. Consequently, the wall thickness of the panel tubes and headers must increase as temperature increases to yield the 30 year creep rupture strength.

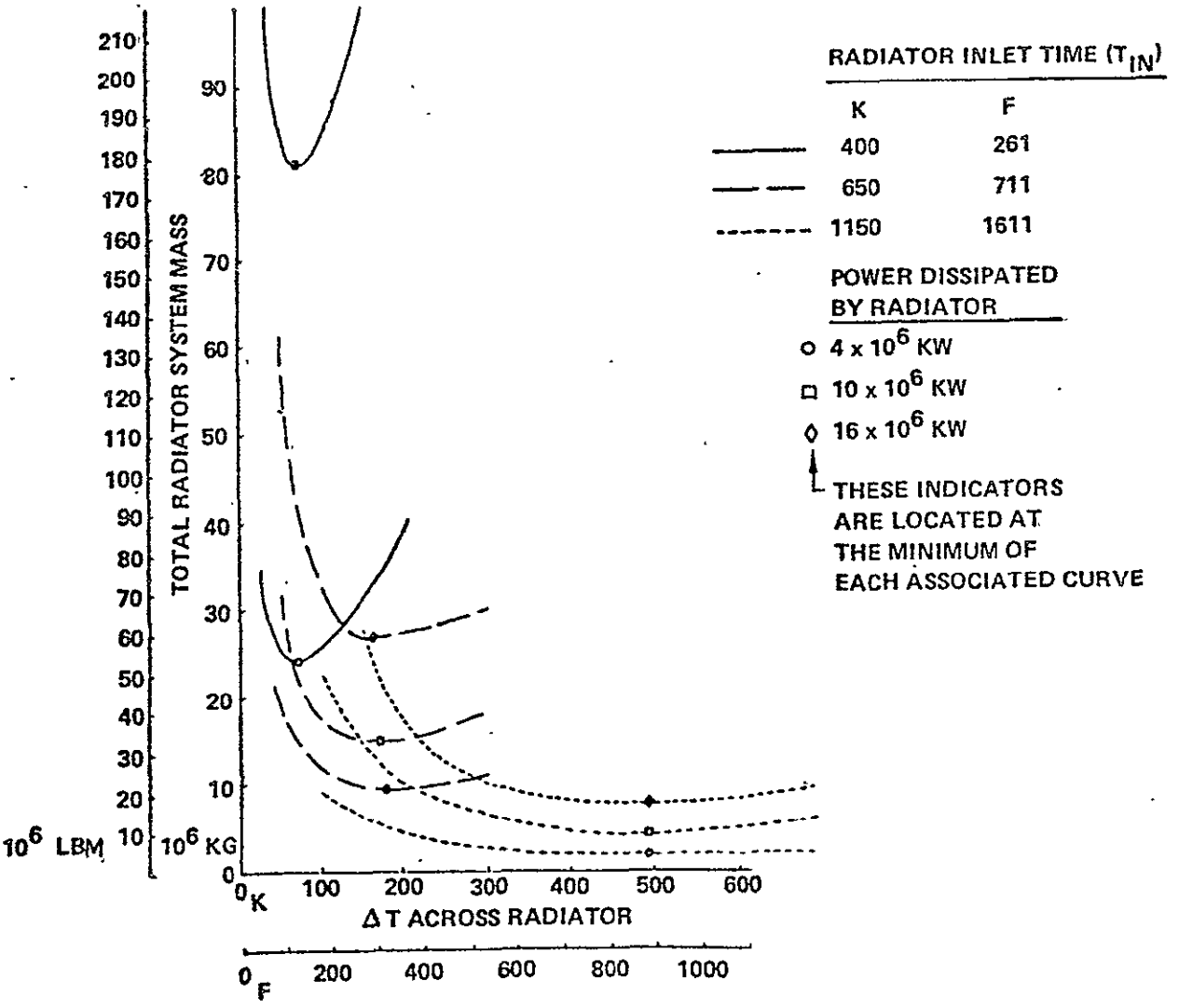

FIGURE 4-62 EFFECT OF SIGNIFICANT RADIATOR PARAMETERS ON TOTAL MASS

In Figure 4-63, minimum radiator specific mass is plotted mersus thermal power dissipated for five inlet temperatures. The variation with power level may be explained as follows: The single source of the power to be dissipated is located at the approximate center of the radiator. If the power level of a radiator is to be increased, additional panel area must be provided around the periphery (the radiator is a single-plane structure to minimize view factor and meteoroid effects). The headers associated with this added area are obviously longer (and, consequently, more massive) than those associated with an equal area near the center. Thus, radiator specific mass is a function of the power level of the system, and becomes an important factor in the selection of ideal power satellite module size, particularly if the radiator operates at a relatively lower temperature range (and is, consequently, more area-intensive).

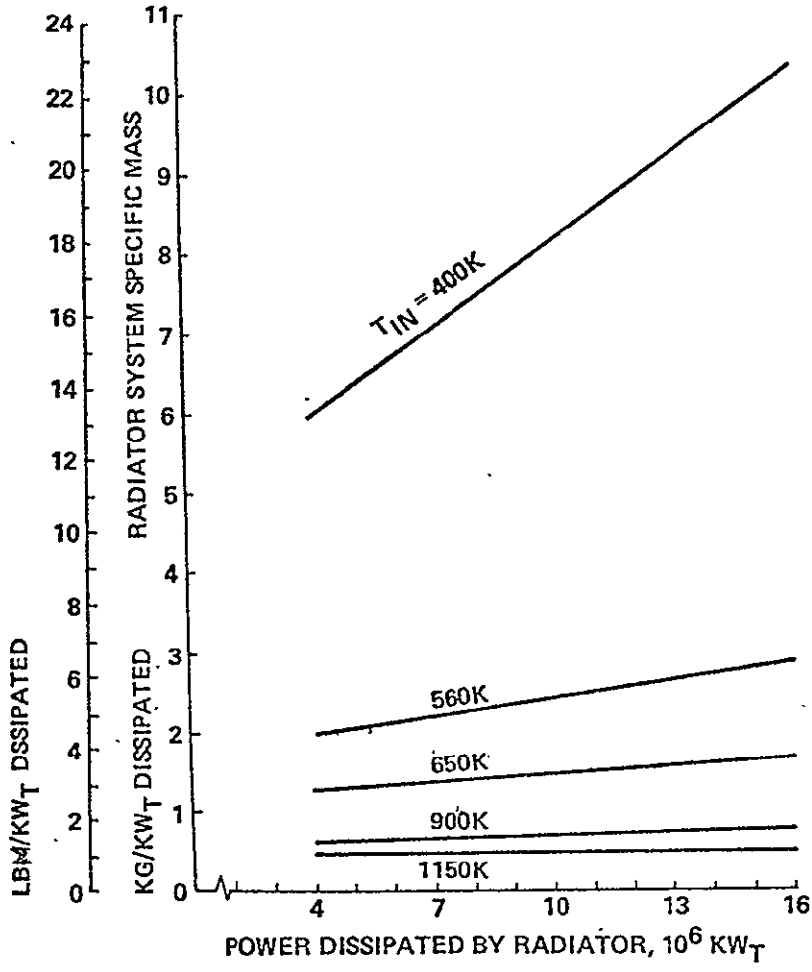

FIGURE 4-63 EFFECT OF POWER LEVEL ON RADIATOR SYSTEM SPECIFIC MASS (OPTIMUM ΔT)

Solar occultation will occur for varying periods of up to 70 minutes (1.167 hours) duration. During these periods, the NaK radiator is subject to cool down from its normal operating temperature. A transient thermal analysis was conducted to determine whether the NaK in the radiator tubing will freeze. The cooling rates with and without circulation were determined. The results Fig. 4-64 indicate a high probability that freezing will occur during longer occultation periods (> 38 minutes). (The NaK helium heat exchanger mass was not included which would delay the freezing time somewhat.) At the end of occultation, to thaw the radiator, it is anticipated that the collector facets can be oriented to direct reflected solar energy to the radiator surface. When the NaK has melted the facets would be redirected to the cavity aperture to start up the cycle.

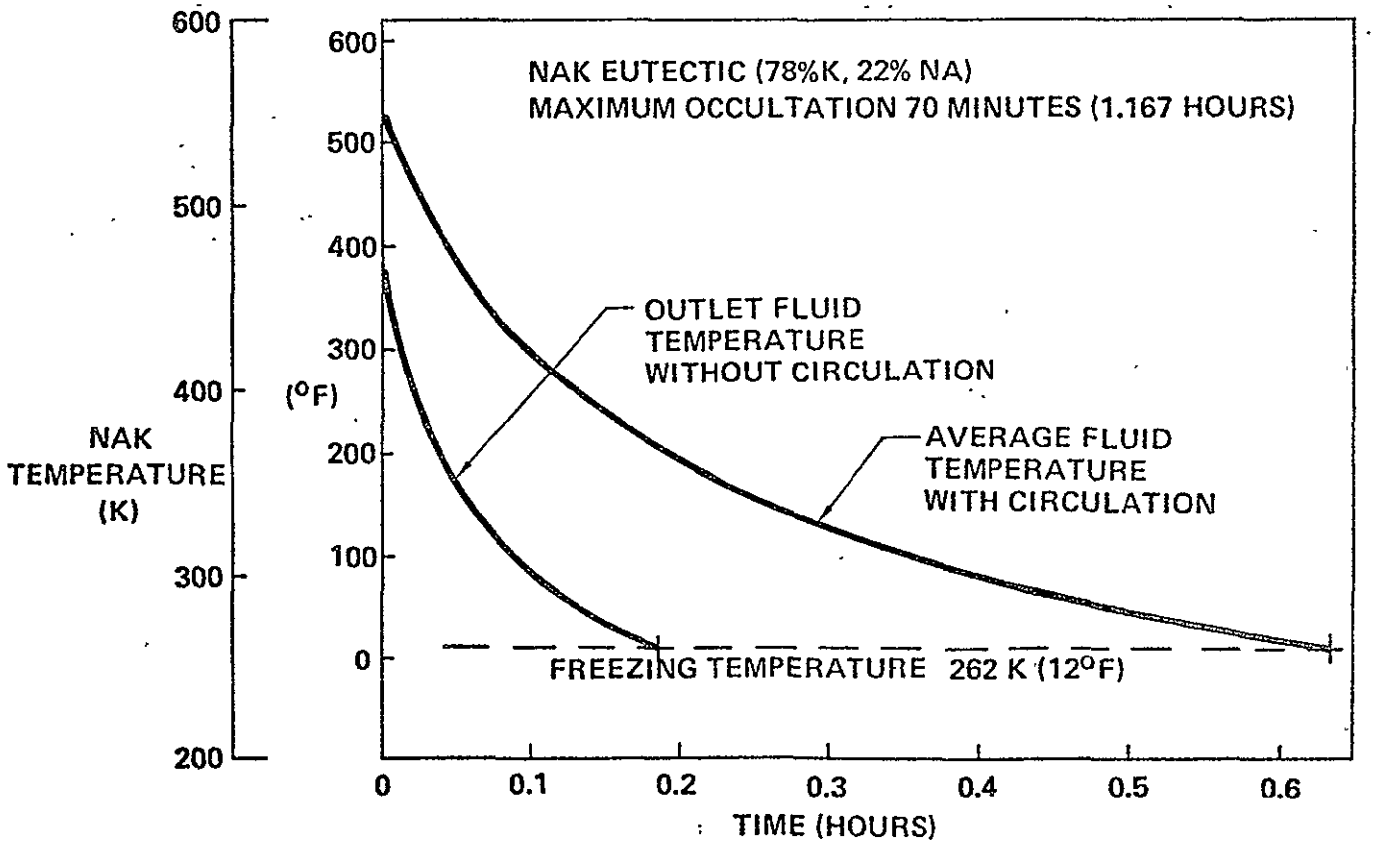

FIGURE 4-64 RADIATOR FLUID TEMPERATURE DURING OCCULATION

Since the analyses was conducted, a ternary eutectic alloy of sodium, potassium and cesium has been proposed which has a lower freezing temperature, 197K (-105°F), than NaK.

Haynes 188 and Columbium B-66 appear to be satisfactory alloys for tubes and headers for, respectively, the low and high temperature radiators. The selected fin/meteoroid bumper materials are aluminum and beryllium. For the thermionic systems the NaK loop can remove heat directly, and would yield a lighter radiator system. Thus, the thermionic systems in this study should use NaK radiators; the Brayton systems should use gas radiators. The helium high temperature radiator above has a mass of 18.5×10^6 kg (4.1×10^7 lbm); the low temperature helium radiator has a mass of 38.5×10^6 kg (8.5×10^7 lbm).

The large number of header connections and requirements for tight joints make the radiator an on-orbit assembly challenge. The correct balance between resistance to meteoroid degradation (which imposes weight penalties) and the system repair rate (with the associated operational costs) is not known; an arbitrary 30% degradation in 30 years was used as a baseline.

The principal conclusions regarding radiators for SPS are:

1. Technology and materials are adequate to begin development of radiators for either the near term (1985, "low" temperature) or 1995, high temperature systems.

2. Closed Brayton cycle systems should use liquid metal radiators.

3. Thermionic systems should use liquid metal radiators.

The fluid-loop thermal radiator design began with an analysis of meteoroid armoring requirements. Armoring places significant design constraints and mass penalties on the radiator.

The average total meteoroid environment (average sporadic plus a derived stream) was derived using the flux-mass model described in Reference A. The flux-mass environment is shown in Figure 4-65. A mass density of 0.5 gm/cm^3 (.018 lbm/in^3) was used for all meteoroid particle sizes.

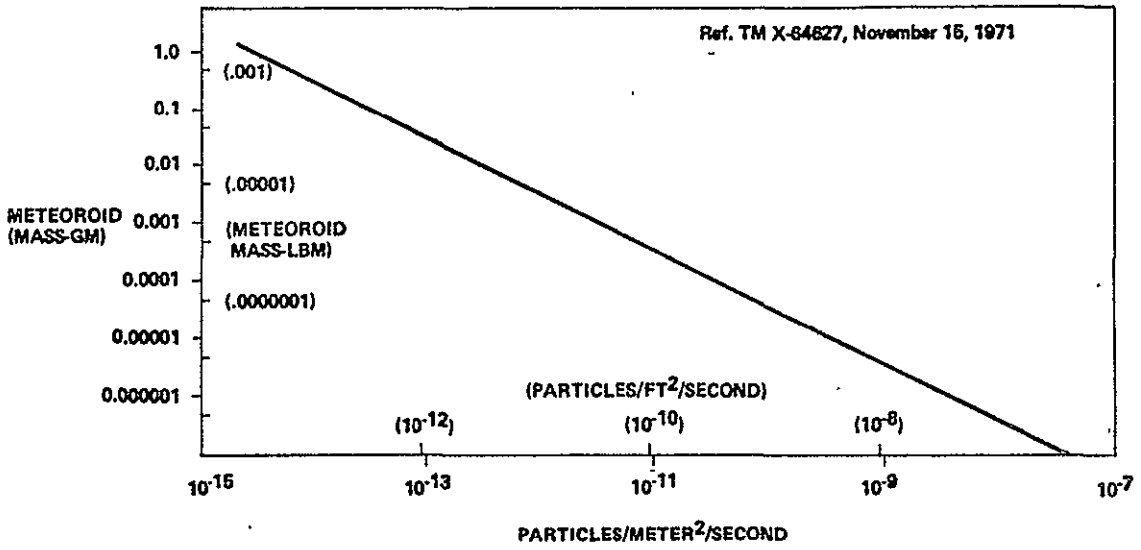

FIGURE 4-65 SPORADIC AND STREAM AVERAGE TOTAL METEROID ENVIRONMENT (OMMDIRECTIONAL)

The meteoroid flux-mass environment shown in Fig 4-65 was calculated on the assumption that the distribution of meteoroid orbital directions with respect to the Earth is uniform. Actually, the majority of meteoroid orbits are close to the ecliptic plane as shown in Figure 4-66.

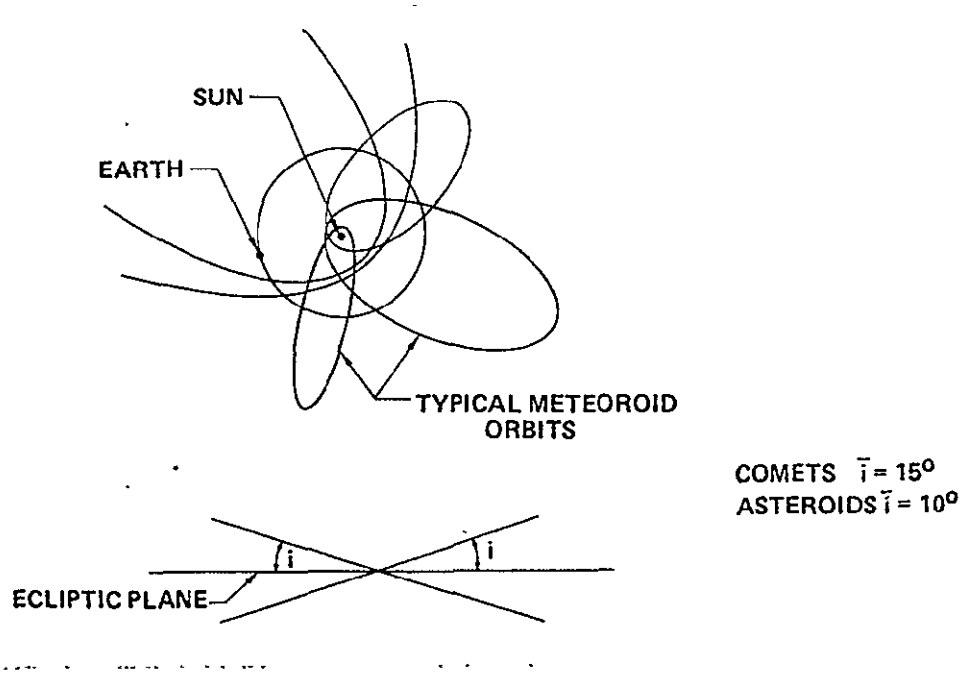

FIGURE 4-66 METEOROID MOTION

Fig. 4-67 was derived from Fig. 4-66. The graph on the left shows the observed meteoroid flux with respect to the ecliptic, and that on the right presents the distribution with respect to solar longitude, in the plane of the ecliptic. These figures were obtained from Reference (b).

Both these distributions are apparent flux densities as observed from Earth; however, they clearly indicate the anisotropic distribution of meteoroids in space.

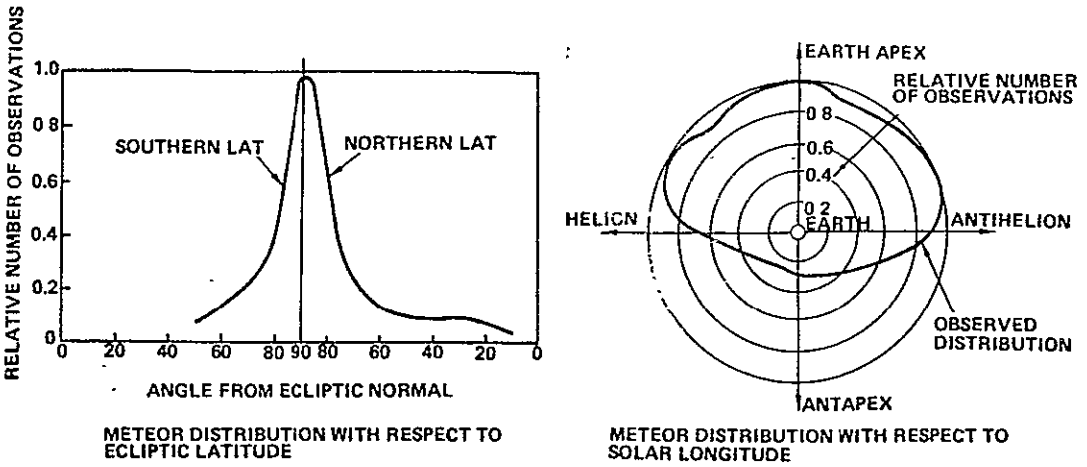

Figure 4-67 RESULTANT INTERACTION WITH OBJECT IN EARTH'S ORBIT

It is possible to preferentially orient the SPS radiators to take advantage of this anistropic distribution of meteoroids in space.

Fig. 4-68 shows that as the SPS orbits the Earth and the Earth orbits the Sun, the SPS is always pointing towards the Sun. The smaller figure shows the radiator oriented to be in the plane of the ecliptic and edgewise to the main meteoroid flux.

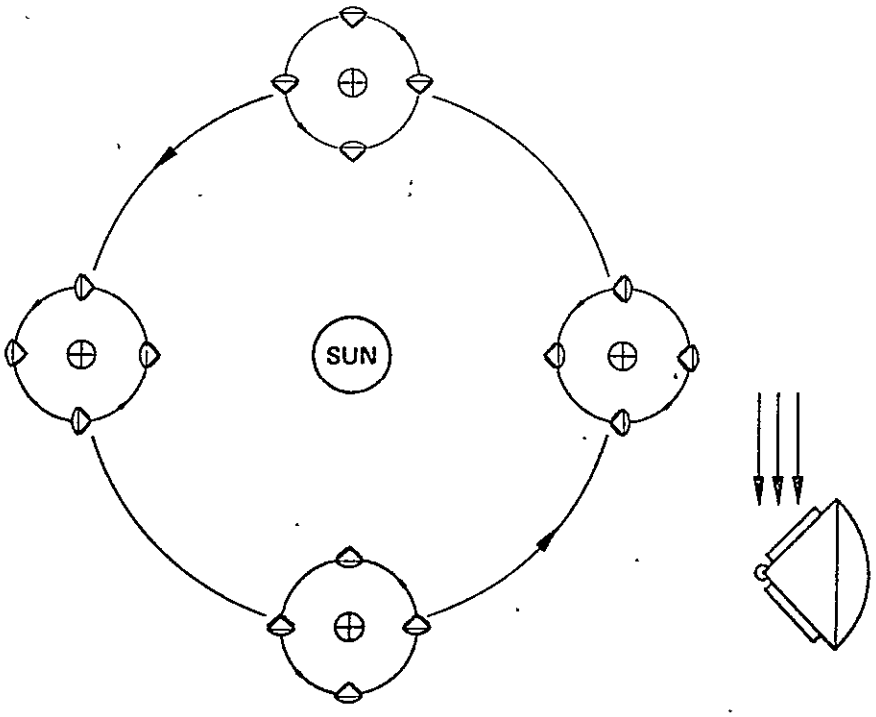

Figure 4-68 SPS RADIATORS CAN BE PREFERENTIALLY ORIENTED

Fig. 4-68 shows the radiator placed in the plane of the ecliptic. Figure 4-69 shows the flux concentrated at a low angle to the ecliptic plane. This angular concentration extends around the leading edge of the radiator from helion to antihelion, as shown in Fig. 4-67. Thus, the radiator sees the meteoroid flux impinging in a concentration at an angle of approximately 15° to its plane of motion.

The radiator consists of thousands of small tubes spaced at 50 mm (2 inches) to 75 mm (3 inches) apart, depending upon design. These tubes are most vulnerable to meteoroid damage since penetration would allow escape of helium. Protection of the tubes by some form of barrier, therefore, is extremely important. To facilitate the design of a minimum weight barrier, a refined flux-mass model was derived taking into account the orientation of the flux concentration.

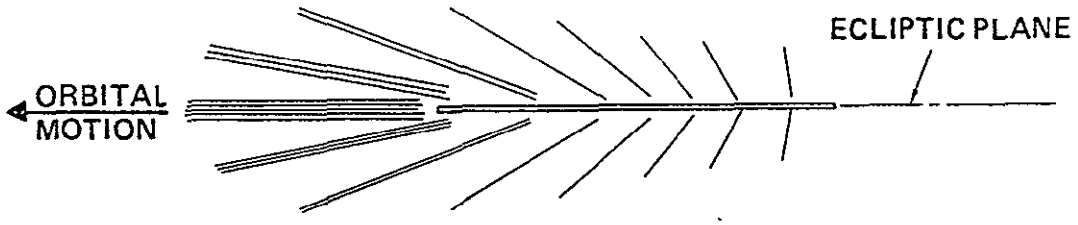

Figure 4-69 FLUX SEEN BY RADIATOR

The refined flux-mass model, taking into account the directional flux concentration, is shown in Table 4-33. It was derived from the graphs in Figure 4-67. The left hand graph was divided into 10° wide increments or strips. The first column of the table is the mean angle of each strip. The second column is the relative number of observations represented by each strip. The third column is the percentage of the total number of observations; i.e., of the total flux, represented by each angular strip. Column four transforms the directional flux to the flux normal to the radiator plane; i.e., the ecliptic plane. It is the flux of column three multiplied by the sine of the appropriate angle. Column five is column four multiplied by the omnidirectional flux for meteoroid particles .001 gm (.0000022 lbm) or greater. Each line represents the proportion of the total flux contributed by each angular strip to the total flux normal to the ecliptic plane. Since the radiator tubes are spaced, the weighted flux of column five must be modified by a view factor to account for particles which are included in the flux, but which pass harmlessly between the tubes. These view factors are different for each angle. They are tabulated in column six for tubes spaced at 50 mm (2 inches) and in column eight for tubes spaced at 75 mm (3 inches). The final derived flux is the weighted flux multiplied by the view factor.

Table 4-33 DERIVED DIRECTIONAL METEROID FLUX

Angle from 0° ecliptic	Relative number of observations	% of total flux	Aspect factor	Weighted hits/ m2/sec (hits/ft2/sec) >001-gm (22^{5} lbm	View factor 50 mm tube	Hits/tube/m2/sec (/ft2/sec) 50 mm (2") tube spacing	View factor 75 mm(3") tube spacing	Hits/tube/m2/sec (/ft2/sec) 75 mm (3") tube spacing
N 5	.895	467	.041	4.92×10^{-13} (4.57×10^{-14})	1 0	4.92×10^{-13} (4.57×10^{-14})	1 0	4.92×10^{-13} (4.57×10^{-14})
15	.362	.189	.049	5.88×10^{-13} (5.46×10^{-14})	73	4.29×10^{-13} (3.98×10^{-14})	.6	3.53×10^{-13} (3.28×10^{-14})
25	.176	.092	039	4.68×10^{13} (4.35×10^{-14})	.49	2.29×10^{-13} (2.13×10^{-14})	38	1.68×10^{-13} (1.56×10^{-14})
35	.114	059	034	4.08×10^{-13} (3.79×10^{14}	.37	1.51×10^{-13} (1.40×10^{-14})	26	1.08×10^{-13} (9.8×10^{15})
45	.090	.047	.033	3.96×10^{13} (3.68×10^{-14})	31	1.23×10^{-13} (1.14×10^{-14})	22	8.71×10^{-14} (8.08×10^{-15})
55	.095	.049	.040	4.8×10^{-13} (4.46×10^{-14})	.28	1.34×10^{-13} (1.24×10^{14})	.19	9.12×10^{-14} (8.47×10^{-15})
65	.095	.049	.044	5.28×10^{-13} (4.9×10^{-14})	.25	1.32×10^{-13} (1.23×10^{14})	.17	8.93×10^{-14} (8.34×10^{15})
75	.067	.035	034	4.08×10^{13} (3.79×10^{-14})	24	9.79×10^{14} (9.1×10^{-15})	.16	6.53×10^{-14} (6.07×10^{-15})
85	.024	.012	.012	1.44×10^{-13} (1.34×10^{-14})	23	3.31×10^{-14} (3.07×10^{-15})	.15	2.16×10^{-14} 2.01×10^{-15}
			Total	3.91×10^{-12} (3.63×10^{13}	Total	1.82×10^{12} (1.69×10^{-13})	Total	1.47×10^{-12} (1.37×10^{13})
S 5	.767	.557	.048	5.76×10^{-13} (5.35×10^{-14})	1 0	5.76×10^{-13} (5.35×10^{-14})	1.0	5.76×10^{-13} (5.35×10^{-14})
15	.281	.204	.053	6.36×10^{-13} (5.91×10^{-14})	.73	4.64×10^{13} (4.31×10^{-14})	6	3.82×10^{-13} (3.55×10^{-14})
25	.176	.128	.054	6.48×10^{-13} (6.02×10^{-14})	.49	3.17×10^{-13} (2.95×10^{-14})	.36	2.33×10^{-13} (2.16×10^{-14})
35	.109	.079	.045	5.4×10^{-13} (5.02×10^{14})	37	2.0×10^{-13} (1.86×10^{-14})	.26	1.4×10^{-13} (1.3×10^{-14})
45	.043	.031	022	2.64×10^{13} (2.45×10^{-14})	31	9.18×10^{-14} (7.6×10^{-15})	.22	5.81×10^{14} (5.4×10^{-15})
			Total	2.66×10^{-12} (2.47×10^{-13})	Total	1.64×10^{-12} (1.52×10^{-13})	Total	1.39×10^{12} (1.29×10^{-13})

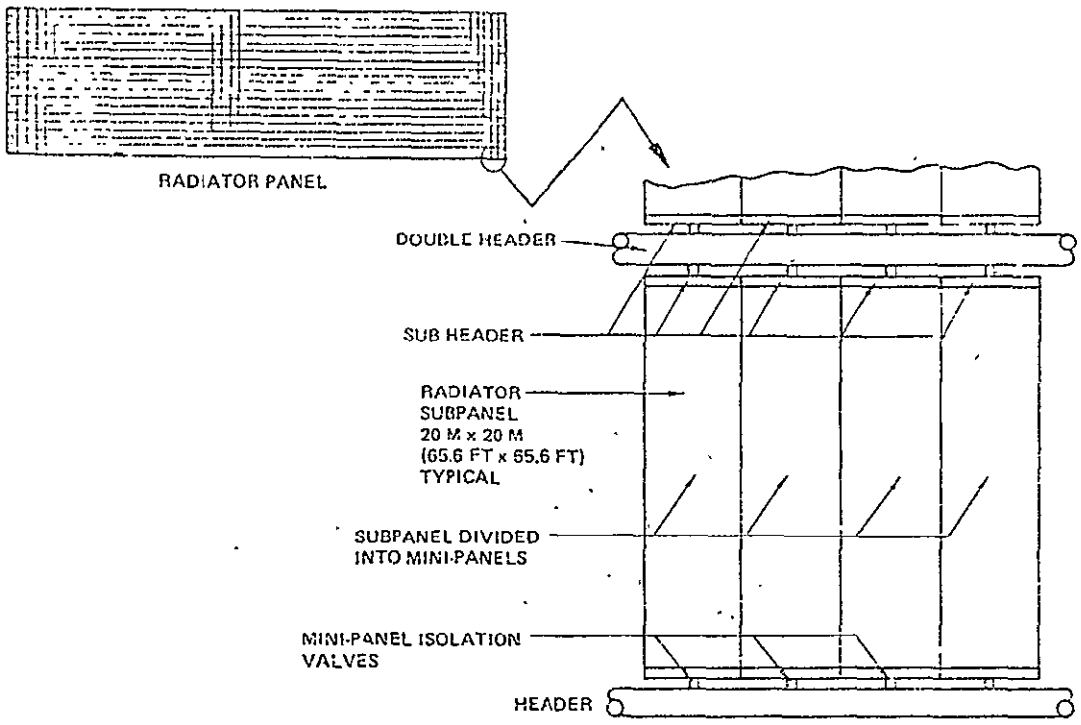

Figure 4-70 METEROID SHIELDING PHILOSOPHY

Three basic radiator configurations were considered and these are shown in Fig. 4-54. Thermal analyses of the configurations is described under "Radiation Analyses".

Fig. 4-71 was used in determining the dimensions of Configurations B and C of Fig. 4-54. The first barrier is the radiator fin and the second is the armor around the tube. The main meteoroid flux is at a shallow angle of the radiator and increases the effective distance between the first and second barriers. Fig. 4-71 , taken from Reference C enables a minimum weight two-sheet aluminum barrier to be chosen for protection against a certain meteoroid particle.

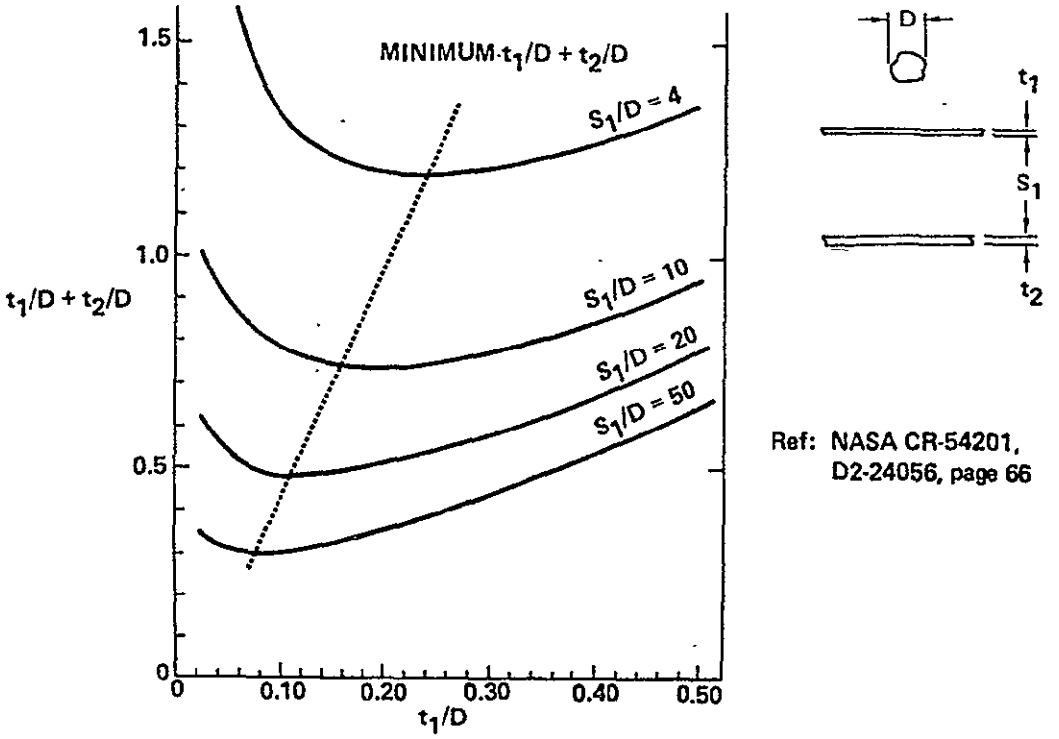

Figure 4-71 MINIMUM WEIGHT TWO-SHEET ALUMINUM BARRIER

Radiator panel arrangements were investigated to obtain a minimum mass design. Concept No. 1 is shown in Fig. 4-72 . This concept consists of input and output headers with a row of radiator panels between them. The headers are fixed in relation to each other at the feeder end and are free to expand at the other end. Due to the temperature difference between them the headers will move laterally relative to each other and the panels will rotate as shown. This lateral movement due to temperature differential will take place during start-up and shutdown and during occultation.

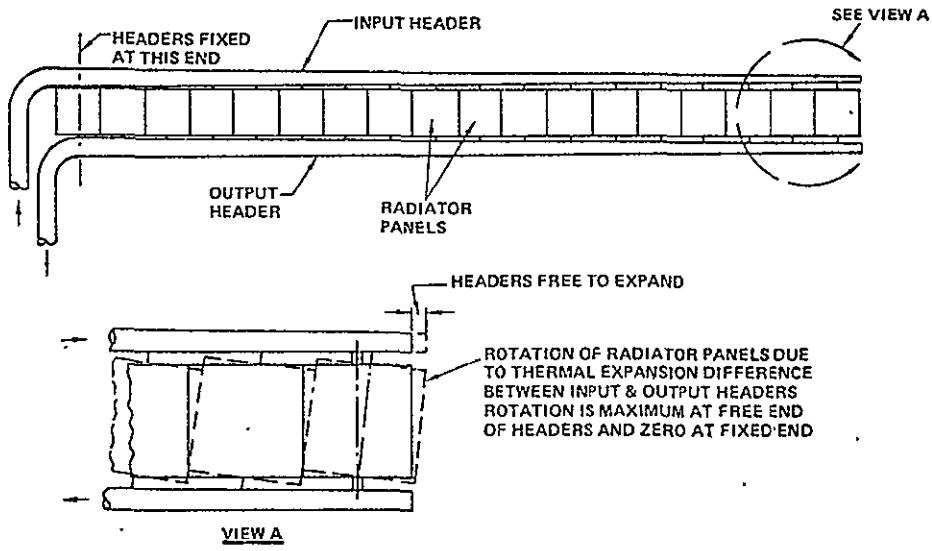

Figure 4- 72 RADIATOR PANEL ARRANGEMENT - CONCEPT No. 1

It is a provisional requirement that 70% of the system must still be operative after a 30-year life without repair or replacement. Applying this philosophy to the radiator, it means that no more than 30% of the tubes must be penetrated and that the damaged tubes must be isolated to prevent loss of coolant. The radiator must be divided into subpanels such that in combination with a barrier against an appropriate particle size, a minimum weight is achieved. A suitable size of subpanel for transportation into orbit in one piece is 20 m x 20 m (65.6 ft. x 65.6 ft.). This will require subdividing into smaller or mini-panels to achieve a radiator degradation of not more than 30% in 30 years. Using the total derived flux, from the previous table, for a particle of .001 gm (.0000022 lbm) or greater, the subpanels will require subdividing irto 5 mini-panels for the 50 mm (2 inches) tube spacing and 4 mini-panels for the 75 mm (3 inches) tube spacing. As shown in Fig. 4-70, each mini-panel will require an inlet and outlet valve for isolation in the event of tube penetration.

Fig. 4-73 shows radiator panel arrangement, Concept No. 2. This concept is similar to the previous arrangement except that the headers are fed at their centers instead of at one end. The headers are fixed relative to each other at their centers with their ends free to expand. If the number of panels is the same as in the previous concept then the rotation of the end panels will be approximately half that of the previous concept, since the differential expansion of the header ends is halved.

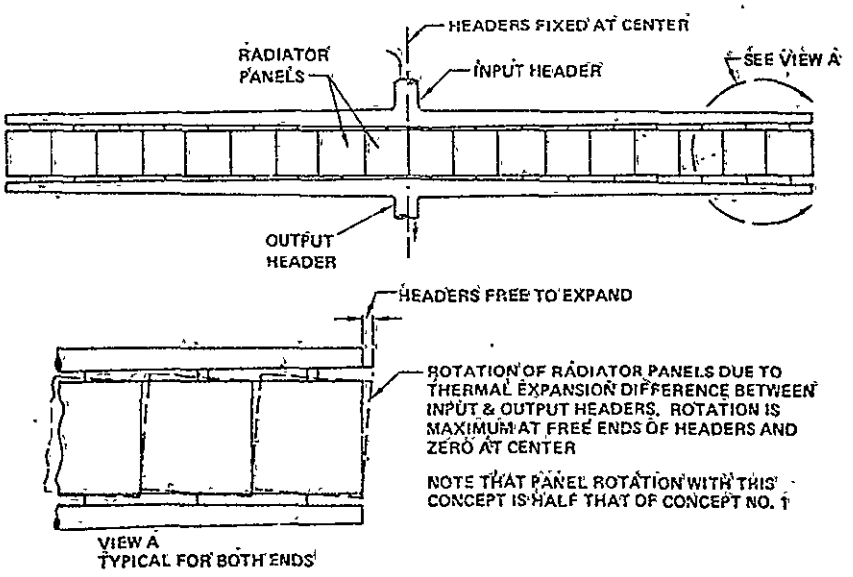

Figure 4-73 RADIATOR PANEL ARRANGEMENT - CONCEPT No. 2

Fig. 4-74 shows radiator panel arrangement, Concept No. 3. This concept is similar to the previous arrangement except that there are two rows of radiators between the input and output headers. As with the previous concept, the headers are fixed at their centers relative to each other and the ends are free to move.

Since the distance between the headers is doubled the angular rotation of the panels is approximatelyhalf that of the previous arrangement, and a quarter that of Concept No. 1.

Note that, although there are two rows of panels, each panel is separately placed between the headers, alternately in the upper and lower rows. A 20m (65.6') long feed tube is required for each panel.

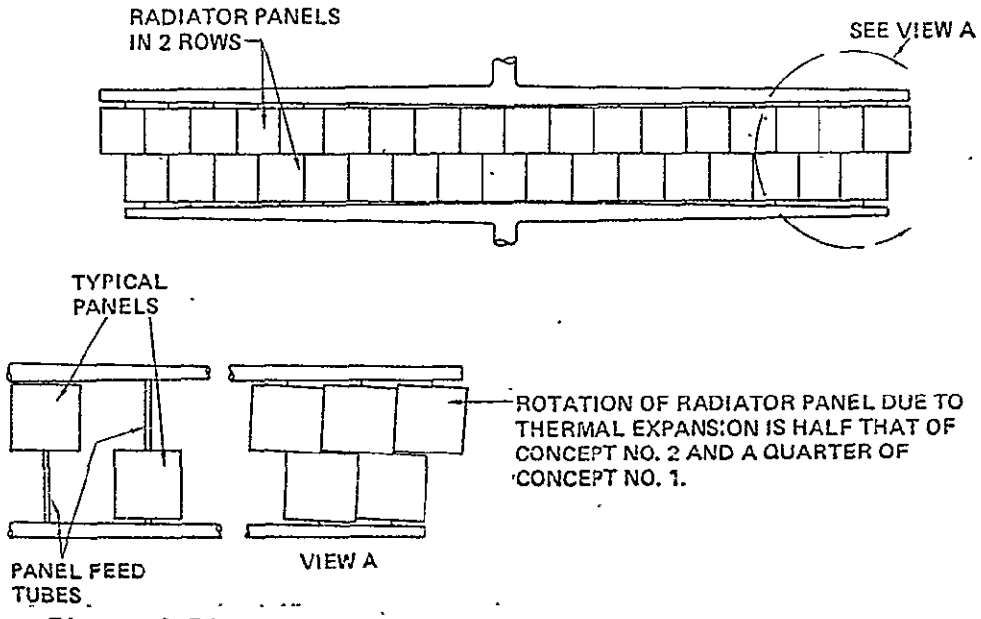

Figure 4-74 RADIATOR PANEL ARRANGEMENT - CONCEPT No. 3

Fig. 4-75 shows a typical arrangement of the radiator area associated with three 300 MWe turbogenerators. Each radiator section required per turbogenerator consists of 70 panels. The tapering headers are fed from the center. Input and output headers are fixed at their centers relative to each other so that movement due to thermal expansion is confined to the ends which are free. The structure which supports the radiator is designed to accommodate feeder length changes.

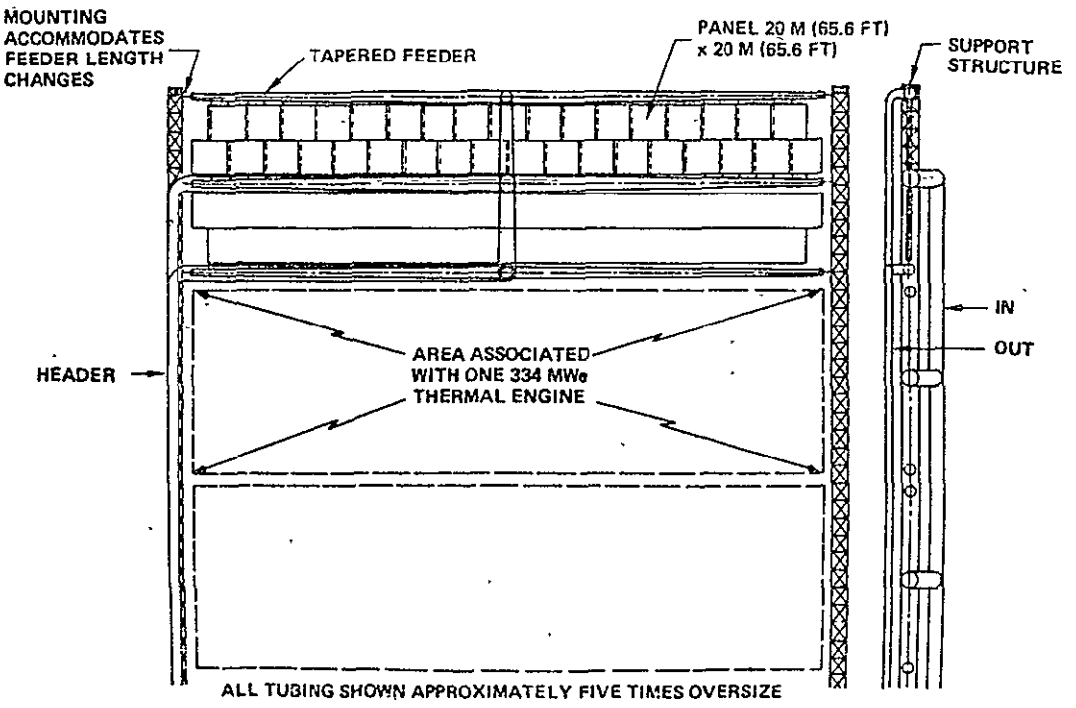

Figure 4-75 RADIATOR CONFIGURATION CONCEPT

In system optimization initial runs produced parametric descriptions of power generation modules with radiators having feeders 1.6 times more massive than the panels which they feed. Consequently, radiator configurations were sought which would have lighter feeders. It was recognized that short feeders were dependent upon clustering the radiator panels as closely as possible about the heat source. Fig. 4-76 shows both the original and a new "halo" configuration which permits a minimum length for the feeders. In both cases the radiator lies in a single plane which is oriented "edge-on" to the predominant meteoroid flow.

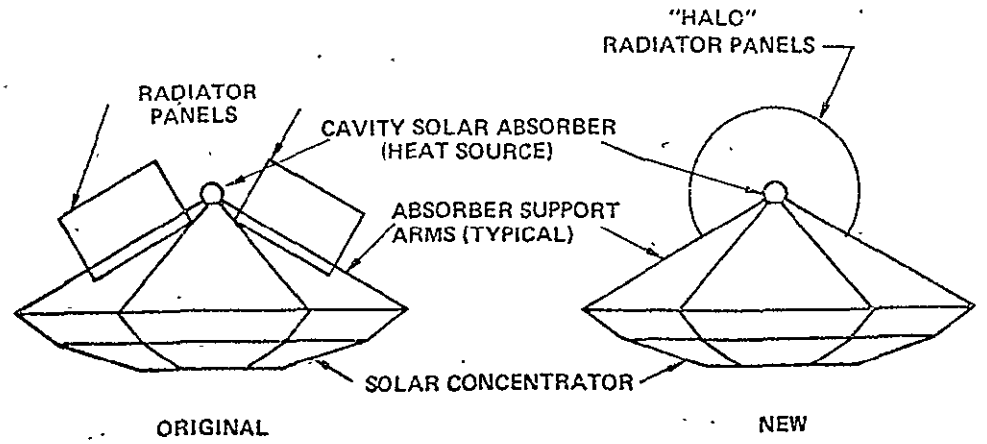

Figure 4-76 ORIGINAL AND NEW RADIATOR CONFIGURATION

Fig. 4-77 shows the original radiator arrangement with both supply and return feeders attached to the center of the headers. Constant supply and return feeder diameters are used up to the radiator panels where tapering headers are introduced.

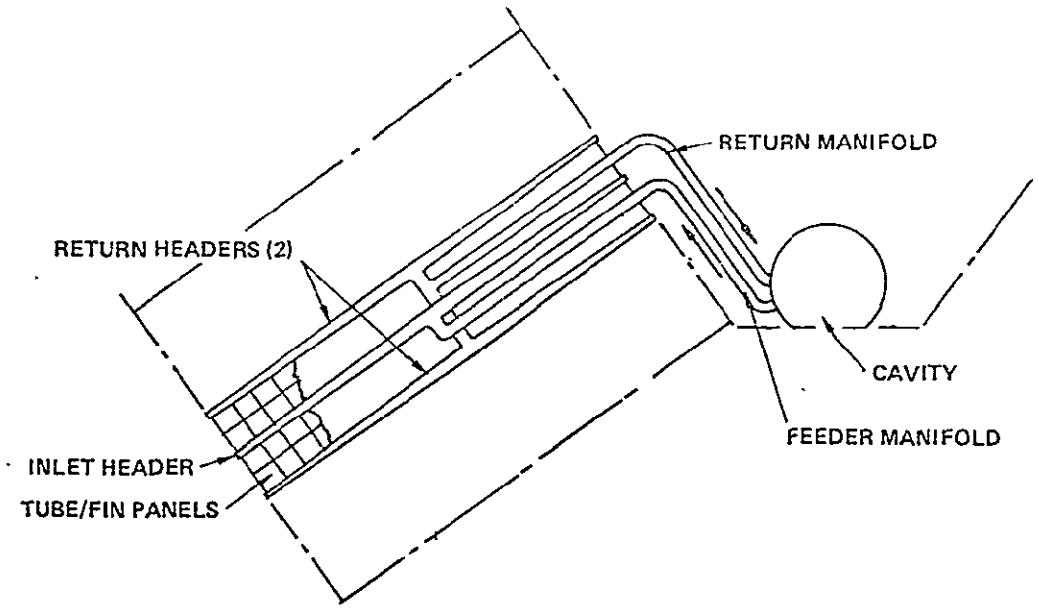

Figure 4-77 ORIGINAL PANEL ARRANGEMENT SHOWING TYPICAL FEEDER PATH TO CENTER FED HEADERS

Fig. 4-78 shows the new "halo" radiator configuration. This is similar to the original configuration in that the headers are center fed. However, the radiator sections have been clustered closely around the cavity absorber to provide the shortest possible supply and return feeders.

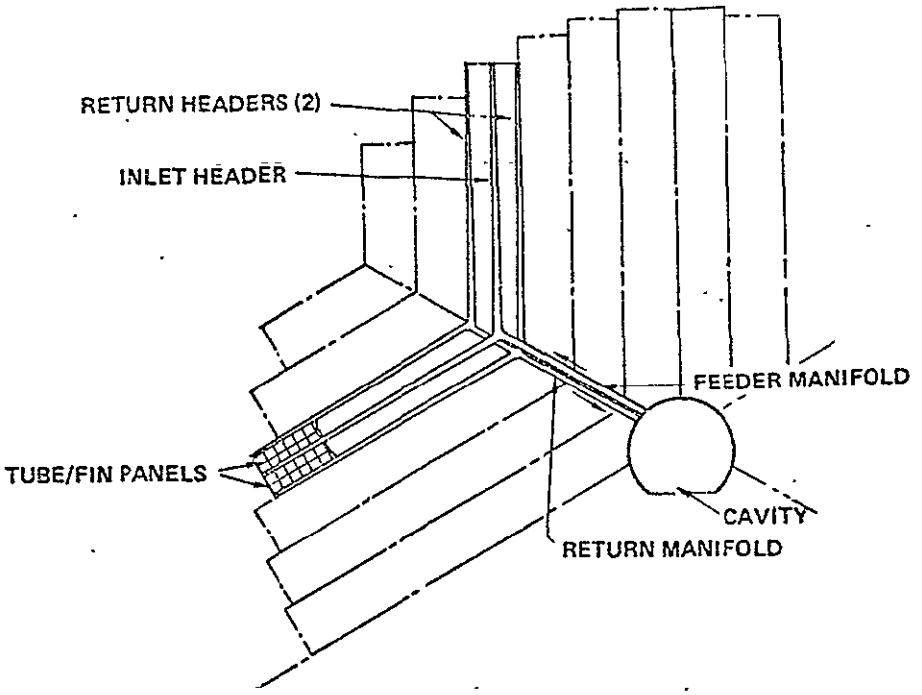

Figure 4-78 "HALO" RADIATOR CONFIGURATION

Fig. 4-79 shows the radiators for one module (4 GWe nominal) of the solar thermionic liquid cooled power satellite system. The radiators are configured in the "halo" design previously described. Supply and return feeders are as close to the solar absorber as possible to minimize weight. Headers are secured to structure at the solar absorber end. Expansion of the radiator elements due to temperature changes and creep is provided for by expansion joints to the peripheral structure. The secondary radiators below the absorber support trusses are for cooling the rotary converter assemblies (direct current to alternating current converters). This arrangement of the radiators is typical for other power satellite systems such as the Solar Brayton Cycle.

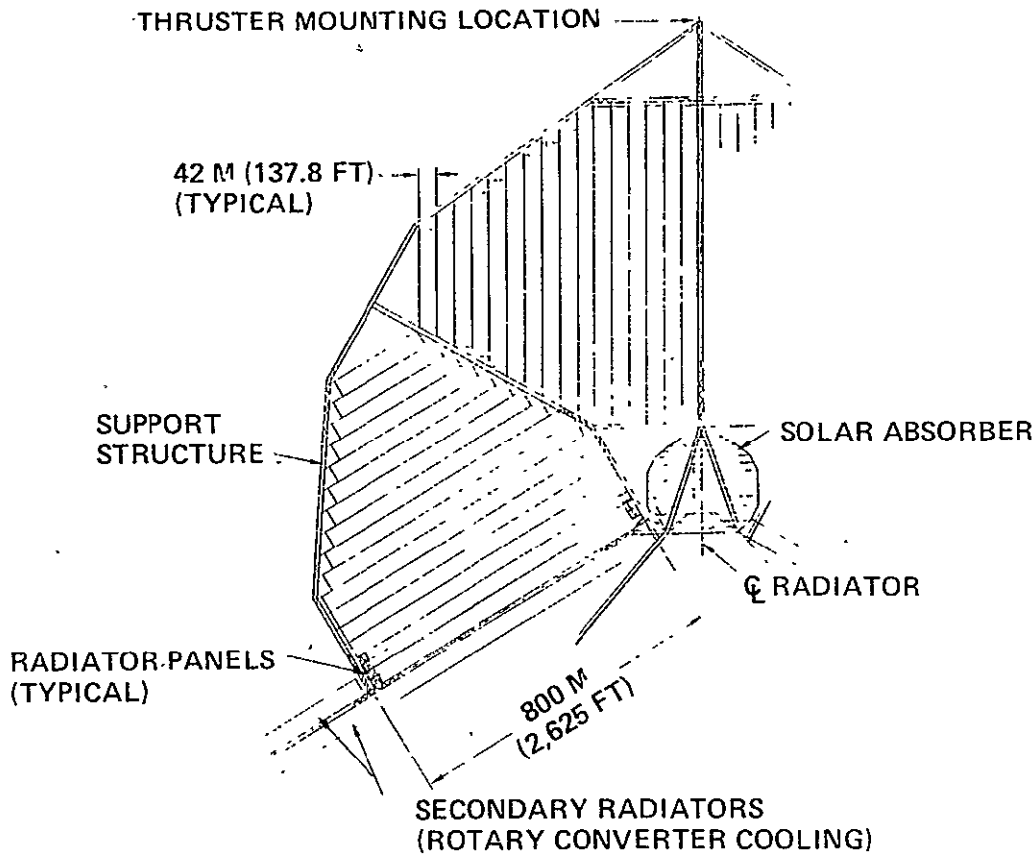

Figure 4-79 RADIATOR SYSTEM, SOLAR THERMIONIC LIQUID COOLED POWER SATELLITE

Fig. 4-80 shows a typical radiator loop using liquid metal (NaK). This arrangement is for cooling diode collectors in the solar thermionic power satellite.

The liquid metal is carried in a multitude of small tubes contacting the diode collectors. The heated metal is pumped through feeders and headers into radiator panels arranged as in Fig. 4-79. The cooled liquid is passed through output headers and feeders and over the diode collectors, completing the cycle. An accumulator is used to provide a positive pressure at the pump inlet.

Isolation valves are provided at the inlet and outlet of each panel to enable any panel(s) to be cut out of the cooling loop to prevent loss of coolant in the event of leaks due to meteoroid puncture or other causes.

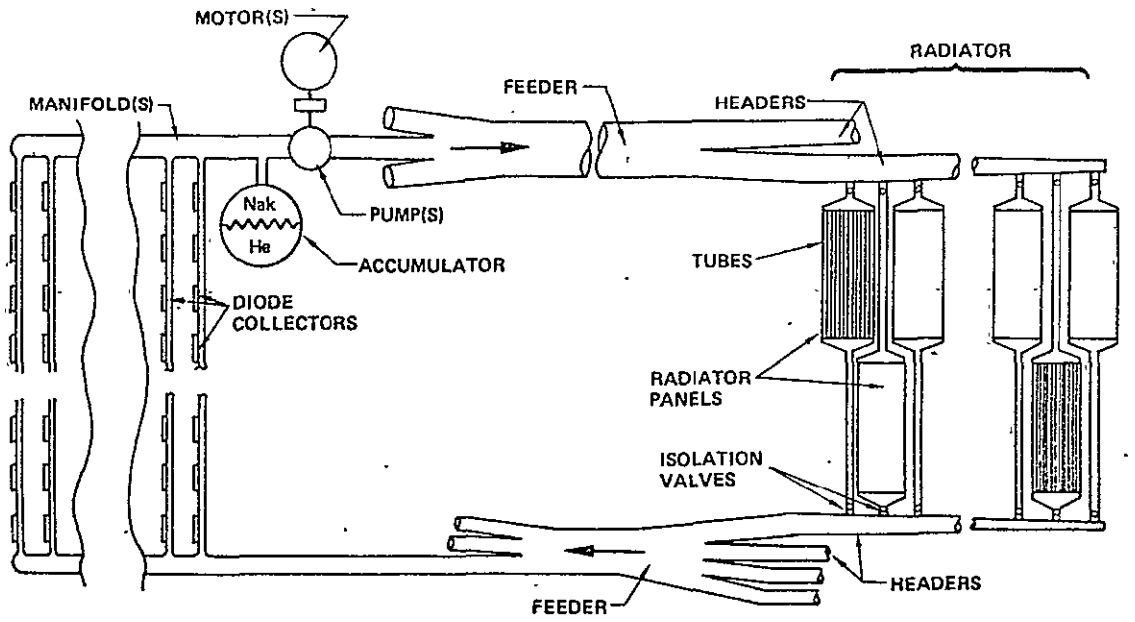

Figure 4-80 LIQUID METAL (NaK) LOOP

It has been shown that the motion of parts of the radiator such as headers and panels relative to each other has been considered in the design. The "halo" configuration of the radiator minimizes relative motion of its parts due to temperature differentials.

Another factor for consideration in the radiator design is metal creep due to stress. Fig. 4-81 shows the creep (or strain) of Haynes 188 material in 30 years as a percentage of original length, plotted against the constant stress level required to produce the creep, for three different temperatures.

Note that a decrease in stress level causes a disproportionate decrease in creep; e.g., a decrease in stress from 7 to 5 x 10^7 N/M^2 at 1033K causes a decrease in the 30 year creep from 7.5 to 0.75 percent.

If the stress level for a creep of 10% in 30 years is reduced by 50% the creep becomes very small - approximately 0.1%.

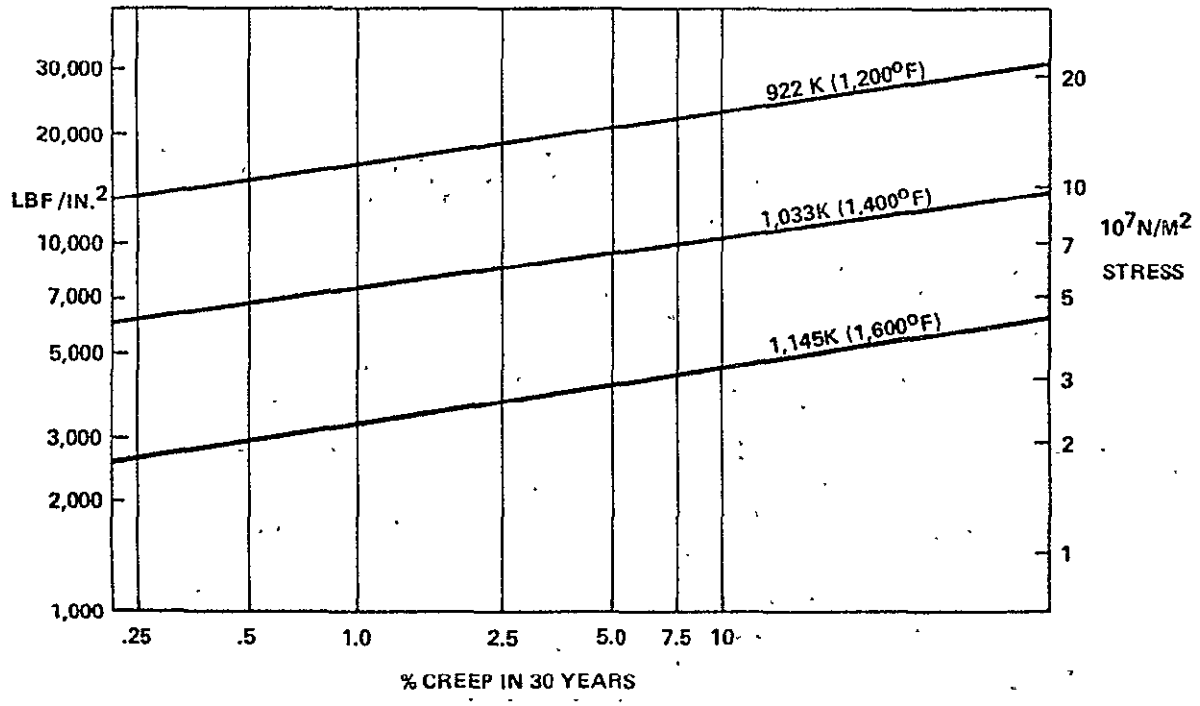

Figure 4-81 STRESS VERSUS CREEP - HAYNES 188

The radiator headers and feeders are designed for relatively high stress such that significant creep (approximately 10%) occurs over the design life (30 years). Fig. 4-82 shows a circular section of feeder or header tube. It should be noted that the circumferential stress is twice the axial stress. The wall thickness of the header or feeder is thus determined by the circumferential stress. However, Fig. 4-81 shows that creep decreases at a much higher rate than stress. Thus, the axial creep will be very small compared to the circumferential creep. The graph in Fig. 4-82 shows that for a 10% creep the volume of the feeder or header increases approximately 22% in 30 years.

This large volume increase is too great for the NaK accumulator to handle. A yearly, or two-yearly, "topping up" of the system will be required.

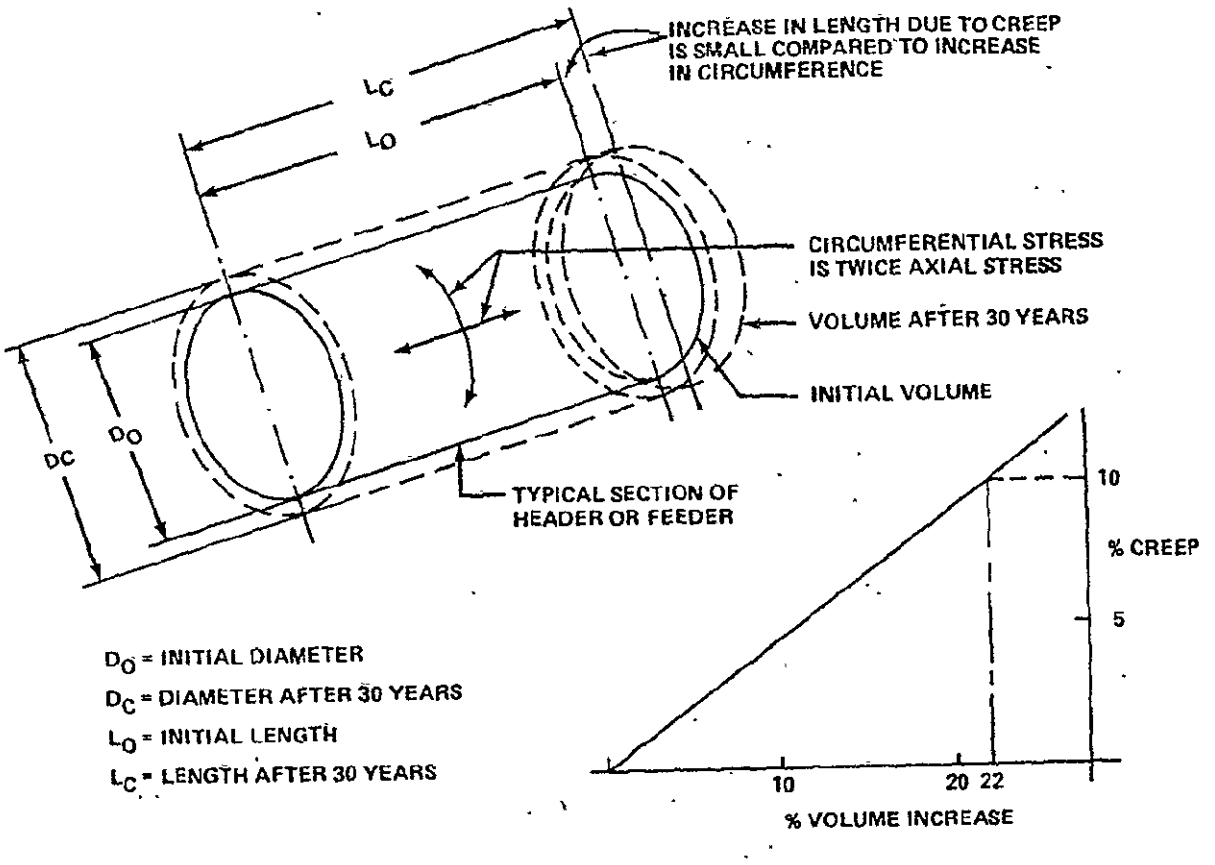

Figure 4-82 HEADER OR FEEDER VOLUME VERSUS CREEP

5.0 SATELLITE SYSTEMS

This section presents mass and size information for the total SPS systems studied. Pictorial representations of all systems are contained in Section 7.0, the cost report. Subsystems are described in Section 4.0; nuclear SPS systems are described in Section 4.6.

5.1 EFFICIENCIES

The baseline microwave power conversion system efficiency was established as 62%, i.e. for a 5.0 GW ground output, the orbital busbar power must be 8.06 GW; for 10 GW ground output 16.12 GW orbit busbar is required. Orbital busbar power must also include provision for parasitic operations such as attitude control and radiator fluid pumping.

Table 5-1 shows a typical satellite "power chain" (for the Brayton thermal engine concept).

TABLE 5-1 POWER LEVELS AT SPECIFIC POINTS (BRAYTON THERMAL ENGINE SATELLITE)

POINT IN ENERGY FLOW	POWER IN GW
Raw Solar Energy Intercepted	85.6
Energy into Cavity Absorbers	60.8
Energy in Helium/Xenon Gas Flow	50.4
Turbomachine Shaft Power	18.1
Generator Output	17.7
Attitude Control, etc.	0.2
Radiator Pumping	1.4
Power to Transmitter	16.1
Ground Output	10.0

This power chain is dependent upon the efficiency levels achieved by various subsystems (solar concentrators, absorbers, etc.) Table 5-2 shows efficiency levels for various elements of the system.

TABLE 5-2 EFFICIENCY CONTRIBUTIONS

SYSTEM ELEMENT	EFFICIENCY
Initial Facet Reflectivity	0.84
Facet Fill Factor (Gaps, etc)	0.88
Shadowing, Blockage, Aperture Spillover	0.96
Solar Concentrator	0.71
Reflection (Out of Aperture) Control	0.97
Wall Losses Through Insulation	0.99
Reradiation Control	0.87
Solar Absorber	0.83
Thermal Engine Cycle	0.358
Generators	0.98

5.2 COMPARISON OF SYSTEM MASSES AND SIZES 10 GWe GROUND OUTPUT

The masses of four solar and one nuclear SPS have been estimated. The nuclear thermionic SPS was not included, since it is not feasible with 1985 technology and a molten salt breeder reactor. Figure 5-1 compares the masses of the five SPS's.

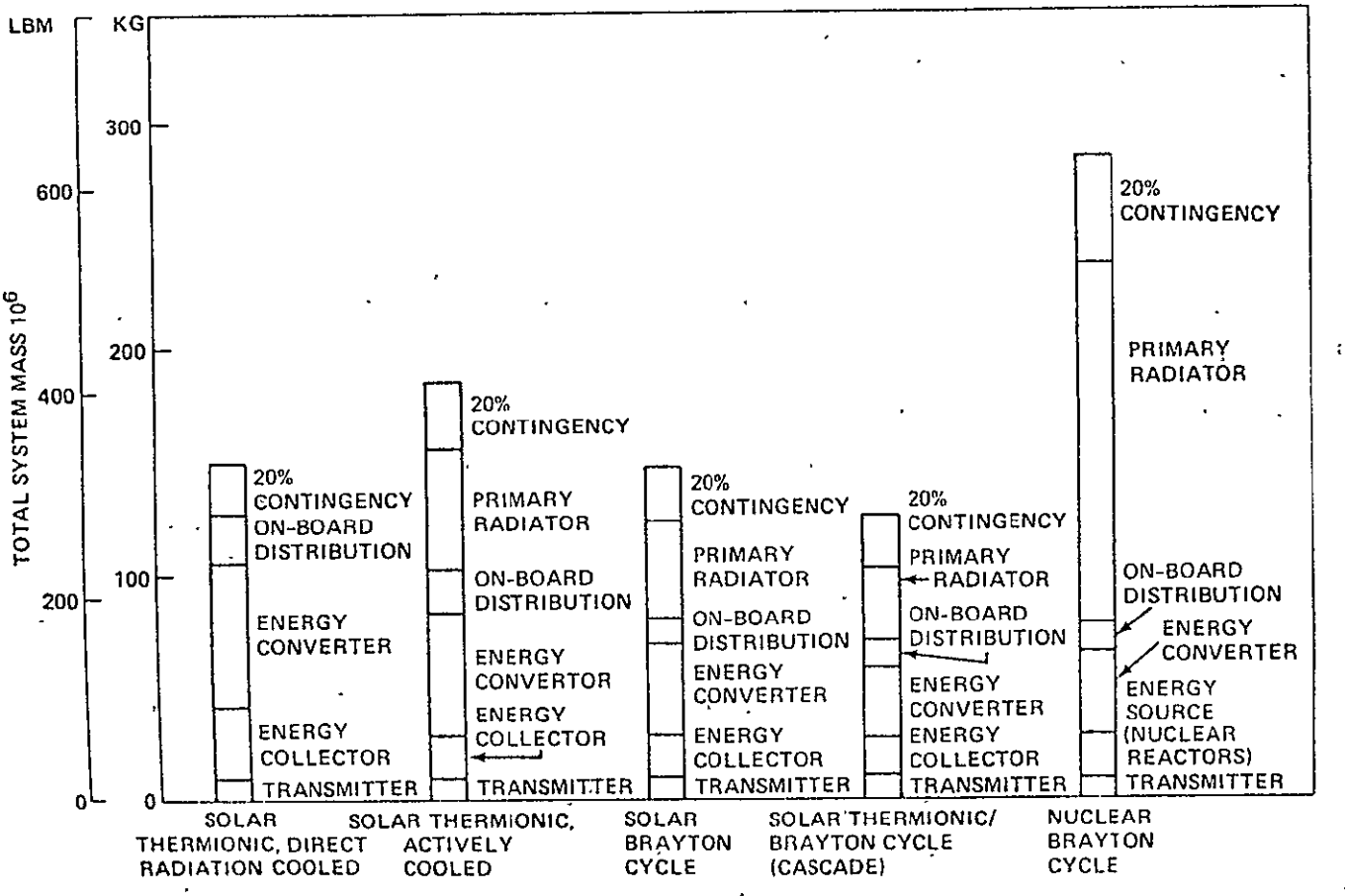

FIGURE 5-1 COMPARISON OF SYSTEM MASSES - 10 GW GROUND OUTPUT

Figure 5-2 is a mass statement for the five SPS. Note that the mass totals for each SPS contain a 20% growth contingency.

	Solar power, four 2.5 GW modules								Nuclear, sixteen 1.0 GW modules		
	Thermionic				Brayton		Cascaded thermionic/ Brayton		Thermionic	Brayton	
	Direct radiation cooled		Liquid cooled								
	10^6 kg	10^6 lbm	10^6 kg	10^6 lbm	10^6 kg	10^6 lbm	10^6 kg	10^6 lbm		10^6 kg	10^6 lbm
Energy collection/prod	(30 16)	(66 49)	(19.76)	(45 36)	(17.08)	(37 65)	(15 44)	(34 04)	(Not feasible	(21 27)	(46.8
Primary structure	15 22	33 55	10.55	23.26	9 12	14.90	8 74	13 47	with 1985	–	–
Secondary structure	7 90	17 42	1 99	4.38	1.72	7.74	1.55	6 99	technology	–	–
Reflectors	7.04	15 52	7.22	15.91	6.24	15 01	5 64	13 58	& molten salt	–	–
Reactor system	–	–	–	–	–	–	–	–	breeder reactor	21.27	46 89
Energy conversion	(64.11)	(141.34)	(53 72)	(118 45)	(42.20	(93.03)	(37 04)	(81.66)		(35.64)	(78 57)
Thermionic diodes	31.71	69 91	42.94	94 67	–	–	8.08	17 81		–	–
Fins/insulation	29 80	65.70	7.91	17.44	2.16	4.76	1.60	3 53		–	–
Cavity structure/tubing	2 60	5.73	2 87	6.34	4 40	9 70	2 20	4 85		–	–
Turbomachines/gen.	–	–	–	–	35.64	78.57	25 16	55 47		35 64	78 57
Primary radiators	(Graphite		(52 68)	(116.13)	(43.32)	(95 5)	(29 98)	(65 87)		(158 24)	(348 6
Panels	fins		12 52	27 60	18 23	18.14	5 68	12 52		46.55	102.6
Manifolds	included		5.96	13.14	27.29	16.07	5.03	11 09		17 25	33 0
Pumps/valves	with		0.35	0.77	0.50	1.10	0.35	0.77		2.10	4.6
Structure	diodes)		2.50	5.51	2.17	4.78	1.50	3 31		7 91	17 4
Fluid			31.35	69.11	25.13	55.40	17 32	38 18		84 13	186
Energy distribution	(19 55)	(43.08)	(19.55)	(43 08)	(11.70)	(25.79)	(13 64)	(30 07)		(11 70)	(25.79)
Rotary converter	7.85	17 30	7 85	17 30	–	–	1 98	4.37		–	–
Controls	1 88	4.14	1.88	4.14	1 88	4 14	1 84	4 06		1.88	4.44
Transformers	4 41	9 72	4.41	9.72	4 41	9 72	4.41	9 72		4 41	9 72
Rectifier/filter	5 41	11.92	5 41	11.92	5 41	11 93	5 41	11 93		5 41	11 93
Transmitter	11 9	26.2	11.9	26 2	11.9	26 2	11.9	26.2		11 9	26.2
Contingency/growth	25 24	55 64	31.52	69.49	25.24	55 66	21 58	47 57		47 75	105 2
Totals	150 96	332.81	189.13	416 96	151.44	333.86	129.48	285.45		286 50	631 62

FIGURE 5-2 MASS STATEMENT - 10 GW GROUND OUTPUT SPS

The five SPS, each with 10 GW ground output, are shown in Figure 53 drawn to the same scale to provide a comparison of sizes. Note that, although the nuclear Brayton cycle is the smallest of the power satellites, it is also the heaviest. This is because its area consists of radiators whose mass density is considerably greater than that of the solar collectors which comprise the major area of the other power satellites.

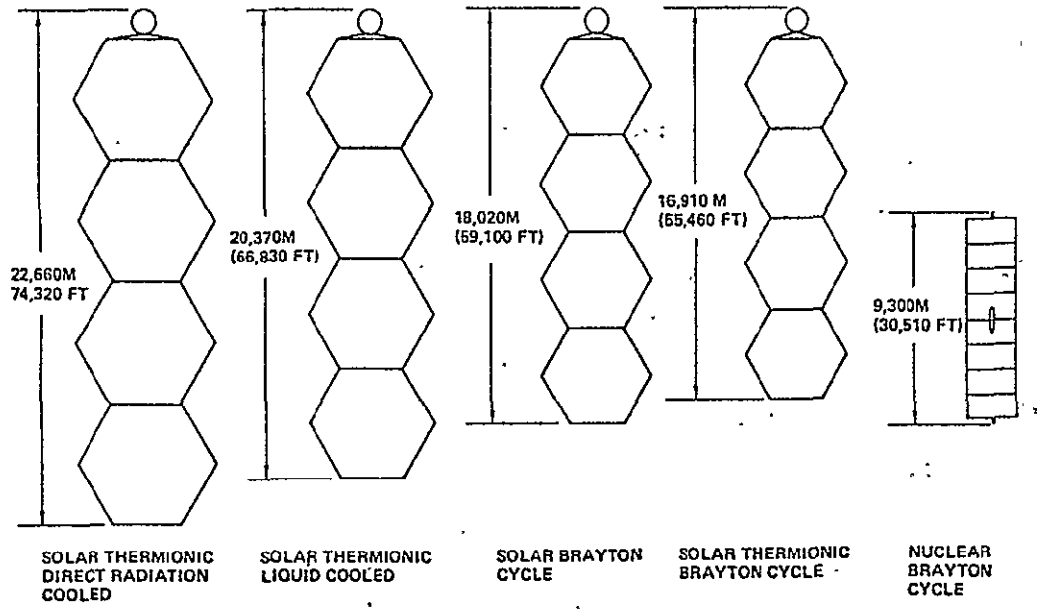

FIGURE 5-3 COMPARISON OF SYSTEM SIZES - ALL SAME SCALE
10 GW GROUND OUTPUT

Figure 5-4 shows four SPS concepts with focal point assemblies. They are drawn to a common scale to provide a comparison of solar absorber and radiator sizes. Note that the solar thermionic direct radiation cooled concept has the largest solar absorber but has no main radiator. It has two radiators, one to cool the motors and the other to cool the generators of the rotary converters.

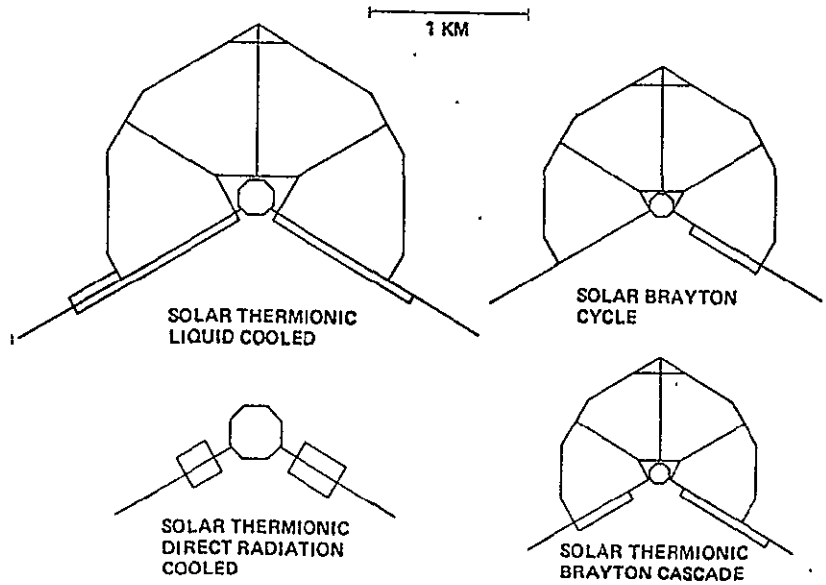

FIGURE 5-4 COMPARISON OF FOCAL POINT ASSEMBLIES
ALL SHOWN TO SCALE. 10 GW GROUND OUTPUT

5.3 BRAYTON CYCLE SOLAR ABSORBER ASSEMBLY

The major element of the solar absorber is a hollow sphere approximately 130 m (426.5 ft.) in diameter. The absorber has an aperture of 83 m (272.3 ft.) diameter. It is attached to a structural ring, supported on 6 trusses extending from the solar concentrator, such that concentrated solar radiation enters the sphere's cavity through the aperture.

The surface of the solar absorber is made up of flat facets. Around the cneter of the absorber is a belt of 28 facets carrying the bulk of the Brayton cycle machinery. These facets are alternately 20 m (65.6 ft.) square and 20 m (65.6 ft.) x 9 m (29.5 ft.). The remainder of the facets are 20 m (65.6 ft.) square with smaller, tapered flat panels in between to complete the sphere's surface. The reason for the basic 20 m (65.6 ft.) square panel is that this is a convenient size for transportation to low Earth orbit. The 4 solar absorbers which comprise a 10 GW power satellite are joined together by a spinal truss of triangular cross section. The main members of the truss carry the 3-phase primary power from the generators to the transmitter. The secondary members of the spinal truss incorporate insulators to electrically isolate the phases from each other. The absorber is attached to the spinal truss by two members extending from the absorber support ring.

The arrangement of the solar absorber is shown in Figure 5-5.

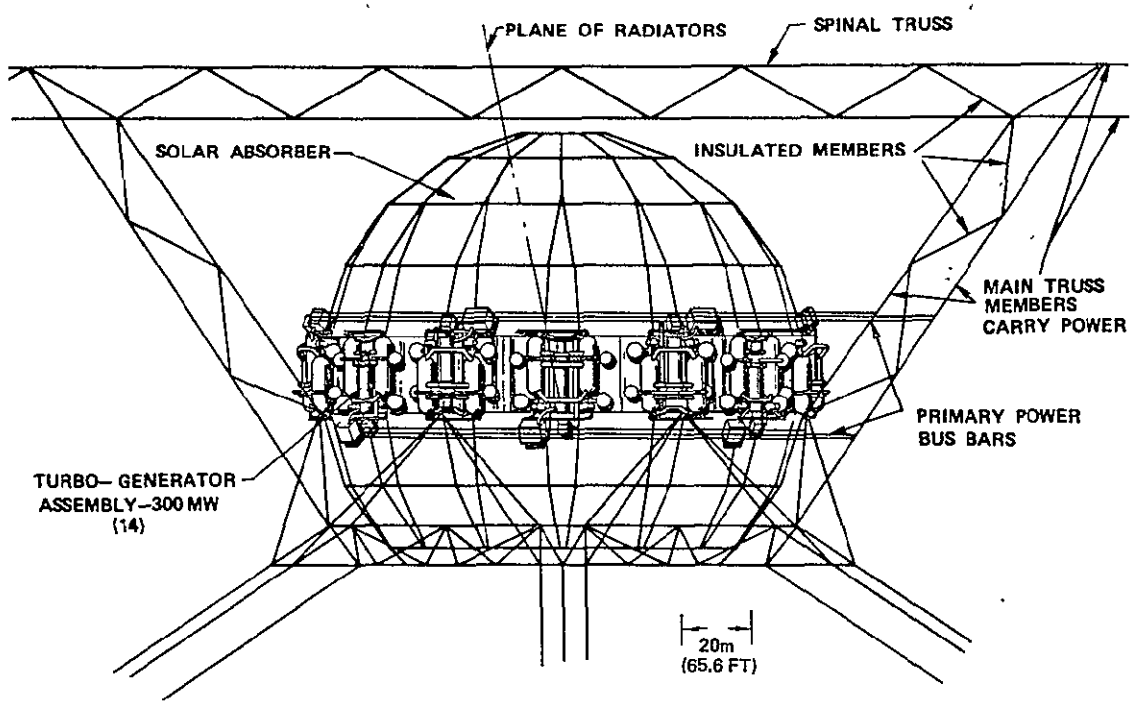

FIGURE 5-5 BRAYTON CYCLE SOLAR ABSORBER ASSEMBLY CONCEPT

Each solar absorber has 14-300 MW generators. These are mounted on the 20 m (65.6 ft.) x 9 m (29.5 ft.) panels which form a part of the central belt described previously. The generators are driven by Brayton cycle turbo-compressors. Alternate turbo-generator assemblies are oriented at 180° to each other in order to nullify rotational effects.

Each turbo-compressor has 2 recuperator/coolers. The recuperator/coolers are mounted on the 20 m (65.6 ft.) square panels adjacent to the turbo-generators. These panels are divided in two since the combined weight of the recuperator/coolers and other equipment exceeds the weight capability of the transporter. Each of the 20 m (65.6 ft.) x 10 m (32.8 ft.) panels support a helium-xenon bottle, a NaK accumulator and a NaK pump in addition to the recuperator/cooler. The helium-xenon bottle provides start-up

capability for the turbo-compressor and the NaK pump and accumulator form part of the turbo-compressor radiator loop.

The 60 kilovolt 3-phase output from the generator is transformed into 380 kilovolt. There is a circuit breakder between the generator and transformer. Figure 5-6 shows the general arrangement of the turbo-generators and associated equipment.

Output from the transformer is carried on two sets of busbars each serving seven turbo-generators. The radiators for the turbo-compressors are similar to those shown in Figure 5-4, for the solar thermionic liquid cooled SPS. The generators and transformers are also liquid cooled.

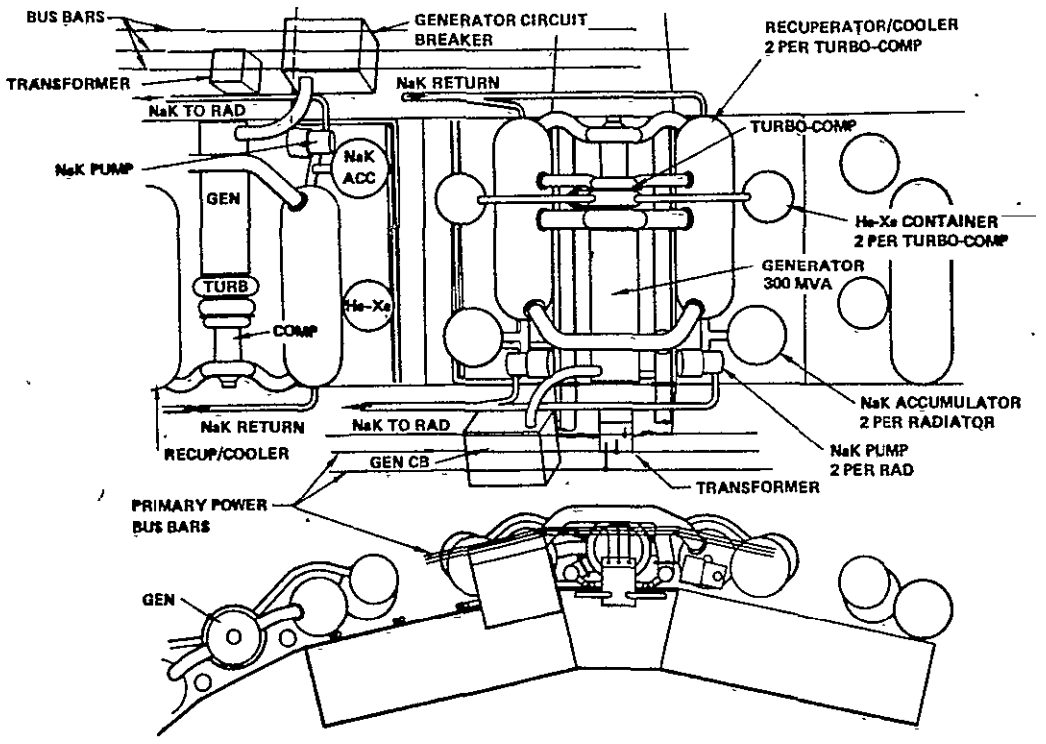

FIGURE 5-6 SOLAR BRAYTON CYCLE TURBO-GENERATOR ASSEMBLY CONCEPT

Solar energy, available in the solar absorber cavity, is removed by the heat absorber assembly. The heat absorber consists of a multitude of 12.5 mm (0.5") diameter tubes shaped and arranged as shown in Figure 5-7. The tubes cover almost the whole of the interior of the absorber. They are arranged in 14 equal area sets, one set to each turbo-compressor. The tubes are attached to input and output headers which connect through feeders to the turbo-compressor. The location of the tubes in the Brayton cycle power system is shown in Figure 5-8.

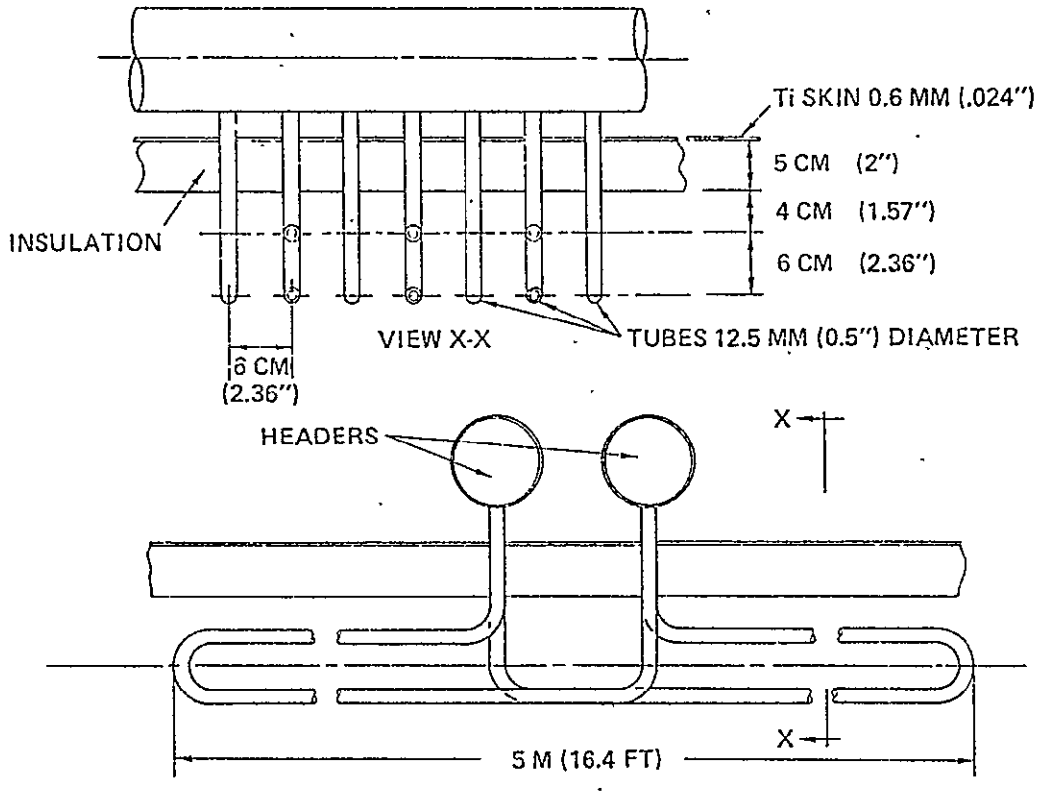

FIGURE 5-7 BRAYTON CYCLE HEAT ABSORBER ASSEMBLY

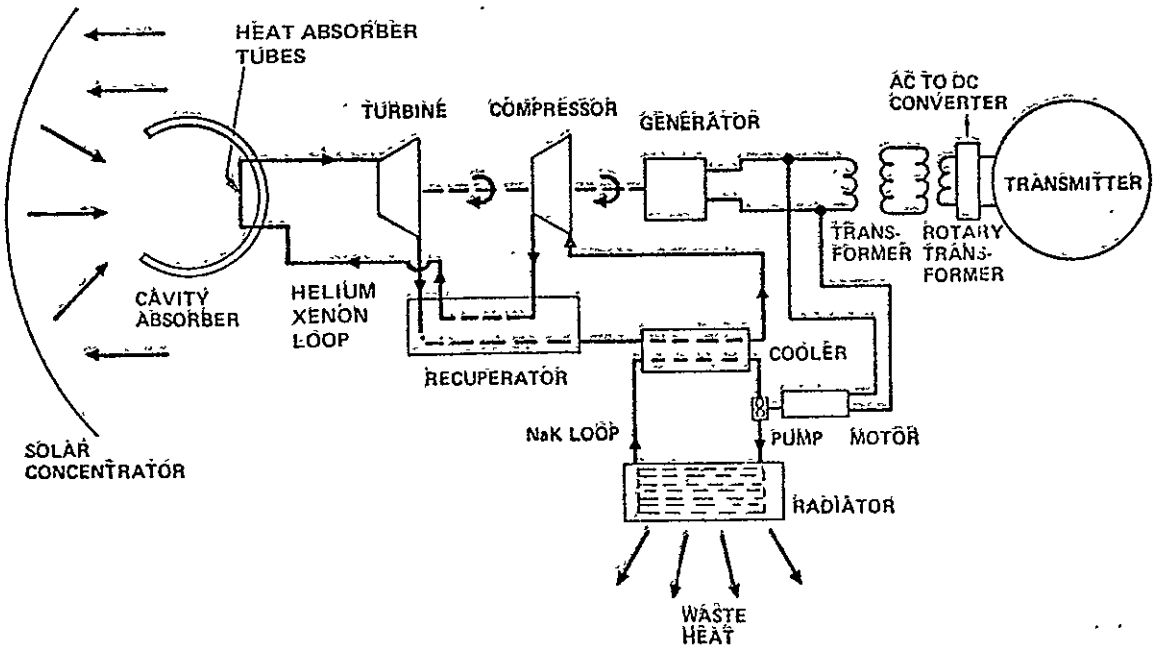

FIGURE 5-8 SOLAR BRAYTON CYCLE

5.4

THE POWER RELAY SYSTEM (GEOSYNCHRONOUS MIRRORS FOR AUGMENTATION OF GROUND-BASED SOLAR POWER PLANTS)

A large mirror in geosynchronous orbit has been proposed to direct solar radiation to a ground-based solar power plant for night operation. Because the sun is not a point source, the minimum size of reflected image from geosynchronous orbit is 134,000 KM^2 (52,000 MI^2). To provide a reflected solar image of one sun intensity, a mirror having the same area is required which would have a system mass of 4×10^{10} KG (45,000,000 tons). If targeted anywhere in the United States, it would involve at least 50,000 inhabitants and the maximum daytime temperature in the affected region could reach 150°F. This could have severe environmental effects.

Figure 5-9 shows a typical target area for the power relay system.

- Optical effects cause minimum image size to be quite large:

  Any target area selected within contiguous U.S. will involve at least 50,000 occupants.

- For "one sun" image strength:

  1) Total mirror area required is $\approx 134{,}000$ km^2 (52,000 mi^2)
  2) System mass is $\approx 4 \times 10^{10}$ kg (45,000,000 tons)

- The mirror system may cause significant environmental effects

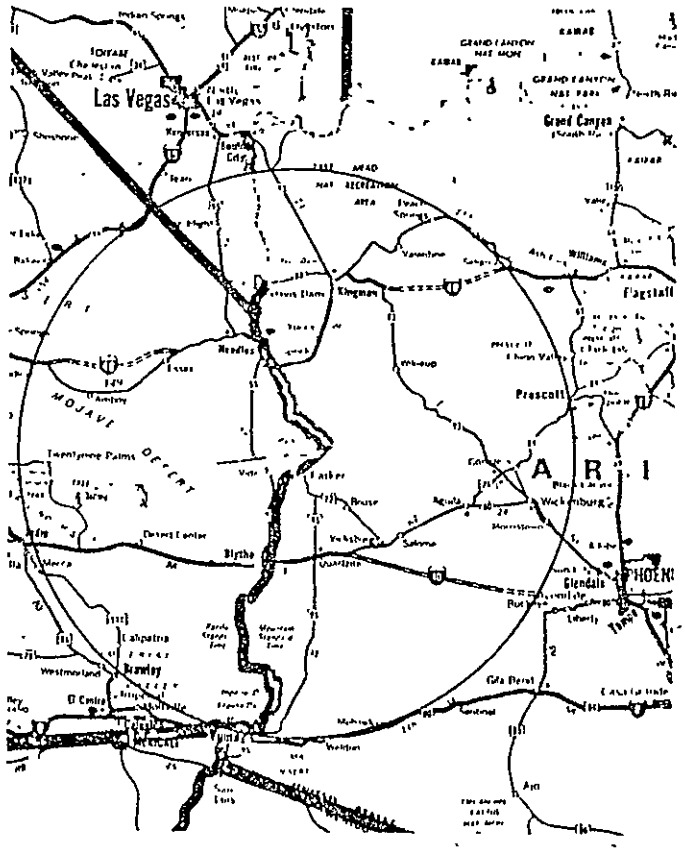

FIGURE 5-9 THE POWER RELAY SYSTEM (GEO-SYNCHRONOUS MIRRORS FOR AUGMENTATION OF GROUND-BASED SOLAR POWER PLANTS)

6.0 IMPACTS

6.1 COMPARISON OF SPS ENERGY BALANCE

In order to assess the potential of an energy producing system such as the SPS, it is necessary to establish a meaningful performance index. MSFC correspondence (1) directed that methods suggested in a recent article in Science (2) be considered. In (2), the author considers all energy necessary to perform functions (e.g., processing of ore to produce metal, transportation of parts, etc.) that are part of total plant construction as subsidy. Thus, the sum of all subsidies represents an energy investment and the useful energy output is the return. The ratio of the return to the subsidy is the performance index used in (2) and below.

Subsidy density (defined as kWh/kg) data has been found in many sources. Wherever possible, those sources have been used that consider primary energy by using the "input-output method of analysis" (see (2)). Also in the case of fuel and plastics, feedstock energies are included in the subsidy.

The approach used in (2) and here is somewhat new, and subsidies are not readily found for all materials or functions. All estimates for materials or functions for which no subsidy could be found were conservatively estimated.

In these calculations energy subsidies are given in terms of kW thermal, as the majority of such quantities are related to hydrocarbon fossil fuels. However, system electrical output is, of course, in kW electric. Thus "energy grade" must be considered. In (2) the method used was to multiply electrical energy by a factor of 3.5, to compensate for the inefficiency of conversion of fossil to electrical energy in power plants. This method is used here, i.e., the 30 year electrical output is multiplied by the factor 3.5. Tables 6-1 through 6-5 summarize the various subsidy components, in terms of their masses and energy contents for each system. The liquid hydrogen is assumed to be produced by electrolysis, and its energy subsidy has, therefore,

been multiplied by the same factor of 3.5. Power availability is assessed at 95%. Figure 6-1 compares the energy balance of the candidate SPS systems. It should be noted that in each of the SPS's analyzed, over 90% of the energy subsidy is used in transporting the system to orbit.

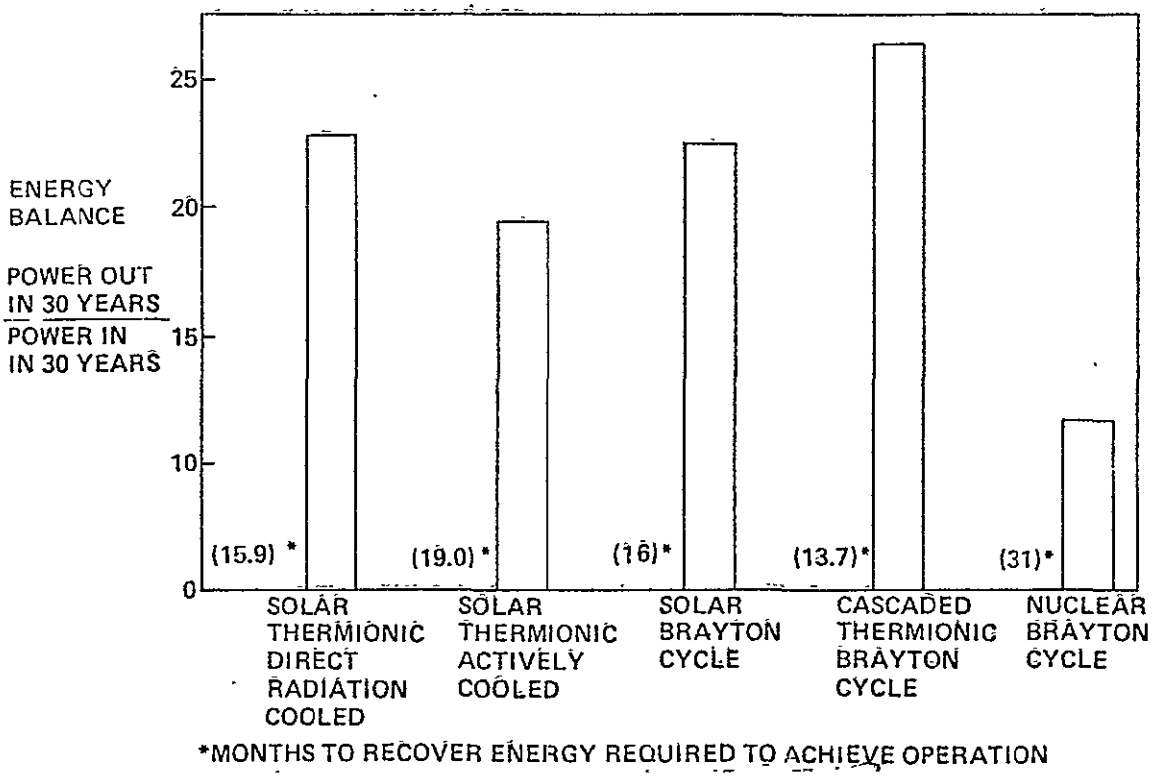

FIGURE 6-1 COMPARISON OF SPS ENERGY BALANCE (10 GW GROUND OUTPUT)

TABLE 6-1 ENERGY BALANCE
SOLAR THERMIONIC RADIATION COOLED

MASS: 150.96 X 10^6 Kg (332.81 X 10^6 Lbm)

	Kg X 10^{-6}	Lbm X 10^{-6}	kWh_{th} X 10^{-9}	Btu X 10^{-12}
Aluminum	71.65	157.99	5.66	19.32
Magnesium	8.54	18.83	0.982	3.35
Steel	10.74	23.68	0.172	0.587
Tedlar/Kapton	2.62	5.78	0.065	0.222
Haynes-188	6.63	14.62	0.431	1.47
NaK	1.81	3.99	0.007	0.024
Molybdenum	33.17	73.14	1.824	6.225
Beryllium	9.68	21.34	0.532	1.816
Min-K	6.12	13.49	0.306	1.044
			9.979	34.058
Ground Transportation (SPS Materials)				
300 mi. (Rail)			0.010	0.034
200 mi. (Truck)			0.027	0.092
			0.037	0.126
30 Year Replacement Parts				
0.5% for 30 years	22.64		0.905	3.089
Orbit Transfer of Satellite and Parts				
Argon	88.59	195.34	0.267	0.911
LH_2	3.49	7.69	0.684	2.334
LO_2	24.28	53.54	0.073	0.249
Propulsion	0.49	1.08	0.043	0.147
			1.067	3.641
Assembly Station Pro-rated	0.08	1.76	.003	0.011
1314 Flights of Low Orbit Transport System X 10^{-2}				
LO_2	109.3	241.00	32.90	112.288
RP^2	7.45	16.43	13.14	44.847
LH_2	16.04	35.37	314.38	1072.979
			360.42	1230.114

TABLE 6-1 ENERGY BALANCE (Cont'd)

Rectenna and Transmission Corridor (Nominal Length, 100 KM = 62 S. Mi.)

Area lost to farming — Assume acreage in corn and complete loss during 30 yr.

	Energy lost	30 Yr. Energy Loss (KW Hrs.)	BTU
Rectenna 100 KM^2	2.5×10^8 kWh/Yr.	7.5×10^9	22.0×10^{12}
Transmission Corridor 100 KM^2	2.5×10^8 kWh/Yr.	7.5×10^9	22.0×10^{12}
		15.0×10^9	44×10^{12}
TOTAL		3.874×10^{11} kWh	15.39×10^{14} BTU

30 Yr. X 10 GW x 0.95 Availability = 2.50×10^{12} kWh

$$\frac{2.5 \times 10^{12} \text{ kWh}_e}{0.38 \times 10^{12}} \times 3.5 \frac{\text{kWh}_t}{\text{kWh}_t} = 22.58$$

TABLE 6-2 ENERGY BALANCE SOLAR THERMIONIC ACTIVELY COOLED

MASS: 185.9×10^6 kg (409.72×10^6 Lbm)

	Kg $\times 10^{-6}$	Lbm $\times 10^{-6}$	Total Energy kWh_{th}	Energy BTU
Aluminum	40.07	88.31	3.165×10^9	10.8×10^{12}
Magnesium	1.91	4.21	0.2196×10^9	0.749×10^{12}
Steel	30.5	67.22	0.488×10^9	1.665×10^{12}
Tedlar/Kapton	1.00	2.204	0.025×10^9	0.085×10^{12}
Molybdenum	27.3	60.17	1.501×10^9	5.125×10^{12}
Beryllium	15.02	33.10	0.826×10^9	2.82×10^{12}
Haynes	8.86	19.53	0.576×10^9	1.965×12^{12}
Ceramics	12.89	28.41	0.120×10^9	0.44×10^{12}
Min-K	9.49	20.92	0.474×10^9	1.62×10^{12}
NaK	38.84	85.6	0.155×10^9	0.53×10^{12}
			7.55×10^9	25.8×10^{12}

Ground Transportation (Satellite Materials)

	KW Hrs.	BTU
300 Mi. (Rail)	1.206×10^7	4.117×10^{10}
200 Mil (Truck)	3.3613×10^7	11.472×10^{10}
	4.57×10^7	15.59×10^{10}

30 Years Replacement Parts

NaK	6.7	14.77	0.0268×10^9	0.09147×10^{12}
Other	18.8	41.44	0.752×10^9	2.57×10^{12}
			0.779×10^9	2.66×10^{-2}

Orbit Transfer of Satellite and Parts

Argon	109.1	240.46	0.329×10^9	1.123×10^{12}
LH_2	4.3	9.48	0.843×10^9	2.877×10^{12}
LO_2	29.9	65.9	0.09×10^9	0.307×10^{12}
Propulsion Modules Pro-rated	0.6	1.32	0.0529×10^9	0.180×10^{12}
			1.315×10^9	4.487×10^{12}
Assembly Station Pro-rated	0.1	0.22	0.004×10^9	0.01365×10^{12}

1600 Flights of Low Orbit Transport System

LO_2	133.1×10^2	293.35×10^2	40.06×10^9	136.72×10^{12}
RP^2	9.07×10^2	19.99×10^2	16.0×10^9	54.61×10^{12}
LH_2	19.53×10^2	43.04×10^2	382.79×10^9	1306.46×10^2
			438.85×10^9	1497.79×10^{12}

TABLE 6-2 ENERGY BALANCE SOLAR THERMIONIC ACTIVELY COOLED (Cont'd)

Area lost to farming Assume acreage in corn and complete loss during 30 yr.

	Energy lost	30 Yr. Energy Loss (KW Hrs.)	BTU
Rectenna 100 KM^2	2.5×10^8 kWh/Yr.	7.5×10^9	22.0×10^{12}
Transmission Corridor 100 KM^2	2.5×10^8 kWh/Yr.	7.5×10^9	22.0×10^{12}
		15.0×10^9	44×10^{12}
TOTAL		4.635×10^{11} kWh	15.82×10^{14} BTU

30 Yr. x 10 GW x 0.95 Availability = 2.50×10^{12} kWh

$$\frac{2.5 \times 10^{12} \text{ kWhe}}{0.4635 \times 10^{12}} \times 3.5 \frac{\text{kWht}}{\text{kWht}} = 18.88$$

TABLE 6-3 ENERGY BALANCE SOLAR BRAYTON CYCLE

MASS: 151.44 X 10^6 (333.86 X 10^6 Lbm)

	Kg X 10^{-6}	Lbm X 10^{-6}	kWh_{th} X 10^9	BTU X 10^{12}
Aluminum	38.75	85.44	3.060	10.444
Magnesium	1.70	3.75	0.196	0.669
Steel	15.78	34.77	0.252	0.860
Tedlar/Kapton	0.90	1.98	0.023	0.078
Min-K	2.66	5.86	0.133	0.454
Copper	6.90	15.21	0.114	0.389
Niobium	35.93	79.21	1.976	6.744
Beryllium	9.90	21.82	0.545	1.860
Haynes-188	8.77	19.34	0.570	1.945
NaK	30.18	66.54	0.121	0.413
			6.99	23.857
Ground Transportation (SPS Materials)				
300 mi (Rail)			0.0098	
200 mi (Truck)			0.0274	
			.0372	0.127
30 Year Replacement Parts				
NaK	6.64	14.64	0.027	0.091
Other	18.19	40.11	0.728	2.483
	24.83	54.75	0.755	2.574
Orbit Transfer of SPS and Parts				
Argon	88.88	195.98	0.267	0.911
LH_2	3.50	7.72	0.686	2.341
LO_2	24.36	53.71	0.073	0.249
Propulsion Modules	0.49	1.08	1.069	3.648
Assembly Station	0.08	0.18	0.007	0.024
1335 Flights of Low Orbit Transport System	X 10^2	X 10^2		
LO_2	110.98	244.71	33.40	113.99
RP^2	7.56	16.67	13.33	45.495
LH_2	16.28	35.89	319.09	1089.05
			365.82	1248.54

TABLE 6-3 ENERGY BALANCE SOLAR BRAYTON CYCLE (Cont'd)

Rectenna and Transmission Corridor (Nominal Length, 100 KM = 62 S. Mi.)

Area lost to farming Assume acreage in corn and complete loss during 30 yr.

	Energy lost	30 Yr. Energy Loss (KW Hrs.)	BTU
Rectenna 100 KM^2	2.5×10^8 kWh/Yr.	7.5×10^9	22.0×10^{12}
Transmission Corridor 100 KM^2	2.5×10^8 kWh/Yr.	7.5×10^9	22.0×10^{12}
		15.0×10^9	44×10^{12}
TOTAL		3.897×10^{11} kWh	13.30×10^{14} BTU

30 Yr. x 10 GW x 0.95 Availability = 250×10^{12} kWh

$$\frac{2.5 \times 10^{12} \text{ kWhe} \times 3.5 \text{ kWht}}{0.3897 \times 10^{12} \text{ kWht}} = 22.45$$

TABLE 6-4 ENERGY BALANCE CASCADED THERMIONIC BRAYTON

MASS: 129.48 X 10^6 Kg (285.45 X 10^6 Lbm)

	Kg X 10^{-6}	Lbm X 10^{-6}	kWh_{th} X 10^{09}	BTU X 10^{-12}
Materials				
Aluminum	34.26	75.54	2.706	9.235
Magnesium	1.49	3.28	0.171	0.584
Steel	19.63	43.28	0.314	1.072
Molybdenum	5.14	11.33	0.283	0.966
Ceramic	2.44	5.38	0.023	0.078
Tedlar/Kapton	0.78	1.72	0.020	0.068
Min-K	1.92	4.23	0.096	0.328
Copper	4.83	10.65	0.080	0.273
Niobium	25.36	55.92	1.395	4.761
Beryllium	6.82	15.04	0.375	1.280
Haynes-188	6.04	13.32	0.393	1.341
NaK	20.77	45.79	0.083	0.283
			5.939	20.269
Ground Transportation				
300 mi (Rail)			.0084	0.029
200 mi (Truck)			.023	0.078
			.0314	0.107
30 Year Replacement Parts				
NaK	4.57	10.07	0.018	0.061
Other	14.85	3.27	0.594	2.027
			0.612	2.088
Orbit Transfer of Satellite & Parts				
Argon	75.99	167.56	0.229	0.781
LH_2	2.99	6.59	0.586	2.000
LO_2	20.82	45.91	0.063	0.215
Propulsion Modules	0.42	0.93	0.037	0.126
			0.915	3.122
Assembly Station Pro-rated	0.07	0.15	0.006	0.020
1130 Flights of Low Orbit Transport System	X 10^2	X 10^2		
LO_2	93.83	206.89	28.24	96.383
RP^2	6.39	14.09	11.27	38.464
LH_2	13.77	30.36	269.89	921.135
			309.40	1055.982

TABLE 6-4 ENERGY BALANCE CASCADED THERMIONIC BRAYTON (Cont'd)

Rectenna and Transmission Corridor (Nominal Length, 100 KM = 62 S. Mi.)

Area lost to farming Assume acreage in corn and complete loss during 30 yr.

	Energy lost	30 Yr. Energy Loss (KW Hrs.)	BTU
Rectenna 100 KM^2	2.5×10^8 kWh/yr.	7.5×10^9	22.0×10^{12}
Transmission Corridor 100 KM^2	2.5×10^8 kWh/yr.	7.5×10^9	22.0×10^{12}
		15.0×10^9	44×10^{12}
TOTAL		3.319×10^{11} kWh	11.328×10^{14} BTU

30 Yr. X 10 GW X 0.95 Availability = 2.50×10^{12} kWh

$$\frac{2.5 \times 10^{12} \text{ kWhe}}{0.3319 \times 10^{12} \text{ kWht}} \times 3.5 = 26.36$$

TABLE 6-5 ENERGY BALANCE NUCLEAR BRAYTON CYCLE

MASS: 286.5 X 10^6 Kg (631.62 X 10^6 Lbm)

	Kg X 10^{-6}	Lbm X 10^{-6}	kWh_{th} X 10^{-9}	BTU X 10^{-12}
Aluminum	26.88	59.27	2.12	7.235
Steel	63.28	139.53	1.01	3.447
Haynes-188	20.70	45.64	1.34	4.573
Beryllium	55.96	123.39	3.08	10.512
Copper	6.83	15.06	0.113	0.386
Graphite	6.83	15.06	0.341	1.164
NaK	101.32	223.41	0.405	1.382
Lithium	0.38	0.84	0.03	0.102
Thorium	2.04	4.50	0.204	0.696
Uranium	0.06	0.13	0.006	0.02
Fluorine	2.13	4.70	0.319	1.089
			8.968	30.608
Ground Transportation				
300 mi (Rail)			0.018	
200 mi (Truck)			0.052	
			0.70	0.239
30 Year Replacement Parts				
NaK	22.29	49.15	0.089	0.304
Other	20.68	45.6	0.827	2.822
Thorium	20.40	44.98	2.04	6.962
	63.37		2.956	10.088
Orbit Transfer of Satellite and Parts				
Argon	180.56	398.13	0.543	1.853
LH_2	7.12	15.70	1.395	4.761
LO_2	49.48	109.10	0.149	0.508
Propulsion Modules	0.99	2.18	0.087	0.297
			2.174	7.42
Assembly Station Pro-rated	0.165	0.363	0.007	0.024
2650 Flights of Low Orbit Transport System X 10^2				
LO_2	220.45	486.09	66.355	226.47
RP^2	15.02	33.12	26.49	90.41
LH_2	32.35	71.33	634.06	2164.05
			726.9	2480.93

TABLE 6-5 ENERGY BALANCE NUCLEAR BRAYTON CYCLE (Cont'd)

Rectenna and Transmission Corridor (Nominal Length, 100 KM = 62 S. Mi.)

Area lost to farming — Assume acreage in corn and complete loss during 30 yr.

	Energy lost	30 Yr. Energy Loss (KW Hrs)	BTU
Rectenna 100 KM^2	2.5×10^8 kWh/yr.	7.5×10^9	22.0×10^{12}
Transmission Corridor 100 KM^2	2.5×10^8 kWh/yr.	7.5×10^9	22.0×10^{12}
		15.0×10^9	44×10^{12}
TOTAL		7.56×10^{11} kWh	25.80×10^{14} BTU

30 Yr. X 10 GW x 0.95 Availability = 2.50×10^{12} kWh

2.5×10^{12} kWhe X 3.5 kWht = 11.57

0.756×10^{12}

REFERENCES

1. MSFC Letter, W. E. Whitacre to D. Gregory, Subject: "Energy Balance Analysis", October 30, 1975.

2. Gilliland, M. W., "Energy Analysis and Public Policy", Science, September 26, 1975.

6.2 LAUNCH VEHICLE EXHAUST EMISSION MASS

Launch vehicle exhaust emission masses for five SPS's were estimated and are shown in Figure 6-2. They are for a Class 4 ballistic SSTO vehicle of the type previously described. The number of launches for each system is in the order of 1100 to 2650, depending on system mass and includes launches for maintenance during a 30-year period. The emissions are for altitudes above 12 Km (40,000 ft.). Below this alttitude, CO and CO_2 emissions would be approximately the same as above 12 Km, but H_2O would be very much less. The maximum H_2O produced (nuclear Brayton cycle) would be somewhat greater than a small thunderstorm, but considerably less than a tropical thunderstorm. The chart shows probable maximum masses of nitrides of oxygen which are too small to be drawn to scale. Also indicated are masses of HCL and Al_2O_3 produced by the space shuttle in associated crew rotation launches.

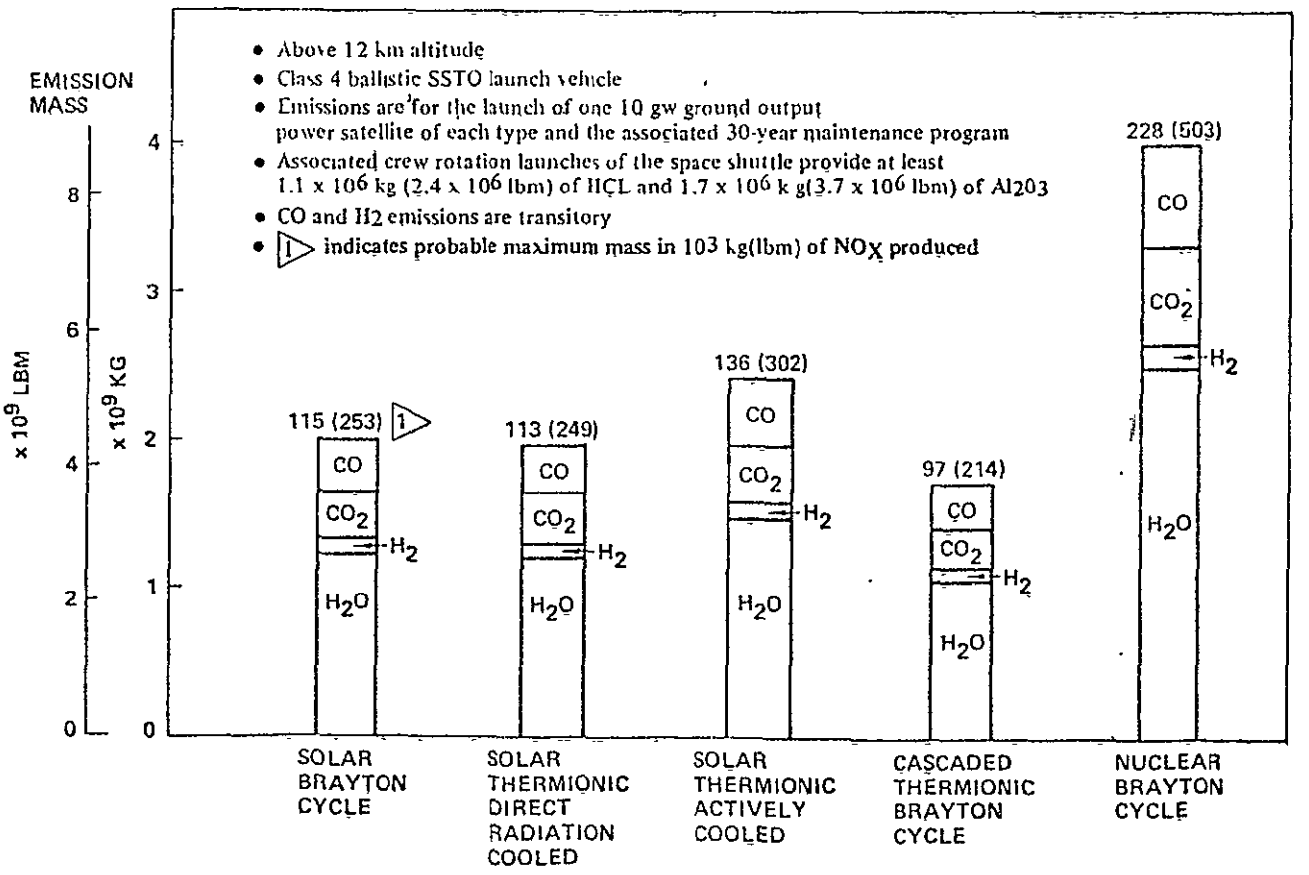

FIGURE 6-2 LAUNCH VEHICLE EXHAUST EMISSION MASS

7.0 SPACE BASED SATELLITE POWER STATION STUDY

COST REPORT

POWER SATELLITE STUDY COST REPORT

INTRODUCTION

7.1 PROGRAM COST SUMMARIES AND COMPARISONS

7.2 GROUND RULES AND ASSUMPTIONS

7.3 WORK BREAKDOWN STRUCTURE

7.4 PROGRAM MASTER SCHEDULE

7.5 HARDWARE IDENTIFICATION AND TIME PHASING

- 7.5.1 SKETCHES, DRAWINGS, AND WEIGHT STATEMENTS OF MAJOR ELEMENTS
- 7.5.2 HARDWARE IDENTIFICATION MATRIX (QUANTITIES BY PROGRAM PHASE AND WBS)
- 7.5.3 HARDWARE TIME PHASING

7.6 COST ESTIMATES

- 7.6.1 SYSTEM ESTIMATES BY WBS
- 7.6.2 SYSTEM ESTIMATES ARRANGED BY HARDWARE ELEMENT
- 7.6.3 HARDWARE ELEMENT COST DETAILS

7.7 ECONOMICS

- 7.7.1 FUNDING DISTRIBUTIONS
- 7.7.2 NET PRESENT VALUE ANALYSIS

INTRODUCTION

This report presents total system cost estimates for five alternative power satellite systems. Included are ground rules and assumptions, hardware descriptions, quantities, schedules, and cost estimates, net present value analysis, f xed cost comparisons, and projected funding levels. Program costs are developed by hardware item and categorized into development, production, and operations phases. The costs are then grouped in a Work Breakdown Structure based on the NASA provided WBS. Each satellite concept includes costs associated with the following hardware:

1. Verification Program Pre-Production Satellite
2. STS Transportation to LEO
3. Heavy Lift LEO Frieghter (HLLV)
4. Full Scale Satellite and Transmitter
5. LEO Manufacturing Base
6. GEO Assembly and Maintenance Base
7. LEO and GEO Manipulators
8. Crew OTV
9. Satellite OTV
10. Ground Rectenna
11. Ground Mission Control Complex

Cost data for the HLLV and STS systems are derived from two other current NASA/Boeing studies. The Ground Rectenna and certain parts of the Satellite are estimated using the RCA Price Parametric Model. All other cost data is developed through use of the Boeing Parametric Cost Model (PCM). All dollars are expressed as constant 1976 values and a fixed ground output of 620 gigawatts is used for each system.

7.1 PROGRAM COST SUMMARIES AND COMPARISONS

TABLE 7-1 SATELLITE POWER STATION
SYSTEM COSTS
BY PHASE

SYSTEM	COST DOLLARS IN BILLIONS DDT&E	PRODUCTION	OPERATIONS	TOTAL
SOLAR THERMIONIC DIRECT RADIATION COOLED	44.25	1,238.98*	672.12	1,955.35
SOLAR THERMIONIC LIQUID COOLED	51.10	1,425.13*	828.59	2,304.82
SOLAR BRAYTON	58.78	1,606.96	674.47	2,340.21
SOLAR THERMIONIC BRAYTON	56.05	1,435.03*	622.19	2,113.27
NUCLEAR BRAYTON	71.45	2,368.51	1,118.55	3,558.51

*Reflects diode costs based on CUM average unit costs

NOTE: Costs have been revised since the Final Report Oral Presentation of April 14, 1976. Revisions reflect Thermionic Diode cost changes and minor Verification Program cost changes in the Transmitter Antenna.

TABLE 7-2 SATELLITE POWER STATION
SYSTEM COST BREAKOUT
BY MAJOR WBS ELEMENT

WBS	ELEMENT	COST - DOLLARS IN BILLIONS				
		THERMIONIC DIRECT RADIATION COOLED	THERMIONIC LIQUID COOLED	BRAYTON	THERMIONIC BRAYTON	NUCLEAR BRAYTON
1.0	PROGRAM MANAGEMENT	11.31	11.31	11.31	11.31	11.31
1.1	SE&I					
1.2	TECHNOLOGY DEVEL.	?	?	?	?	?
1.3	SYSTEM DEVELOPMENT (VERIFICATION PROGRAM	11.61	11.61	11.61	11.61	24.16
1.4	LEO TRANSPORT	743.13	923.40	745.48	684.10	1,257.46
1.5	LEO-GEO CREW OTV	2.16	2.16	2.16	2.16	2.16
1.6	SATELLITE ASSEMBLY OTV	14.69	14.69	14.69	14.69	14.69
1.10	SATELLITE POWER STATION	999.49	1,168.69	1,382.00	1,211.76	2,052.93
1.11	GROUND RECTENNA	125.58	125.58	125.58	125.58	125.58
1.12	OPS. SUPPORT	20.93	20.93	20.93	25.61	43.77
1.13	GROUND CONTROL COMPLEX	26.45	26.45	26.45	26.45	26.45
	TOTAL	1,955.35	2,304.82	2,340.21	2,113,27	3,558,51

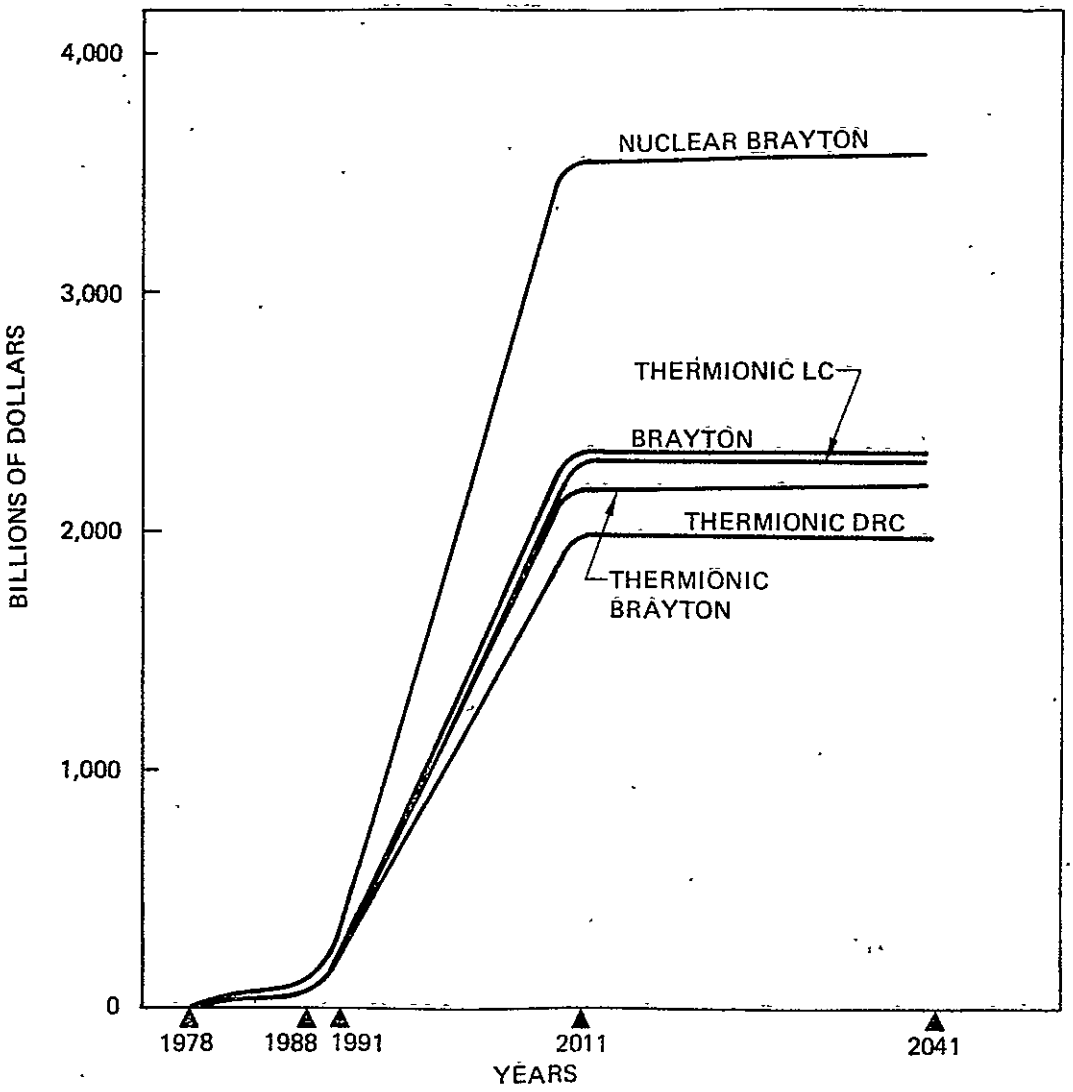

FIGURE 7-1 GRAPHICAL COST COMPARISON CUMULATIVE IN TIME

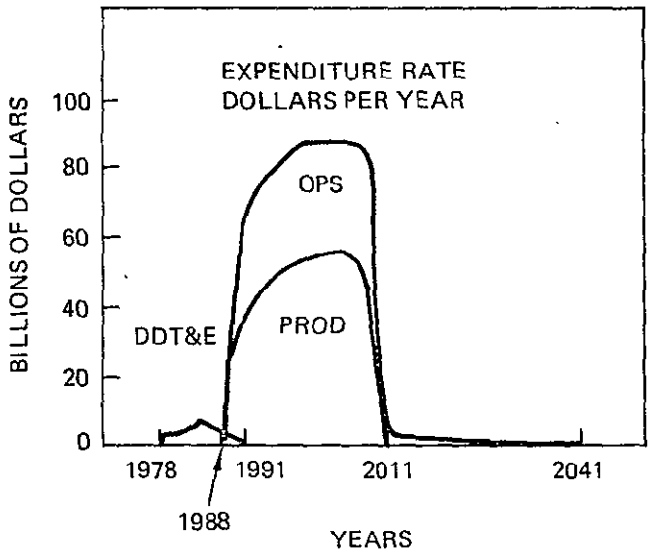

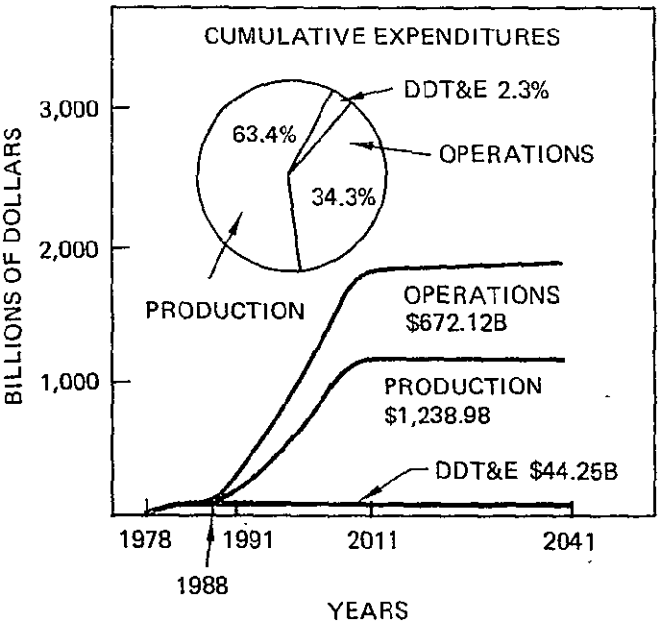

FIGURE 7-2 TYPICAL FUNDING CURVES
(THERMIONIC DIRECT RADIATION COOLED EXAMPLE)

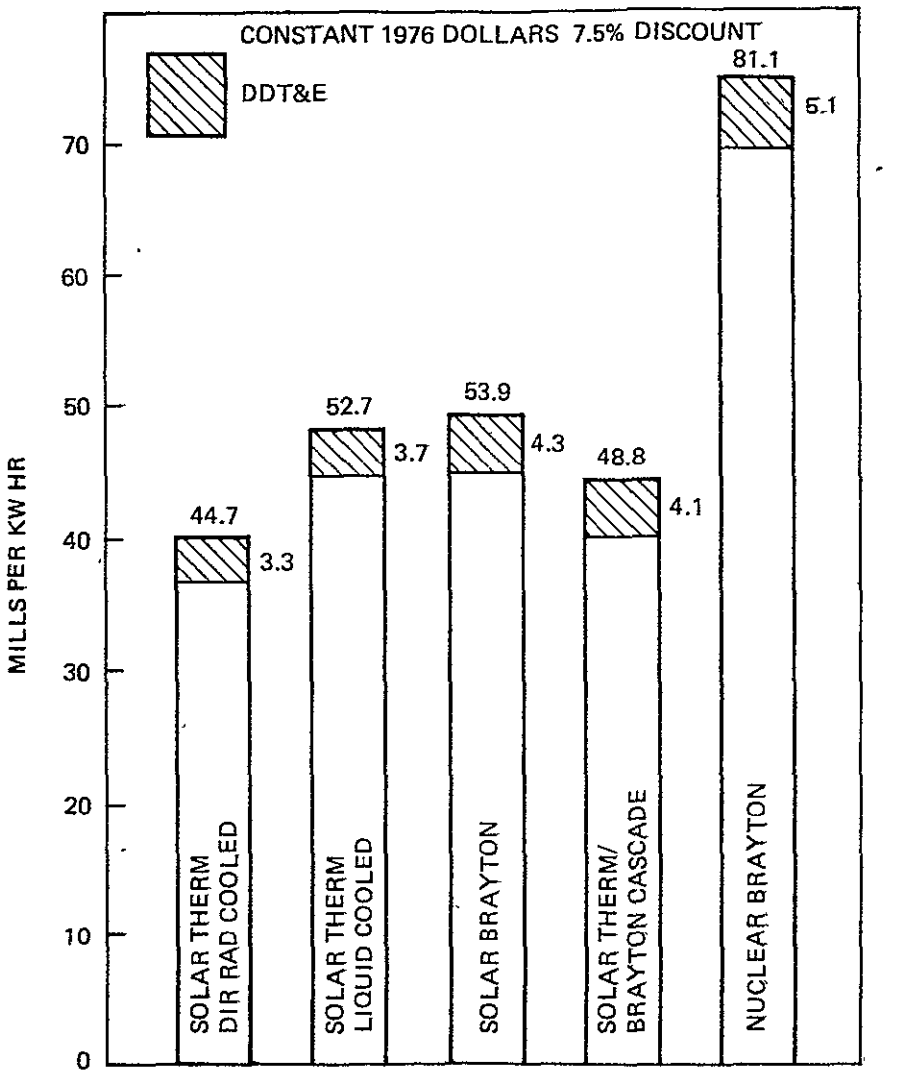

FIGURE 7-3 GENERATING COST OUTPUT FROM GROUND RECTENNA

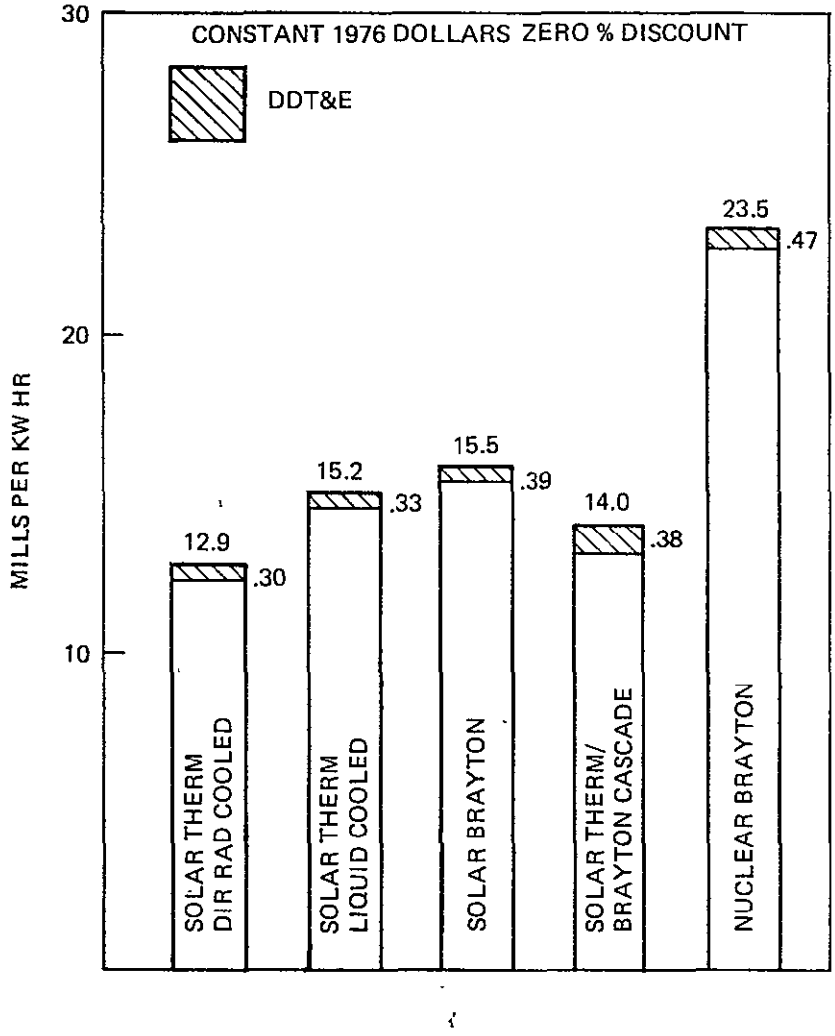

FIGURE 7-4 GENERATING COST OUTPUT FROM GROUND RECTENNA

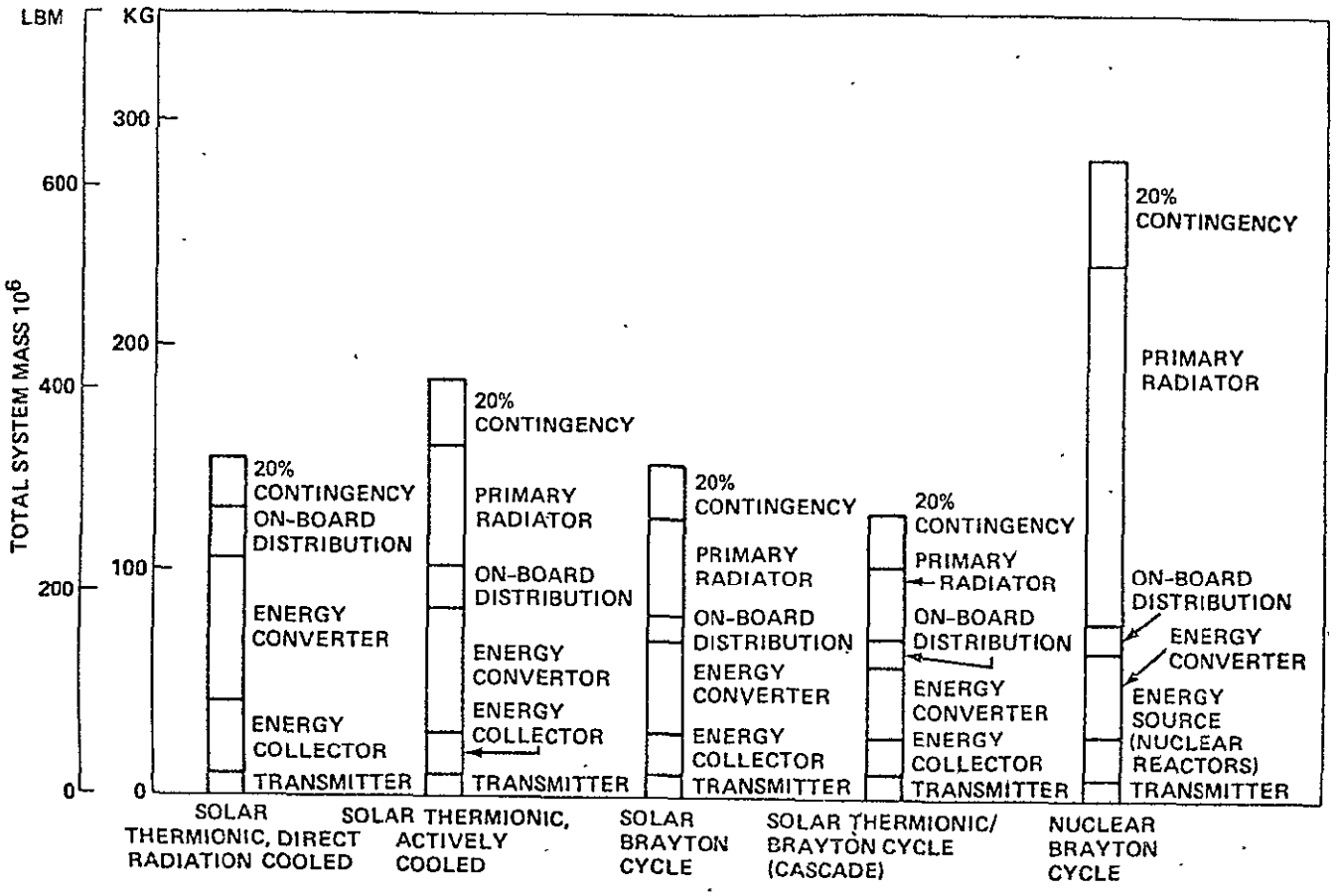

FIGURE 7-5 GRAPHICAL COMPARISON OF SYSTEM MASSES

7.2 GROUND RULES AND ASSUMPTIONS

COSTS

1. All dollars in 1976 values.

2. Discount rate is 7-1/2% on constant 1976 dollars for net present value analysis.

3. STS transportation costs are based on NASA Baseline (1971) cost per flight data escalated to 1976 values.

4. Expendable propellants and fluids are included in HLLV costs. All other program expendables including Nuclear Brayton NaK are excluded from program cost.

5. An allowance of 10% of hardware production cost is made to cover system spares.

6. Pilot program costs are assumed to be the same for all versions except Nuclear Brayton.

7. Satellite assembly is in Low Earth Orbit with no orbital manufacturing.

HARDWARE DETAILS

1. Sixty-two power satellites in each system generating 605 GW ground output.

2. Average packaging factor for HLLV payloads is 96%.

3. Numbers of ground and flight test units are based on consideration of total unit sizes and representative core section sizes.

4. STS will provide LEO crew transport with 100 person capacity payload bay pods.

5. STS will provide all verification program LEO transport.

6. No salvage consideration or values are made for any spent hardware.

ORBITAL CREW DETAILS

1. Crew Tasks

   - Deploy structural modules
   - Install solar cells and reflectors

1. (Continued)
   - Attach structural modules together
   - Attach microwave modules
   - Perform test and checkout
   - Re-perform all procedures as maintenance requires
2. Crew Work Cycle is 90 Days On-Orbit
3. Base Provisions
   - Means of operating for prolonged periods in space
   - Means of mobility throughout 10 square mile work area
   - Means of handling and controlling massive structures

HARDWARE LIFE TIME

1. STS - 500 flights
2. HLLV - 500 flights
3. Satellite OTV - 12 flights
4. Crew OTV - 20 flights
5. Power Satellite - 30 years
6. Ground Rectenna - indefinite
7. Ground Control Complex - indefinite
8. LEO Base - indefinite
9. GEO Base - indefinite
10. GEO and LEO Manipulators - indefinite

SCHEDULE - See Section 4.0

QUANTITIES - See Sections 5.2 and 5.3

7.3 WORK BREAKDOWN STRUCTURE

The Work Breakdown Structure used to format systems cost is based on direction received from NASA MSFC. We have attempted to conform to this breakdown; at t first breakout level. However, cost for items 1.7, 1.8 and 1.9 will be includ in other items as indicated on the WBS. Identification of these costs is not available.

WORK BREAKDOWN STRUCTURE

Adapted from NASA-Provided WBS

SATELLITE POWER STATION

1.0 Overall Program Management

1.1 SE&I

1.2 Technology Development Program

1.3 System Development Program - Verification

1.4 Earth-Low Earth Orbit Transportation Program

- 1.4.1 HLLV
- 1.4.2 STS

1.5 Low Earth Orbit - Geosynchronous Earth Orbit Transportation Program

1.6 Assembly Transportation Program

1.7 Logistics Transportation Program (will not be identified)

1.8 Maintenance Transportation Program (will not be identified)

1.9 Crew Transport Program (Will be included in 1.4 and 1.5)

1.10 Satellite Power Station Program

1.11 Ground Microwave Station Program

1.12 Operations Support Program

- 1.12.1 Low Earth Orbit Base
- 1.12.2 Geosynchronous Earth Orbit Base

1.13 Ground Control Complex

7.4 MASTER SCHEDULE

The following foldout presents a preliminary power satellite station master schedule. From this schedule the hardware time phasing (Section 5.3) is developed.

7.5 HARDWARE IDENTIFICATION

This section presents a description of the hardware in the Power Satellite System, identifies the hardware by WBS, and establishes quantities by program phase and time period.

7.5.1 SKETCHES, DRAWINGS, AND WEIGHT STATEMENTS OF MAJOR ELEMENTS.

TABLE 7-12 HARDWARE TIME PHASING SOLAR THERMIONIC DIRECT RADIATION COOLED

ITEM	YEAR 1980	1981	1982	1983	1984	1985	1986	1987	1988	1989	1990	1991	1992	1993	1994	1995	1996	1997	1998	1999	2000	2001	2002	2003	2004	2005	2006	2007	2008	2009	2010	2011	TOTAL
1. CW On-Line each Year												5	5	5	10	10	20	20	20	20	20	20	40	40	40	40	40	50	50	50	50	50	605
2. Cumm. GW On-Line												5	10	15	25	35	55	75	95	115	135	155	195	235	275	315	355	405	455	505	555	605	
3. Number of Power SATS/Year												1	1	1	1	1	2	2	2	2	2	2	4	4	4	4	4	5	5	5	5	5	62
4. Number of LEO Stations/Year										1					1		2					4					2						10
5. Number of Trans. Assemblers/Year										1																	1						2
6. Number of GEO Stations/Year											1								1				1			1			1		1		6
7. Number of Crew OTV Sets/Year												1				1		1		1	1	1	1	1	1	1	2	3	3	3	3	3	27
8. No. of SAT OTV Sets/Year										1				1		2						4					2						10
Replacement															1		2		2			2			2			2		2	1		14
9. Number of STS Launches/Year			3	Verification 4	20	40	5	5	10	10	10	10	10	10	10	15	16	16	17	18	18	18	33	36	36	36	43	45	46	47	48	49	667
10. Number of STS Buys/Year			1			1																				1							3
11. Number of HLLV Launches/Year									2	4	575	575	575	1150	1150	2300	2300	2300	2300	2300	2300	4600	4600	4600	4600	4600	5750	5750	5750	5750	5750		69,581
12. Number of HLLV For Replacement*													2	2	2	4	4	4	4	4	4	4	4	4	4	6	6	6	6	6	4		80
For Payload**									1	1	4			6		12						24					12						60
13. No. of Rectennas Instal/Year												1	1	1	1	1	2	2	2	2	2	2	4	4	4	4	4	5	5	5	5	5	62
14. No. of People in LEO						24	24			100	100	100	100	100	180	180	355	355	355	355	355	355	705	705	705	705	875	875	875	875	875	875	
15. No. of People in GEO											12	12	13	13	18	23	33	43	56	68	78	88	113	133	158	178	198	223	253	278	303	333	

* 500 Flight Life Req Replacement

**If the HLLV had infinite life, would need this many to place payload.

FOLDOUT FRAME

FOLDOUT FRAME 2

TABLE 7-13 HARDWARE TIME PHASING SOLAR THERMIONIC ACTIVELY COOLED

ITEM	YEAR 1980	1981	1982	1983	1984	1985	1986	1987	1988	1989	1990	1991	1992	1993	1994	1995	1996	1997	1998	1999	2000	2001	2002	2003	2004	2005	2006	2007	2008	2009	2010	2011	TOTAL
1. CW On-Line each Year												5	5	5	10	10	20	20	20	20	20	20	40	40	40	40	40	50	50	50	50	50	605
2. Cumm. CW On-Line												5	10	15	25	35	55	75	95	115	135	155	195	235	275	315	355	405	455	505	555	605	
3. Number of Power SATS/Year												1	1	1	1	1	2	2	2	2	2	2	4	4	4	4	4	5	5	5	5	5	62
4. Number of LEO Stations/Year										1					1		2					4					2						10
5. Number of Trans. Assemblers/Year										1																	1						2
6. Number of GEO Stations/Year											1								1				1			1			1		1		6
7. Number of Crew OTV Sets/Year												1				1		1		1	1	1	1	1	1	1	2	3	3	3	3	3	27
8. No. of SAT OTV Sets/Year										1				1		2						4					2			2			10
Replacement															1		2		2			2			2			2		2	1		14
9. Number of STS Launches/Year			3	4	20	40	5	5	10	10	10	10	10	10	10	19	19	20	20	21	39	39	40	41	42	52	52	53	55	55	55	55	824
10. Number of STS Buys/Year			1		1																					1							3
11. Number of HLLV Launches/Year									2	5	717	717	717	1433	1433	2866	2866	2866	2866	2866	2866	5732	5732	5732	5732	5732	7165	7165	7165	7165	7165	7165	86,705
12. Number of HLLV For Replacement*													2	3	4	4	5	5	5	5	5	5	5	5	5	5	7	7	7	6	5		95
For Payload									1	1	6			8		16						31					16						79
13. No. of Rectennas Instal/Year												1	1	1	1	1	2	2	2	2	2	2	4	4	4	4	4	5	5	5	5	5	62
14. No. of People in LEO									132	132	132	132	132	220	220	440	440	440	440	440	880	880	880	880	880	1100	1100	1100	1100	1100	1100	1100	
15. No. of People in GEO											12	12	12	13	18	23	33	43	56	68	78	88	113	133	158	178	198	223	253	278	303	333	

*500 Flight Life

FOLDOUT FRAME 1

FOLDOUT FRAME 2

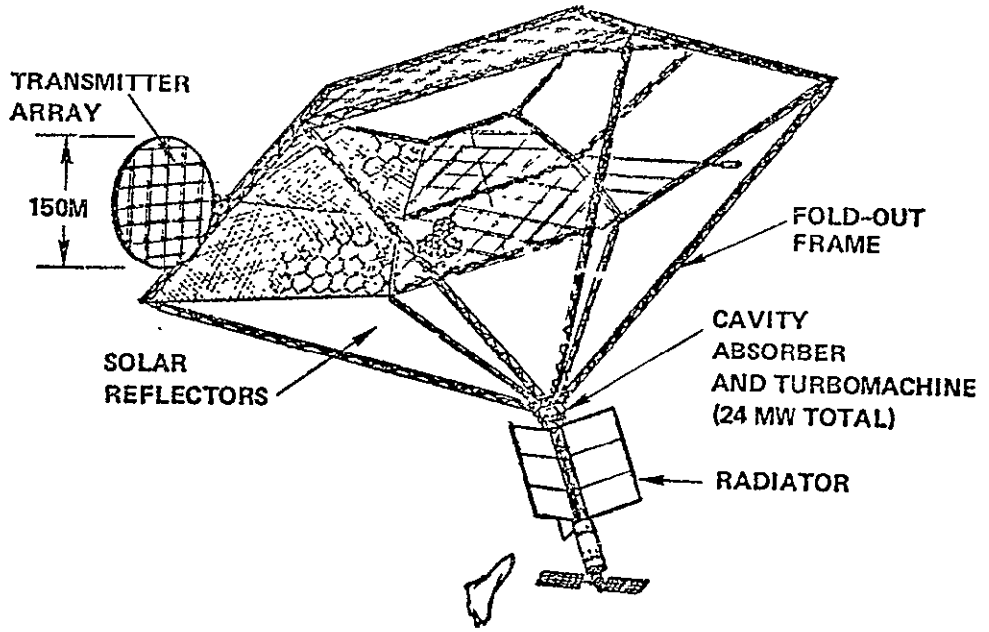

FIGURE 7-7 VERIFICATION POWER SATELLITE

TABLE 7-3 VERIFICATION POWER SATELLITE
MASS STATEMENT

	10^3 kg	10^3 lbm
Energy Collection		
Primary Structure	55	121
Secondary Structure	45	99
Reflectors	150	331
Energy Conversion		
Cavity Absorber	40	88
Turbogenerators	210	463*
Primary Radiator	280	617
Power Distribution	70	154*
Transmitter		
Waveguides/Structure	700	1543
Tubes	50	133
	1610	3549
Contingency/Growth	322	710
TOTAL	1932	4259

*Costing assumes 55 x 10^3 lbm from these two values to be thermionic diodes.

TABLE 7-14 HARDWARE TIME PHASING SOLAR RADIATION BRAYTON CYCLE

ITEM	1980	1981	1982	1983	1984	1985	1986	1987	1988	1989	1990	1991	1992	1993	1994	1995	1996	1997	1998	1999	2000	2001	2002	2003	2004	2005	2006	2007	2008	2009	2010	2011	TOTAL
	YEAR																																
1. CW On-Line each Year												5	5	5	10	10	20	20	20	20	20	20	40	40	40	40	40	50	50	50	50		605
2. Cumm. GW On-Line												5	10	15	25	35	55	75	95	115	135	155	195	235	275	315	355	405	455	505	555	605	
3. Number of Power SATS/Year												1	1	1	1	1	2	2	2	2	2	2	4	4	4	4	4	5	5	5	5	5	62
4. Number of LEO Stations/Year										1					1		2					4					2						10
5. Number of Trans. Assemblers/Year										1																	1						2
6. Number of GEO Stations/Year											1								1				1			1			1		1		6
7. Number of Crew OTV Sets/Year												1				1		1		1	1	1	1	1	1	1	2	3	3	3	3	3	27
8. No. of SAT OTV Sets/Year Replacement										1				1	1	2	2		2			2 4			2		2	2		2	1		14 10
9. Number of STS Launches/Year			3	4	20	40	5	5	10	10	10	10	10	10	10	19	19	20	20	21	39	39	40	41	42	52	52	53	55	55	55	55	824
10. Number of STS Buys/Year			1		1																					1							3
11. Number of HLLV Launches/Year										2	4	575	575	575	1150	1150	2300	2300	2300	2300	2300	2300	4600	4600	4600	4600	4600	5750	5750	5750	5750		69.581
12. Number of HLLV For Replacement* For Payload										1	1	4	2	2	3	3	4 12	4	4	4	4	4	4 24	4	4	4	5	6 12	6	5	4		80 60
13. No. of Rectennas Instal/Year												1	1	1	1	1	2	2	2	2	2	2	4	4	4	4	4	5	5	5	5	5	62
14. No. of People in LEO									132	132	132	132	132	220	220	440	440	440	440	440	880	880	880	880	880	1100	1100	1100	1100	1100	1100	1100	
15. No. of People in GEO											12	12	12	12	13	18	23	33	43	56	68	78	88	113	133	158	178	198	223	253	278	333	

*500 Flight Life

FOLDOUT FRAME 1

FOLDOUT FRAME 2

TABLE 7-15 HARDWARE TIME PHASING SOLAR THERMIONIC/BRAYTON CYCLE

ITEM	YEAR 1980	1981	1982	1983	1984	1985	1986	1987	1988	1989	1990	1991	1992	1993	1994	1995	1996	1997	1998	1999	2000	2001	2002	2003	2004	2005	2006	2007	2008	2009	2010	2011	TOTAL
1. GW on-Line each Vehicle	-	-	-	-	-	-	-	-	-	-	-	5	5	5	10	10	20	20	20	20	20	20	40	40	40	40	40	50	50	50	50	50	605
2. Gumm. GW on-Line	-	-	-	-	-	-	-	-	-	-	-	5	10	15	25	35	55	75	95	115	135	155	195	235	275	315	355	405	455	505	555	605	
3. Number of Power SATS/Year	-	-	-	-	-	-	-	-	-	-	-	1	1	1	1	1	2	2	2	2	2	2	4	4	4	4	4	5	5	5	5	5	62
4. Number of LEO Stations/Year	-	-	-	-	-	-	-	-	-	1	-	-	-	-	1	-	2	-	-	-	-	4	-	-	-	-	2	-	-	-	-	-	10
5. Number of Trans. Assemblers/Year	-	-	-	-	-	-	-	-	-	1	-	-	-	-	-	-	-	-	-	-	-	-	-	-	-	-	1	-	-	-	-	-	2
6. Number of GEO Stations/Year	-	-	-	-	-	-	-	-	-	-	1	-	-	-	-	-	-	-	1	-	-	-	1	-	-	1	-	-	1	-	1	-	6
7. Number of Crew OTV Sets/Year	-	-	-	-	-	-	-	-	-	-	-	1	-	-	-	1	-	1	-	1	1	1	1	1	1	1	2	3	3	3	3	3	27
8. Number of SAT OTV Sets/Year	-	-	-	-	-	-	-	-	-	1	-	-	-	1	-	2	-	-	-	-	-	4	-	-	-	-	2	-	-	-	-	-	10
Replacements															1		2		2			2			2		2		1				14
9. Number of STS Launches/Year	-	-	3	4	20	40	5	5	10	10	10	10	10	10	10	19	19	20	20	21	39	39	40	41	42	52	52	53	55	55	55	55	824
	← Verification →																																
10. Number of STS Buys/Year	-	-	1	-	1	-	-	-	-	-	-	-	-	-	-	-	-	-	-	-	-	-	-	-	-	1	-	-	-	-	-	-	3
11. Number of HLLV Launches/Year	-	-	-	-	-	-	-	-	2	4	491	491	981	981	1962	1962	1962	1962	1962	1962	3924	3924	3924	3924	3924	4905	4905	4905	4905	4905	4905	-	63,772
12. Number of HLLV Replacement	-	-	-	-	-	-	-	-	-	-	-	-	-	2	2	2	3	4	4	4	4	4	4	4	4	4	6	6	6	5	4	-	72
Payload	-	-	-	-	-	-	-	-	1	1	5	-	5	-	11	-	-	-	-	-	21	-	-	-	-	11	-	-	-	-	-	-	55
13. Number of Rectannas Instal/Year	-	-	-	-	-	-	-	-	-	-	-	1	1	1	1	1	2	2	2	2	2	2	4	4	4	4	4	5	5	5	5	5	62
14. Number of People in LEO	-	-	-	-	-	-	-	-	132	132	132	132	132	220	220	440	440	440	440	440	880	880	880	880	880	1100	1100	1100	1100	1100	1100	1100	
15. Number of People in GEO	-	-	-	-	-	-	-	-	-	-	12	12	12	13	18	23	33	43	56	68	78	88	113	133	158	178	198	223	253	278	303	333	

TABLE 7-16 HARDWARE TIME PHASING NUCLEAR/BRAYTON CYCLE

ITEM	YEAR 1980	1981	1982	1983	1984	1985	1986	1987	1988	1989	1990	1991	1992	1993	1994	1995	1996	1997	1998	1999	2000	2001	2002	2003	2004	2005	2006	2007	2008	2009	2010	2011	TOTAL
1. GW On-Line each Year												5	5	5	10	10	20	20	20	20	20	20	40	40	40	40	40	50	50	50	50	50	605
2. Cumm. GW On-Line												5	10	15	25	35	55	75	95	115	135	155	195	235	275	315	355	405	455	505	555	605	
3. Number of Power SATS/Year												1	1	1	1	1	2	2	2	2	2	2	4	4	4	4	4	5	5	5	5	5	62
4. Number of LEO Stations/Year										1					1		2					4					2						10
5. Number of Trans. Assemblers/Year										1																	1						2
6. Number of GEO Stations/Year											1								1				1			1			1		1		6
7. Number of Crew OTV Sets/Year												1				1		1		1	1	1	1	1	1	1	2	3	3	3	3	3	27
8. No. of SAT OTV Sets/Year										1				1		2						4					2						10
Replacements															1		2		2			2			2			2		2	1		14
9. Number of STS Launches/Year			3	Verification 4	20	40	5	5	10	10	10	10	10	20	20	40	40	41	41	42	80	81	82	82	84	100	101	102	102	103	105	106	1,499
10. Number of STS Buys/Year			1		1																2					1							5
11. Number of HLLV Launches/Year									2	4	966	966	1931	1931	1931	3862	3862	3862	3862	3862	3862	7724	7724	7724	7724	7724	9655	9655	9655	9655	9655		117,798
12. Number of HLLV Replacement												3	4	5	6	6	7	6	7	6	7	6	7	6	7	6	8	9	9	8	7		130
Payload									1		10		11			21						42						21					106
13. No. of Rectennas Instal/Year													1	1	1	1	2	2	2	2	2	2	4	4	4	4	4	5	5	5	5	5	62
14. No. of People in LEO									240	240	240	240	240	480	480	960	960	960	960	960	1920	1920	1920	1920	1920	2304	2304	2304	2304	2304	2304	2304	
15. No. of People in GEO											12	12	12	13	18	23	33	43	56	68	78	88	113	133	158	178	198	273	253	278	303	333		

FOLDOUT FRAME 1

FOLDOUT FRAME 2

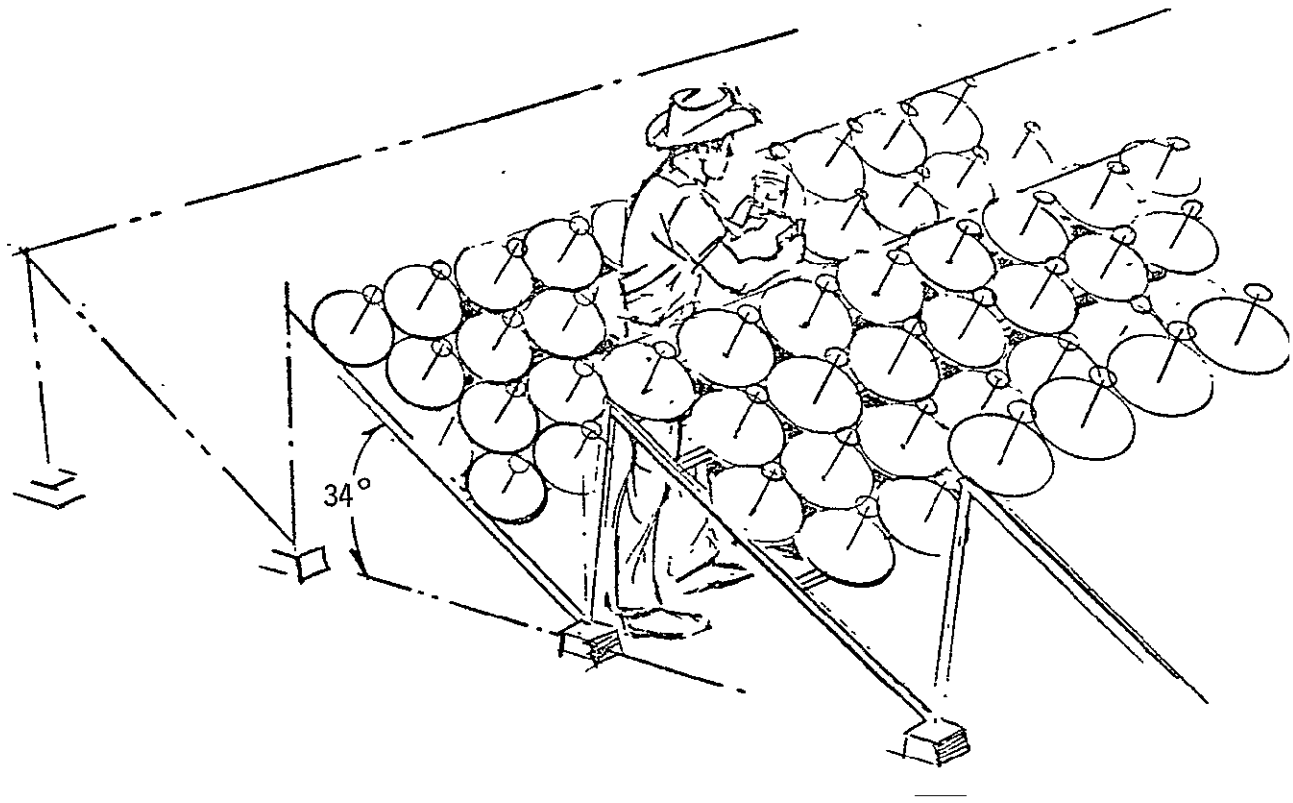

MASS STATEMENT

Element 5' X 5'	279 lbm - Estimated using RCA Price Guidelines
Complete 3Km^2 ground Rectenna Containing 952,512 Elements	265,750,848 lbm

FIGURE 7-8 GROUND RECTENNA—VERIFICATION

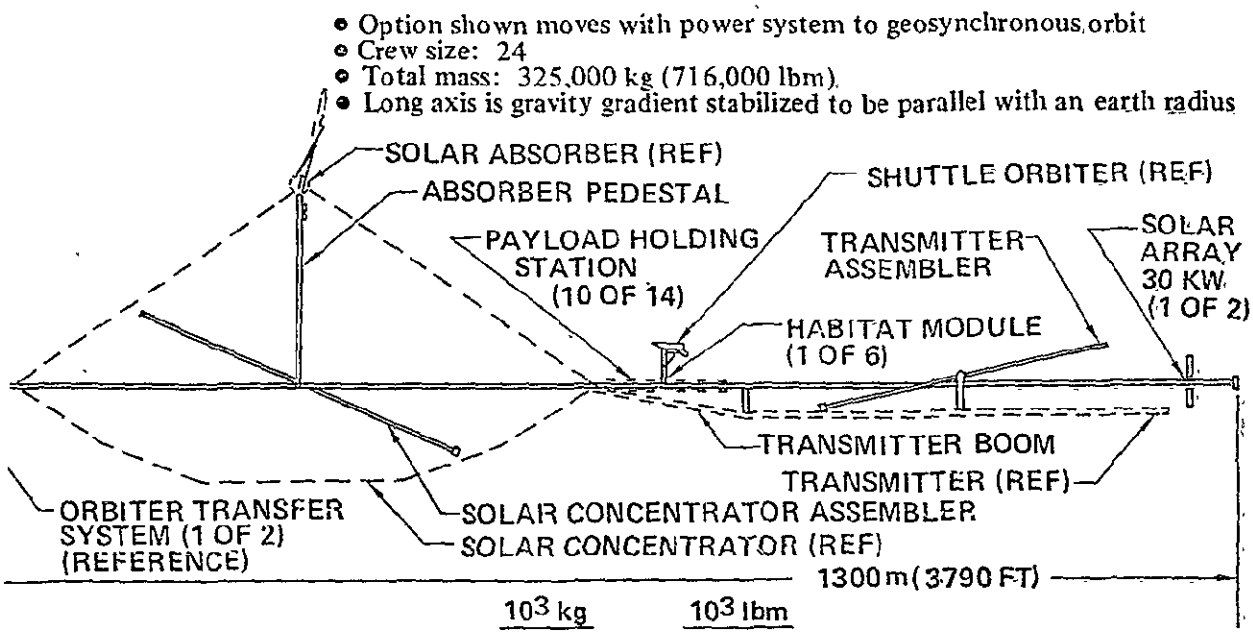

	10^3 kg	10^3 lbm	
Habitat	150	331	
Frames	50	110	
Assembler systems	50	110	
Power systems	15	33	
Payload holding	10	22	
Contingency	50	110	
	325	716	≈ 13 shuttle flights

MASS STATEMENT

	lbm
Habitat	331,000
Frames	110,000
Assembler Systems	110,000
Power Systems	33,000
Payload Holding	22,000
Contingency	110,000
TOTAL	716,000

FIGURE 7-9 ASSEMBLY STATION--VERIFICATION

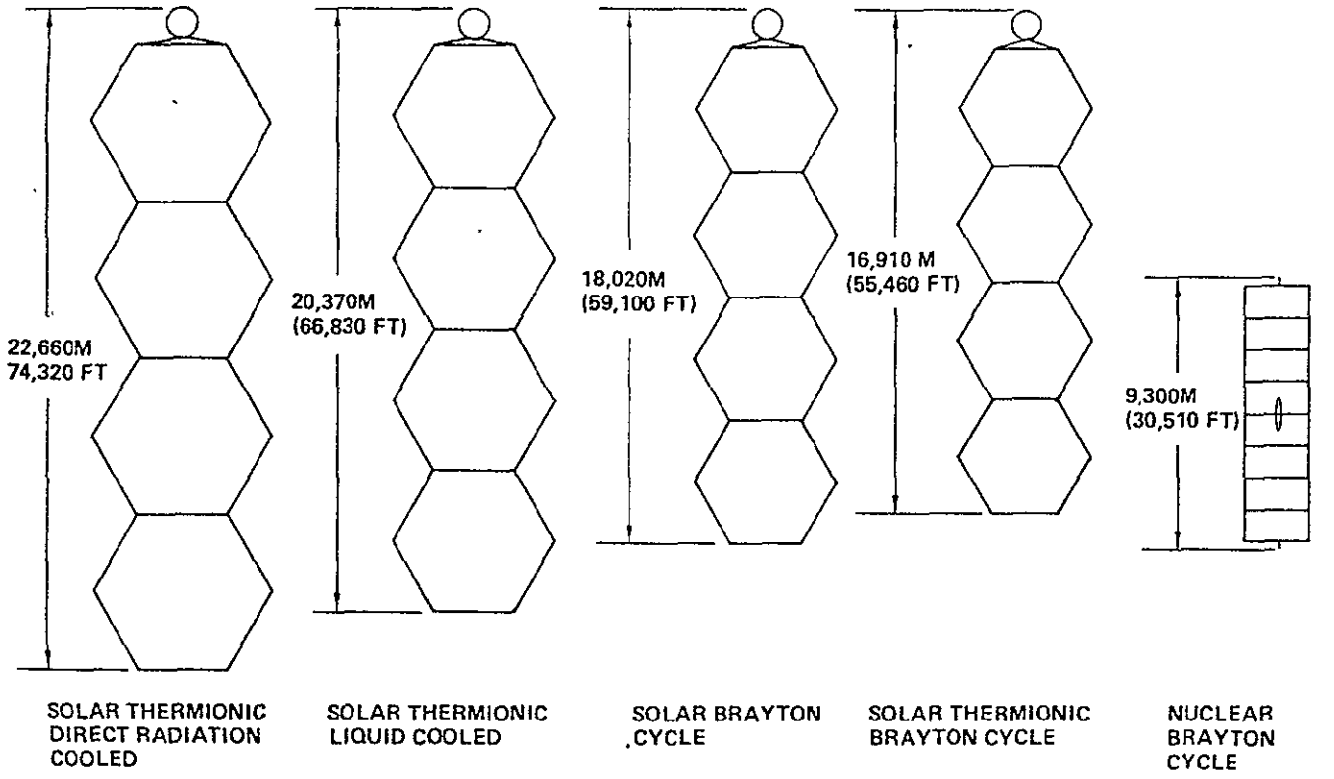

FIGURE 7-10 PLAN VIEWS OF POWER SYSTEMS

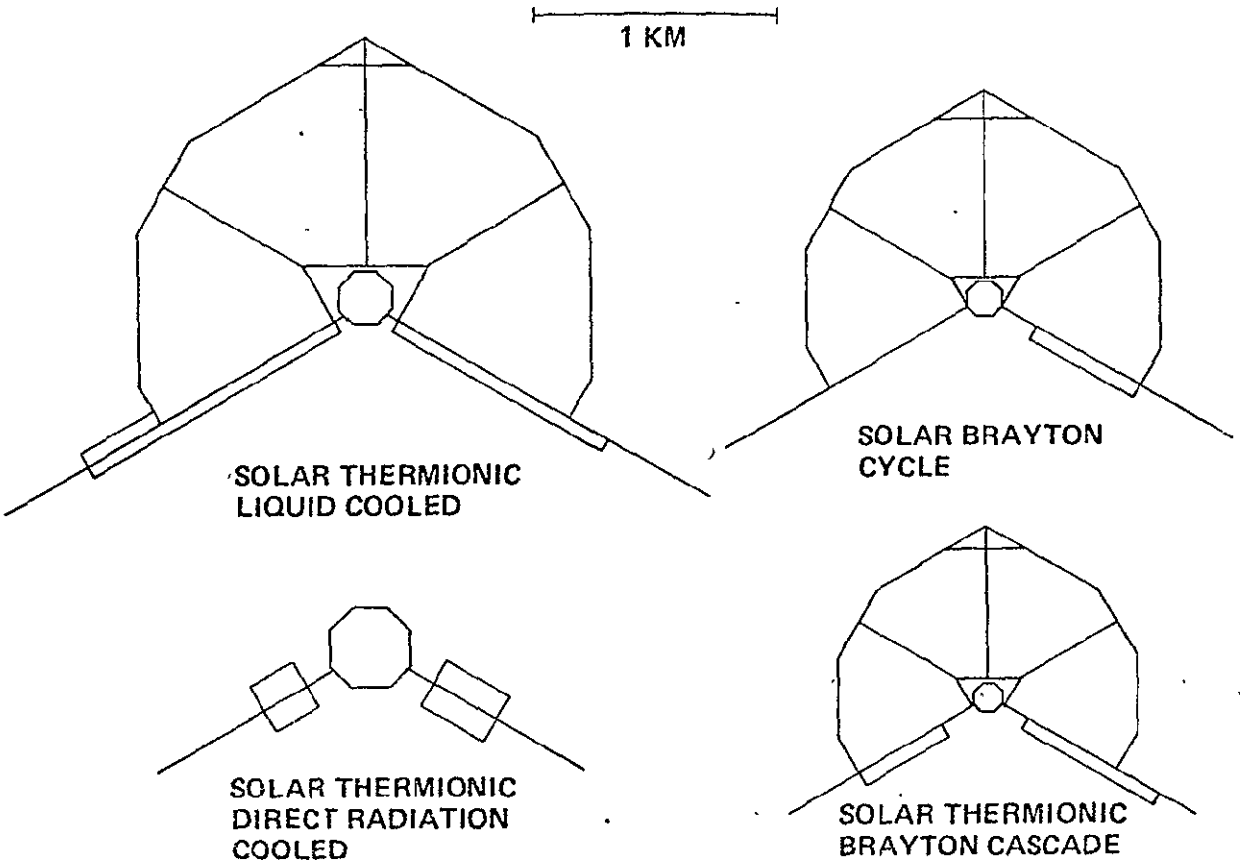

FIGURE 7-11 ELEVATION VIEWS OF CAVITIES AND RADIATORS

TABLE 7-4 MASS STATEMENT

FULL SCALE POWERSATS

	Solar power, four 2.5 GW modules								Nuclear, sixteen 1.0 GW modules		
	Thermionic				Brayton		Cascaded thermionic/ Brayton		Thermionic	Brayton	
	Direct radiation cooled		Liquid cooled								
	10^6 kg	10^6 lbm	10^6 kg	10^6 lbm	10^6 kg	10^6 lbm	10^6 kg	10^6 lbm		10^6 kg	10^6 lbm
Energy collection/prod.	(30.16)	(66.49)	(19.76)	(45.36)	(17.08)	(37.65)	(15.44)	(34.04)	(Not feasible	(21.27)	(46.8
Primary structure	15.22	33.55	10.55	23.26	9.12	14.90	8.74	13.47	with 1985	–	–
Secondary structure	7.90	17.42	1.99	4.38	1.72	7.74	1.55	6.99	technology	–	–
Reflectors	7.04	15.52	7.22	15.91	6.24	15.01	5.64	13.58	& molten salt	–	–
Reactor system	–	–	–	–	–	–	–	–	breeder reactor	21.27	46.89
Energy conversion	(64.11)	(141.34)	(53.72)	(118.45)	(42.20	(93.03)	(37.04)	(81.66)		(35.64)	(78.57)
Thermionic diodes	31.71	69.91	42.94	94.67	–	–	8.08	17.81		–	–
Fins/insulation	29.80	65.70	7.91	17.44	2.16	4.76	1.60	3.53		–	–
Cavity structure/tubing	2.60	5.73	2.87	6.34	4.40	9.70	2.20	4.85		–	–
Turbomachines/gen.	–	–	–	–	35.64	78.57	25.16	55.47		35.64	78.57
Primary radiators	(Graphite		(52.68)	(116.13)	(43.32)	(95.5)	(29.98)	(65.87)		(158.24)	(348.6)
Panels	fins		12.52	27.60	18.23	18.14	5.68	12.52		46.55	102.6
Manifolds	included		5.96	13.14	27.29	16.07	5.03	11.09		17.25	38.0
Pumps/valves	with		0.35	0.77	0.50	1.10	0.35	0.77		2.10	4.6
Structure	diodes)		2.50	5.51	2.17	4.78	1.50	3.31		7.91	17.4
Fluid			31.35	69.11	25.13	55.40	17.32	38.18		84.13	186
Energy distribution	(19.55)	(43.08)	(19.55)	(43.08)	(11.70)	(25.79)	(13.64)	(30.07)		(11.70)	(25.79)
Rotary converter	7.85	17.30	7.85	17.30	–	–	1.98	4.37		–	–
Controls	1.88	4.14	1.88	4.14	1.88	4.14	1.84	4.06		1.88	4.44
Transformers	4.41	9.72	4.41	9.72	4.41	9.72	4.41	9.72		4.41	9.72
Rectifier/filter	5.41	11.92	5.41	11.92	5.41	11.93	5.41	11.93		5.41	11.93
Transmitter	11.9	26.2	11.9	26.2	11.9	26.2	11.9	26.2		11.9	26.2
Contingency/growth	25.24	55.64	31.52	69.49	25.24	55.66	21.58	47.57		47.75	105.2
Totals	150.96	332.81	189.13	416.96	151.44	333.86	129.48	285.45		286.50	631.62

MASS STATEMENT

Element 10' x 10'	700 lbm - Estimated using RCA PRICE Guidelines
Complete 10 Km diameter ground rectenna combining 8,453,186 elements	5,917,230,200 lbm

FIGURE 7-12 GROUND RECTENNA

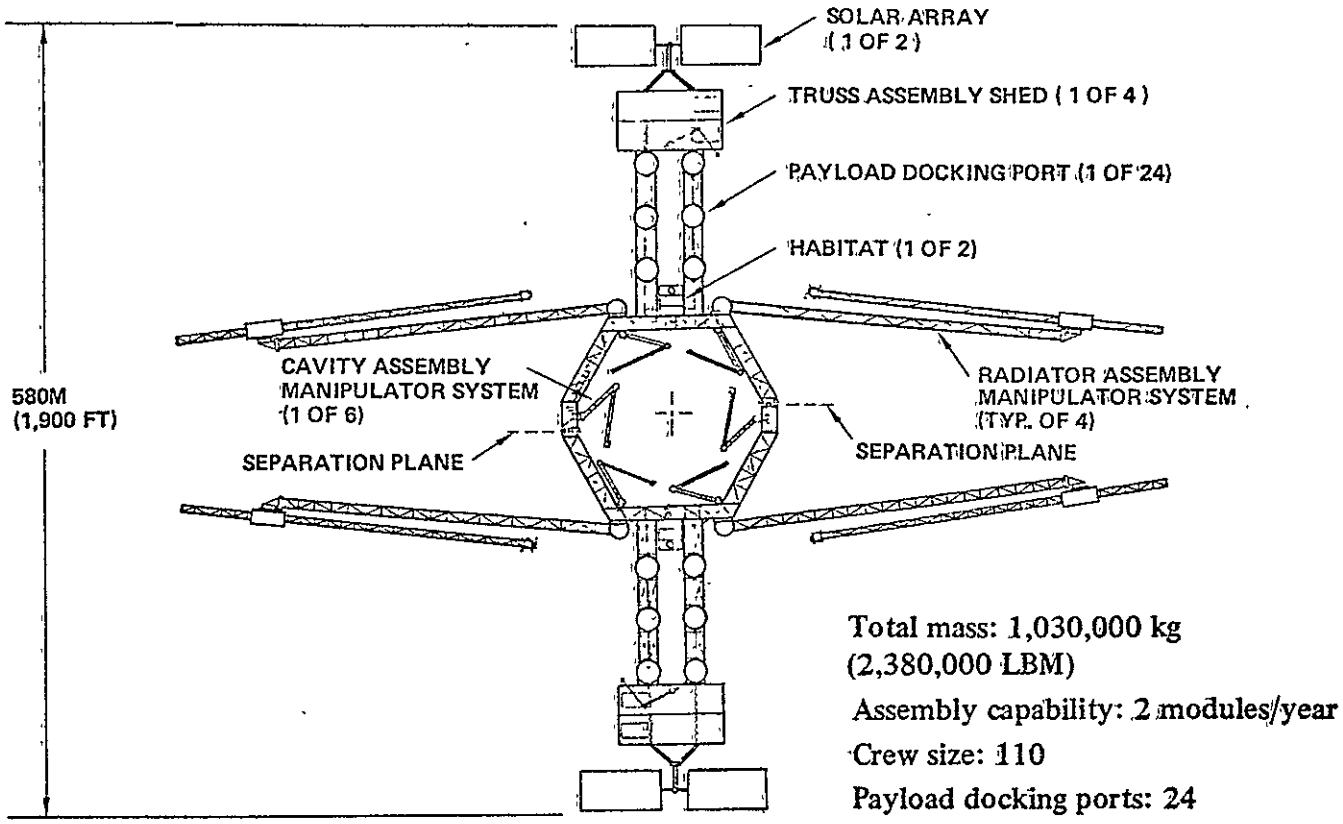

FIGURE 7-14 LEO BASE THERMIONIC LIQUID COOLED THERMIONIC BRAYTON

Assembly capability: eight 1 GW modules/year
Total mass: 2,750,000 KG (6,063,000 LBM)

Crew size: 240
Payload docking ports: 62

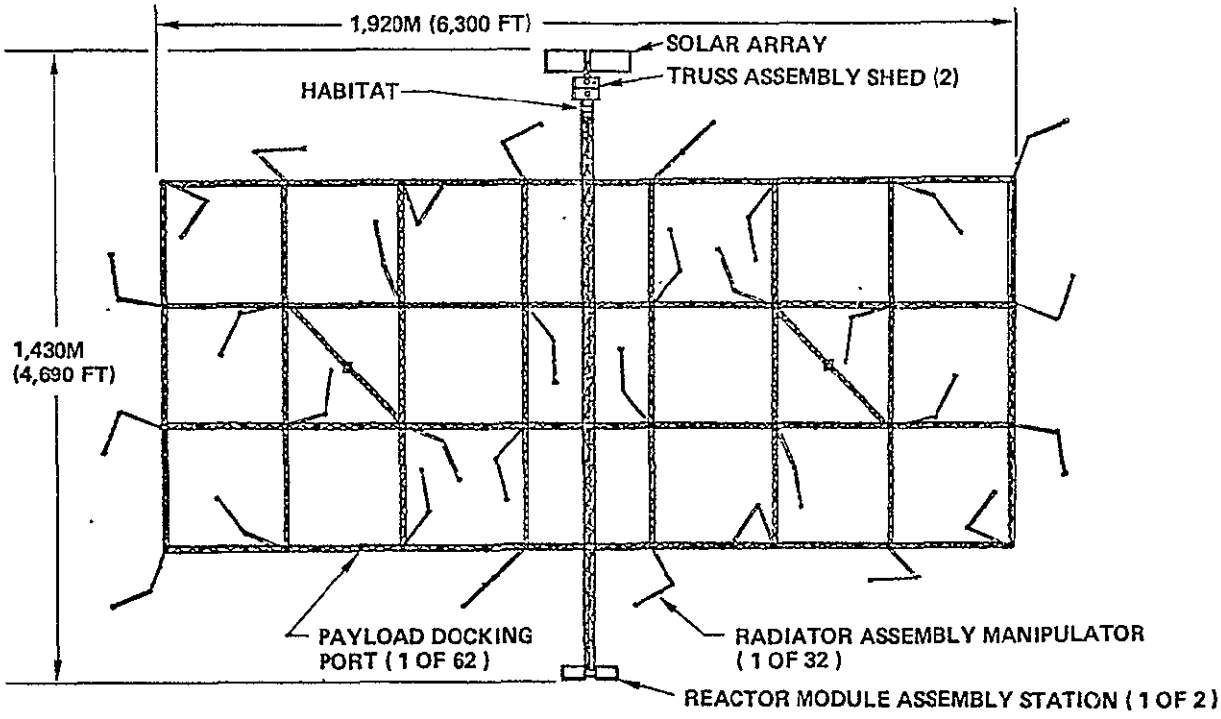

MASS STATEMENT

	LBM
Habitat	150,000
Docking Parts	80,000
Structure	1,160,000
TOTAL	1,390,000

FIGURE 7-15 LEO BASE NUCLEAR BRAYTON

TABLE 7-5 LEO BASES

MASS STATEMENT

ASSEMBLY STATIONS	THERMIONIC DRC THERMIONIC LC BRAYTON		THERMIONIC BRAYTON		NUCLEAR BRAYTON	
	10^3kg	10^3lbm	10^3kg	10^3lbm	10^3kg	10^3lbm
Structure	106	233	32	70.4	293	644.6
Manipulators	56	123	152	334.4	512	1126.4
Habitat	260	572	330	726.0	720	1584
Tools/"Pods"	60	132	110	242	240	528
Power Supply	11	24.2	16	35.2	64	141
Docking/Payload Holding	51	112.2	77	169.4	104	229
Assembler Modules	80	176.0	144	316.8	267	587
Misc/Contingency	156	343	216	475.2	550	1210
TOTALS	780		1080		2750	

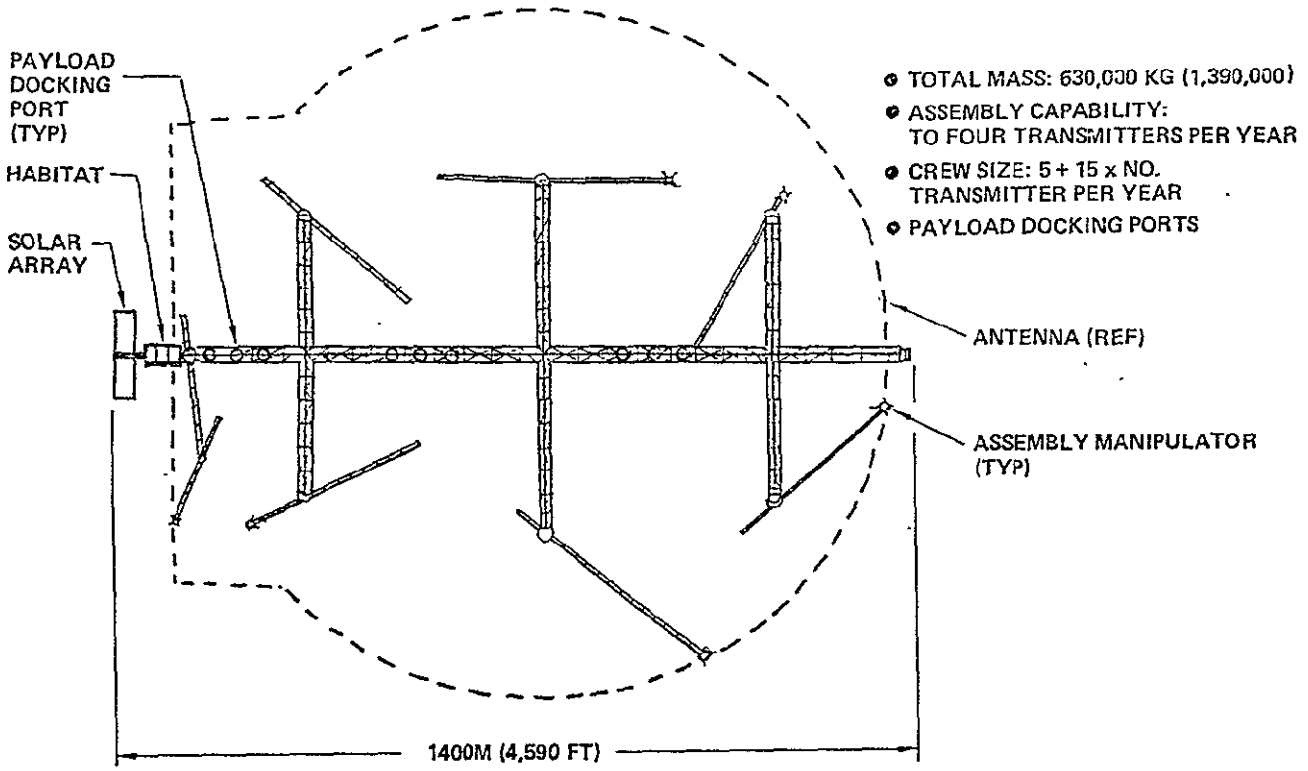

FIGURE 7-16 TRANSMITTER ANTENNA ASSEMBLER

- Total mass (without spares or support vehicles) : 600,000 KG
- Support capability: up to Powersats producing a total of 100 GW ground output
- Payload docking ports: 21
- Maximum crew size: 50
- Placement: by arriving Powersat module

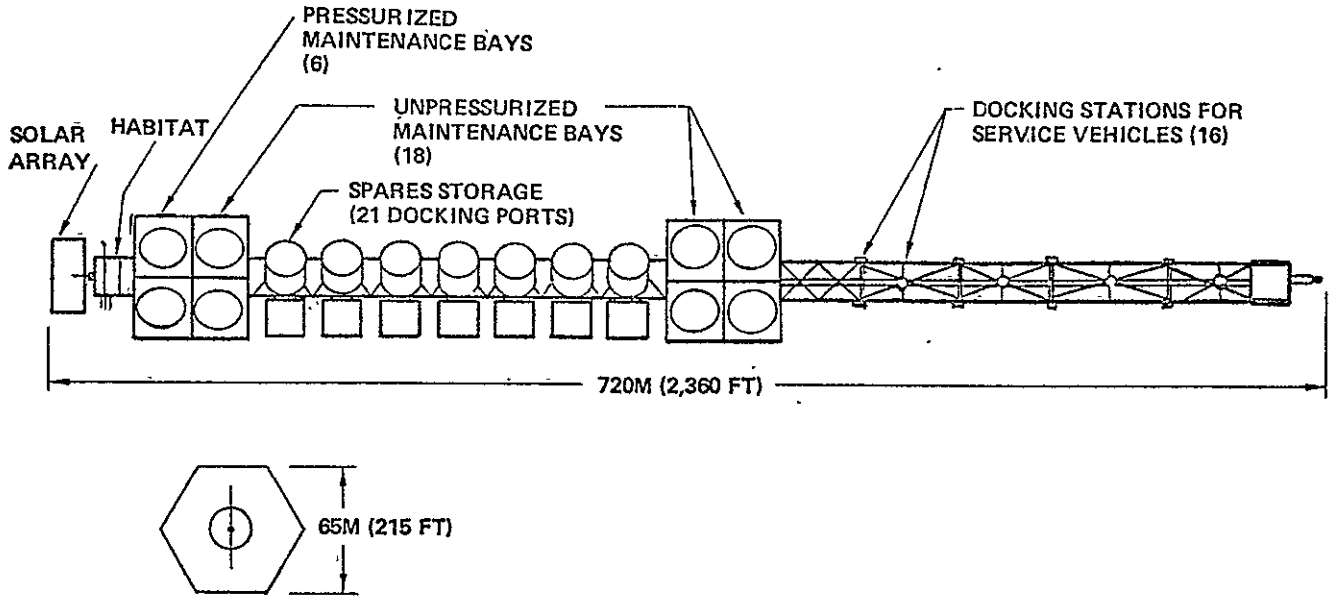

	lbm
Habitat	150,000
Maintenance Bay	400,000
Spares Storage	300,000
Main Frame	470,000
TOTAL	1,320,000

FIGURE 7-17 GEO BASE

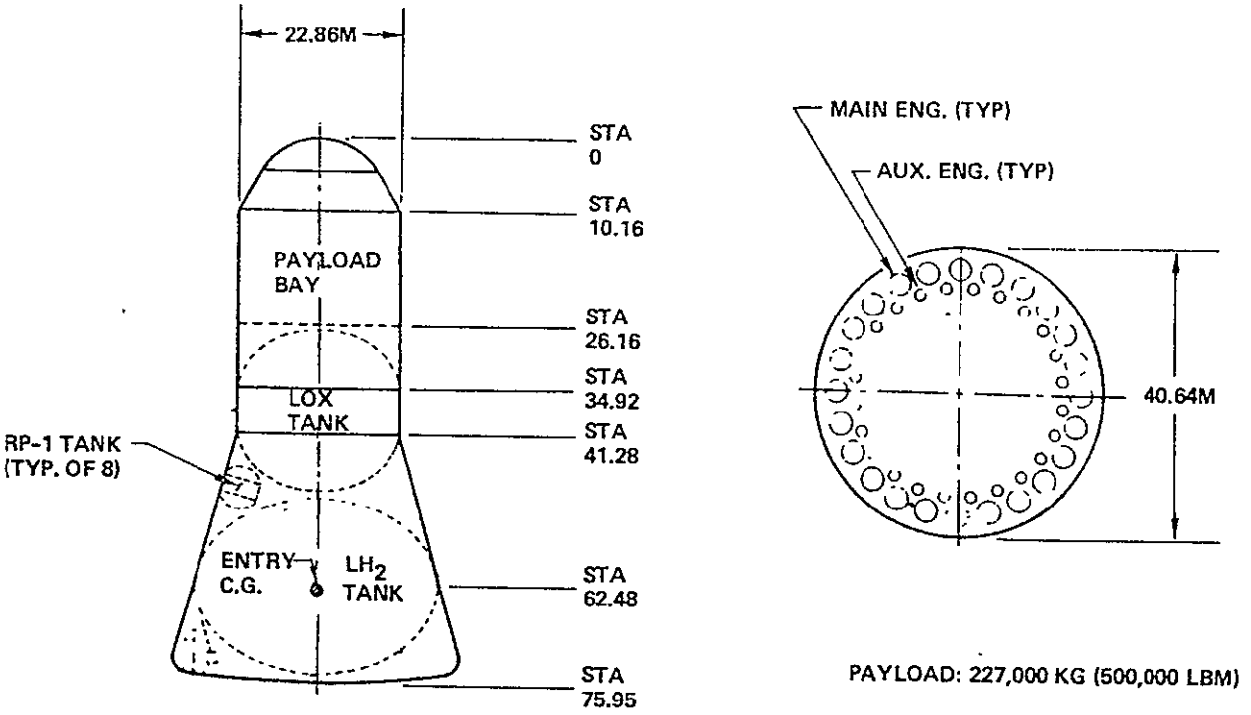

FIGURE 7-18 HLLV LEO FREIGHTER

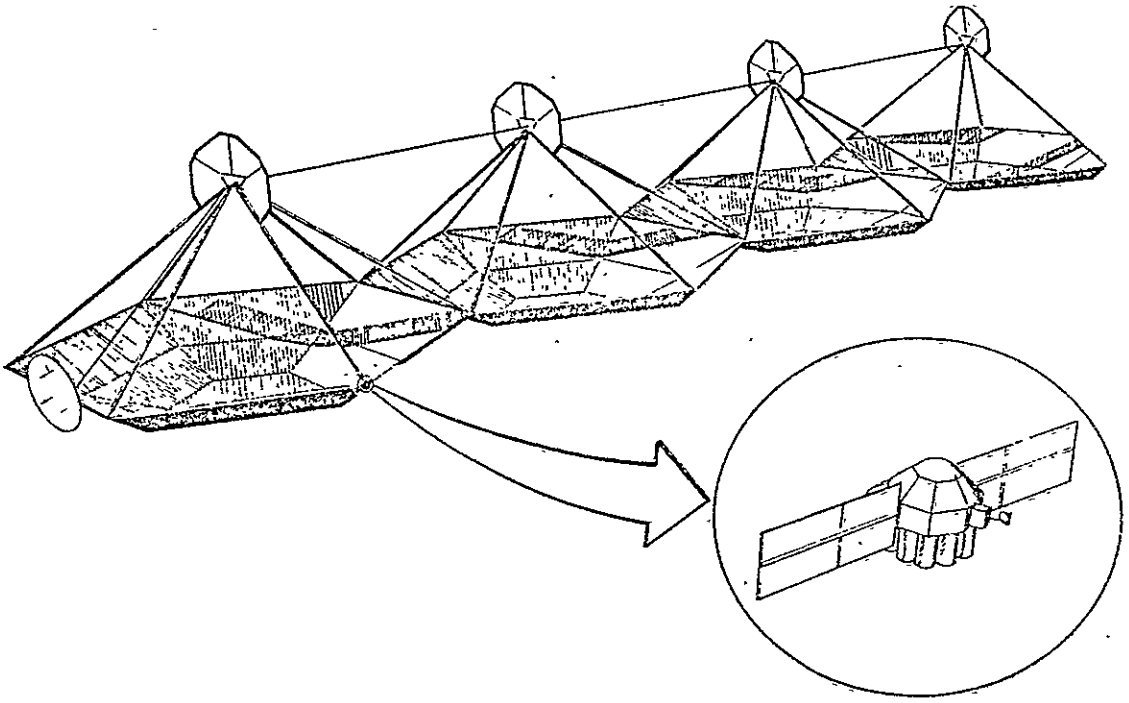

MASS STATEMENT

	lbm
Reaction Control	10,000
Structures	200,000
Avionics	8,000
Power Conditioning Equip	50,000
Electrical System	9,000
TOTAL	277,000

FIGURE 7-19 SATELLITE OTV

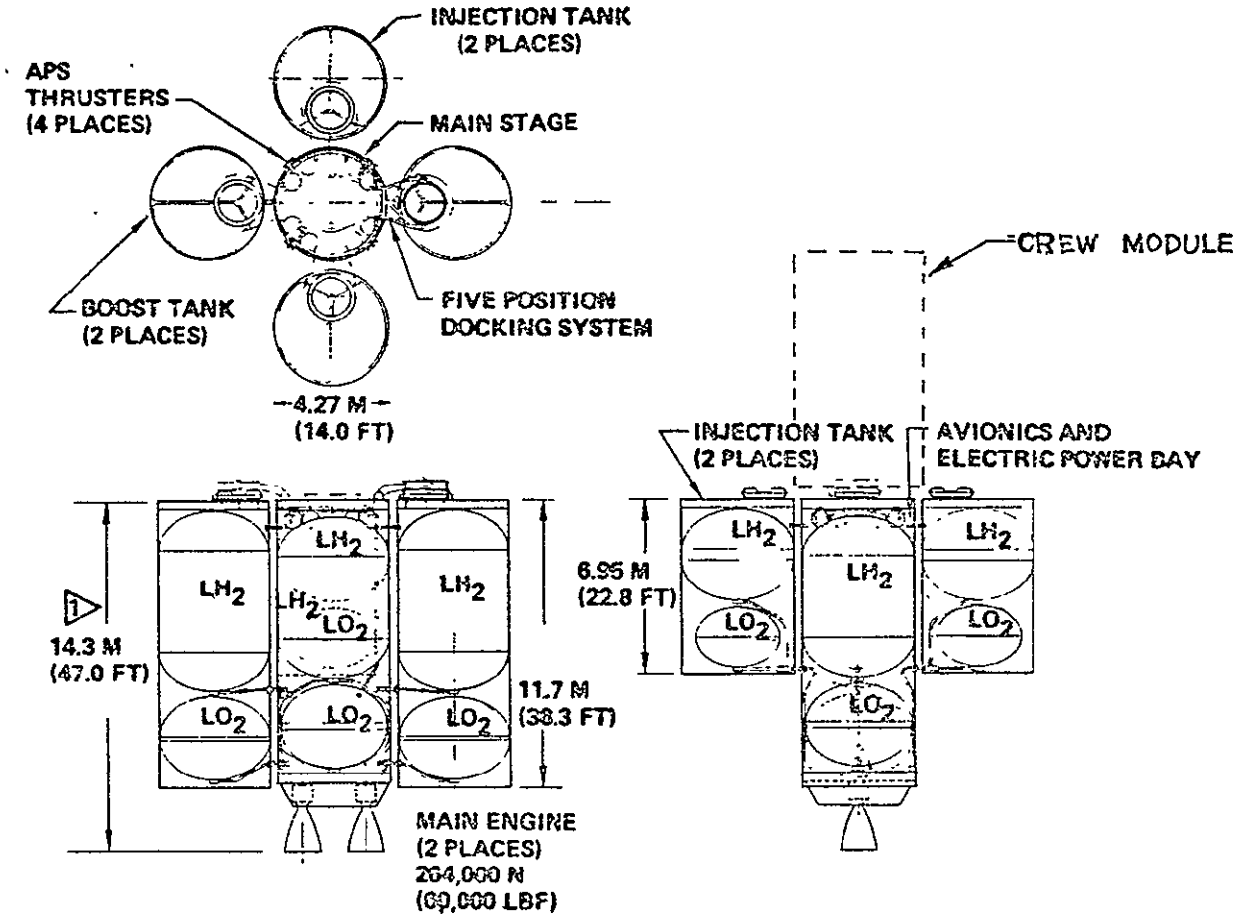

FIGURE 7-20 CREW OTV USING FSTSA DEVELOPED VEHICLE

TABLE 7-6 CREW OTV
MASS STATEMENT

	lbm
Main Stage Burnout	15,720
Drop Tanks Burnout	16,675
Crew Module	35,000
TOTAL DRY WEIGHT	67,395
Main Stage Propellant	86,000
Drop Tank Propellant	269,000
TOTAL PROPELLANT	355,010

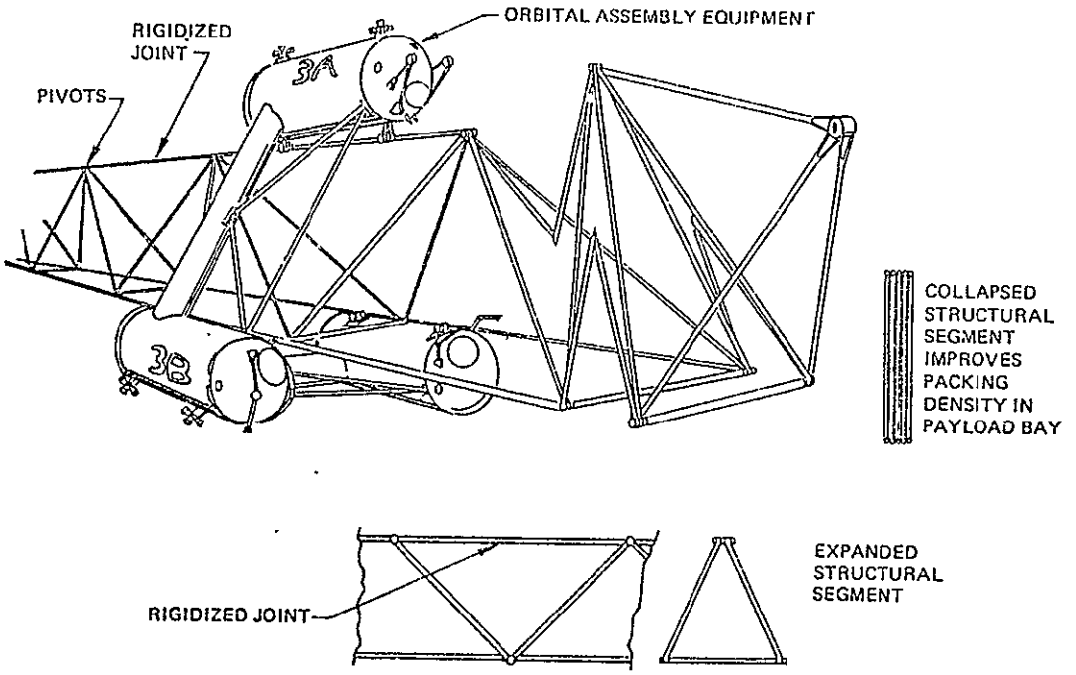

MASS STATEMENT

Total unit mass 208,000 lbm

FIGURE 7-21 LEO MANIPULATOR

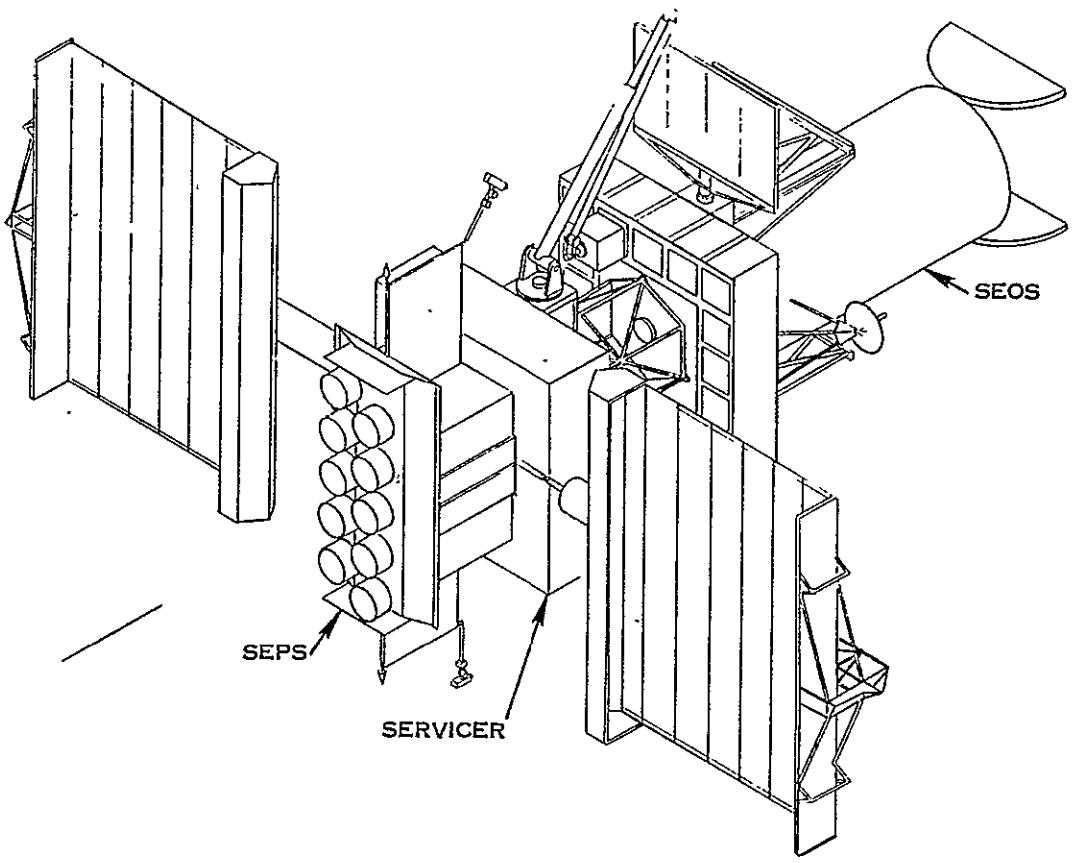

MASS STATEMENT

Total Mass	35,000 lbm

Weight from SEPS System Analysis Study

FIGURE 7-22 GEO MANIPULATOR WING SEPS DEVELOPED VEHICLE

LEGEND:
- GTU - GROUND TEST UNIT
- PROTO - PROTOTYPE
- GEO - GEOSYNCHRONOUS EARTH ORBIT
- OTV - ORBIT TRANSFER VEHICLE
- LEO - LOW EARTH ORBIT
- HLLV - HEAVY LIFT LAUNCH VEHICLE
- STS - SPACE SHUTTLE TRANSP. SYS.

TABLE 7-7 HARDWARE IDENTIFICATION
SOLAR BRAYTON

	PROGRAM PHASE					
	DDT&E		PRODUCTION		OPERATIONS	
	HARDWARE NAME	QTY	HARDWARE NAME	QTY	HARDWARE NAME	QTY
SATELLITE POWER STATION						
1.0 OVERALL PROGRAM MANAGEMENT	NO HARDWARE		NO HARDWARE		NO HARDWARE	
1.1 SE&I	NO HARDWARE		NO HARDWARE		NO HARDWARE	
1.2 TECHNOLOGY DEVELOPMENT PROGRAM						
1.3 SYSTEM DEVELOPMENT PROGRAM-VERIF.	VERIFICATION POWER SAT GTU	0.1				
	PROTO	1.0				
	CREW OTV GTU	1.0				
	PROTO	1.0				
	SAT OTV GTU	1.0	CHARGED TO DDT&E		CHARGED TO DDT&E	
	PROTO	1.0				
	ASSEMBLY STA.	1.0				
	SHUTTLE LAUNCHES	7.2				
	DEMO ANTENNA	1.0				
1.4 EARTH-LEO TRANSPORTATION PROGRAM	HLLV GROUND TEST UNITS	2.0	STS VEHICLES	3	STS FLIGHTS	752
	HLLV FLIGHT TEST UNITS	1.5	HLLV VEHICLES	140	HLLV FLIGHTS	69581
1.5 LEO-GEO TRANSPORTATION PROGRAM	CREW OTV GTU	1.5	CREW OTV	27		
	PROTO	1.0				
1.6 ASSEMBLY TRANSPORTATION PROGRAM	SAT OTV (EA) GTU	1.5	SAT OTV (SETS)	10		
	PROTO	1.0				
1.7 LOGISTICS TRANSPORTATION PROGRAM	N/A		N/A			
1.8 MAINTENANCE TRANSPORTATION PROGRAM	N/A		N/A			
1.9 CREW TRANSPORT PROGRAM	(INCLUDED IN 1.4 & 1.5)		(INCLUDED IN 1.4 & 1.5)			
1.10 SATELLITE POWER STATION PROGRAM	POWER SATELLITE GTU	0.01	POWER SATELLITES	62		
	SPACE ANTENNA GTU	0.1	SPACE ANTENNAS	62		
1.11 GROUND MICROWAVE STATION PROG.	(DEMO RECTENNA IN 1.3)		RECTENNAS	62		
1.12 OPERATIONS SUPPORT PROGRAM	LEO BASE GTU	.01	LEO BASE	10		
	LEO MANIPULATOR GTU	.3	LEO MANIPULATOR	30		
	ANTENNA ASSEMBLER GTU	.01	ANTENNA ASSEMBLER	2		
	GEO BASE GTU	.01	GEO BASE	6		
	GEO MANIPULATOR GTU	1.5	GEO MANIPULATOR	36		
1.13 CENTRAL CONTROL STATION PROGRAM	MISSION CONTROL COMPLEX	1	CHARGED TO DDT&E			

LEGEND:
- GTU - GROUND TEST UNIT
- PROTO - PROTOTYPE
- GEO - GEOSYNCHRONOUS EARTH ORBIT
- OTV - ORBIT TRANSFER VEHICLE
- LEO - LOW EARTH ORBIT
- HLLV - HEAVY LIFT LAUNCH VEHICLE
- STS - SPACE SHUTTLE TRANSP. SYSTEM

TABLE 7-8 HARDWARE IDENTIFICATION
NUCLEAR BRAYTON

SATELLITE POWER STATION	PROGRAM PHASE					
	DDT&E		PRODUCTION		OPERATIONS	
	HARDWARE NAME	QTY	HARDWARE NAME	QTY	HARDWARE NAME	QTY
1.0 OVERALL PROGRAM MANAGEMENT	NO HARDWARE		NO HARDWARE		NO HARDWARE	
1.1 SE&I	NO HARDWARE		NO HARDWARE		NO HARDWARE	
1.2 TECHNOLOGY DEVELOPMENT PROGRAM						
1.3 SYSTEM DEVELOPMENT PROGRAM-VERIF.	VERIFICATION POWER SAT-GTU	0.1				
	PROTO	1.0				
	CREW OTV GTU	1.0				
	PROTO	1.0				
	SAT OTV GTU	1.0				
	PROTO	1.0	CHARGED TO DDT&E		CHARGED TO DDT&E	
	ASSEMBLY STA	1.0				
	SHUTTLE LAUNCHES	7.2				
	DEMO RECTENNA	1.0				
1.4 EARTH-LEO TRANSPORTATION PROG.	HLLV GROUND TEST UNITS	2.0	STS VEHICLES	5	STS FLIGHTS	1427
	HLLV FLIGHT TEST UNITS	1.5	HLLV VEHICLES	236	HLLV FLIGHTS	117,798
1.5 LEO-GEO TRANSPORTATION PROGRAM	CREW OTV GTU	1.5	CREW OTV	27		
	PROTO	1.0				
1.6 ASSEMBLY TRANSPORTATION PROGRAM	SAT OTV (EA) GTU	1.5	SAT OTV (SETS)	10		
	PROTO	1.0				
1.7 LOGISTICS TRANSPORTATION PROGRAM						
1.8 MAINTENANCE TRANSPORTATION PROGRAM						
1.9 CREW TRANSPORT PROGRAM	(INCLUDED IN 1.4 & 1.5)		(INCLUDED IN 1.4 & 1.5)			
1.10 SATELLITE POWER STATION PROG.	POWER SATELLITE GTU	0.01	POWER SATELLITES	62		
	SPACE ANTENNA GTU	0.1	SPACE ANTENNAS	62		
1.11 GROUND MICROWAVE STATION PROG.	(DEMO RECTENNA IN 1.3)		RECTENNAS	62		
1.12 OPERATIONS SUPPORT PROGRAM	LEO BASE GTU	.01	LEO BASE	10		
	LEO MANIPULATOR GTU	.3	LEO MANIPULATOR	30		
	ANTENNA ASSEMBLER GTU	.01	ANTENNA ASSEMBLER	2		
	GEO BASE GTU	.01	GEO BASE	6		
	GEO MANIPULATOR GTU	1.5	GEO MANIPULATOR	36		
1.13 CENTRAL CONTROL STATION PROGR.	MISSION CONTROL COMPLEX	1	CHARGED TO DDT&E			

LEGEND:
- GTU - GROUND TEST UNIT
- PROTO - PROTOTYPE
- GEO - GEOSYNCHRONOUS EARTH ORBIT
- OTV - ORBIT TRANSFER VEHICLE
- LEO - LOW EARTH ORBIT
- HLLV - HEAVY LIFT LAUNCH VEHICLE
- STS - SPACE SHUTTLE TRANSP. SYS.

TABLE 7-9 HARDWARE IDENTIFICATION
SOLAR THERMIONIC BRAYTON

SATELLITE POWER STATION	PROGRAM PHASE: DDT&E HARDWARE NAME	QTY	PRODUCTION HARDWARE NAME	QTY	OPERATIONS HARDWARE NAME	QTY
1.0 OVERALL PROGRAM MANAGEMENT	NO HARDWARE		NO HARDWARE		NO HARDWARE	
1.1 SE&I	NO HARDWARE		NO HARDWARE		NO HARDWARE	
1.2 TECHNOLOGY DEVELOPMENT PROGRAM						
1.3 SYSTEM DEVELOPMENT PROGRAM-VERIF.	VERIFICATION POWER SAT-GTU	0.1				
	PROTO	1.0				
	CREW OTV GTU	1.0				
	PROTO	1.0				
	SAT OTV GTU	1.0	CHARGED TO DDT&E		CHARGED TO DDT&E	
	PROTO	1.0				
	ASSEMBLY STA	1.0				
	SHUTTLE LAUNCHES	7.2				
	DEMO RECTENNA	1.0				
1.4 EARTH-LEO TRANSPORTATION PROG.	HLLV GROUND TEST UNITS	2.0	STS VEHICLES	3	STS FLIGHTS	752
	HLLV FLIGHT TEST UNITS	1.5	HLLV VEHICLES	127	HLLV FLIGHTS	63772
1.5 LEO-GEO TRANSPORTATION PROGRAM	CREW OTV GTU	1.5	CREW OTV (SETS)	10		
	PROTO	1.0				
1.6 ASSEMBLY TRANSPORTATION PROGRAM	SAT OTV (EA) GTU	1.5	SAT OTV (SETS)	10		
	PROTO	1.0				
1.7 LOGISTICS TRANSPORTATION PROGRAM	N/A		N/A			
1.8 MAINTENANCE TRANSPORTATION PROG.	N/A		N/A			
1.9 CREW TRANSPORT PROGRAM	(INCLUDED IN 1.4 & 1.5)		(INCLUDED IN 1.4 & 1.5)			
1.10 SATELLITE POWER STATION PROG.	POWER SATELLITE GTU	0.01	POWER SATELLITES	62		
	SPACE ANTENNA GTU	0.1	SPACE ANTENNAS	62		
1.11 GROUND MICROWAVE STATION PROGR.	(DEMO RECTENNA IN 1.3)		RECTENNAS	62		
1.12 OPERATIONS SUPPORT PROGRAM	LEO BASE GTU	.01	LEO BASE	10		
	LEO MANIPULATOR GTU	.3	LEO MANIPULATOR	30		
	ANTENNA ASSEMBLER GTU	.01	ANTENNA ASSEMBLER	2		
	GEO BASE GTU	.01	GEO BASE	6		
	GEO MANIPULATOR GTU	1.5	GEO MA IPULATOR	36		
1.13 CENTRAL CONTROL STATION PROGR.	MISSION CONTROL COMPLEX	1	CHARGED TO DDT&E			

LEGEND:
- GTU - GROUND TEST UNIT
- PROTO - PROTOTYPE
- GEO - GEOSYNCHRONOUS EARTH ORBIT
- OTV - ORBIT TRANSFER VEHICLE
- LEO - LOW EARTH ORBIT
- HLLV - HEAVY LIFT LAUNCH VEHICLE
- STS - SPACE SHUTTLE TRANSP. SYSTEM

TABLE 7-10 HARDWARE IDENTIFICATION
SOLAR THERMIONIC LIQUID COOLED

	PROGRAM PHASE					
	DDT&E		PRODUCTION		OPERATIONS	
	HARDWARE NAME	QTY	HARDWARE NAME	QTY	HARDWARE NAME	QTY
SATELLITE POWER STATION						
1.0 OVERALL PROGRAM MANAGEMENT	NO HARDWARE		NO HARDWARE		NO HARDWARE	
1.1 SE&I	NO HARDWARE		NO HARDWARE		NO HARDWARE	
1.2 TECHNOLOGY DEVELOPMENT PROGRAM						
1.3 SYSTEM DEVELOPMENT PROG-VERIF.	VERIFICATION POWER SAT-GTU	0.1				
	PROTO	1.0				
	CREW OTV GTU	1.0				
	PROTO	1.0				
	SAT OTV GTU	1.0	CHARGED TO		CHARGED TO	
	PROTO	1.0	DDT&E		DDT&E	
	ASSEMBLY STA.	1.0				
	SHUTTLE LAUNCHES	7.2				
	DEMO RECTENNA	1.0				
1.4 EARTH-LEO TRANSPORTATION PROG.	HLLV GROUND TEST UNITS	2.0	STS VEHICLES	3	STS FLIGHTS	752
	HLLV FLIGHT TEST UNITS	1.5	HLLV VEHICLES	174	HLLV FLIGHTS	86705
1.5 LEO-GEO TRANSPORTATION PROG.	CREW OTV GTU	1.5	CREW OTV	27		
	PROTO	1.0				
1.6 ASSEMBLY TRANSPORTATION PROG.	SAT OTV (EA) GTU	1.5	SAT OTV (SETS)	10		
	PROTO	1.0				
1.7 LOGISTICS TRANSPORTATION PROG.	N/A		N/A			
1.8 MAINTENANCE TRANSPORTATION PROG.	N/A		N/A			
1.9 CREW TRANSPORT PROGRAM	(INCLUDED IN 1.4 & 1.5)		(INCLUDED IN 1.4 & 1.5)			
1.10 SATELLITE POWER STATION PROG.	POWER SATELLITE GTU	0.01	POWER SATELLITES	62		
	SPACE ANTENNA GTU	0.1	SPACE ANTENNAS	62		
1.11 GROUND MICROWAVE STATION PROG.	(DEMO RECTENNA IN 1.3)		RECTENNAS	62		
1.12-OPERATIONS SUPPORT PROGRAM	LEO BASE GTU	.01	LEO BASE	10		
	LEO MANIPULATOR GTU	.3	LEO MANIPULATOR	30		
	ANTENNA ASSEMBLER GTU	.01	ANTENNA ASSEMBLER	2		
	GEO BASE GTU	.01	GEO BASE	6		
	GEO MANIPULATOR GTU	1.5	GEO MANIPULATOR	36		
1.13 CENTRAL CONTROL STATION PROGRAM	MISSION CONTROL COMPLEX	1	CHARGED TO DDT&E			

LEGEND.
- GTU - GROUND TEST UNIT
- PROTO - PROTOTYPE
- GEO - GEOSYNCHRONOUS EARTH ORBIT
- OTV - ORBIT TRANSFER VEHICLE
- LEO - LOW EARTH ORBIT
- HLLV - HEAVY LIFT LAUNCH VEHICLE
- STS - SPACE SHUTTLE TRANSP. SYSTEM

TABLE 7-11

HARDWARE IDENTIFICATION

SOLAR THERMIONIC DIRECT RADIATION COOLED

SATELLITE POWER STATION	PROGRAM PHASE					
	DDT&E		PRODUCTION		OPERATIONS	
	HARDWARE NAME	QTY	HARDWARE NAME	QTY	HARDWARE NAME	QTY
1.0 OVERALL PROGRAM MANAGEMENT	NO HARDWARE		NO HARDWARE		NO HARDWARE	
1.1 SE&I	NO HARDWARE		NO HARDWARE		NO HARDWARE	
1.2 TECHNOLOGY DEVELOPMENT PROGRAM						
1.3 SYSTEM DEVELOPMENT PROGRAM-VERIFICATION	VERIFICATION					
	POWER SAT GTU	0.1				
	PROTO	1.0				
	CREW OTV GTU	1.0				
	PROTO	1.0				
	SAT OTV GTU	1.0	CHARGED TO DDT&E		CHARGED TO DDT&E	
	PROTO	1.0				
	ASSEMBLY STATION	1.0				
	SHUTTLE LAUNCHES	7.2				
	DEMO RECTENNA	1.0				
1.4 EARTH-LEO TRANSPORTATION PROGRAM	HLLV GROUND TEST UNITS	2.0	STS VEHICLES	3	STS LAUNCHES	595
	HLLV FLT TEST UNITS	1.5	HLLV VEHICLES	140	HLLV LAUNCHES	69,581
1.5 LEO-GEO TRANSPORTATION PROGRAM	CREW OTV GTU	1.5	CREW OTV	27		
	PROTO	1.0				
1.6 ASSEMBLY TRANSPORTATION PROGRAM	SAT OTV (EA) GTU	1.5	SATELLITE OTV (SETS)	10		
	PROTO	1.0				
1.7 LOGISTICS TRANSPORTATION PROGRAM	N/A		N/A			
1.8 MAINTENANCE TRANSP. PROGRAM	N/A		N/A			
1.9 CREW TRANSPORT PROGRAM	(INCLUDED IN 1.4 & 1.5)		(INCLUDED IN 1.4 & 1.5)			
1.10 SATELLITE POWER STATION PROGRAM	POWER SATELLITE GTU	.01	POWER SATELLITES	62		
	SPACE ANTENNA GTU	.1	SPACE ANTENNAS	62		
1.11 GROUND MICROWAVE STATION PROGRAM	(DEMO RECTENNA IN 1.3)		RECTENNA	62		
1.12 OPERATIONS SUPPORT PROGRAM	LEO BASE GTU	.01	LEO BASE	10		
	LEO MANIPULATOR GTU	.3	LEO MANIPULATOR	30		
	ANTENNA ASSEMBLER GTU	.01	ANTENNA ASSEMBLER	2		
	GEO BASE GTU	.01	GEO BASE	6		
	GEO MANIPULATOR GTU	1.5	GEO MANIPULATOR	36		
1.13 CENTRAL CONTROL STATION PROGRAM	MISSION CONTROL COMPLEX	1	CHARGED TO DDT&E			

7.6 COST ESTIMATES

In this section cost is summarized two ways; first by hardware element in Section 7.6.2, and secondly by WBS in Section 7.6.1. Backup for the summaries in Section 7.6.3, provides detail estimates for each hardware item. Costs are based on the weights in Section 7.5.1. Many of the elements are common among the five system concepts such as the HLLV and Satellite OTV. Figure 7.6-1 displays the family tree regarding hardware commonality used in cost estimating. The cost estimate flow is from detail estimates in Section 7.6.3 to hardware elements in Section 7.6.2 utilizing the family tree in Table 7-1; 7.6-1. Costs from Section 7.6.2 are then transferred to the WBS in Section 7.6.1.

7.6.1 TABLE 7-17 HARDWARE FAMILY TREE (COSTING PURPOSES)

BASIC SYSTEM HARDWARE	POWER SATELLITE TYPE (1) ST/ DRC	(2) ST/ AC	(3) S/ BRAYTON	(4) ST/ BRAYTON	(5) NUC/ BRAYTON
Verification Prog. - Satellite	Same	Same	Same	Same	Ratio of (1)
- Assembly Base	Same	Same	Same	Same	Ratio of (1)
- SAT OTV	Same	Same	Same	Same	Same
- Crew OTV	Same	Same	Same	Same	Same
- Shuttle Launches	Same	Same	Same	Same	Ratio of (1)
- Demo Antenna	Same	Same	Same	Same	Same
Full Scale - Satellite	ST/DRC	ST/AC	S/BRAY	ST/BRAY	NUC/BRAY
- Transmitter & Distribution	ST/DRC	Same as (1)	S/BRAY	ST/BRAY	Same as (3)
- Leo Assy Base	ST/DRC	Same as (4)	Same as (4)	ST/BRAY	NUC/BRAY
- Leo Ant. Assembler	Same	Same	Same	Same	Same
- Leo Manipulators	Same	Same	Same	Same	Same
- SAT OTV	Same	Same	Same	Same	Same
- Crew OTV	Same	Same	Same	Same	Same
- Geo Base	Same	Same	Same	Same	Same
- Geo Manipulators	Same	Same	Same	Same	Same
- Rectenna	Same	Same	Same	Same	Same
HLLV (Cost per unit & per flight)	Same	Same	Same	Same	Same
STS (Cost per unit & per flight)	Same	Same	Same	Same	Same
Ground Facility	Same	Same	Same	Same	Same

7.6.1 SYSTEM ESTIMATED BY WBS

TABLE 7-18 THERMIONIC DIRECT RADIATION COOLED

WBS		COST-DOLLARS IN BILLIONS DDT&E	PROD	OPS	TOTAL
SATELLITE POWER STATION		44.25	1,238.98	672.12	1,955.35
1.0	Overall Prog. Mgmt }				
1.1	SE&I }			11.31	11.31
1.2	Technology Development Prog.				
1.3	System Devel - Verification	11.61			11.61
1.4	LEO Transport	8.92	99.05	635.16	743.13
	1.4.1 HLLV	8.92	98.00	626.23	733.15
	1.4.2 STA		1.05	8.93	9.98
1.5	LEO-GEO Transport - Crew	.80	1.36		2.16
1.6	Assembly Transport - Sat.	1.41	13.28		14.69
1.7	Logistics Transport	N/A	N/A	N/A	N/A
1.8	Maintenance Transport	N/A	N/A	N/A	N/A
1.9	Crew Transport	- Included in 1.4.2 and 1.5 -			
1.10	Satellite Power Station	11.99	987.50*		999.49
1.11	Ground Microwave	.38	125.20		125.58
1.12	Operations Support	8.34	12.59		20.93
	1.12.1 LEO Base	6.11	9.97		16.08
	1.12.2 GEO Base	2.23	2.62		4.85
1.13	Ground Control	.80		25.65	26.45

*Reflects revised Thermionic Diode calculations

7.6.1 SYSTEM ESTIMATES BY WBS

TABLE 7-19 THERMIONIC LIQUID COOLED

WBS		COST - DOLLARS IN BILLIONS DDT&E	PROD	OPS	TOTAL
SATELLITE POWER STATION		51.10	1,425.13	828.59	2,304.82
1.0	Overall Prog Mgmt			11.31	11.31
1.1	SE&I				
1.2	Technology Development Prog				
1.3	System Devel - Verification	11.61			11.61
1.4	LEO Transport	8.92	122.85	791.63	923.40
	1.4.1 HLLV	8.92	121.80	780.35	911.07
	1.4.2 STS		1.05	11.28	12.33
1.5	LEO-GEO Transport - Crew	.80	1.35		2.16
1.6	Assembly Transport - Sat.	1.41	13.28		14.69
1.7	Logistics Transport	N/A	N/A	N/A	N/A
1.8	Maintenance Transport	N/A	N/A	N/A	N/A
1.9	Crew Transport	- Included in 1.4.2 & 1.5 -			
1.10	Satellite Power Station	18.84	1,149.85*		1,168.69
1.11	Ground Microwave	.38	125.20		125.58
1.12	Operations Support	8.34	12.59		20.93
	1.12.1 LEO Base	6.11	9.97		16.08
	1.12.2 GEO Base	2.23	2.62		4.85
1.13	Ground Control	.80		25.65	26.45

*Reflects revised Thermionic Diode calculations.

7.6.1 SYSTEM ESTIMATES BY WBS

TABLE 7-20 BRAYTON

WBS		COST - DOLLARS IN BILLIONS DDT&E	PROD	OPS	TOTAL
SATELLITE POWER STATION		58.78	1,606.96	674.47	2,340.21
1.0	Overall Prog Mgmt.				
1.1	SE&I			11.31	11.31
1.2	Technology Development Prog				
1.3	System Devel - Verification				
1.4	LEO Transport	8.92	99.05	637.51	745.48
	1.4.1 HLLV	8.92	98.00	626.23	733.15
	1.4.2 STS		1.05	11.28	12.33
1.5	LEO-GEO Transport - Crew	.80	1.36		2.16
1.6	Assembly Transport - Sat.	1.41	13.28		14.69
1.7	Logistics Transport	N/A	N/A	N/A	N/A
1.8	Maintenance Transport	N/A	N/A	N/A	N/A
1.9	Crew Transport	- Included in 1.4.2 & 1.5 -			
1.10	Satellite Power Station	26.52	1,355.48		1,382.00
1.11	Ground Microwave	.38	125.20		125.58
1.12	Operations Support	8.34	12.59		20.93
	1.12.1 LEO Base	6.11	9.97		16.08
	1.12.2 GEO Base	2.23	2.62		4.85
1.13	Ground Control	.80		25.65	26.45

7.6.1 SYSTEM ESTIMATES BY WBS

TABLE 7-21 Thermionic Brayton

WBS		COST - DOLLARS IN BILLIONS DDT&E	PROD	OPS	TOTAL
SATELLITE POWER STATION		56.05	1,435.03	622.19	2,113.27
1.0	Overall Prog. Mgmt				
1.1	SE&I			11.31	11.31
1.2	Technology Development Prog.				
1.3	System Devel - Verification	11.61			11.61
1.4	LEO Transport	8.92	89.95	585.23	684.10
	1.4.1 HLLV	8.92	88.90	573.95	671.77
	1.4.2 STS		1.05	11.28	12.33
1.5	LEO-GEO Transport - Crew	.80	1.35		2.16
1.6	Assembly Transport - Sat.	1.41	13.28		14.69
1.7	Logistics Transport	N/A	N/A	N/A	N/A
1.8	Maintenance Transport	N/A	N/A	N/A	N/A
1.9	Crew Transport	- Included in 1.4.2 & 1.5 -			
1.10	Satellite Power Station	22.35	1,189.41*		1,211.76
1.11	Ground Microwave	.38	125.20		125.58
1.12	Operations Support	9.78	15.83		25.61
	1.12.1 LEO Base	7.55	13.21		20.76
	1.12.2 GEO Base	2.23	2.62		4.85
1.13	Ground Control	.80		25.65	26.45

*Reflects revised Thermionic Diode calculations.

7.6.1 SYSTEM ESTIMATES BY WBS

TABLE 7-22 NUCLEAR BRAYTON

WBS		COST - DOLLARS IN BILLIONS DDT&E	PROD	OPS	TOTAL
SATELLITE POWER STATION		71.45	2,368.51	1,118.55	3,558.51
1.0	Overall Prog. Mgmt				
1.1	SE&I			11.31	11.31
1.2	Technology Development Prog				
1.3	System Devel - Verification	24.16			24.16
1.4	LEO Transport	8.92	166.95	1,081.59	1,257.46
	1.4.1 HLLV	8.92	165.20	1,060.18	1,234.30
	1.4.2 STS		1.75	21.41	23.16
1.5	LEO-GEO Transport - Crew	.80	1.36		2.16
1.6	Assembly Transport - Sat.	1.41	13.28		14.69
1.7	Logistics Transport	N/A	N/A	N/A	N/A
1.8	Maintenance Transport	N/A	N/A	N/A	N/A
1.9	Crew Transport	- Included in 1.4.2 & 1.5 -			
1.10	Satellite Power Station	19.70	2,033.23*		2,052.93
1.11	Ground Microwave	.38	125.20		125.58
1.12	Operations Support	15.28	28.49		43.77
	1.12.1 LEO Base	13.05	25.87		38.92
	1.12.2 GEO Base	2.23	2.62		4.85
1.13	Ground Control	.80		25.65	26.45

*Reflects revised Thermionic Diode calculations.

7.6.2 SYSTEM ESTIMATE BY HARDWARE ELEMENT

TABLE 7-23 THERMIONIC DIRECT RADIATION COOLED

	COST-DOLLARS IN BILLIONS							
	DDT&E			PRODUCTION			OPS	
Cost Item	Dev	Test Hdwe	Total Cost	First Unit Cost	Qty	Total Cost	Total Cost	Total
Preproduction Satellite	3.53	1.58	5.11					5.11
Assembly Station	2.05	.81	2.86					2.86
Satellite OTV (4 in Set)	.85	.47	1.32					1.32
Crew OTV	.50	.04	.54					.54
Shuttle Launches	---	---	1.08					1.08
Demo Rectenna	---	---	.70					.70
Subtotal Verification Program			11.61					11.61
Technical Devel Program			Unknown					Unknown
STS Buys	---	---	---	.35	3	1.05		1.05
HLLV Buys	---	---	8.92	.80	140	98.00		106.92
Crew OTV	---	---	.80	.07	27	1.36		2.16
Power Satellite	---	---	9.48	18.83	62	866.56*		876.04
Transmitter & Dist	---	---	2.51	3.13	62	120.94		123.45
GEO Base	---	---	1.78	.44	6	2.25		4.03
GEO Manipulator	---	---	.45	.03	18	.37		.82
Rectenna	---	---	.38	3.24	62	125.20		125.58
LEO Base	---	---	3.65	.92	10	7.31		10.96
Antenna Assembler	---	---	2.01	.64	2	1.22		3.23
LEO Manipulator	---	---	.45	.07	30	1.44		1.89
Satellite OTV	---	---	1.41	.78	24	13.28		14.69
STS Launches							8.93	8.93
HLLV Launches							626.23	626.23
Control Complex	---	---	.80				25.65	26.45
Subtotal Operations							660.81	
Overall Program Management and SE&I							11.31	11.31
TOTAL PROGRAM COST			44.25	29.20		1,238.98	672.12	1,955.35

*Reflects revised Thermionic Diode calculations.

7.6.2 SYSTEM ESTIMATE BY HARDWARE ELEMENT

TABLE 7-24 THERMIONIC LIQUID COOLED

COST-DOLLARS IN BILLIONS

Cost Item	DDT&E Dev	DDT&E Test Hdwe	DDT&E Total Cost	PRODUCTION First Unit Cost	PRODUCTION Qty	PRODUCTION Total Cost	OPS Total Cost	Total
Preproduction Satellite	3.53	1.58	5.11					5.11
Assembly Station	2.05	.81	2.86					2.86
Satellite OTV (4 in Set)	.85	.47	1.32					1.32
Crew OTV	.50	.04	.54					.54
Shuttle Launches	---	---	1.08					1.08
Demo Rectenna	---	---	.70					.70
Subtotal Verification Program			11.61					11.61
Technical Devel Program			Unknown					Unknown
STS Buys	---	---	---	.35	3	1.05		1.05
HLLV Buys	---	---	8.92	.80	174	121.80		130.72
Crew OTV	---	---	.80	.07	27	1.36		2.16
Power Satellite	---	---	16.33	23.03	62	1,028.91*		1,045.24
Transmitter & Dist	---	---	2.51	3.13	62	120.94		123.45
GEO Base	---	---	1.78	.44	6	2.25		4.03
GEO Manipulator	---	---	.45	.03	18	.37		.82
Rectenna	---	---	.38	3.24	62	125.20		125.58
LEO Base	---	---	3.65	.92	10	7.31		10.96
Antenna Assembler	---	---	2.01	.64	2	1.22		3.23
LEO Manipulator	---	---	.45	.07	30	1.44		1.89
Satellite OTV	---	---	1.41	.78	24	13.28		14.69
STS Launches							11.28	11.28
HLLV Launches							780.35	780.35
Control Complex	---	---	.80				25.65	26.45
Subtotal Operations							817.28	
Overall Program Management and SE&I							11.31	11.31
TOTAL PROGRAM COST			51.10	33.40		1,425.13	828.59	2,304.82

*Reflects revised Thermionic Diode calculations.

7.6.2 SYSTEM ESTIMATE BY HARDWARE ELEMENT

TABLE 7-25 BRAYTON

COST-DOLLARS IN BILLIONS

	DDT&E			PRODUCTION			OPS	
Cost Item	Dev	Test Hdwe	Total Cost	First Unit Cost	Qty	Total Cost	Total Cost	Total
Preproduction Satellite	3.53	1.58	5.11					5.11
Assembly Station	2.05	.81	2.86					2.86
Satellite OTV (4 in Set)	.85	.47	1.32					1.32
Crew OTV	.50	.04	.54					.54
Shuttle Launches	---	---	1.08					1.08
Demo Rectenna	---	---	.70					.70
Subtotal Verification Program			11.61					11.61
Technical Devel Program			Unknown					Unknown
STS Buys	---	---	---	.35	3	1.05		1.05
HLLV Buys	---	---	8.92	.80	140	98.00		106.92
Crew OTV	---	---	.80	.07	27	1.36		2.16
Power Satellite	---	---	25.02	33.21	62	1,283.23		1,308.25
Transmitter & Dist	---	---	1.50	1.87	62	72.25		73.75
GEO Base	---	---	1.78	.44	6	2.25		4.03
GEO Manipulator	---	---	.45	.03	18	.37		.82
Rectenna	---	---	.38	3.24	62	125.20		125.58
LEO Base	---	---	3.65	.92	10	7.31		10.96
Antenna Assembler	---	---	2.01	.64	2	1.22		3.23
LEO Manipulator	---	---	.45	.07	30	1.44		1.89
Satellite OTV	---	---	1.41	.78	24	13.28		14.69
STS Launches							11.28	11.28
HLLV Launches							626.23	626.23
Control Complex	---	---	.80				25.65	26.45
Subtotal Operations							663.16	
Overall Program Management and SE&I							11.31	11.31
TOTAL PROGRAM COST			58.78	42.32		1,606.96	674.47	2,340.21

7.6.2 SYSTEM ESTIMATE BY HARDWARE ELEMENT

TABLE 7-26 THERMIONIC BRAYTON

COST-DOLLARS IN BILLIONS

	DDT&E			PRODUCTION			OPS	
Cost Item	Dev	Test Hdwe	Total Cost	First Unit Cost	Qty	Total Cost	Total Cost	Total
Preproduction Satellite	3.53	1.58	5.11					5.11
Assembly Station	2.05	.81	2.86					2.86
Satellite OTV (4 in Set)	.85	.47	1.32					1.32
Crew OTV	.50	.04	.54					.54
Shuttle Launches	---	---	1.08					1.08
Demo Rectenna	---	---	.70					.70
Subtotal Verification Program			11.61					11.61
Technical Devel Program			Unknown					Unknown
STS Buys	---	---	---	.35	3	1.05		1.05
HLLV Buys	---	---	8.92	.80	127	88.90		97.82
Crew OTV	---	---	.80	.07	27	1.36		2.16
Power Satellite	---	---	19.84	27.61	62	1,105.18*		1,125.02
Transmitter & Dist	---	---	2.51	2.18	62	84.23		86.74
GEO Base	---	---	1.78	.44	6	2.25		4.03
GEO Manipulator	---	---	.45	.03	18	.37		.82
Rectenna	---	---	.38	3.24	62	125.20		125.58
LEO Base	---	---	5.09	1.32	10	10.55		15.64
Antenna Assembler	---	---	2.01	.64	2	1.22		3.23
LEO Manipulator	---	---	.45	.07	30	1.44		1.89
Satellite OTV	---	---	1.41	.78	24	13.28		14.69
STS Launches							11.28	11.28
HLLV Launches							573.95	573.95
Control Complex	---	---	.80				25.65	26.45
Subtotal Operations							610.88	
Overall Program Management and SE&I							11.31	11.31
TOTAL PROGRAM COST			56.05	37.43		1,435.03	622.19	2,113.27

*Reflects revised Thermionic Diode calculations

7.6.2 SYSTEM ESTIMATE BY HARDWARE ELEMENT

TABLE 7-27 NUCLEAR BRAYTON

	COST-DOLLARS IN BILLIONS							
	DDT&E			PRODUCTION			OPS	
Cost Item	Dev	Test Hdwe	Total Cost	First Unit Cost	Qty	Total Cost	Total Cost	Total
Preproduction Satellite*	6.78	4.26	11.04					11.04
Assembly Station*	5.95	2.56	8.51					8.51
Satellite OTV (4 in Set)	.85	.47	1.32					1.32
Crew OTV	.50	.04	.54					.54
Shuttle Launches **	---	---	2.05					2.05
Demo Rectenna	---	---	.70					.70
Subtotal Verification Program			24.16					24.16
Technical Devel Program			Unknown					Unknown
STS Buys	---	---	---	.35	5	1.75		1.75
HLLV Buys	---	---	8.92	.80	236	165.20		174.12
Crew OTV	---	---	.80	.07	27	1.36		2.16
Power Satellite	---	---	18.20	50.75	62	1,960.98		1,979.18
Transmitter & Dist	---	---	1.50	1.87	62	72.25		73.75
GEO Base	---	---	1.78	.44	6	2.25		4.03
GEO Manipulator	---	---	.45	.03	18	.37		.82
Rectenna	---	---	.38	3.24	62	125.20		125.58
LEO Base	---	---	10.59	2.91	10	23.21		33.80
Antenna Assembler	---	---	2.01	.64	2	1.22		3.23
LEO Manipulator	---	---	.45	.07	30	1.44		1.89
Satellite OTV	---	---	1.41	.78	24	13.28		14.69
STS Launches							21.41	21.41
HLLV Launches							1,060.18	1,060.18
Control Complex	---	---	.80				25.65	26.45
Subtotal Operations							1,107.24	
Overall Program Management and SE&I							11.31	11.31
TOTAL PROGRAM COST			71.45	61.85		2,368.51	1,118.55	3,558.51

*Costs established by ratio of full scale dev. and prod. costs of nuclear Brayton to Thermionic Direct Radiation Cooled applied to Validation costs.

**Costs established by ratio of full scale satellite weights of Nuclear Brayton to Thermionic DRC applied to Validation flights.

TABLE 7-28 DETAIL COST BACKUP STS

	DDT & E	COST PER FLIGHT
Costs from JSC Cost Per Flight Control Document (See Appendix)	Will be Completed Separately	$15 M

RECURRING COSTS

	LAUNCHES*	COST TOTAL - MILLIONS
Thermionic DRC	595	8,925
Thermionic LC	752	11,280
Brayton	752	11,280
Thermionic Brayton	752	11,280
Nuclear Brayton	1427	21,405

*Not Including Verification Launches

	BUYS	COST TOTAL - MILLIONS
Thermionic DRC	3	1,050
Thermionic LC	3	1,050
Brayton	3	1,050
Thermionic Brayton	3	1,050
Nuclear Brayton	5	1,750

DETAIL COST BACKUP

SHUTTLE LAUNCHES - VERIFICATION

Launches = 72 - Section 5.3

Cost/launch = $15 M - STS escallated cost from Cost Per Flight Control Document (See Appendix)

72 launches X $15 M/launch = $1,080 M TOTAL

Cost for Nuclear Brayton launches based on ratio of full scale satellite weights of Nuclear Brayton to Thermionic DRC applied to Validation flights.

i.e. $\frac{631.62}{332.81}$ X 72 = 137 flights

137 launches X $15 M/launch = $2,055 TOTAL

TABLE 7-29 DETAIL COST BACKUP HLLV

	DDT & E	COST PER FLIGHT	COST PER 1st UNIT
Costs from HLLV Study (see Appendix)	$7,000 M	$9 M	$800 M
32 Launch Pads @ 60M	1,920		
TOTAL	$8,920 M		

RECURRING COSTS

	LAUNCHES	COST TOTAL - MILLIONS
Thermionic DRC	69,581	626,229
Thermionic LC	86,705	780,345
Brayton	69,581	626,229
Thermionic Brayton	63,772	573,948
Nuclear Brayton	117,798	1,060,182

	BUYS	COST TOTAL - MILLIONS
Thermionic DRC	140	98,000
Thermionic LC	174	121,800
Brayton	140	98,000
Thermionic Brayton	127	88,900
Nuclear Brayton	236	165,200

TABLE 7-30 DETAIL COST BACKUP THERMIONIC DIODES

Cost per diode in production quantity is $238 Estimate from Manufacturing Group -- See Appendix

Quantities are estimated by .64 KW/diode

COSTS

	UNIT GENERATING REQUIREMENTS	UNIT QTY	UNIT COST (MILLIONS)
Thermionic DRC	16,000,000 KW	25,000,000	5,950
Thermionic LC	16,000,000 KW	25,000,000	5,950
Thermionic Brayton	4,413,000 KW	6,895,313	1,641

Unit Costs represent cum average for entire production run.

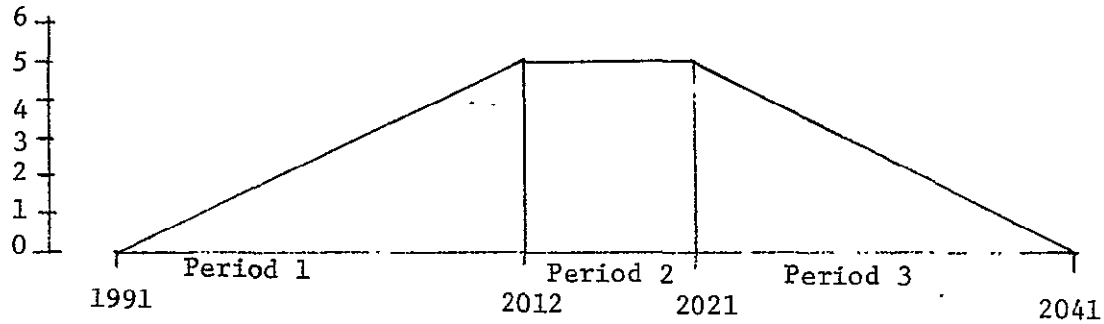

FACILITY MANNING PROFILE

COSTING

ASSUME $50,000/MAN YEAR -- INCLUDES LABOR AND SUPPORT

PERIOD	MAN YEARS	COST - MILLIONS
1	63,000	3,150,000
2	45,000	2,250,000
3	63,000	3,150,000
	SUB TOTAL	8,550,000
	THREE SHIFT EFFORT X 3	
	TOTAL	$25,650,000
	FACILITY	$ 800,000

FIGURE 7-23 DETAIL COST BACKUP GROUND CONTROL FACILITY

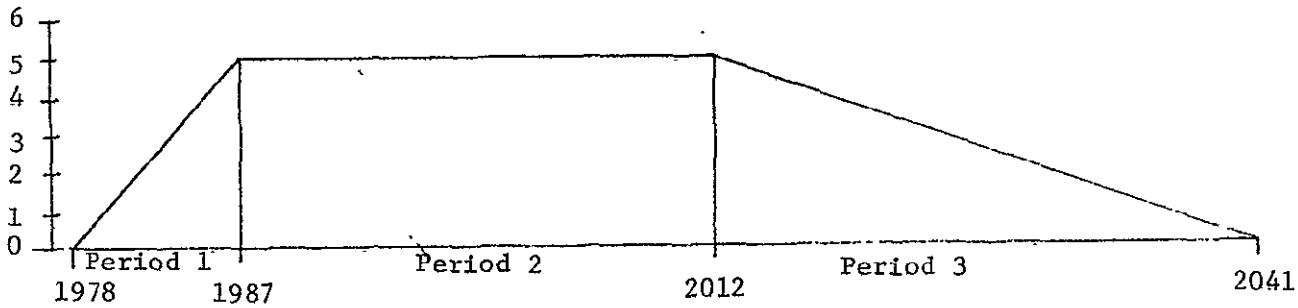

MANNING PROFILE

COSTING

ASSUME $50,000/MAN YEAR -- INCLUDES LABOR AND SUPPORT

PERIOD	MAN YEARS	COST - MILLIONS
1	22,500	1,310,000
2	125,000	6,250,000
3	75,000	3,750,000
	TOTAL	11,310,000

FIGURE 7-24 DETAIL COST BACKUP PROGRAM MANAGEMENT AND SE&I

TABLE 7-31 DETAIL COST BACKUP POWER SATELLITE
THERMIONIC DIRECT RADIATION COOLED

$ in Millions
Weight in lbs X 10^3

COST ELEMENTS	$ RDT&E	FIRST UNIT	$ PROD	QTY	UNIT WEIGHT	CER
Total Program	9,477	18,826	866,563	62	207,780	
Program Management	536	1,007	38,915			
System Engr & Integ	2,184	244	9,427			
System Hardware	5,179	15,702	745,836			
Energy Collection	1,978	3,456	133,557		50,920	Simple Structure
					15,520	Reflector Units
Energy Conversion	3,098	6,296	243,317		5,730	Nominal Structure
					65,700	Simple Structure
Diodes	104	5,951	368,962*		69,910	Independent Calculation from Manufacturing
Software Engineering	303					
Systems Test Labor	228					
Systems Test Hardware	158					
Vehicle GSE	688	234	9,041			
Tooling	201	717	27,711			
Engr Support & Liason		125	4,831			
Initial Spares		797	30,802			
Flt Test Hdwe						

*Unit cost is cum average
No learning curve is shown

TABLE 7-32 DETAIL COST BACKUP POWER SATELLITE
THERMIONIC LIQUID COOLED

$ in Millions
Weight in lbs X 10^3

COST ELEMENTS	$ RDT&E	FIRST UNIT	$ PROD	QTY	UNIT WEIGHT	CER
Total Program	16,329	23,032	1,028,911	62	209,030	
Program Management	924	1,224	47,291			
System Engr & Integ	3,661	409	15,802			
System Hardware	8,741	18,246	843,997			
Energy Collection	1,362	2,775	107,216		27,640	Simple Structure
					15,920	Reflectors Unit
Energy Conversion	2,351	3,010	116,296		6,340	Nominal Structure
					17,440	Simple Structure
Diodes	104	5,951	368,962*		94,670	
Radiators	4,924	6,510	251,523		19,420	Nominal Structure
					27,600	Simple Structure
Software Engineering	501					
Systems Test Labor	379					
Systems Test Hardware	323					
Vehicle GSE	1,382	470	18,159			
Tooling	418	1,491	57,607			
Engr Support & Liason		256	9,891			
Initial Spares		936	36,164			
Flt Test Hdwe						

*Unit cost is cum average
No learning curve is shown

TABLE 7-33 DETAIL COST BACKUP POWER SATELLITE BRAYTON

$ in Millions
Weight in lbs X 10^3

COST ELEMENTS	$ RDT&E	FIRST UNIT	$ PROD	QTY	UNIT WEIGHT	CER
Total Program	25,019	33,209	1,283,231	62	170,770	
Program Management	1,416	1,761	68,047			
System Engr & Integ	5,498	614	23,726			
System Hardware	13,299	25,812	997,441			
Energy Collection	2,217	2,049	79,176		22,640	Simple Structure
					15,010	Reflector Units
Energy Conversion	6,325	17,116	661,380		83,330	Nominal Structure
					9,700	Simple Structure
Radiators	4,758	6,647	256,885		21,950	Nominal Structure
					18,140	Simple Structure
Software Engineering	734					
Systems Test Labor	560					
Systems Test Hardware	530					
Vehicle GSE	2,280	775	29,947			
Tooling	702	2,496	96,448			
Engr Support & Liason		421	16,268			
Initial Spares		1,329	51,354			
Flt Test Hdwe						

TABLE 7-34 DETAIL COST BACKUP POWER SATELLITE THERMIONIC BRAYTON

$ in Millions
Weight in lbs X 10^3

COST ELEMENTS	$ RDT&E	FIRST UNIT	$ PROD	QTY	UNIT WEIGHT	CER
Total Program	19,842	27,607	1,105,184	62	143,340	
Program Management	1,123	1,466	56,652			
System Engr & Integ	4,398	491	18,974			
System Hardware	10,563	21,694	876,682			
Energy Collection	2,023	1,941	75,008*		20,460	Simple Structure
					13,580	Reflector Units
Energy Conversion	4,990	13,342	515,638		57,145	Nominal Structure
					6,705	Simple Structure
Diodes	104	1,641	101,742**		17,810	Independent Calculation from Manufacturing
Radiators	3,446	4,769	184,294		15,120	Nominal Structure
					12,520	Simple Structure
Software Engineering	597					
Systems Test Labor	453					
Systems Test Hardware	412					
Vehicle GSE	1,759	598	23,109			
Tooling	538	1,916	74,042			
Engr Support & Liason		327	12,637			
Initial Spares		1,115	43,088			
Flt Test Hdwe						

* $29,250 for Reflector
**Unit cost is cum average
No learning curve is shown

TABLE 7-35 DETAIL COST BACKUP POWER SATELLITE NUCLEAR BRAYTON

$ in Millions
Weight in lbs X 10^3

COST ELEMENTS	$ RDT&E	FIRST UNIT	$ PROD	QTY	UNIT WEIGHT	CER
Total Program	18,193	50,750	1,960,980	62	288,130	
Program Management	1,030	2,718	105,024			
System Engr & Integ	4,061	454	17,543			
System Hardware	9,595	42,750	1,651,898			
Reactor	2,122	9,718	375,542		46,890	Nominal Structure
Turbomachinery	3,300	15,507	599,190		78,570	Nominal Structure
Radiators	4,172	17,525	677,166		60,000	Nominal Structure
					102,670	
Software Engineering	555					
Systems Test Labor	420					
Systems Test Hardware	388					
Vehicle GSE	1,641	558	21,561			
Tooling	504	1,796	69,397			
Engr Support & Liason		308	11,901			
Initial Spares		2,165	83,656			
Flt Test Hdwe						

TABLE 7-36 DETAIL COST BACKUP TRANSMITTER AND DISTRIBUTION
THERMIONIC DIODE - DIRECT RADIATION AND LIQUID COOLED

$ in Millions
Weight in lbs X 10^3

COST ELEMENTS	$ RDT&E	FIRST UNIT	$ PROD	QTY	UNIT WEIGHT	CER
Total Program	2,508	3,134	120,943	62	69,280	
Program Management	196	183	7,062			
System Engr & Integ	144	37	1,428			
System Hardware	684	2,838	109,520			
Rotary Converter	333	1,070	41,208		17,300	RCA Price
Transmitter	62	476	18,392		26,200	RCA Price
Transformers; Controls	289	1,292	49,920		25,780	RCA Price
Software Engineering						
Systems Test Labor						
Systems Test Hardware	1,293					
Vehicle GSE						
Tooling	191	76	2,933			
Engr Support & Liason						
Initial Spares						
Flt Test Hdwe						

TABLE 7-37 DETAIL COST BACKUP TRANSMITTER AND DISTRIBUTION THERMIONIC BRAYTON

$ in Millions
Weight in lbs X 10^3

COST ELEMENTS	$ RDT&E	FIRST UNIT	$ PROD	QTY	UNIT WEIGHT	CER
Total Program	2,508	2,180	84,230	62	56,280	
Program Management	196	102	3,941			
System Engr & Integ	144	14	541			
System Hardware	684	2,018	77,971			
Rotary Converter	333	250	9,659		4,370	RCA Price
Transmitter	62	476	18,392		26,200	RCA Price
Transformers, Controls	289	1,292	49,920		25,710	RCA Price
Software Engineering						
Sytems Test Labor						
Systems Test Hardware	1,293					
Vehicle GSE						
Tooling	191	46	1,777			
Engr Support & Liason						
Initial Spares						
Flt Test Hdwe						

TABLE 7-38 DETAIL COST BACKUP TRANSMITTER AND DISTRIBUTION BRAYTON - SOLAR AND NUCLEAR

$ in Millions
Weight in lbs X 10^3

COST ELEMENTS	$ RDT&E	FIRST UNIT	$ PROD	QTY	UNIT WEIGHT	CER
Total Program	1,500	1,870	72,254	62	51,980	
Program Management	115	64	2,473			
System Engr & Integ	79	9	348			
System Hardware	351	1,768	68,312			
Transmitter	62	476	18,392		26,200	RCA Price
Transformers, Controls	289	1,292	49,920		25,780	RCA Price
Software Engineering						
Systems Test Labor						
Systems Test Hardware	838					
Vehicle GSE						
Tooling	117	29	1,121			
Engr Support & Liason						
Initial Spares						
Flt Test Hdwe						

TABLE 7-39 DETAIL COST BACKUP DEMO RECTENNA - VERFIICATION

$ in Millions
Weight in lbs X 10^3

COST ELEMENTS	$ RDT&E	FIRST UNIT	$ PROD	QTY	UNIT WEIGHT	CER
Total Program	665			1	265,751	
Program Management	42					
System Engr & Integ						
System Hardware	604					
Rectenna	604				265,751	RCA Price
Software Engineering						
Systems Test Labor						
Systems Test Hardware						
Vehicle GSE						
Tooling	19					
Engr Support & Liason						
Initial Spares						
Flt Test Hdwe						

TABLE 7-40 DETAIL COST BACKUP SATELLITE - VERIFICATION

$ in Millions
Weight in lbs X 10^3

COST ELEMENTS	$ RDT&E	FIRST UNIT	$ PROD	QTY	UNIT WEIGHT	CER
Total Program	3,525	1,584	1,584	1	4,259	
Program Management	198	69	69			
System Engr & Integ	832	93	93			
System Hardware	1,804	648	648			
Energy Collection	739	209	209		220	Nominal Structure
					568	Simple Structure
Radiators	465	128	128		853	Simple Structure
Conversion & Dist	557	154	154		88	Nominal Structure
					652	Simple Structure
Transmitter	42	157	157		146	Batteries Electrical
					56	Diode Independent Calc
					1,676	RCA Price
Software Engineering	32					
Systems Test Labor	361					
Systems Test Hardware	49					
Vehicle GSE	208	141	141			
Tooling	42	540	540			
Engr Support & Liason		28	28			
Initial Spares		63	63			
FLT Test Hdwe						

TABLE 7-41 DETAIL COST BACKUP SATELLITE OTV - VERIFICATION

$ in Millions
Weight in lbs X 10^3

COST ELEMENTS	$ RDT&E	FIRST UNIT	$ PROD	QTY	UNIT WEIGHT	CER
Total Program	846	468	468	1	166	
Program Management						
System Engr & Integ						
System Hardware						
SAT OTV						
Software Engineering						
Systems Test Labor						
Systems Test Hardware						
Vehicle GSE						
Tooling						
Engr Support & Liason						
Initial Spares						
Flt Test Hdwe						

NOTE: All costs and weights 60% of full scale OTV

TABLE 7-42 DETAIL COST BACKUP ASSEMBLY SYSTEM - VERIFICATION

$ in Millions
Weight in lbs X 10^3

COST ELEMENTS	$ RDT&E	FIRST UNIT	$ PROD	QTY	UNIT WEIGHT	CER
Total Program	2,053	810	810	1	716	
Program Management	116	39	39			
System Engr & Integ	497	56	56			
System Hardware	1,034	279	279			
Habitat	609	171	171		331	Nominal Structure
Pwr Sys & P/L Holding	318	86	86		22	Machinery
					33	Battery Electrical
Frames & Assembler	108	22	22		110	Nominal Structure
					110	Simple Structure
					110	Contingency
Software Engineering	20					
Systems Test Labor	212					
Systems Test Hardware	28					
Vehicle GSE	122	83	83			
Tooling	23	302	302			
Engr Support & Liason		16	16			
Initial Spares		16	16			
Flt Test Hdwe						

TABLE 7-43 DETAIL COST BACKUP LEO BASE THERMIONIC DIODE - DRC AND LC - BRAYTON

$ in Millions
Weight in lbs X 10^3

COST ELEMENTS	& RDT&E	FIRST UNIT	& PROD	QTY	UNIT WEIGHT	CER
TOTAL PROGRAM	3,652	920	7,312	10	1,715.4	
PROGRAM MANAGEMENT	207	43	342			
SYSTEM ENGR & INTEG	823	12	92			
SYSTEM HARDWARE	1,883	538	4,273			
LEO BASE	1,883	538	4,273		112.2	Docking & Payload Holding
					233.0	Structure 2
					343.0	Contingency 2
					1,003.0	Manipulators, Assemblers, Tools 3
					24.2	Power System 4
SOFTWARE ENGINEERING	28				1	Machinery
SYSTEMS TEST LABOR	377				2	Simple Structure
SYSTEMS TEST HARDWARE	57				3	Nominal Structure
VEHICLE GSE	226	97	769		4	Battery Electrical
TOOLING	51	163	1,299			
ENGR SUPPORT & LIASON		4	33			
INITIAL SPARES		63	504			
FLT TEST HDWE						

TABLE 7-44 DETAIL COST BACKUP LEO BASE THERMIONIC BRAYTON

$ in Millions
Weight in lbs X 10^3

COST ELEMENTS	$ RDT&E	FIRST UNIT	$ PROD	QTY	UNIT WEIGHT	CER
TOTAL PROGRAM	5,091	1,320	10,550	10	2,369.4	
PROGRAM MANAGEMENT	288	62	494			
SYSTEM ENGR & INTEG	1,128	16	126			
SYSTEM HARDWARE	2,635	770	6,159			
LEO BASE	2,635	770	6,159		169.4	Docking & Payload Holding 1
					70.4	Structure 2
					475.2	Contingency 2
					1,619.2	Manipulators, Assemblers, Tools 3
					35.2	Power System 4
SOFTWARE ENGINEERING	36				1	Machinery
					2	Simple Structure
SYSTEMS TEST LABOR	524				3	Nominal Structure
					4	Battery Electrical
SYSTEMS TEST HARDWARE	83					
VEHICLE GSE	323	137	1,100			
TOOLING	75	238	1,901			
ENGR SUPPORT & LIASON		6	47			
INITIAL SPARES		91	726			
FLT TEST HDWE						

TABLE 7-45 DETAIL COST BACKUP LEO BASE NUCLEAR BRAYTON

$ in Millions
Weight in lbs X 10^3

COST ELEMENTS	$ RDT&E	FIRST UNIT	$ PROD	QTY	UNIT WEIGHT	CER
TOTAL PROGRAM	10,589	2,910	23,207	10	6,049.6	
PROGRAM MANAGEMENT	599	136	1,088			
SYSTEM ENGR & INTEG	2,257	32	252			
SYSTEM HARDWARE	5,525	1,689	13,473			
LEO BASE	5,525	1,689	13,473		229.0	Docking & Payload Holding 1
					644.6	Structure 2
					1,210.0	Contingency 2
					3,825.0	Manipulators, Assemblers, Tools 3
					141.0	Power System 4
SOFTWARE ENGINEERING	66					
SYSTEMS TEST LABOR	1,085					
SYSTEMS TEST HARDWARE	181					
VEHICLE GSE	707	302	2,404			
TOOLING	169	539	4,299			
ENGR SUPPORT & LIASON		13	103			
INITIAL SPARES		199	1,588			
FLT TEST HDWE						

1 Machinery
2 Simple Structure
3 Nominal Structure
4 Battery Electrical

TABLE 7-46 DETAIL COST BACKUP ANTENNA (TRANSMITTER) ASSEMBLER

$ in Millions
Weight in lbs X 10^3

COST ELEMENTS	$ RDT&E	FIRST UNIT	$ PROD	QTY	UNIT WEIGHT	CER
TOTAL PROGRAM	2,017	640	1,226	2	1,390	
PROGRAM MANAGEMENT	114	29	56			
SYSTEM ENGR & INTEG	470	27	52			
SYSTEM HARDWARE	1,035	283	543			
ANTENNA ASSEMBLER	1,035	283	543		150	Habitat *
					80	Docking Ports
					1,160	Simple Structure
SOFTWARE ENGINEERING						
SYSTEMS TEST LABOR	17					
SYSTEMS TEST HARDWARE	209					
VEHICLE GSE	29	85	161			
TOOLING	119	170	326			
ENGR SUPPORT & LIASON	25	9	17			
INITIAL SPARES		37	70			
FLT TEST HDWE						

* Same CER (Nominal Structure)

TABLE 7-47 DETAIL COST BACKUP LEO MANIPULATOR

$ in Millions
Weight in lbs X 10^3

COST ELEMENTS	$ RDT&E	FIRST UNIT	$ PROD	QTY	UNIT WEIGHT	CER
TOTAL PROGRAM	454	70	1,440	30	208	
PROGRAM MANAGEMENT	26	3	70			
SYSTEM ENGR & INTEG	110	1	12			
SYSTEM HARDWARE	219	53	1,084			
LEO MANIPULATOR	219	53	1,084		30	Nominal Structure
					170	Simple Structure
					8	Battery Electrical
SOFTWARE ENGINEERING	5					
SYSTEMS TEST LABOR	45					
SYSTEMS TEST HARDWARE	18					
VEHICLE GSE	27	4	91			
TOOLING	5	3	62			
ENGR SUPPORT & LIASON			3			
INITIAL SPARES		6	118			
FLT TEST HDWE						

TABLE 7-48 DETAIL COST BACKUP SATELLITE OTV

$ in Millions
Weight in lbs X 10^3

COST ELEMENTS	$ RDT&E	FIRST UNIT	$ PROD	QTY	UNIT WEIGHT	CER
TOTAL PROGRAM	1,410	780	13,284	24	277	
PROGRAM MANAGEMENT	80	37	632			
SYSTEM ENGR & INTEG	254	2	28			
SYSTEM HARDWARE	537	608	10,350			
SAT OTV	537	608	10,350		10	Reaction Control
					50	Machinery
					100	Nominal Structure
					100	Simple Structure
					4	Complex Avionics
					4	Simple Avionics
					9	Battery Electrical
SOFTWARE ENGINEERING	10					
SYSTEMS TEST LABOR	110					
SYSTEMS TEST HARDWARE	208					
VEHICLE GSE	60	58	981			
TOOLING	12	9	151			
ENGR SUPPORT & LIASON			8			
INITIAL SPARES		66	1,133			
FLT TEST HDWE	139					

TABLE 7-49 DETAIL COST BACKUP CREW OTV

$ in Millions
Weight in lbs X 10^3

COST ELEMENTS	$ RDT&E	FIRST UNIT	$ PROD	QTY	UNIT WEIGHT	CER
TOTAL PROGRAM	795	73	1,360	27	68	
PROGRAM MANAGEMENT	40	4	75			
SYSTEM ENGR & INTEG	9					
SYSTEM HARDWARE	480	69	1,285			
CORE STAGE	221	25	484		16	FSTSA
DROP TANKS	12	11	186		17	FSTSA
CREW CAPSULE	247	33	615		35	FSTSA
SOFTWARE ENGINEERING	7					
SYSTEMS TEST LABOR	17					
SYSTEMS TEST HARDWARE	139					
VEHICLE GSE	19					
TOOLING	2					
ENGR SUPPORT & LIASON						
INITIAL SPARES						
FLT TEST HDWE	82					

FSTSA = FUTURE SPACE TRANSPORTATION SYSTEM ANALYSIS STUDY

TABLE 7-50 DETAIL COST BACKUP GEO BASE

$ in Millions
Weight in lbs X 10^3

COST ELEMENTS	& RDT&E	FIRST UNIT	& PROD	QTY	UNIT WEIGHT	CER
TOTAL PROGRAM	1,777	440	2,248	6	1,320	
PROGRAM MANAGEMENT	101	18	94			
SYSTEM ENGR & INTEG	416	9	46			
SYSTEM HARDWARE	910	239	1,223			
GEO BASE	910	239	1,223		150	Habitat *
					400	Maintenance BAT **
					300	Spares Storage
					470	Main Frame
SOFTWARE ENGINEERING	15					
SYSTEMS TEST LABOR	184					
SYSTEMS TEST HARDWARE	25					
VEHICLE GSE	104	84	424			** . SAME CER (SIMPLE STRUCTURE)
TOOLING	22	55	281			
ENGR SUPPORT & LIASON		3	14			
INITIAL SPARES		32	165			
FLT TEST HDWE						

TABLE 7-51 DETAIL COST BACKUP GEO MANIPULATOR

$ in Millions
Weight in lbs X 10^3

COST ELEMENTS	& RDT&E	FIRST UNIT	& PROD	QTY	UNIT WEIGHT	CER
TOTAL PROGRAM	450	28	370	18	35	
PROGRAM MANAGEMENT	26	2	21			
SYSTEM ENGR & INTEG	46	1	12			
SYSTEM HARDWARE	168	25	333			
	168	25	333		35	SEPS System Analysis Study
SOFTWARE ENGINEERING	26		3			
SYSTEMS TEST LABOR	4		1			
SYSTEMS TEST HARDWARE	45					
VEHICLE GSE	135					
TOOLING						
ENGR SUPPORT & LIASON						
INITIAL SPARES						
FLT TEST HDWE						

TABLE 7-52 DETAIL COST BACKUP RECTENNA

$ in Millions
Weight in lbs X 10^3

COST ELEMENTS	& RDT&E	FIRST UNIT	& PROD	QTY	UNIT WEIGHT	CER
TOTAL PROGRAM	381	3,241	125,200	62	5,917,000	
PROGRAM MANAGEMENT	84	222	8,576			
SYSTEM ENGR & INTEG	3	8	309			
SYSTEM HARDWARE	42	466	18,002			
RECTENNA	42	466	18,002		5,917,000	RCA Price
SOFTWARE ENGINEERING						
SYSTEMS TEST LABOR						
SYSTEMS TEST HARDWARE	231					
VEHICLE GSE						
TOOLING	21	2,545	98,313			
ENGR SUPPORT & LIASON						
INITIAL SPARES						
FLT TEST HDWE						

7.7 ECONOMICS

By using the master schedule and hardware time phasing information presented in Section 7.5.3, funding distributions are developed for each Powersat alternative. Funding by phase is possible by relating to the hardware identification matrix of Section 7.5.2, which is time phased.

The funding distributions allow the development of net present values for the alternatives which are then used for comparison purposes in Section 7.1, Program Cost Comparisons.

7.7.1 FUNDING DISTRIBUTIONS

Preparatory to doing a present value analysis, the system costs must be time spread. Using the program schedule (Section 7.4) distribution profiles were made for DDT&E, Production, and Operations. The following charts show each system spread by the distribution profile. Major start and stop points are shown in the table below:

	START	FINISH
DDT&E	1978	1989
Production	1988	2011
Ops-LEO Transport-HLLV	1988	2011
Ops-Mission Control	1991	2041
Power Production	1991	2041

Power generation profile (in GW) is included for a reference in the distribution charts. The hump in DDT&E is the Verification Program, and the majority of operations costs result from the HLLV low earth orbit launch cycle.

Non HLLV operations costs are for mission control and their cost profile follows that of the 62 satellite ground power output. Production cost profile represents a rapid build up to meet the high initial production rate, followed by a leveling off as efficiency improves but production continues to build.

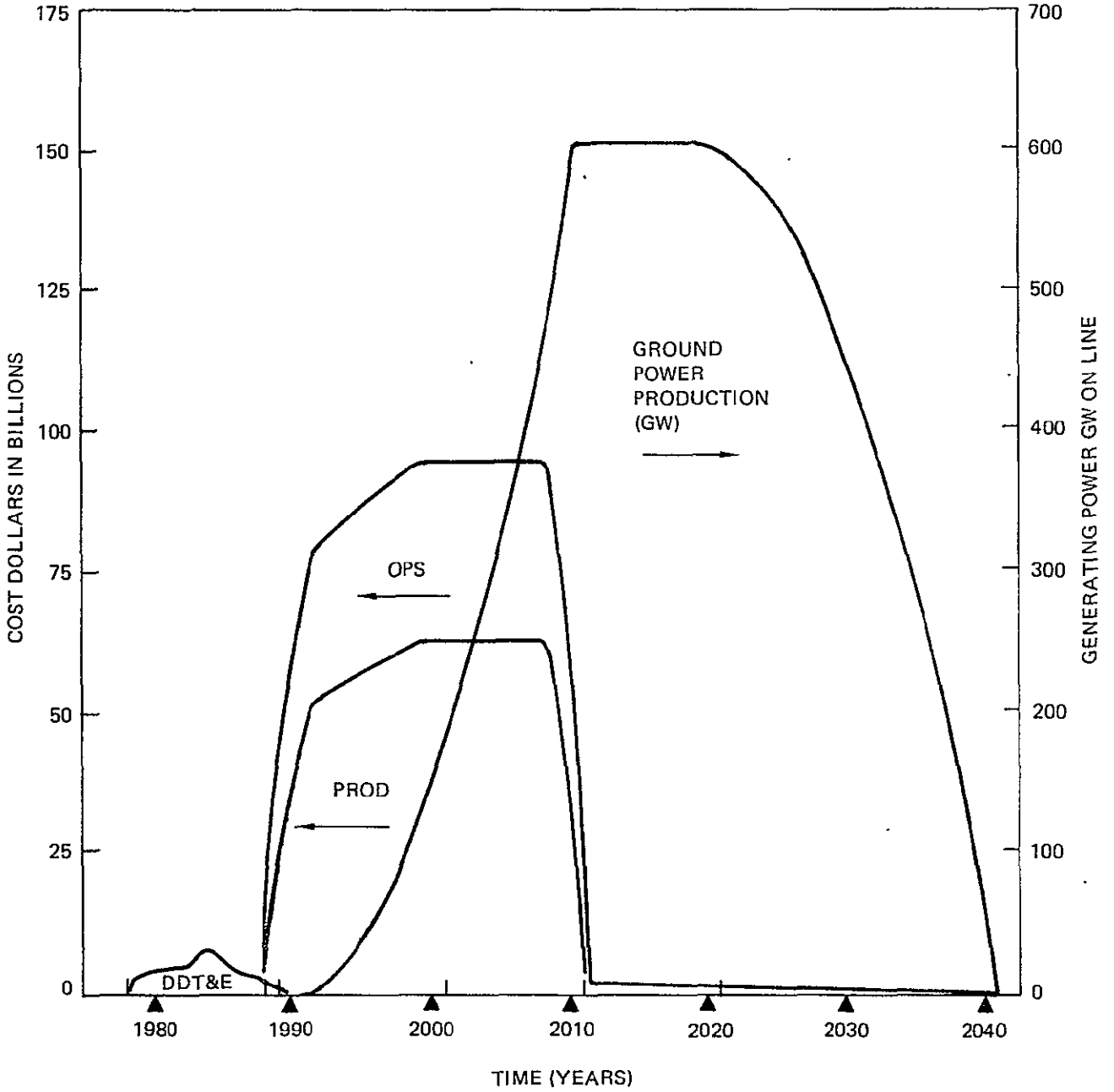

FIGURE 7-25 FUNDING DISTRIBUTION THERMIONIC DIRECT RADIATION COOLED

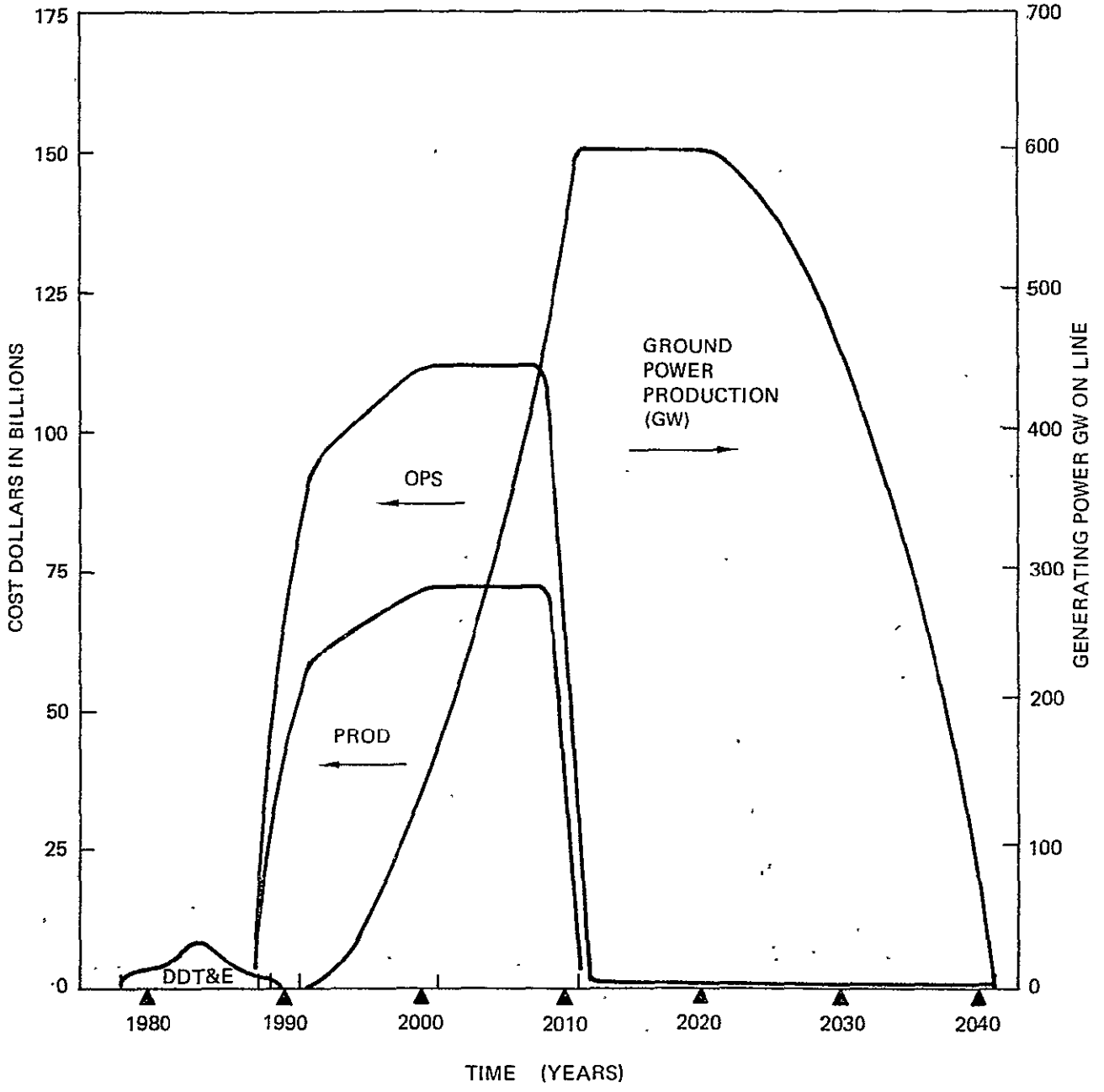

FIGURE 7-26 FUNDING DISTRIBUTION THERMIONIC LIQUID COOLED

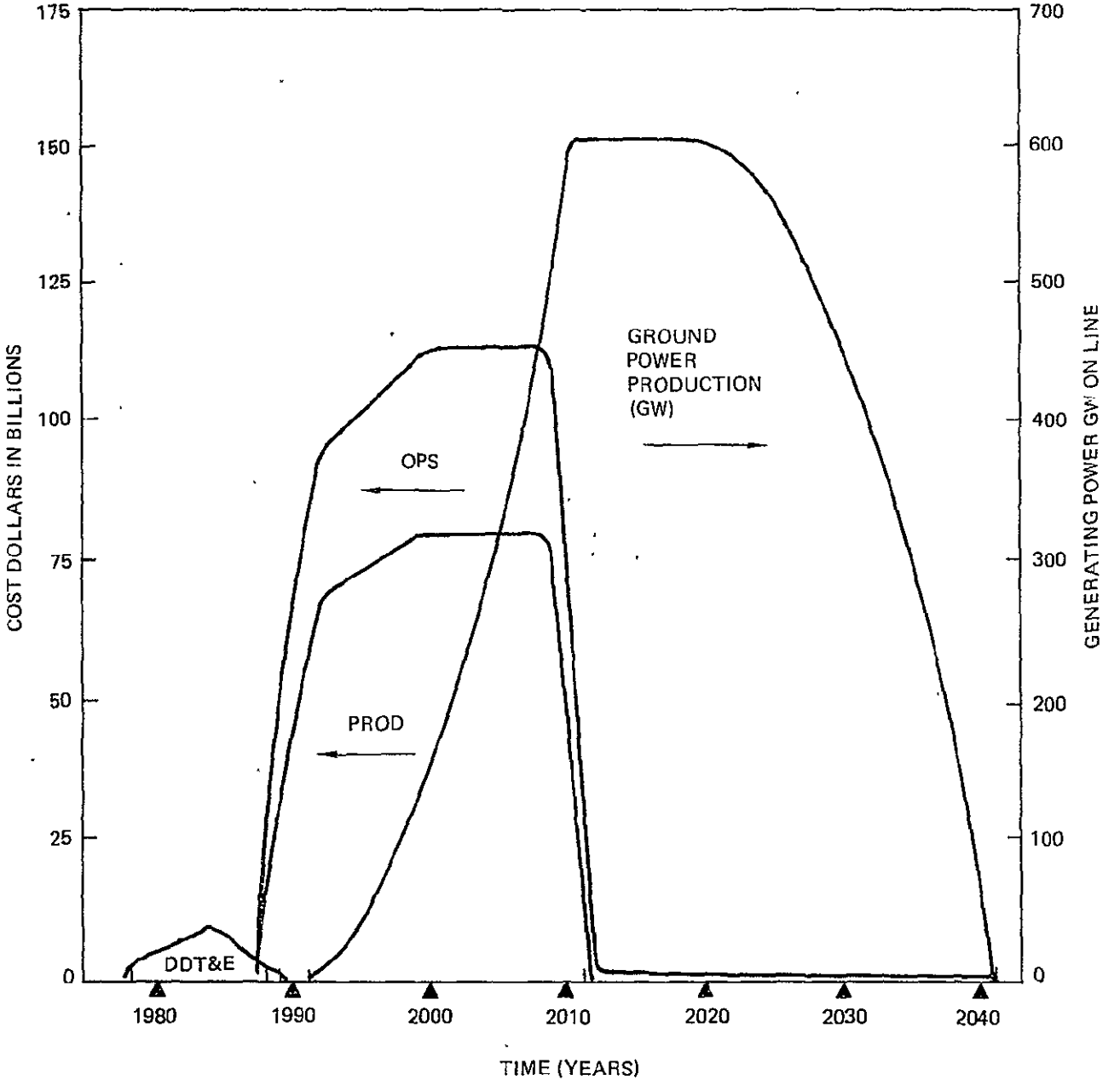

FIGURE 7-27 FUNDING DISTRIBUTION BRAYTON

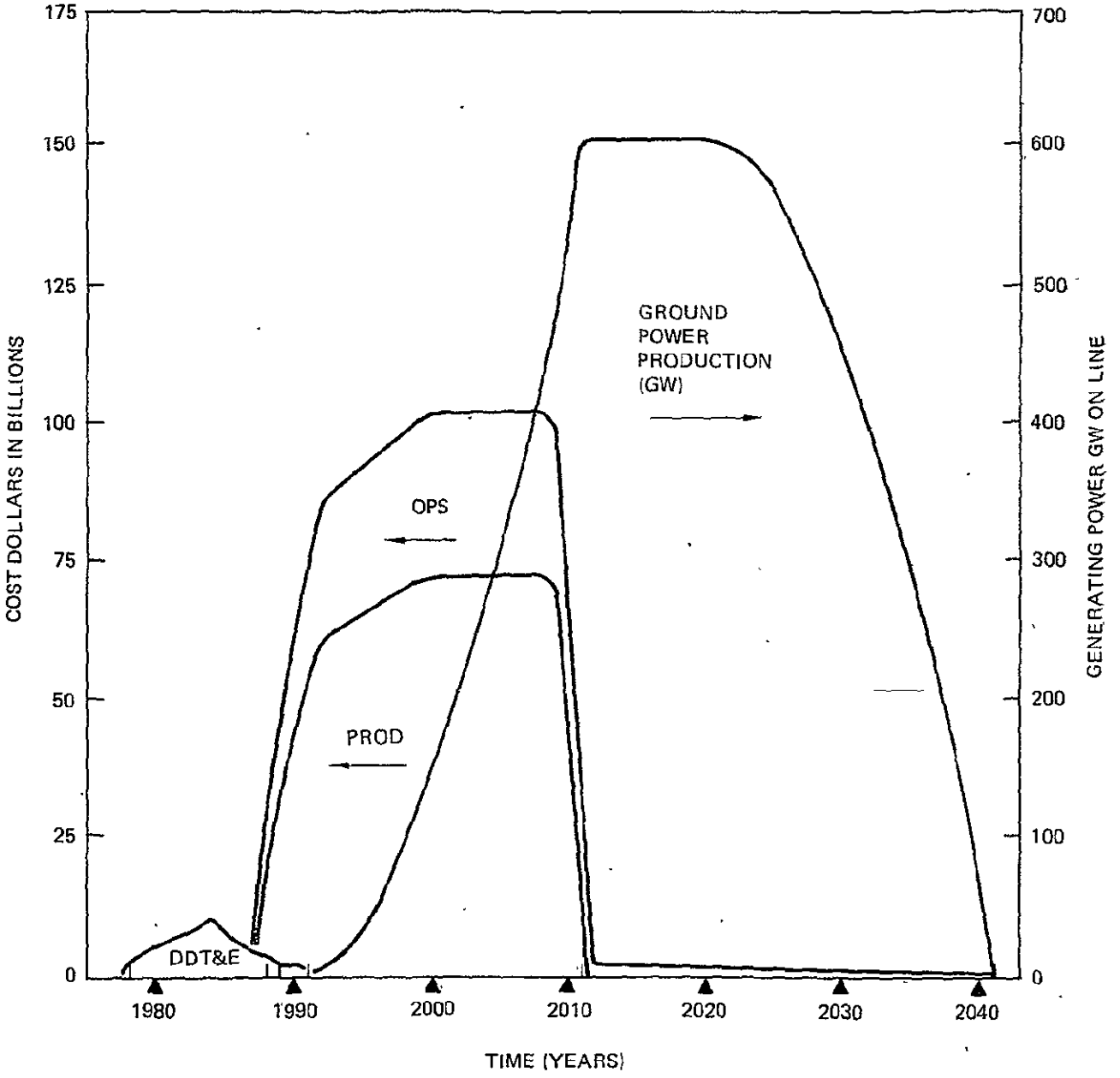

FIGURE 7-28 FUNDING DISTRIBUTION THERMIONIC BRAYTON

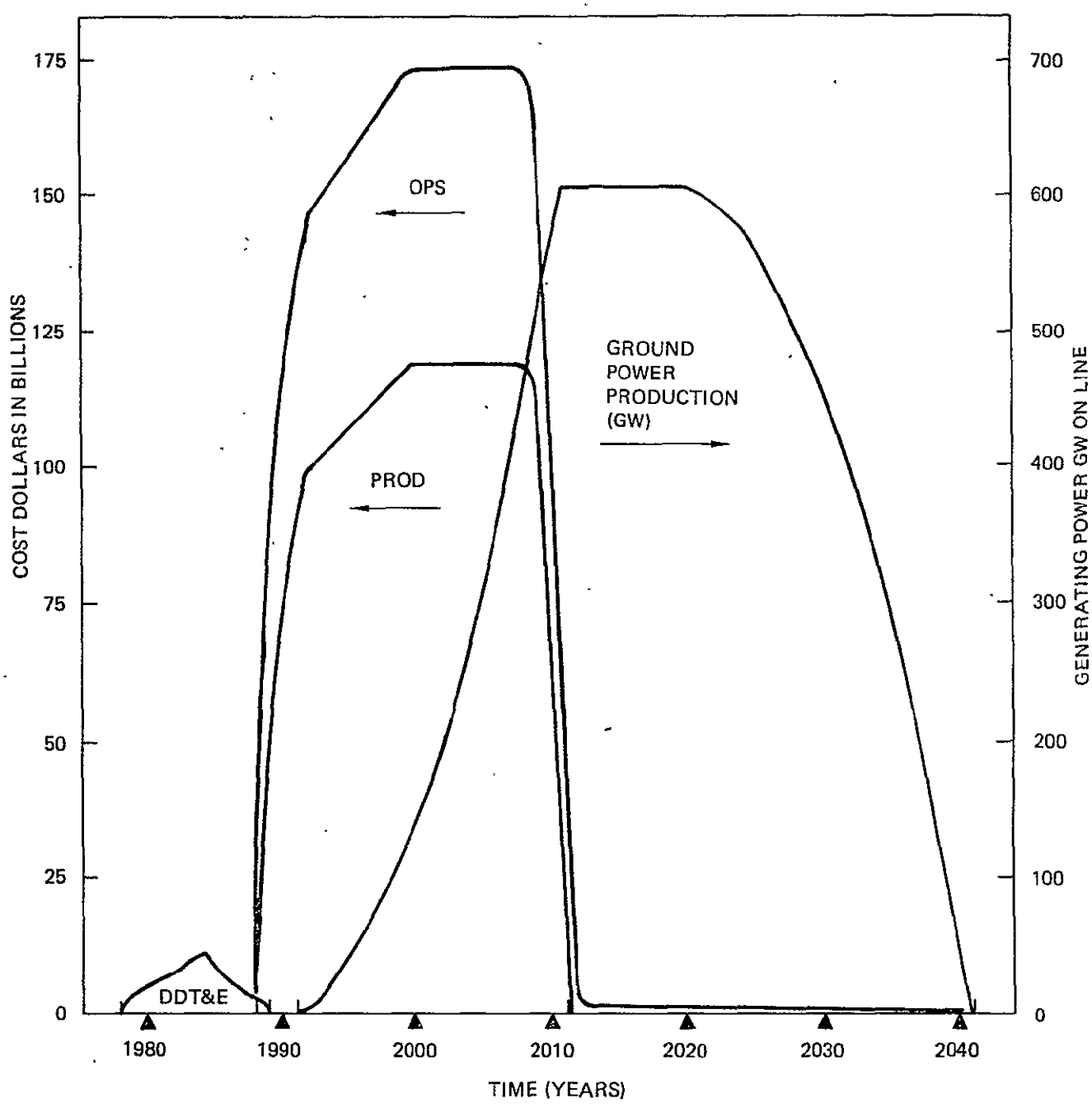

FIGURE 7-29 FUNDING DISTRIBUTION NUCLEAR BRAYTON

7.7.2 NET PRESENT VALUE ANALYSIS

This section contains a zero net present value summary on each of the five power systems. The method of analysis is to establish the present value of the system's costs, and then determine the value each KW-HR of ground available output must have to give the same present value. Summing the equal cost debits and generated power credits results in a zero net present value.

The process of analysis uses the cost-time spreads and power output-time spread of Section 7.1. A present value for each year's costs is calculated using the following formula:

$$p = \frac{f}{(1+i)^n}$$

where p = present value

f = future value

i = interest rate - compound

n = time periods - years

This results in 64 present values from 1978 through 2041. The present values are all summed to establish the system present value. All present values are stated as of 1 January 1976.

Present value for power output is established in the same manner, except that a cost rate must first be assumed. By trial and error the cost rate is adjusted until the power output has the same present value as the system costs. The final cost rate becomes the present value cost per KW-HR.

Two present value cases representing two interest rates are calculated - 0% and 7.5%. A power output efficiency factor of 95% is used to allow for occultation and maintenance. The results are shown in Table 7-53 The 0% case is a baseline assuming not time value of money. The 7.5% case represents a possible cost of money for this project. It should be noted that 7.5% is calculated on constant 1976 dollars whereas a typical realtime rate in a 8% per year inflation would be 15.5%. The results of Table 7-53 are used for system comparison in Section 7.1.

TABLE 7-53 NET PRESENT VALUE CALCULATIONS

	7.5% INTEREST RATE			
	SYSTEM PRESENT VALUE 1 Jan 1976	DDT&E PRESENT VALUE 1 Jan 1976	% DDT&E	COST PER KW-HR
Thermionic DRC	$ 366,259 x 10^6	$26,929 x 10^6	7.4	.0447
Thermionic LC	$ 431,625 x 10^6	$30,771 x 10^6	7.1	.0527
Brayton	$ 440,908 x 10^6	$35,078 x 10^6	8.0	.0539
Thermionic Brayton	$ 399,115 x 10^6	$33,564 x 10^6	8.4	.0488
Nuclear Brayton	$ 664,507 x 10^6	$42,183 x 10^6	6.3	.0811

	0% INTEREST RATE			
	SYSTEM PRESENT VALUE 1 Jan 1976	DDT&E PRESENT VALUE 1 Jan 1976	% DDT&E	COST PER KW-HR
Thermionic DRC	$1,955,350 x 10^6	$44,250 x 10^6	2.3	.0129
Thermionic LC	$2,304,820 x 10^6	$51,100 x 10^6	2.2	.0152
Brayton	$2,340,210 x 10^6	$58,780 x 10^6	2.5	.0155
Thermionic Brayton	$2,113,270 x 10^6	$56,050 x 10^6	2.7	.0140
Nuclear Brayton	$3,558,510 x 10^6	$71,450 x 10^6	2.0	.0235

APPENDICES

CONTENTS:

APPENDIX I

PCM MODEL

PARAMETRIC COST MODEL
(PCM)

THIS MODEL PREDICTS AEROSPACE PROGRAM COST IN TERMS OF BOEING'S FUNCTIONAL ORGANIZATION STRUCTURE. THE MODEL IS BASED ON MANHOUR AND COST HISTORY FROM BOEING AEROSPACE HARDWARE DEVELOPMENT AND PRODUCTION PROGRAMS.

NOTE: This model is computerized and running- See PCM Users Manual to make computerized estimates - Contact Steve Otrosa for further information.

BOEING AEROSPACE COMPANY

JUNE 1975

ECONOMETHODS GROUP

STEVE OTROSA, TEAM LEADER

TABLE OF CONTENTS

INTRODUCTION

This cost model predicts the cost of Aerospace programs from a set of preliminary physical or performance inputs. The model's working units are manhours. They are converted to dollars using rates and factors for any time period desired.

Boeing historical manhour data collected in the Estimating Information System (EIS) data bank provides the raw information from which functional Manhour Estimating Relationships (MERS) are formed. These "MERS" relate program inputs to the model's internal working logic. Each major functional area (e.g., project engineering, developmental shop, etc.), making up Boeing's organizational mix, is represented and interrelated in the model. These functional areas are ultimately expressed in terms of required manhours to fulfill the objectives of the program.

This model takes the form of a family of models in that certain elements are changed to predict cost of different types of Aerospace programs. The models in the family cover:

PCM (LV-A)	Launch Vehicle
PCM (LASER)	Laser Weapons
PCM (TUG)	Space Tugs (OTV & LTV)
PCM (SAT-A)	Spacecraft
PCM (BOAT)	Boats
PCM (MISIL)	Missiles
PCM (TANK)	Tracked Vehicles

TABLE A-1 compares "PCM" to three other estimating models to highlight its features. The capability to handle the cost effects of "off the shelf hardware" and the cost effect of using existing designs with various levels of modification are particularly noteworthy. These features reflect the drive to employ the maximum amount of off the shelf hardware (or mods of existing designs) to new programs to minimize the costs of space hardware.

TABLE A-1 COST MODEL COMPARISONS

Feature/parameter	Boeing PCM	Aerospace	Econo-metrics	KOELLE
Working units	Manhours	Dollars	Dollars	Manhours
Level of hardware manhour/ cost visibility	Subsystem	Subsystem	Subsystem	System*
Level of manhour/cost element visibility				
Total DDT&E	Yes	Yes	No	Yes
First unit	Yes	Yes	Yes	Yes
System engineering	Yes	Yes	No	No
System test	Yes	Yes	No	No
Software engineering	Yes	No	No	No
Quality control	Yes	No	No	No
Assembly and checkout	Yes	Yes	No	No
Factory labor	Yes	No	No	No
Tooling	Yes	Yes	No	No
Design engineering	Yes	No	No	No
Developmental shop	Yes	No	No	No
Management	Yes	Yes	No	No
Support equipment	Yes	Yes	No	No
Facility workload	No	No	No	Yes
Length of prog effects	No	No	No	Yes
Off-the-shelf hardware effect	Yes	Limited	No	No
Existing design modification effect	Yes	Limited	No	No

*With the exception of one subsystem area; i.e., liquid rocket engines

1. The working units of the cost model are manhours; resulting costs are displayed in 1976 dollars.

2. Manhours are converted to dollars using current Boeing direct and indirect labor and material rates and factors.

3. Model is based upon a detailed breakout of all functional organization effort contributing to space programs in which Boeing has participated.

4. No direct attempt is made to adjust these data to represent future technology. However, the model does reflect discrete levels of design sophistication.

5. Ground support equipment is considered to be a specialized design to support the unique vehicle hardware. It does not require the use of converted factory support equipment or use of generalized support equipment.

6. The value of tooling depends upon production run rates and total number of vehicles produced.

7. Program management includes the contractors effort only. NASA program management is not included.

8. Spares are valued as a percentage of production hardware.

9. No fee is included.

FIGURE A-1 COSTING GROUND RULES AND ASSUMPTIONS

WBS/COST MATRIX

THE TWO FOLLOWING TABLES ILLUSTRATE TWO WBS/COST MATRICES THAT CAN BE ASSEMBLED FROM PCM OUTPUT.

TABLE A-2 WBS/COST MATRIX

Cost element	DDT&E cost	First unit	Prod cost	Ops cost	Life cycle cost
Program management	x	x	x	x	x
Systems engineering and integration	x				x
Flight hardware					
Structure and mechanism	x	x	x		x
Avionics	x	x	x		x
Electrical power	x	x	x		x
Main engines	x	x	x		x
Prop plumbing	x	x	x		x
Retro rockets	x	x	x		x
Reaction control	x	x	x		x
Assembly and checkout		x	x		x
Systems test engineering	x				x
Systems test hardware	x				x
Flight test program	x				x
GSE	x		x		x
Tooling	x		x		x
Facilities					
Manufacturing	x				x
Systems test	x				x
Launch	x				x
Mission control	x				x
Recovery	x				x
Operations					
Launch				x	x
Flight				x	x
Recovery				x	x
Spares				x	x
Propellant				x	x

10-15-75

TABLE A-3 FSTSA WBS/COST MATRIX

CASE: LO_2/LH_2 Single Stage OTV

COST ELEMENT	DOLLARS IN MILLIONS DDT&E	FIRST UNIT
FLIGHT HARDWARE	(251.118)	(32.384)
STRUCTURES & MECHANISMS	12.568	4.084
MAIN PROPULSION [1]	206.938	6.645
AUXILIARY PROPULSION	9.667	3.630
AVIONICS	11.070	10.346
ELECTRICAL POWER	4.078	2.813
THERMAL CONTROL	6.797	3.768
ASSEMBLY AND CHECKOUT		1.098
SYSTEMS ENGINEERING & INTEGRATION	(6.035)	
SOFTWARE ENGINEERING	(4.874)	
SYSTEMS TESTING	(139.746)	
GROUND TEST HARDWARE	80.959	
FLIGHT TEST HARDWARE	48.575	
TEST LABOR	10.212	
GROUND SUPPORT EQUIPMENT	(10.644)	
INITIAL TOOLING	(1.278)	
PROGRAM MANAGEMENT	(24.822)	(1.943)
SUBTOTAL	438.517	34.327
COST EQUIVALENT OF MASS CONTINGENCY		
TOTAL		

[1] DDT&E
ENGINE 200M
Non Eng 6.938M
1st UNIT
ENGINE 6M
Non Eng .645M

BOEING

COST ELEMENT DEFINITIONS

PROGRAM MANAGEMENT - This element includes that effort relating to the technical and business management of the program. It includes the contractor effort of directing and assuring that approved plans are implemented by the responsible organizations; and controlling the program in a cost-effective and technically excellent manner.

Specific areas of effort are:

Planning and Controls
Finance Management
Configuration Management
Data Management
Facility Coordination
Personnel Training and Certification

SYSTEM ENGINEERING AND INTEGRATION - This element includes the activities directed at assuring a totally integrated engineering effort. It includes the effort to establish system, subsystem, GSE and Test requirements and criteria, to define and integrate technical interfaces to optimize total system definition and design, to allocate performance parameters to the subsystem level, to identify, define and control interface requirements between system elements, to monitor design and equipment to determine CEI compliance, to provide and maintain inertial properties analyses, support and documentation, to develop and maintain system specification to provide parts, standards and materials and processes surveillance and to integrate product assurance activities. Fundamental to this WBS element is the documentation of system-level design requirements as derived from NASA-established requirements and guidelines and through functional analyses.

Specific areas of effort are:

System Design and Integration
Configuration
Flight Hardware Requirements
Operations Requirements
GSE Requirements
System Test Requirements
Mass Properties
Interfaces
Materials, Processes, and Standards
Product Assurance
Service and Maintenance Requirements

SOFTWARE - This element includes the costs of the design, development, production, checkout, maintenance and delivery of computer software. Included are test, on-board and mission or flight software.

GSE - This element includes the costs to design, develop, fabricate, assemble, test, and deliver all ground support equipment. Also included under GSE are mockups and simulators where required. Cost of development of test procedures and reports associated with the acceptance and qualification of GSE are included

FLIGHT HARDWARE - This element includes the costs to design, develop, fabricate, assemble, and test all flight article subsystems, the assembly of these subsystems and the test and checkout of the flight article. Included are the costs associated with all test procedures and reports preparation and the Quality Control inspection effort. Also included are costs of operation/test-unique support equipment (including factory support and special test equipment), and the cost of handling and transportation of items between operation/test locations.

GROUND TEST HARDWARE - This element includes the cost of engineering liaison, fabrication, assembly and test of ground test hardware. Ground test hardware includes the static, dynamic, thermal and firing (if required) test articles.

Excluded are engineering subsystem design effort

FLIGHT TEST HARDWARE - Includes the fabrication, assembly and checkout of the flight test vehicle(s) including spares to support the test.

SYSTEMS TEST - Manpower to conduct the ground and flight tests.

TOOLING - Includes (a) initial and (b) production (if required) tooling jigs and fixtures. Initial tooling is that needed to fabricate and assemble the test hardware and first unit. This is "soft" tooling. Production tooling is "hard" tooling designed for repetitive use in fabricating and assembling recurring production units. Production tooling includes sustaining and replenishment tooling.

SPARES - This element includes the costs of developing and documenting requirements for, and the fabrication, assembly, test, storage, delivery, and accountability of spare components, assemblies, or subsystems to be used as test production or mission support spares. Also included is the cost of refurbishment of test spares to a flight hardware configuration. Excluded are production spares, such as fasteners, electronic parts, etc. Included within this element is the cost of developing an inventory-control documentation system and the costs of shipping and distribution of spares to maintain designated inventory levels.

DDT&E (NON-REDURRING COST) - Consists of the "one-time" cost of designing, developing, testing, and evaluating an item. Specifically it includes; development engineering and development support, major test hardware, captive and ground test, flight test, ground support equipment, tooling and special test equipment; manufacturing, test, mission control or launch site activation (if required), initial spares and other program peculiar costs not associated with repetitive production.

FIRST UNIT COST (RECURRING COST) - This is the first production configured flight or mission article in a hardware production program. If there is only

one designated flight or mission article in the program, this would be called the first unit as differentiated from any developmental hardware such as a prototype. First unit cost is that cost associated with producing the first flight or mission article through acceptance of the hardware by the government and includes all costs associated with: (1) the fabrication, assembly and checkout of flight or mission hardware, (2) ground test and factory checkout of flight or mission hardware

NOTE: Initial spares are priced in DDT&E and cover the support of the first unit; additional spares would be a function of a production program for the vehicle and would be included in recurring production costs for spares. Maintenance of tooling and special test equipment would also be part of production recurring costs.

ESTIMATING FLOW DIAGRAM

Figures A-2 and A-3 illustrate the working relationships between functional cost elements which make up the logic of the model. These relationships mirror the actual approach used to develop and produce technically advanc d hardware.

Using Boeing history to quantify these relationships allows the development of a cost prediction model that is comprehensive and accountable at any level in the models logic or the program's WBS estimating level. The model has the additional benefit of providing visibility at the organizational level to allow cost target allocation.

This model has two major working subprograms as portrayed in Figures A-2 and A-3; DDT&E cost development and first unit production cost. Together these two programs develop the cost of a program's principle hardware items. Facilities Operations and Program Management costs are calculated separately. Production phase costs are based on first unit cost, inventory quantities and appropriate learning curves.

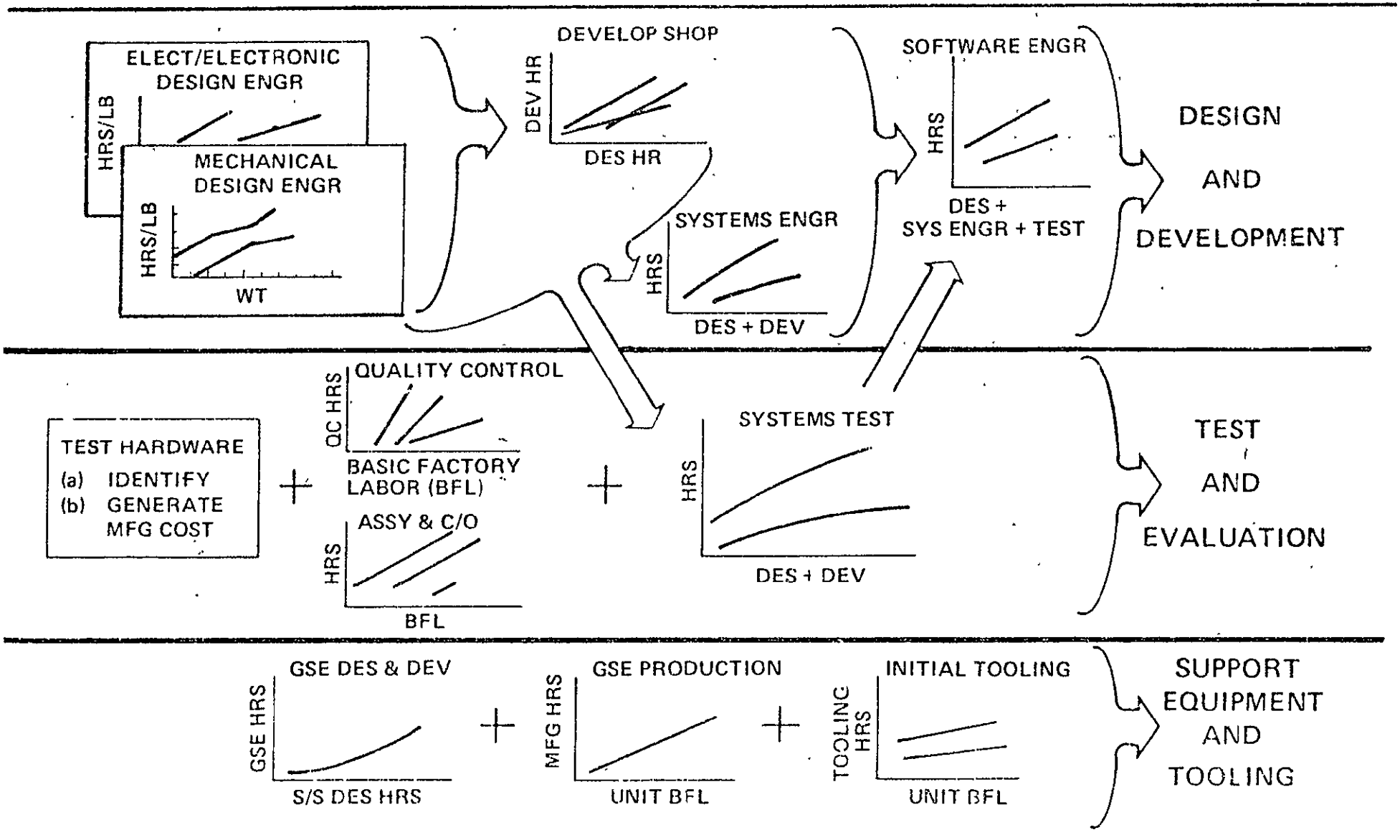

FIGURE A-2 BOEING PCM METHODOLOGY DDT&E

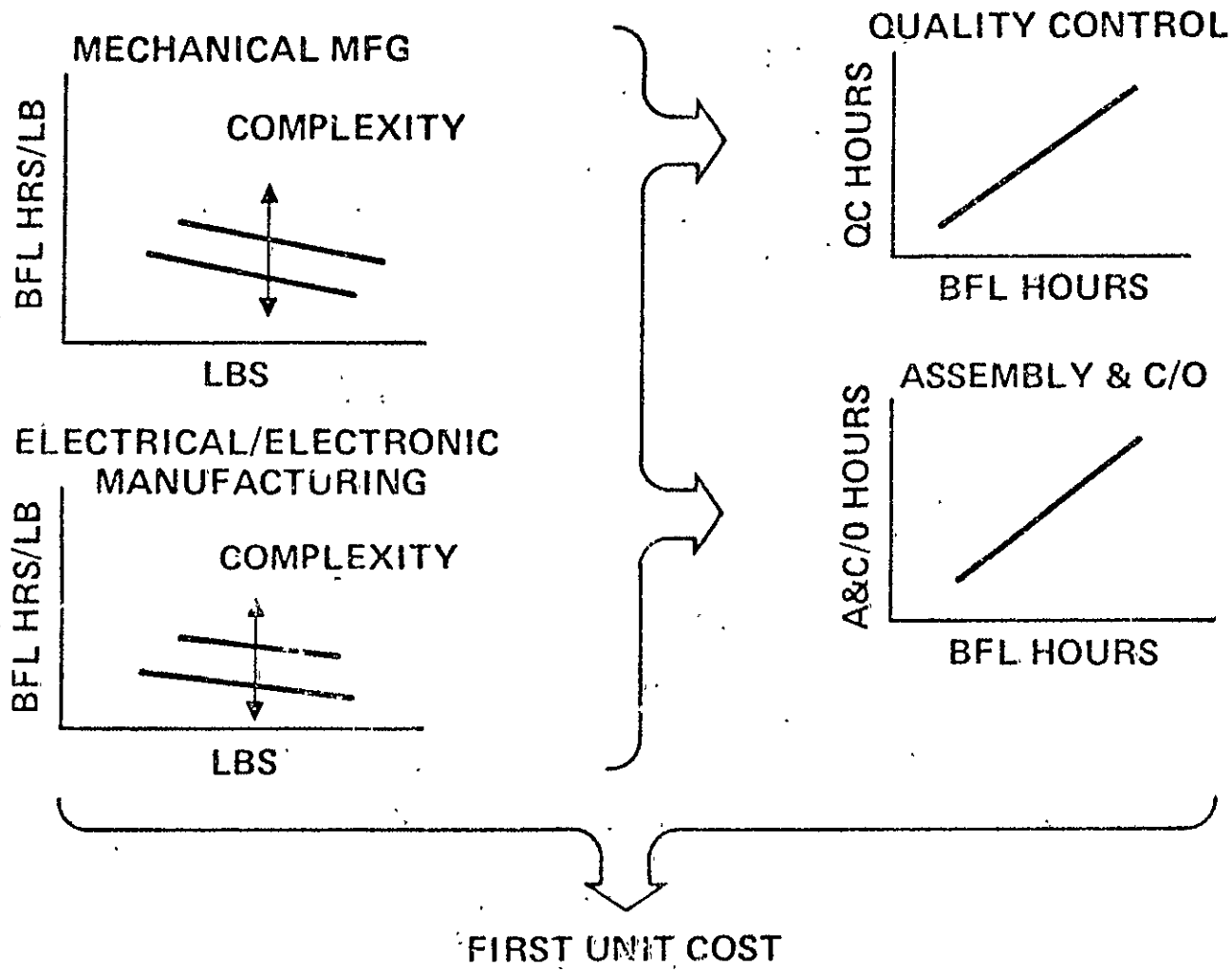

FIGURE A-3 BOEING PCM METHODOLOGY
FIRST UNIT COST

MODEL ESTIMATING LOGIC

This section illustrates in detail the estimating logic for the hardware, associated facilities support, production hardware operations and program management.

(a) Mechanical - By Subsystem

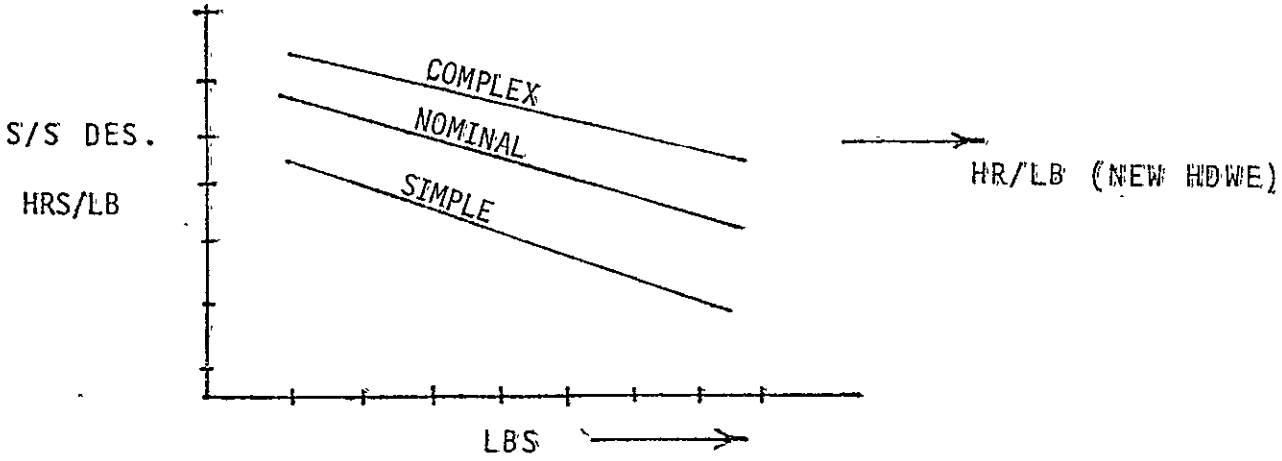

Hr/LB $[1-(MOD \times F)]$ $[(1-OTS)]$ → DES. Hr/# (This Hdwe)

DES. Hr x $/Hr. ⟶ Des. Engr. Labor $

(b) Electrical - by Subsystem

(Same as above but use electrical estimating graph).

OTS = % of off the shelf hardware expressed as decimal.
MOD = % of mod hdwe.
F = Complexity of mod.

FIGURE A-4 PARAMETRIC COST MODEL LOGIC DDT&E DESIGN ENGINEERING

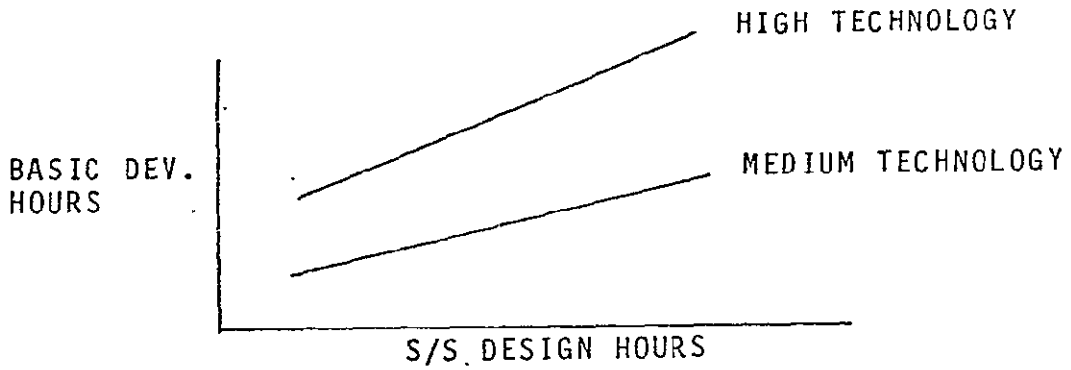

(a) Basic dev. hr. x factor x $/Hr ⟶ Dev. $

(b) Basic Hr x $/Hr ⟶ Dev. mat'l $

FIGURE A-5 DEVELOPMENTAL SHOP

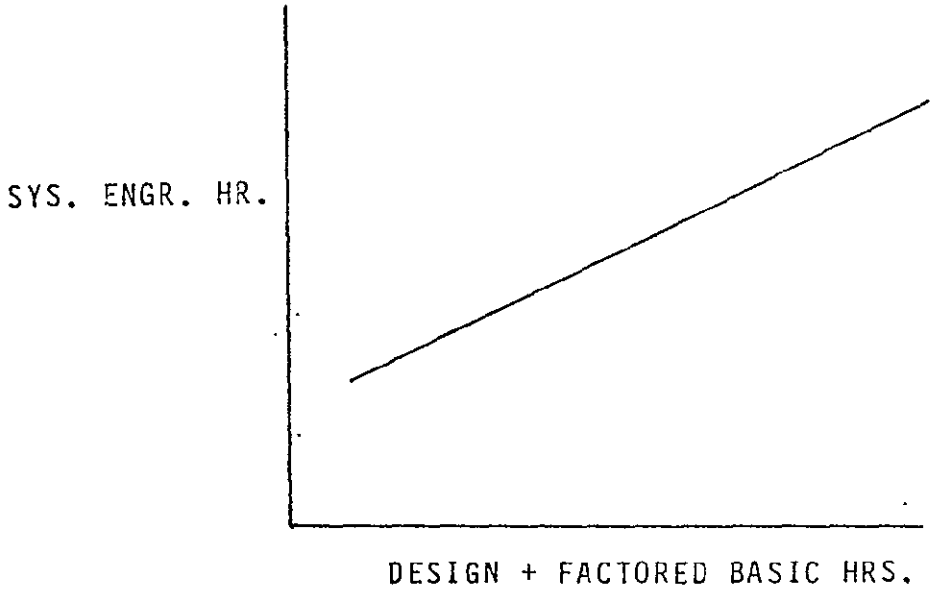

FIGURE A-6 SYSTEM ENGINEERING AND INTEGRATION

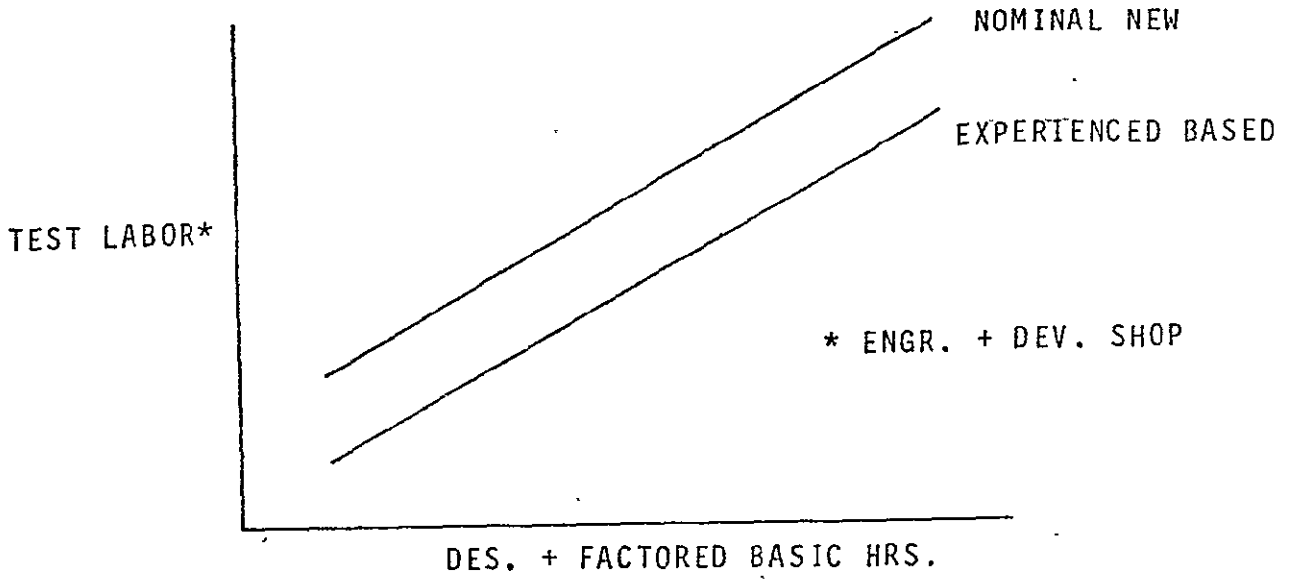

FIGURE A-7 SYSTEMS TEST

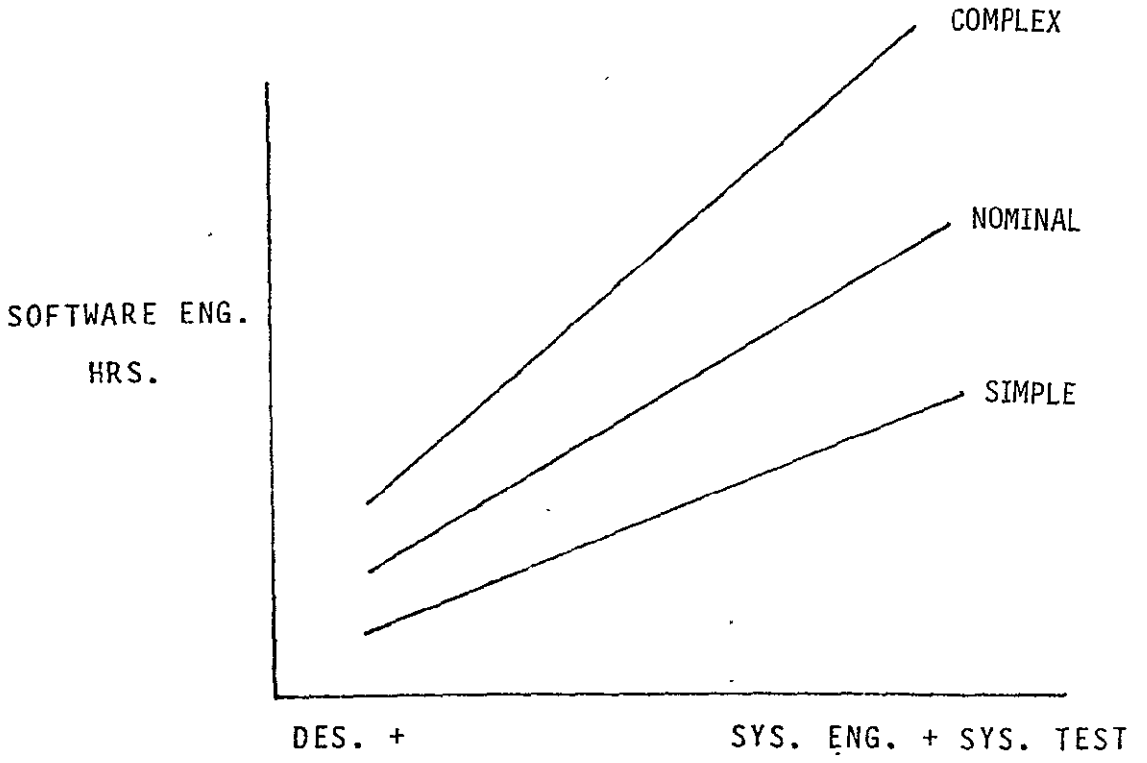

FIGURE A-8 SOFTWARE ENGINEERING

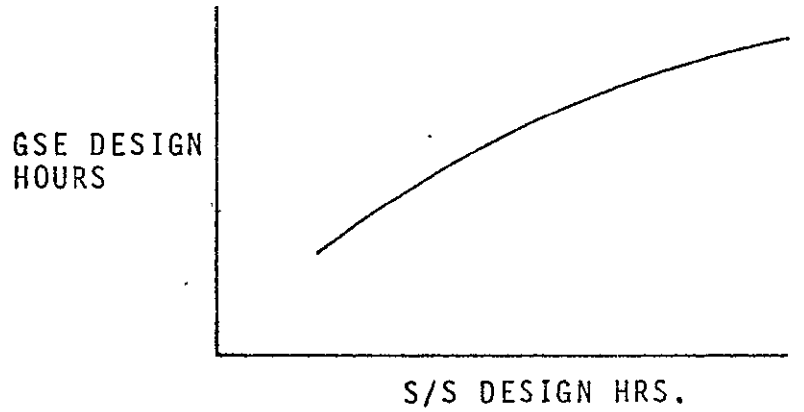

(a) GSE Design Hours x 1.26 [1] → Des. & Dev. Shop Hrs (factor

(b) Design & Dev. Shop Hour x $/Hr.* → GSE Des & Dev. $

FIGURE A-9 GSE DESIGN AND DEVELOPMENT

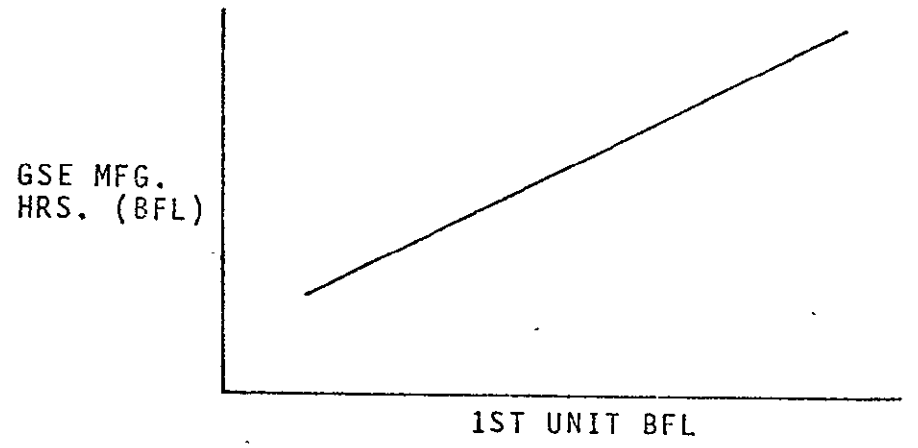

(a) GSE Mfg. Hrs x 2.0 [2] → GSE DFL (including QC)

(b) GSE DFL x $/Hr* → GSE $

*Rate includes material.

[1] Includes ratio for basic dev. and dev. factor.

[2] Includes ratio for labor factor (1.8) and QC (.2)

FIGURE A-10 GSE MFG. (FIRST SET)

SYS. TEST HARDWARE

(a) Identify hdwe & weights.

(b) Use unit cost estimating curves.

QUALITY CONTROL

(a) Developmental Shop QC

(b) System test hdwe QC

QC Hr. x $/Hr ⟶ QC $

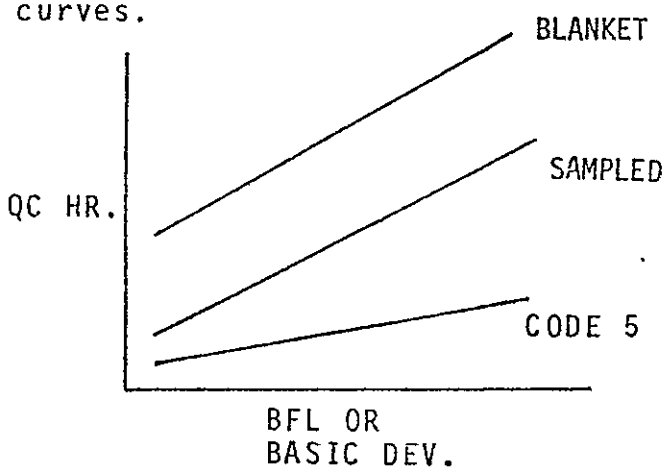

FIGURE A-11

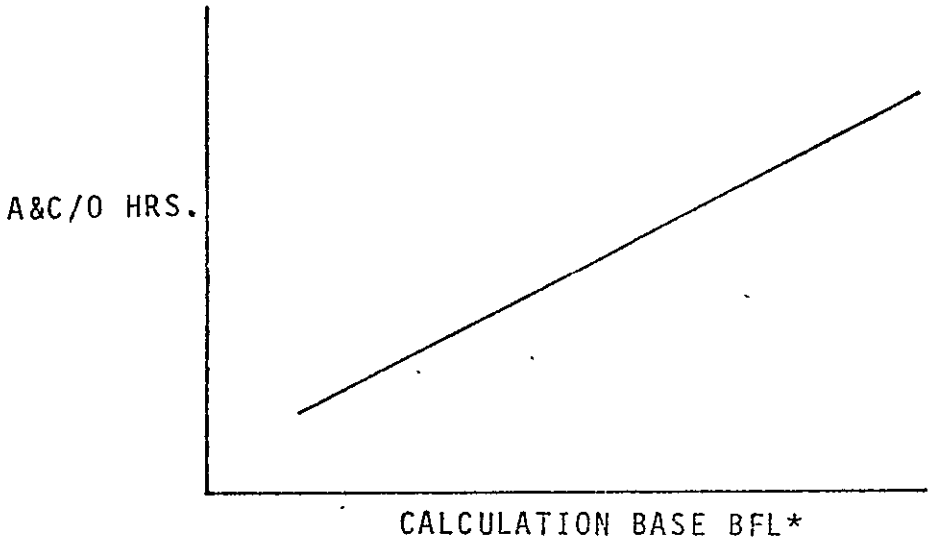

*Calculation base BFL is an input from first unit production ERs covered in the Production section.

FIGURE A-12 TEST HARDWARE ASSEMBLY AND C/O

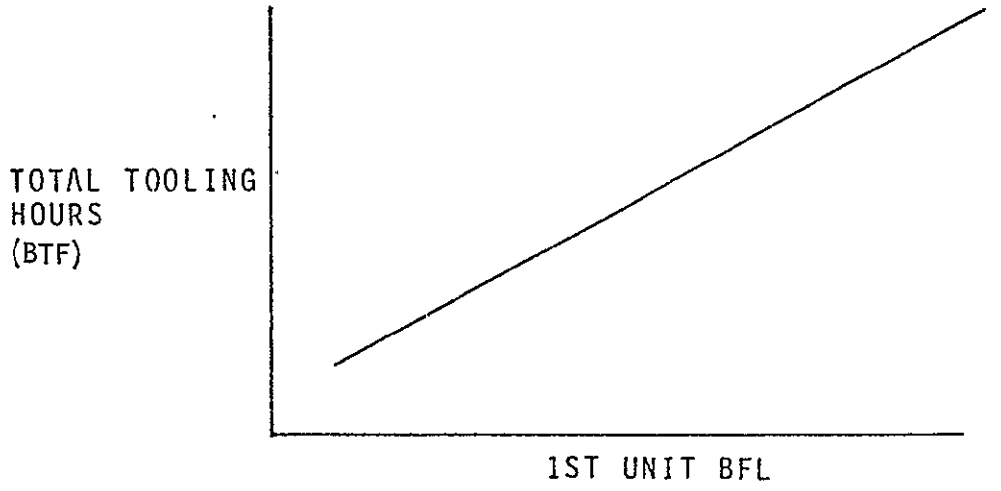

(a) Total tooling hrs. → x $/Hr* → Tooling Labor $
→ X 2.0**

*Includes Mat'l factor.

**BTF TO DTF FACTOR

This yields soft tooling dollars, for hard tooling factor by 1

FIGURE A-13 TOOLING

First Unit Mechanical MFG. Hours - By Subsystem

(a) Labor

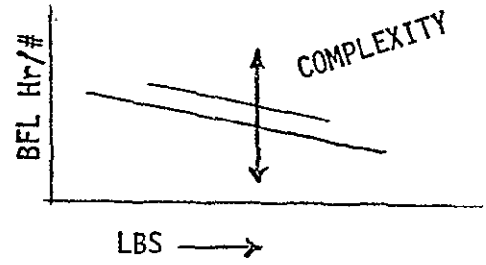

BFL Hrs (1-OTSF) = New BFL

BFL Hrs (OTSF) = OTS Hrs

OTS Hrs x .6* = CURRENT OTS HRS

NEW BFL + CURRENT OTS HRS = CALCULATION BASE BFL

CALCULATION BASE X LABOR FACTOR X $/HR → LABOR $

(NEW BFL + OTS HRS) X $/HR → MATERIAL $

FIGURE A-14 PRODUCTION

(a) Labor

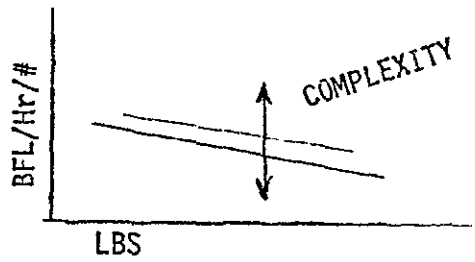

BFL Hrs (1-OTSF) = New BFL

BFL Hrs (OTSF) = OTS Hrs

OTS HRS x .6 = CURRENT OTS HOURS

NEW BFL + CURRENT OTS → CALCULATION BASE

CALCULATION BASE X LABOR FACTOR X $/HR → ELECT. LABOR $

(b) MATERIAL

(NEW BFL + OTS HRS) X $/HR → MATERIAL $

OTSF= OFF THE SHELF FACTOR; % off the shelf expressed as decimal
OTS= OFF THE SHELF
BFL= BASIC FACTORY LABOR

* 30th UNIT (λ = 90)

FIGURE A-15 ELECTRICAL MFG - BY SUBSYSTEM

A = BFL (1-OTS) + BFL(OTS)6 → CAL. BASE HRS

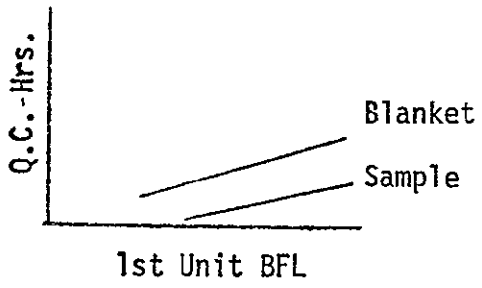

Q.C. Hr x $/Hr → Q.C. $

FIGURE A-16 QUALITY CONTROL

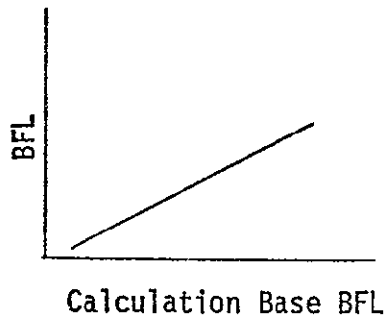

Spares

% of Flight Hardware (Depends on spare philosophy - 3 - 12%)

Program Management

% of Total Cost (6-10%)

FIGURE A-17 ASSEMBLY AND C/O

INPUTS/OUTPUTS

OUTPUTS from PCM take the form of a WBS/Cost Matrix. This type of format summarizes cost information in a form easily used "as is" or for analysis. Additionally, manhour data is available at the functional level.

INPUTS can be physical values such as subsystem weights, or performance parameters such as rocket engine thrust. Inputs can also be "thru puts" if the cost of a subsystem element is known (such as the unit cost of an existing engine). It can be input directly and will be then included into the total cost and placed in its proper place in the WBS.

The following are examples of inputs and outputs.

PCM COST MODEL INPUTS

A. GLOBAL INPUTS

PROGRAM (PROJECT) TITLE:_____

(1) Estimate is in what year dollars?_____, Follow on years excalation ____% per y

(2) PRODUCTION QUANTITIES: (See Following pages for details on major elements)

	Major Element 1		Major Element 2		Major Element 3		Major Element 4	
NAME								
	Qty.	Learning Curve%	Qty.	Learning Curve %	Qty.	Learning Curve %	Qty.	Learning Curve %
Category 1 Items (GENERATED)								
Category 2 Items (KNOWN VALUE)								

(3) Tooling, GSE & Spares:

Sets of Prod. Tooling _____

Sets of GSE Needed _____

Initial Spares % _____

(4) Test Hardware:

	ELM'T 1	ELM'T 2	ELM'T 3	ELM'T 4
Ground Test Units	_____	_____	_____	_____
Flight Test Units	←———	(———)	———	———→

(5) Thru-Put Information:

DDT&E

Line No. _____, Value _____($M)

Line No. _____, Value _____($M)

Line No. _____, Value _____($M)

Production

Line No. _____, Value _____($M)

Line No. _____, Value _____($M)

Line No. _____, Value _____($M)

Facilities (See Facilities Estimates)

Line No. _____, Value _____($M)

Operations (See Operations Estimates)

Line No. _____, Value _____($M)

Line No. _____, Value _____($M)

FIGURE A-18

B. MAJOR ELEMENT INPUTS (ONE PAGE FOR EACH ELEMENT) FILE NO._____

This major element name:_____

(1) HARDWARE DESCRIPTION:

ITEM	VALUE (LBS OR THRUST)	MOD. %	MOD* FACTOR	OTS %
M1 MECHANISMS				
M2 REACTION CONTROL				
M3 LOX/RP ENGINE				
M4 SOLID ROCKET MOTOR				
M5 MACHINERY				
M6 COMPLEX STRUCTURES				
M7 NOMINAL STRUCTURES				
M8 SIMPLE STRUCTURES				
M9 THERMAL CONTROL				
MO LOX/LH_2 ENGINE				
E1 HI-PERF. COMPUTER				
E2 MED. PERF COMPUTER				
E3 G&N				
E6 COMPLEX AVIONICS				
E7 SIMPLE AVIONICS				
E9 BAT. POWER SYS				
EO SWITCHING & REQ				

* (SIMPLE = .8, NOMINAL = .5, COMPLEX = .2)

(2) FUNCTIONAL CODES (ENTER C, M OR S)

Developmental Support _____, SE&I _____,
Systems Test _____, Software Engr. _____,
GSE Design _____, Dev. Q.C. _____,
Mfg. Q.C. _____, Tooling _____,
Assembly & C/O _____, GSE Mfg. _____

CMPX = _____

(3) CATEGORY 2 ITEMS, PRODUCTION KNOWN VALUE

_____ OR _____ _____
VALUE VALUE START POST

FIGURE A-18 CONTINUED

TABLE A-4 COST INPUT--LAUNCH VEHICLE CHARACTERISTICS

CONFIGURATION: 165 S I-W-OC II-W-OH

PERFORMANCE DATA

Σ_{Isp}=340

λ'_I = .867	λ'_{II} = .830	λ'_{III} =
ΔV_I = 10,000	ΔV_{II} = 19,000	ΔV_{III} =
WP_I = 2,575,400	WP_{II} = 965,500	WP_{III} =
WIN_I = 395,100	WIN_{II} = 197,700	WIN_{III} =

LAUNCH WEIGHT = 4,299,000

WEIGHT DATA

	STG I	STG II	STG III
STAGE STRUCTURE	185,600	75,100	
INTERSTAGE STRUCTURE	15,400	—	
~~CLUSTERING~~ SHROUD STRUCTURE	—	5,300	
MAIN TANKS	51,500	23,200	
AVIONICS	2,500	4,200	
MAIN ENGINES	58,300	14,000	
PROPULSION PLUMBING	25,000	13,000	
ELECTRICAL POWER	3,400	5,900	
RETRO ROCKETS	2,800	—	
REACTION CONTROL SYSTEM	4,000	5,600	
OTHER EQUIP. FLUIDS	8,000	2,500	
	38,600	29,300	
TOTAL INERTS	325,100	197,700	
PROPELLANT	2,575,400	965,500	
TOTAL STAGE	2,970,500	1,163,200	

OTHER DATA

	STG I	STG II	STG III
NUMBER OF ENGINES	3	3	
STAGE TYPE	W-OC	W-OH	
THRUST PER ENGINE	1.79×10^6	$.47 \times 10^6$	
DEVELOPMENT STATE	NEW	SSME	

TABLE A-5 DOLLAR 'THRU PUTS'

The following dollar values represent costs received from NASA or other sources and used 'as is' in the model

Item	First unit cost	Learning	Source
SRM	$5.25 M	95%	NASA
SSME	11.26 M	90%	NASA
SRM recovery system	.394 M	97%	NASA
F-1	—	95%	Rocketdyne
ET	10.76	85%	NASA

TABLE A-6 SAMPLE COST OUTPUT

09:44 SPACE PROGRAM
CASE NO. 160, LIQUID 2 STAGE -165K PAYLOAD- 7/YR. 10/02/75

1975 DOLLARS IN MILLIONS

	WBS	RDT&E COSTS	FIRST UNIT COSTS	TOTAL PRODUCTION COSTS	OPERATIONS COSTS	TOTAL LC COSTS
1	HEAVY LIFT LAUNCH VEHICLE	$4,698	$536	$2,035	$768	$7,501
2	PROGRAM MANAGEMENT	$266	$30	$84		$350
3	SYSTEM ENGR. & INTEG.	$88				$88
4	VEHICLE HARDWARE	$1,651	$506	$1,359		$3,010
5	STAGE 1	$1,144	$219	$589		$1,733
6	STAGE 2	$506	$287	$770		$1,276
7	STAGE 3					
8	SYSTEMS TEST ENGR.	$209				$209
9	SYSTEMS TEST HARDWARE	$1,021				$1,021
10	FLIGHT TEST PROGRAM	$975				$975
11	VEHICLE GSE	$162		$475		$637
12	TOOLING	$22		$41		$63
13	FACILITIES	$306				$306
14	MANUFACTURING	$100				$100
15	SYSTEM TEST	$30				$30
16	LAUNCH	$138				$138
17	MISSION CONTROL	$38				$38
18	RECOVERY					
19	OPERATIONS			$76	$768	$844
20	LAUNCH				$480	$480
21	FLIGHT				$120	$120
22	RECOVERY					
23	SPARES			$76	$136	$212
24	PROPELLANT				$32	$32

MANHOUR ESTIMATING RELATIONSHIPS (MER'S)

The following graph is a sample of the estimating relationships used in the cost model. The complete set contains 35 to 40 such relationships for each model in the family.

The complete set is contained in a companion volume and is expanded and modified as new data becomes available.

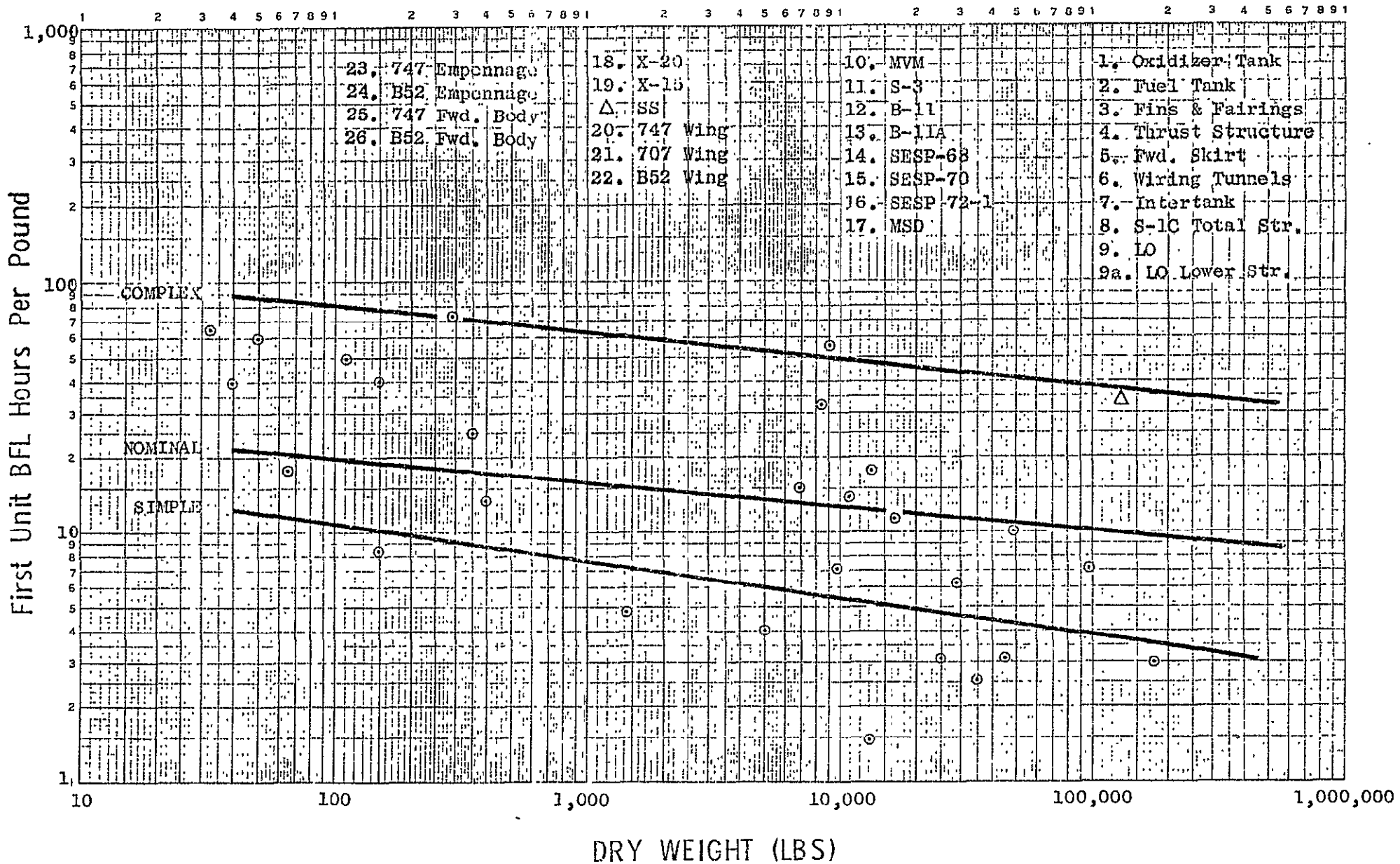

FIGURE A-19 MECHANICAL SUBSYSTEMS - STRUCTURE CATEGORY (BASIC FACTORY LABOR - BFL)

RATES AND FACTORS

The rates and factors used in "PCM" are basically the same as those used in Boeing's "bottom up" pricing. The rates are amalgamated into wrap-around values. Labor factors are composite values for electrical and manufacturing, but do reflect developmental, production or tooling effort.

The rates and factors used are a function of the pricing period. The following are for 1975.

WRAP-AROUND RATES	$/HOUR
Engineering	
Developmental Shop	
Tooling	
Production	
Quality Control	
Developmental Material	
Tooling Material	
Production Material	
Mechanical $	DELETED
Electrical $	

LABOR FACTORS	
Developmental	
Mechanical	%
Electrical	%
Tooling	
Mechanical	%
Electrical	%
Production	
Mechanical	%
Electrical	%

SPECIAL FACTORS

Modification Factor (F)

Simple Mod.	F = 80%
Medium Mod.	F = 50%
Complex Mod.	F = 20%

Off the Shelf Recurring Adjustment

60% of Equipments First Unit Value Generated by "MER"
(Represents Approximately 30th Unit on 90% λ.)

APPENDIX II
RCA PRICE MODEL

The RCA PRICE parametric estimating model was used to estimate several parts of the Solar Power system. Costs for the ground rectenna, satellite microwave transmitter, and satellite power distribution and control systems were derived from RCA PRICE. The transmitter, power distribution, and control costs are included in the Solar Satellite cost category. The ground rectenna costs are complete as shown in the Rectenna cost category.

RCA PRICE is a commercially available estimating technique evolved from RCA electronics estimating. It keys on weight, volume, schedule, and a hardware complexity factor. It is intended for use on any combination of electrical and mechanical hardware. Output is consistent with the Boeing PCM by separating development and production costs. The Solar Power Satellite system is larger than any system normally estimated by RCA PRICE, but by breaking the system down to subelements (i.e. a 10' x 10' rectenna panel) and producing a large quantity of the elements, a cost estimate can be made consistent with the hardware definition and the Boeing PCM.

APPENDIX III

Future Space Transportation System Analysis Study

Boeing Document D180-189269

Contract NAS9014323

The propulsion system design and cost for the Crew OTV is taken from the FSTSA study design - LO_2l LH_2 1 1/2 Stage OTV GSS Mission.

APPENDIX IV

Systems Concepts for STS Derived Heavy Lift Launch Vehicles Study

Contract NAS9-14710

Costs for lifting satellites and assembly equipment into Low Earth Orbit are based on the Ballistic single stage 48 engine 500,000 16m payload launch vehicle.

APPENDIX V

JSC Control Document JSC 07700

Vol XVI

Aug 16, 1974

Cost per flight data for STS originates in this document.

APPENDIX VI

Concept Definition and System Analysis Study for a Solar Electric Propulsion Stage

Boeing Document D180-18553-5

Geosynchronous Orbit assembly and maintenance manipulators are based on a concept in this document.

APPENDIX VII

Thermionic Diode Detail Cost Analysis

Below is the text of the memo transmitting the thermionic diode cost study. The study was done by Manufacturing New Business on March 17, 1976.

The following is provided in response to your verbal request for an estimate of the manufg. cost to produce the subject diodes at n rate of 30,000,000 per year.

Estimating Assumptions

1. A developmental program will precede the production program and the design and manufacturing problems will be resolved so that automatic production is realized.
2. This estimate will be for the unit cost when production rates have been achieved.
3. The emiter and collector will be formed in a press by a Sintering process and the parts will be pressure tight. This is a risky assumption - The parts have a wall thickness of 0.2 cm (0.08") and the sintering process may result in a part that is porous. If sintering is not successful, the parts would be formed in a press at high temperature or machined from blocks at approximately double the cost.
4. Tungsten powder is estimated to cost $130 per pound. This is based on the cost of 3/4" X 2" Tungsten bar that is in a Boeing Store and the

cost was $195 per foot or $159 per pound. An assumption is made that the price would be reduced to $130 per pound when the material is purchased by the ton.

5. The cecium reservior will be made of stainless steel; the cups will be welded to the pipe and the pipe will be threaded for attachment to the collecton.

The Estimate

An automotive sealed beam head lamp is a similar part and this estimate will be made by comparison. The size and weight are approximately the same; the materials are different but the manufacturing steps should be proportional to the number of different parts.

There are 13 in the diode and 6 parts in the headlamp. The complexity factor is estimated to be 3 because the diode is to be reliable space hardware and is obviously more complicated than the headlamp. Both parts are evacuated and sealed. The lamp cost is $2.30 retail.

Material Cost Estimate

Tungsten -- 1.7# @ $130 per #	$222.00
Carbon -- 1# @ 25¢/#	.25
Stainless Steel - i/2¢/# @ $1.00 per # =	.50
Cesium Pellet	.50
TOTAL MATERIAL COST =	$223.25

The cost estimate will be based on the following equation:

$$\text{(Headlamp Cost)} \quad \frac{\text{No. of parts in diode}}{\text{No. of parts in lamp}} \qquad \text{(cont)}$$

(Complexity Factor) + Material Cost

per the above --

$$\frac{(2.30)(13)(3)}{(6)} + 223 = \$238 \quad \text{Diode Cost}$$

Note that the high cost of Tungsten makes other costs relatively unimportant.

Conclusions

1. The production rate of 115,000 per day will require a factory that is dedicated to the production of diodes.
2. Automatic equipment is required to manufacture them -- Similar to a headlamp factory.
3. There are several manufacturing development problems involved such as:
   a. Forming the Tungsten parts.
   b. Making the seal between the Tungsten parts.
   c. Producing parts that will remain pressure tight.
   d. Automation of the manufacturing process.
4. 25,000 tons of Tungsten will be required per year.
5. The estimated cost, based on this 8 hour estimate, is $238 each.

EARTH ORBIT RENDEZVOUS

WITH PROPELLANT TRANSFER USING 2-STAGE SATURN C-3

MISSION SUCCESS PROBABILITY- 92
(.877 W/O APOLLO STANDBY)
(.75 WITH NO STANDBY LAUNCHES)

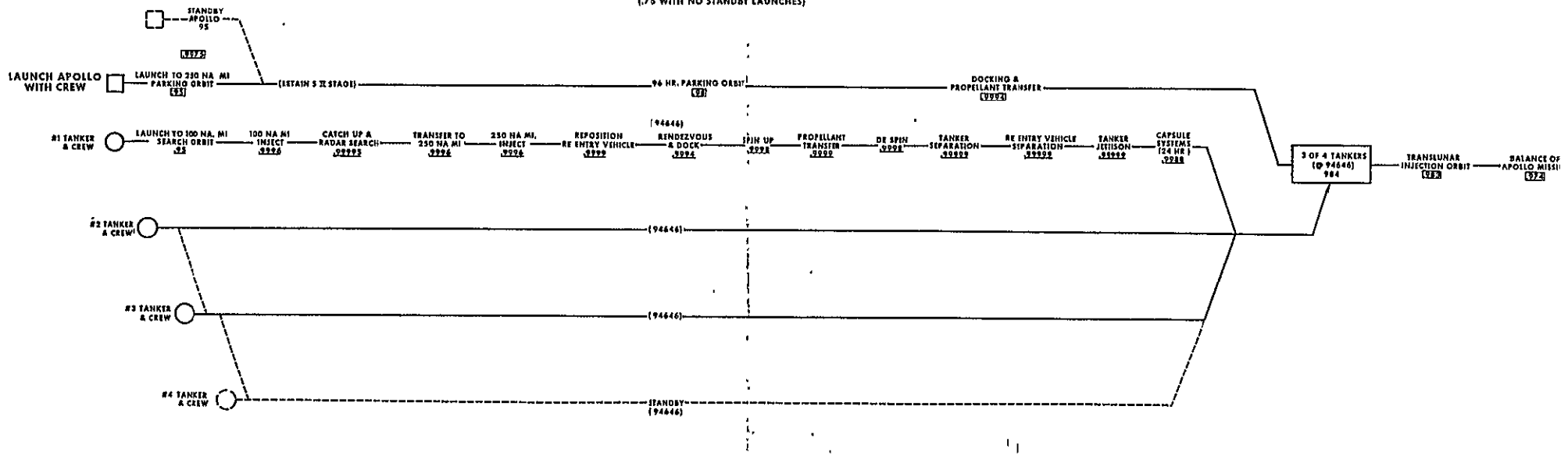

WITH PROPELLANT TRANSFER USING 2-STAGE SATURN C-4

MISSION SUCCESS PROBABILITY-.85

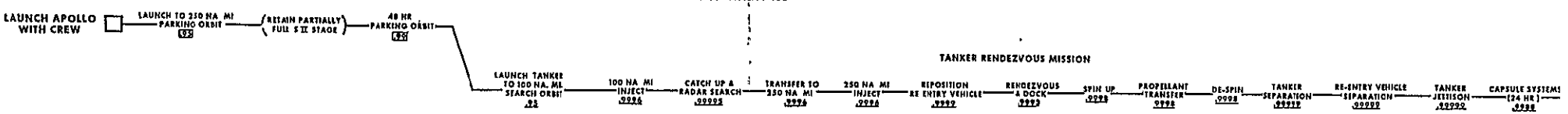

FIGURE 3.5-2

APPLICATIONS OF RENDEZVOUS
FOR THE
APOLLO MISSION

EARTH ORBIT RENDEZVOUS

WITH PROPELLANT TRANSFER USING 2-STAGE SATURN C-3

MISSION SUCCESS PROBABILITY- 92
(.877 W/O APOLLO STANDBY)
(.76 WITH NO STANDBY LAUNCHES)

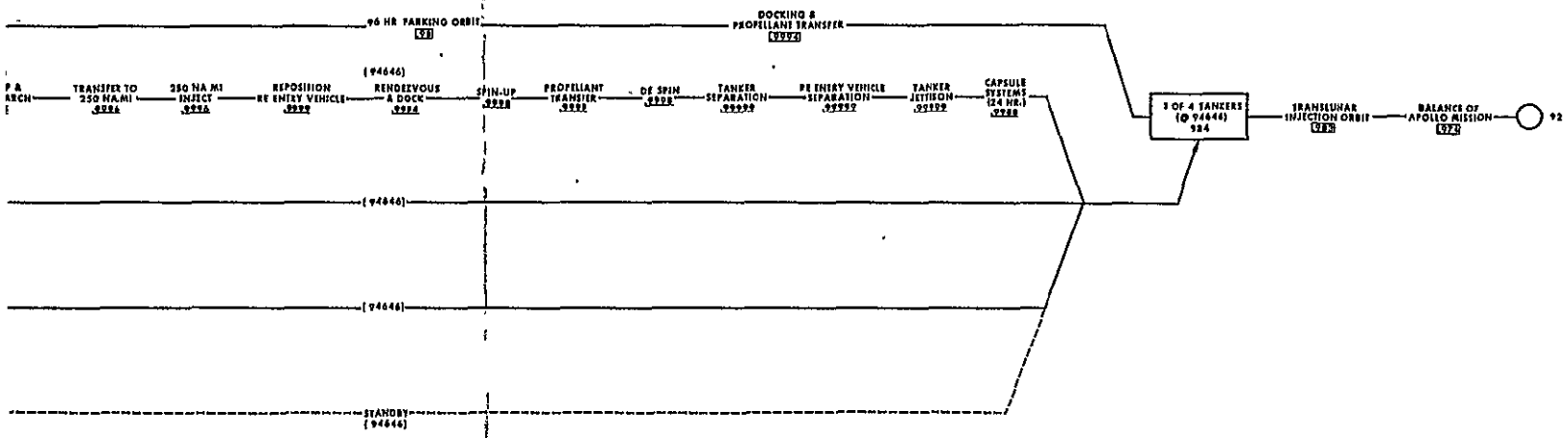

WITH PROPELLANT TRANSFER USING 2-STAGE SATURN C-4

MISSION SUCCESS PROBABILITY-.85

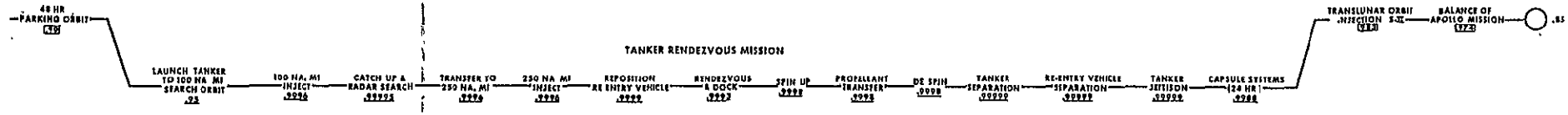

FIGURE 3.5-2

APPLICATIONS OF RENDEZVOUS FOR THE APOLLO MISSION

EARTH ORBITAL RENDEZVOUS

ORBITAL ASSEMBLY SATURN C-3 (2 STAGE)

MISSION SUCCESS PROBABILITY-.92
(.88 WITHOUT APOLLO STANDBY)
(.76 WITH NO STANDBY LAUNCHES)

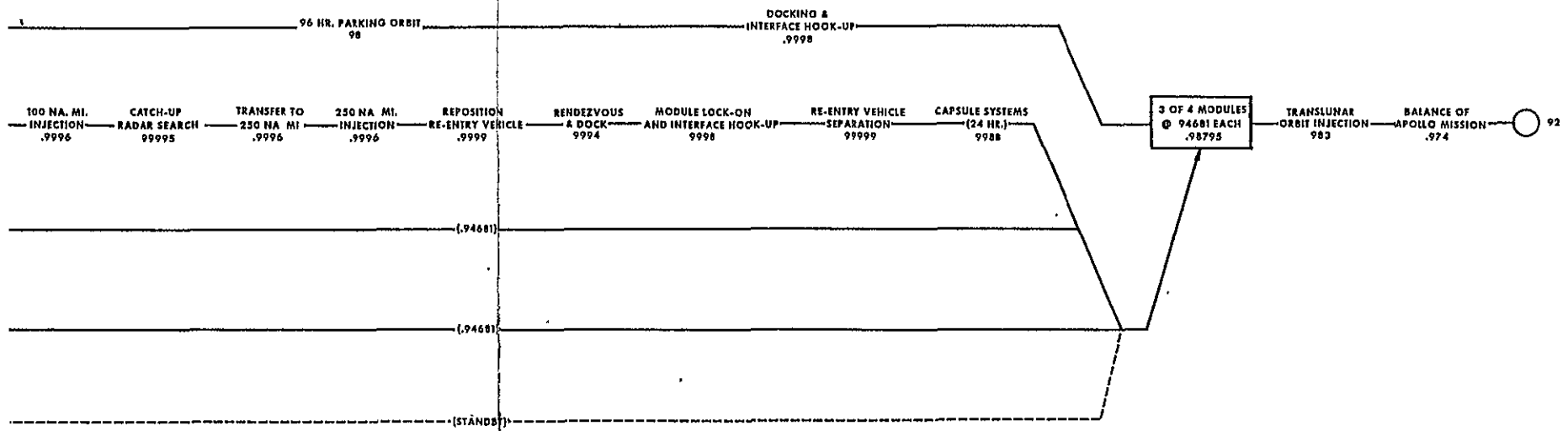

ORBITAL ASSEMBLY SATURN C-4

MISSION SUCCESS PROBABILITY- .85

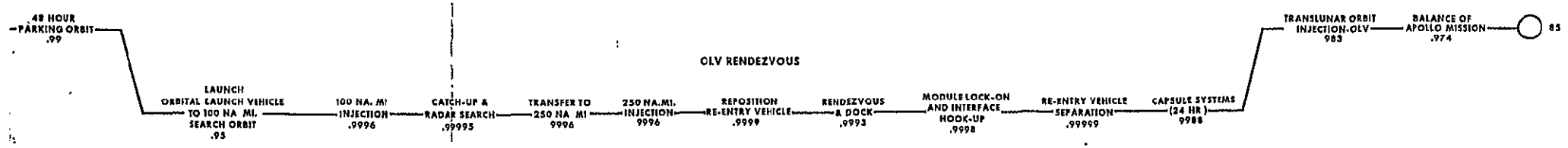

FIGURE 3.5-1

103-B

103-C

~~CONFIDENTIAL~~

APPLICATIONS OF RENDEZVOUS FOR THE APOLLO MISSION

EARTH ORBITAL RENDEZVOUS

ORBITAL ASSEMBLY SATURN C-3 (2 STAGE)

MISSION SUCCESS PROBABILITY-.92
(.88 WITHOUT APOLLO STANDBY)
(.76 WITH NO STANDBY LAUNCHES)

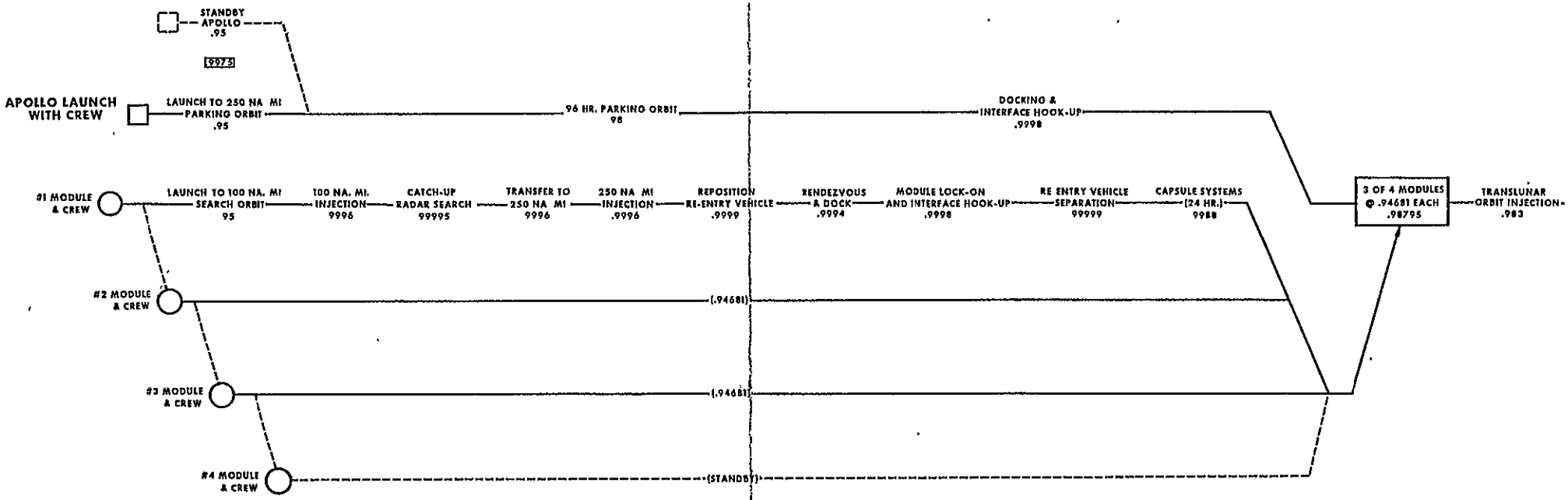

ORBITAL ASSEMBLY SATURN C-4

MISSION SUCCESS PROBABILITY- .85

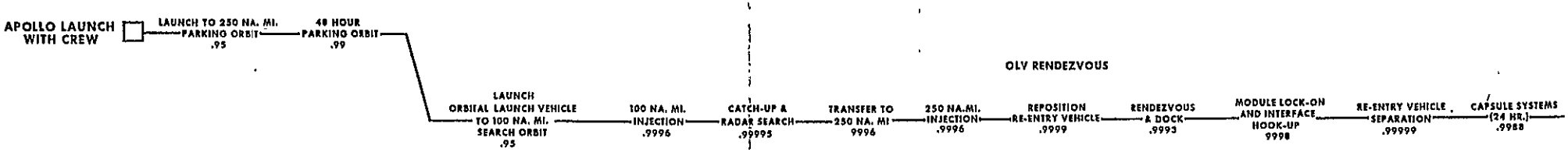

FIGURE 3.5-1

APPLICATIONS OF RENDEZVOUS
FOR THE
APOLLO MISSION

TRANSLUNAR RENDEZVOUS–SATURN C-4

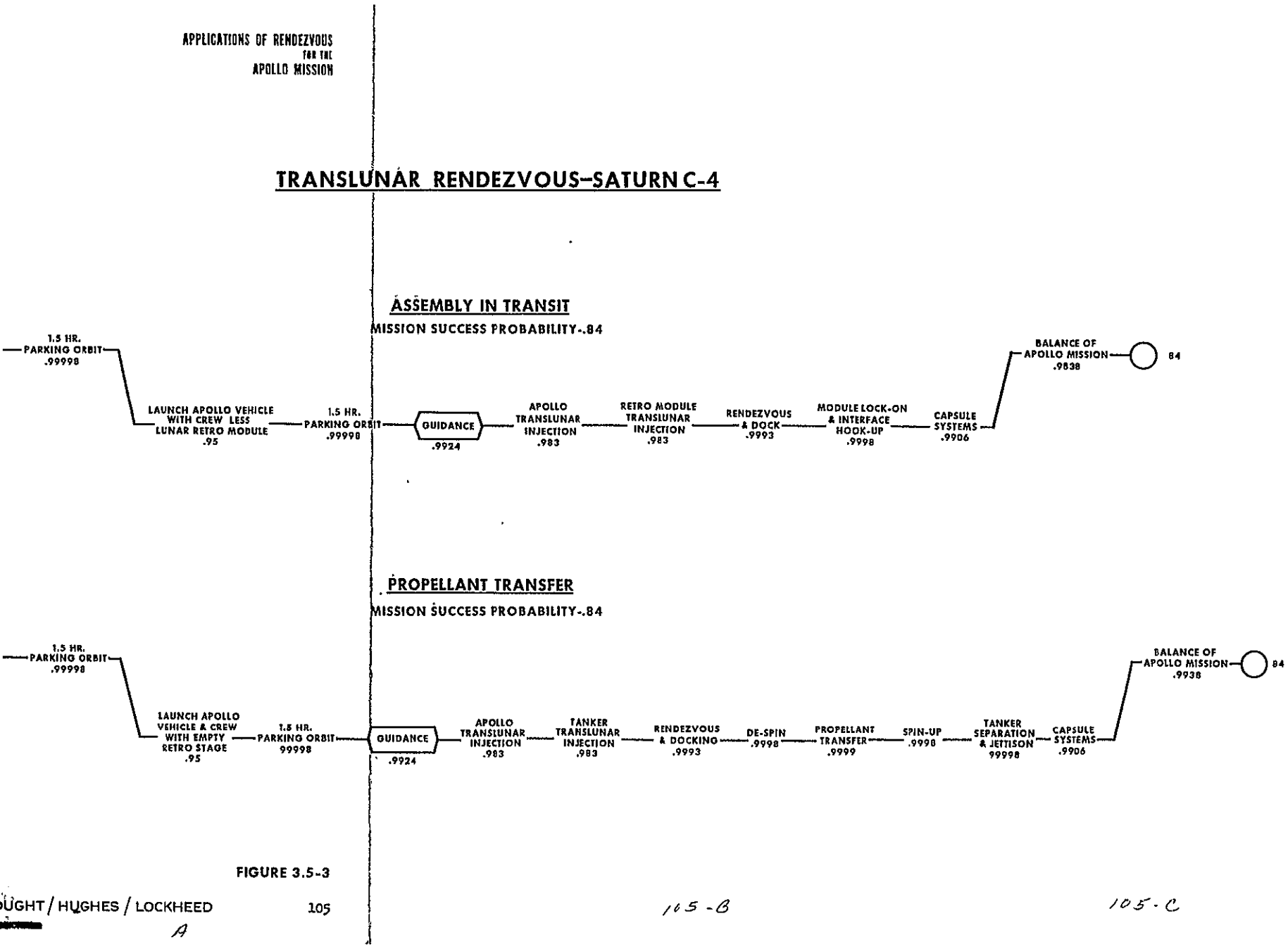

FIGURE 3.5-3

105-B

105-C

APPLICATIONS OF RENDEZVOUS
FOR THE
APOLLO MISSION

TRANSLUNAR RENDEZVOUS–SATURN C-4

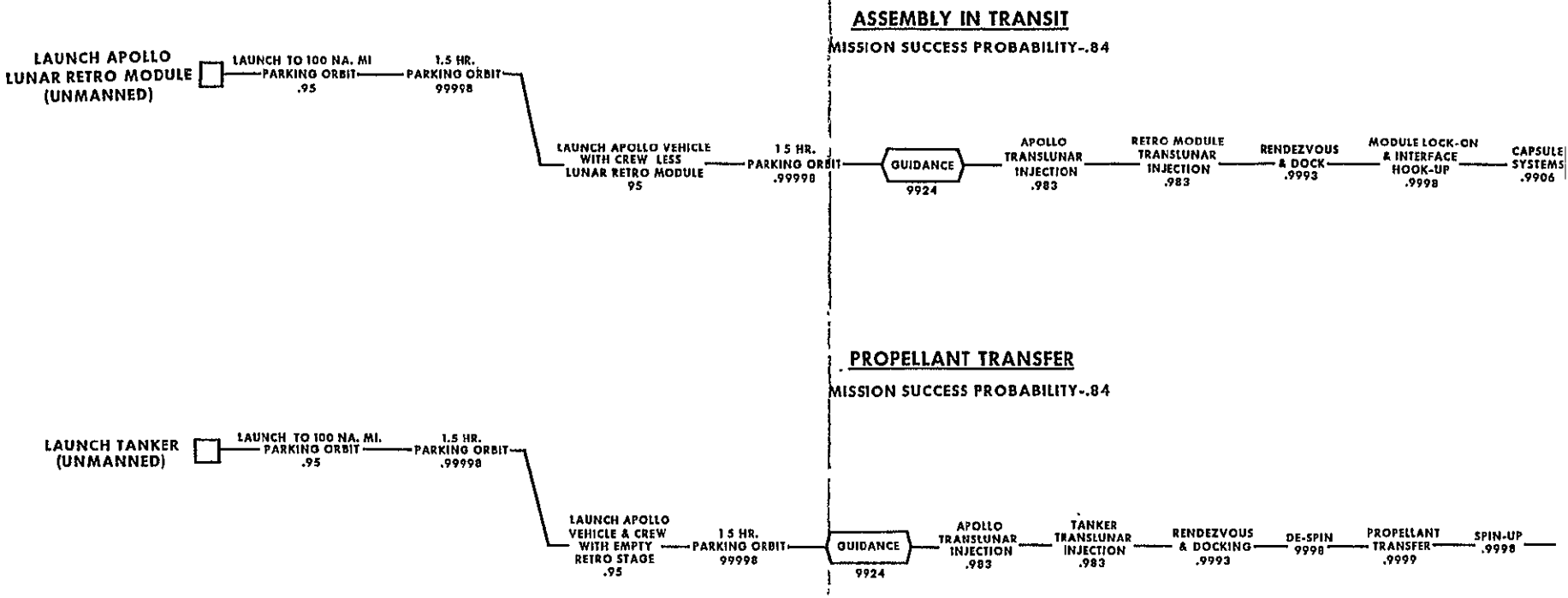

FIGURE 3.5-3